CATALYTIC PYROLYSIS OF BIOMASS FOR IMPROVED LIQUID FUEL QUALITY

ELIZABETH HELEN SALTER
BEng(Hons)

Doctor of Philosophy

Aston University

April 2001

CATALYTIC PYROLYSIS OF BIOMASS FOR IMPROVED LIQUID FUEL QUALITY

Key words: biomass, catalysis, fast pyrolysis, fuel quality, 'green' fuel.

THESIS SUMMARY

Fast pyrolysis of biomass creates pyrolysis liquid that is relatively unstable compared to liquid fossil fuels. It changes considerably with time and temperature, particularly with respect to an increase in viscosity. The objective of the work was the production of a more stable liquid that is also lower in viscosity than standard pyrolysis liquid and not sensitive to its local environment. Catalytic pyrolysis was selected as the process for quality improvement following the success of initial experiments. This is a process in which the newly formed pyrolysis vapours are contacted with catalysts.

Catalysts were incorporated into the fast pyrolysis process in four modes of operation: co-feeding catalyst with biomass; replacing the inert sand fluid bed with a catalytic one; including catalysts close-coupled in this primary reactor and close-coupling catalysts in a secondary reactor. The catalysts employed were ZSM-5 zeolite, Y-zeolite, char and thermally-expanded slate. The bio-oil produced was analysed for evidence of modification, upgrading and stabilisation. The change in composition of the liquid product was measured by HPLC, water content and acidity testing. The viscosity of fresh and artificially aged pyrolysis liquid was measured to assess stability using the newly developed 'Aston Viscosity Index'.

The slate fluid bed gave the best quality pyrolysis liquid as measured by initial viscosity, stability, water content and liquid yield. The maximum organic yield using slate was greater than that using an inert sand fluid bed and found to be at 475°C, lower than that of pyrolysis when using sand. This method of creating better quality pyrolysis liquid has economic and technological advantages and disadvantages associated with it. Economically, using a low cost substance such as slate, which also improves the economics of the pyrolysis process by reducing the operating temperature, is advantageous. However, the possible need to regenerate the slate should be compared to the cost of incorporating a chemical into the liquid product. This is the main alternative method of liquid improvement. Such a chemical, stabilising the pyrolysis liquid in such a successful way, is yet to be found.

The quality of the pyrolysis liquid has been improved through this project. The catalytic route is considered to offer technical and economic promise. Although the stability has been significantly improved, it is still necessary to establish if this improvement is sufficient for wider commercial use. Further work to move towards this goal is therefore recommended.

Acknowledgements

I would like to thank my supervisor Professor Tony Bridgwater for all his expert advice and input. His assistance has been much appreciated.

I would also like to thank the past and present members of the Bio-Energy Research Group (BERG), formally known as the Energy Research Group. Special thanks to Dr. Bob Hague, Dr. Cordner Peacock, Dr. Anna Weekes and Dr. Husam Sheena for sharing their knowledge and providing support. Thanks also to Nick Robinson, Louise Cooke, Colin Dick, Karen Dowden, Nina Ahrendt, Claire Humphreys, George Drahun, Nigel Overton and John Brammer for their friendships in and out of work.

I am grateful to Dr. Steve Bodman for making the pillared clay catalysts used in this project and sharing his knowledge on them.

This project was funded by the European Commission in the framework of the Non Nuclear Energy Programme, Joule III, contract JOR CT95-0081. I would like to thank the other members of the contract for their collaboration - Twente University in the Netherlands; the University of Naples, Italy; CPE Research Institute and Sapemus of Greece; Union Electrica Fenosa, Spain and particularly the Institute for Wood Chemistry in Hamburg, Germany and my colleagues there, Dr. Dietrich Meier and Dr. Peter Wulzinger.

I must also acknowledge the support of my family and friends. Thank you very much Mum, Dad, Ann, Jo, Catherine, Christina, Greg, Mario and Anna (again).

Contents

		Page
THESIS SUMMARY		**2**
Acknowledgements		**3**
Contents		**4**
List of Tables		**10**
List of Figures		**15**
1	**INTRODUCTION**	**19**
1.1	Pyrolysis Liquid	19
1.2	Objectives	21
1.3	Structure of Thesis	22
2	**BACKGROUND TO PYROLYSIS LIQUID MODIFICATION**	**24**
2.1	Biomass Pyrolysis	24
2.1.1	Pyrolysis of Wood	25
2.1.2	Calculation of Chemical Diameter	30
2.2	The Nature of Pyrolysis Liquid	30
2.3	Modification of Pyrolysis Liquid	33
2.3.1	Hydrotreating	36
2.3.1.1	Summary of Hydrotreating Upgrading	38
2.3.2	Chemical Treatment of the Liquid Product	39
2.3.3	Catalytic Cracking	40
2.3.3.1	Zeolite Catalytic Cracking	40
2.3.3.2	Clay Catalytic Cracking	46
2.3.3.3	Cracking of Gasification Tars	46
2.3.3.4	Summary of Catalytic Cracking Upgrading	47
2.4	Catalysts	47
2.4.1.1	Brönsted Acid and Base	47
2.4.1.2	Lewis Acid and Base	48
2.4.1.3	Catalyst Poisoning	48
2.4.1.4	Catalyst Blinding	48
2.4.1.5	Catalyst De-Activation	48
2.4.2	Catalyst Variables	48
2.4.2.1	Shape Selectivity	49
2.4.3	Catalytic Cracking	49
2.4.4	Zeolite Catalysts	49
2.4.5	Clay Catalysts	53
2.4.5.1	Pillared Clay	53
2.5	Catalyst Addition Technology	55
2.5.1	Fixed Bed Technology	56
2.5.2	Fluid Bed Technology	56
2.5.2.1	Minimum Fluidising Velocity	57
2.5.2.2	Particle Terminal Falling Velocity	58
2.5.2.3	Density and Voidage	59
2.6	Summary	60

3 CATALYST SCREENING 62

3.1 Catalyst Screening Apparatus and Experimentation Description 63
3.2 Catalysts Screened 64
3.3 Catalyst Screening Results 66
3.3.1 Manipulation of Screening Information 67
3.3.1.1 Chromatograph Peak Area Minus Blank Runs (Method 1) 68
3.3.1.2 Chromatograph Peak Area Difference as a Percentage of Blank (Method 2) 69
3.3.1.3 Comparison of the Number of Peaks (Method 3) 70
3.3.1.4 Average GC Peak Area (Method 4) 71
3.3.1.5 Sum of Peak Area Difference as Percentage of Blank Area (Methods 5 – 7) 72
3.3.2 Catalyst Screening Assumptions 75
3.3.3 Comparison of Chromatographs from Screening 76
3.3.4 Molecular Weight Hypothesis 77
3.4 Catalysts Recommended Following Screening Experiments 80

4 EXPERIMENTAL FAST PYROLYSIS 82

4.1 Apparatus Description 82
4.1.1 Small Fluid Bed - Commissioning Configuration 83
4.1.1.1 The Feed System 83
4.1.1.2 The Reactor 86
4.1.1.3 Char Separation 93
4.1.1.4 The Liquid Product Collection System 94
4.1.1.5 Residual Gas Handling 97
4.1.2 Small Fluid Bed - Experimental Configuration 97
4.1.2.1 The Liquid Product Collection System 99
4.1.2.2 Design of Condenser 102
4.1.2.3 Residual Gas Handling 106
4.2 Biomass Feed, Preparation and Handling 106
4.3 Apparatus Operation 108
4.3.1 Preparation 108
4.3.2 Start Up 108
4.3.3 Problems 111
4.3.4 Shutdown 111
4.4 Incorporation of Catalyst into the Process 111
4.4.1 Co-Feeding Biomass and Catalyst 113
4.4.2 Replacement of Fluidising Medium by Catalyst 114
4.4.3 Close-Coupled In-bed Catalyst 115
4.4.4 Close-Coupled Catalyst in a Secondary Reactor 117
4.5 Catalysts Used in the Apparatus 119
4.5.1 ZSM-5 120
4.5.2 Y-Zeolite 120
4.5.3 Slate 121
4.5.4 Char 121
4.6 Experimental Description 122
4.7 Pyrolysis Product Analysis Techniques 125
4.7.1 Karl Fischer Water Testing 125
4.7.2 Gas Chromatography 126

4.7.2.1 Use of In-line Gas Chromatography Equipment 127
4.8 Small Fluid Bed Pyrolysis Mass Balance 129
4.8.1 Mass Balance Calculation Development 130
4.8.2 Errors Associated with Mass Balance Calculations 133
4.9 Discussion of Mass Balance Results 135
4.10 Comparison of Mass Balance Results to Wulzinger and Cooke 142
4.10.1 Experimental Comparison with Wulzinger 142
4.10.2 Mass Balance Comparison with Wulzinger 145
4.10.3 Experimental Comparison with Cooke 148
4.10.4 Mass Balance Comparison with Cooke 149

5 CHEMICAL ANALYSIS OF THE LIQUID PYROLYSIS PRODUCT 151

5.1 Water Content 151
5.1.1 Water Content Results 151
5.2 Discussion of Water Content Results 154
5.2.1 Water Content Comparison with Wulzinger 156
5.3 High Performance Liquid Chromatography 158
5.3.1 High Performance Liquid Chromatography Results 159
5.3.1.1 Comments on the Occurrence of Chemicals 162
5.3.1.2 Quantities of Chemicals Found 163
5.3.1.3 Hydroxyacetaldehyde Results 164
5.3.1.4 Levoglucosan Results 167
5.3.1.5 Acetic Acid Results 169
5.3.1.6 Lignin Results 170
5.4 Discussion of Liquid Product Chemical Analysis Results 174
5.4.1 Hydroxyacetaldehyde, Levoglucosan and Acetic Acid Results 174
5.4.2 Lignin Results 177
5.4.3 Summary of Discussion of Liquid Product Chemical Analysis Results 179

6 PHYSICAL ANALYSIS OF THE LIQUID PYROLYSIS PRODUCT 180

6.1 Viscosity Testing 180
6.1.1 Haake Rotary Viscometer 180
6.1.2 Capillary Viscometry 180
6.1.3 Procedure for Use of Capillary Viscometers 181
6.2 Viscosity Testing Results 183
6.2.1 Single Test Over Extended Time Period 183
6.2.2 Initial Viscosity 184
6.3 Discussion of Initial Viscosity Results 185
6.4 Comparison of Viscosity Results to Wulzinger 187

7 LIQUID PRODUCT QUALITY TESTING 189

7.1 Stability Testing 189
7.1.1 Stability Testing Development 189
7.1.1.1 Aston Viscosity Index 190
7.1.2 Procedure For Pyrolysis Liquid Stability Testing 191
7.2 Stability Results 191
7.2.1 Adjusted Aston Viscosity Index 192
7.3 Discussion of Stability Results 194
7.3.1 Modelling and Ranking of AVI Results 194

7.3.2 Modelling and Ranking of Adjusted AVI Results 195
7.3.3 Aston Viscosity Index Error Analysis 196
7.4 Acidity Testing 197
7.5 Summary of Discussion of Liquid Product Quality Testing 197

8 CATALYTIC PYROLYSIS PROCESS SCALE UP 199

8.1 Large Fluid Bed Apparatus Description 199
8.2 Large Fluid Bed Apparatus Operation 201
8.3 Large Fluid Bed Stability Results 202
8.3.1 Change of Stability with Time 203
8.4 Large Fluid Bed Homogeneity Testing 205
8.4.1 Pyrolysis Liquid Filtration 207
8.5 Scale-Up Comparison with Wulzinger 208
8.6 Scale-Up Comparison with Cooke 210

9 CATALYST REGENERATION AND SCANNING ELECTRON MICROSCOPY 213

9.1 Scanning Electron Microscopy Results 215

10 Summary of Discussions 216

10.1 Catalyst Screening 216
10.1.1 Catalyst Screening Hypotheses 217
10.1.1.1 Unknown and Identifiable Compounds 217
10.1.1.2 Chemical Difference from Blank Run 217
10.1.1.3 Number of Chemical Compounds 218
10.1.1.4 Ratio of Low Molecular Chemicals to High Molecular Chemicals 219
10.1.1.5 Catalyst Pore Size 220
10.1.1.6 Pre-Screening for Bench Scale Pyrolysis 220
10.2 Pyrolysis Heat Transfer During Condensation 220
10.3 Mass Balance Analysis 221
10.3.1 Empirical Comparison 221
10.4 Liquid Product Chemical Analysis 222
10.4.1 Pyrolysis Liquid Water Content 222
10.4.2 High Performance Liquid Chromatography 222
10.5 Liquid Product Physical Analysis 223
10.6 Small Fluid Bed Pyrolysis Product Stability 223
10.6.1 Comparison of Stability to Initial Viscosity 225
10.6.2 Comparison of Stability and Initial Viscosity to Chemical Production 225
10.7 Scale -Up of Bench Scale Pyrolysis 225
10.8 Follow-Up of Objectives 225
10.8.1 How is 'Best Quality Pyrolysis Liquid' Defined? 226
10.8.2 What is the Best Catalyst to Produce the Best Quality Pyrolysis Liquid? 226
10.8.3 Where is the Best Place in the Pyrolysis Process to Incorporate Catalysts? 226
10.8.4 What Chemicals within the Pyrolysis Liquid Influence Quality? 226

11 CONCLUSIONS 227

12 RECOMMENDATIONS 229
12.1 Catalyst Recommendations 229
12.1.1 Scaling 229
12.1.2 Mode of Operation 229
12.1.3 Catalyst Mixes 229
12.1.3.1 Catalyst Modes 230
12.1.4 Catalyst Regeneration 230
12.1.5 Catalyst Concentration 230
12.1.6 Slate Reaction Investigation 230
12.2 Process Modifications 231
12.2.1 Addition of Steam 231
12.2.2 Modification of Condensation Temperature 231
12.3 Further Testing of Current Process 231
12.3.1 Tarry Liquid Analysis 231
12.4 Chemistry Recommendations 232
12.4.1 Lignin Ratio 232
12.4.2 Acidity of Pyrolysis Liquid 232
12.4.3 Homogeneity of Pyrolysis Liquid 232

13 Nomenclature 234

14 References 237
14.1 Contents of References 237
14.2 Alphabetical References 237

Appendix A – Publications 252

Appendix B – Results Proforma 253

Appendix C – Excel Spreadsheets 255

Appendix D – Catalyst Screening Graphs and Tables 259

Appendix E – Mass Balance Tabulated Results 270

Appendix F – Mass Balance Graphical Results 277

Appendix G – Water Content Graphs and Tables 279

Appendix H – HPLC Analysis Technique and Tabulated Results 285
Analysis of Resulting HPLC Chromatographs 285

Appendix J – HPLC Graphical Results 310

Appendix K – Viscosity Tabulated Results 312

Appendix L – Viscosity Graphical Results 316

Appendix M – Stability Tabulated Results 318

Appendix N – Stability Graphical Results 324

Appendix P – Large Fluid Bed Viscosity and Homogeneity Testing Results 328
Procedure for Homogeneity Testing 333

Appendix Q – Scanning Electron Microscopy Pictures 335

Appendix R – Catalyst Screening Chromatographs and Acetate Overlay 341

List of Tables

		Page
Table 1	Structures of Chemical Products of Wood Pyrolysis	29
Table 2	Molecular Size Based on Van der Waal's Second-Virial-Coefficient Data (Barrow, 1988)	30
Table 3	Physical Properties of Petroleum and Pyrolysis Liquids	32
Table 4	Functional Groups in Fast Pyrolysis Liquid	33
Table 5	Main Institutions Involved with Hydrotreating Pyrolysis Liquid	38
Table 6	Main Institutions Involved with Catalytic Cracking of Re-Vaporised Biomass Derived Liquids or Model Compounds	43
Table 7	Main Institutions Involved with Catalytic Cracking of Freshly Produced Fast Pyrolysis Vapours	44
Table 8	Typical Characteristics of Zeolite Catalysts	52
Table 9	Classification of Particles by Reynolds Number and Corresponding Terminal Falling Velocity	59
Table 10	Physical Properties of Bed Materials and Feed	60
Table 11	Catalysts Recommended for Screening Tests	61
Table 12	Catalyst Screened in IWC Micro-reactor	65
Table 13	Ranking of Results from Screening Analysis Methods	77
Table 14	Screened Catalysts Recommended for Further Testing	80
Table 15	Fluidising Properties of Reactor Sand and Feed, Calculated at STP	90
Table 16	Calculation of Nitrogen Flow-rate	91
Table 17	Fluidising Properties of Char Produced in Reactor, Calculated at STP	92
Table 18	Calculation of Nitrogen Flow-rate	93
Table 19	Numbers used for Calculation of Terminal Falling Velocity of the Smallest Particle Retained by Cyclone, Calculated at STP	94
Table 20	Calculation of Tube Flow Area at Different Condenser Positions	104
Table 21	GC Analysis of Pinewood and Beechwood Fast Pyrolysis Liquids (Meier, 1997#2)	107
Table 22	Readings Taken Throughout an Experimental Run	110
Table 23	Fluidising Properties of Fluidising Medium Replacement Materials, Calculated at STP	115
Table 24	Catalysts and Potential Configurations of Use in150 g/h Fluid Bed	120
Table 25	Summary of Commissioning Run Variables, (Three Product)	125
Table 26	Summary of Experimental Run Variables, (Single Product)	125
Table 27	Comparison of Gas Sampling Systems	127
Table 28	Calibration Gas Standards	128
Table 29	Temperature and Time Settings for GC	128
Table 30	Location of Pyrolysis Products (Both Configurations)	132
Table 31	Accuracy of Apparatus	134
Table 32	Calculated Mass Balance Errors	135
Table 33	Runs on 150 g/h Apparatus, Beech Wood Feed, No Catalyst	136
Table 34	R^2 Values for Equation 36 to Equation 43	141
Table 35	Variation of Experimental Results	142
Table 36	Average Percentage Difference between Pyrolysis Liquid Water Content and 'Model' Water Content (Ranked)	156
Table 37	HPLC Analysis - Main Fraction of Liquid, Wt% on Dry Wood Basis of Chemicals Found and Pyrolytic Lignin, No Catalyst	160

Table 38	HPLC Analysis - Secondary Fraction of Liquid, Wt% on Dry Wood Basis of Chemicals Found and Pyrolytic Lignin, No Catalyst	161
Table 39	Line Fit for Hydroxyacetaldehyde Graphs, Figure 51 to Figure 52	166
Table 40	Line Fit for Levoglucosan Graphs, Figure 53 to Figure 54	168
Table 41	Line Fit for Acetic Acid Graphs, Figure 51 to Figure 52	170
Table 42	Line Fit for Graphs Lignin, Figure 57 to Figure 58	173
Table 43	Average Percentage Difference between Pyrolysis Liquid Aqueous Fraction Hydroxyacetaldehyde Content and 'Model' Hydroxyacetaldehyde Content (Ranked)	176
Table 44	Average Percentage Difference between Pyrolysis Liquid Aqueous Fraction Levoglucosan Content and 'Model' Levoglucosan Content (Ranked)	176
Table 45	Average Percentage Difference between Pyrolysis Liquid Aqueous Fraction Acetic Acid Content and 'Model' Acetic Acid Content (Ranked)	177
Table 46	Comparison of Organic Yield and Lignin Percentage Production	178
Table 47	Average Percentage Difference between Pyrolytic Lignin Content and 'Model' Lignin Content (Ranked)	179
Table 48	Average Percentage Difference between Initial Viscosity of Pyrolysis Liquid and 'Model' Initial Viscosity (Ranked)	186
Table 49	Percentage Difference between Initial Viscosity of One Pyrolysis Liquid and 'Model' Initial Viscosity at Maximum Organic Yield Temperature (Ranked)	187
Table 50	Average Percentage Difference between Pyrolysis Liquid AVI and 'Model' AVI (Ranked)	194
Table 51	Percentage Difference between AVI of One Pyrolysis Liquid and 'Model' AVI at Maximum Organic Yield Temperature (Ranked)	195
Table 52	Average Percentage Difference between Pyrolysis Liquid Adjusted AVI and 'Model' Adjusted AVI (Ranked)	196
Table 53	Percentage Difference between Adjusted AVI of One Pyrolysis Liquid and 'Model' Adjusted AVI at Maximum Organic Yield Temperature (Ranked)	196
Table 54	Errors Associated with Viscosity Testing	197
Table 55	Large Fluid Bed Results	202
Table 56	Comparison of Large and Small Fluid Bed Stability Results	202
Table 57	Experimental Conditions and Results from the Laboratory Scale Apparatus of Wulzinger (Wulzinger, 1998)	209
Table 58	Results from 1 kg/h Reactor at Aston Reported by Cooke	212
Table 59	Source of Samples for Scanning Electron Microscope Images	214
Table 60	Ranking of Results from Screening Analysis Methods	216
Table 61	Degree of Chemical Difference to Blank Run Compared to Stability	218
Table 62	Degree of Chemical Difference to Blank Run Compared to Stability	219
Table 63	Ranking of the Catalysts used to Produce Pyrolysis Liquid High in Low Molecular Weight Compounds	220
Table 64	Ranked Properties of Pyrolysis Liquid Compared to Stability Expressed as Aston Viscosity Index	224
Table 65	Mass Balance Spreadsheet, Mass Balance Tab 1 of 2	255
Table 66	Mass Balance Spreadsheet, Mass Balance Tab 2 of 2	256
Table 67	Mass Balance Spreadsheet, Water Tab	257
Table 68	Mass Balance Spreadsheet, Gas Tab	258

Table 69	Mass Balance Spreadsheet, Summary Tab	258
Table 70	Identification of Detected Chemicals in Micro-reactor Screening	268
Table 71	Runs on 150 g/h Apparatus, Beech Wood Feed, Slate Fluid Bed	272
Table 72	Runs on 150 g/h Apparatus, Beech Wood Feed, Y-Zeolite Close-Coupled in Primary Reactor	273
Table 73	Runs on 150 g/h Apparatus, Beech Wood Feed, Char Co-Fed and Char in the Secondary Reactor	274
Table 74	Runs on 150 g/h Apparatus, Beech Wood Feed, Char Fluid Bed, Slate Co-Fed and Slate in the Secondary Reactor	275
Table 75	Runs on 150 g/h Apparatus, Pine Wood Feed (Commissioning Configuration)	276
Table 76	Line Fit for Graphs, Figure 87 and Figure 88	281
Table 77	Calculation of Percentage Difference from 'Model' (No catalyst) Water Content for No Catalyst Runs	281
Table 78	Calculation of Percentage Difference from 'Model' (No catalyst) Water Content for Slate Fluid Bed Runs	282
Table 79	Calculation of Percentage Difference from 'Model' (No catalyst) Water Content for Y-Zeolite In-bed and Co-fed Char Runs	282
Table 80	Calculation of Percentage Difference from 'Model' (No catalyst) Water Content for Char in Secondary Reactor and Char Fluid Bed Runs	283
Table 81	Calculation of Percentage Difference from 'Model' (No catalyst) Water Content for Co-fed Slate and Slate Secondary Bed Runs	284
Table 82	HPLC 'Standard' Components in Order of Retention Times	287
Table 83	Terms Used in Equation 57 to Equation 62 (in order of appearance)	288
Table 84	HPLC Analysis - Main Fraction of Liquid, Wt% on Dry Wood Basis of Chemicals Found and Pyrolytic Lignin, Slate Fluid Bed	290
Table 85	HPLC Analysis - Main Fraction of Liquid, Wt% on Dry Wood Basis of Chemicals Found and Pyrolytic Lignin, Y-Zeolite Close Coupled in Primary Reactor	291
Table 86	HPLC Analysis - Main Fraction of Liquid, Wt% on Dry Wood Basis of Chemicals Found and Pyrolytic Lignin, Char Co-Fed and Char in Secondary Reactor	292
Table 87	HPLC Analysis - Main Fraction of Liquid, Wt% on Dry Wood Basis of Chemicals Found and Pyrolytic Lignin, Char Fluid Bed, Slate Co-Fed and Slate in Secondary Reactor	293
Table 88	HPLC Analysis - Secondary Fraction of Liquid, Wt% on Dry Wood Basis of Chemicals Found and Pyrolytic Lignin, Slate Fluid Bed	295
Table 89	HPLC Analysis - Secondary Fraction of Liquid, Wt% on Dry Wood Basis of Chemicals Found and Pyrolytic Lignin, Y-Zeolite Close Coupled in the Primary Reactor	296
Table 90	HPLC Analysis - Secondary Fraction of Liquid, Wt% on Dry Wood Basis of Chemicals Found and Pyrolytic Lignin, Char Co-Fed and Char in the Secondary Reactor	297
Table 91	HPLC Analysis - Secondary Fraction of Liquid, Wt% on Dry Wood Basis of Chemicals Found and Pyrolytic Lignin, Char Fluid Bed, Slate Co-Fed and Slate in the Secondary Reactor	298
Table 92	Numbering of Catalyst Systems for Table 93 and Table 94	299
Table 93	Initial Assessment of HPLC Results, Main Fraction of Liquid	300
Table 94	Initial Assessment of HPLC Results, Secondary Fraction of Liquid	301

Table 95	Calculation of Percentage Difference from 'Model' (No catalyst) Hydroxyacetaldehyde, Levoglucosan and Acetic Acid Content for Non-Catalytic Runs	302
Table 96	Calculation of Percentage Difference from 'Model' (No catalyst) Hydroxyacetaldehyde, Levoglucosan and Acetic Acid Content for Slate Fluid Bed Runs	303
Table 97	Calculation of Percentage Difference from 'Model' (No catalyst) Hydroxyacetaldehyde, Levoglucosan and Acetic Acid Content for Y-Zeolite in Primary Reactor and Char Co-fed Runs	304
Table 98	Calculation of Percentage Difference from 'Model' (No catalyst) Hydroxyacetaldehyde, Levoglucosan and Acetic Acid Content for Char in Secondary Reactor, Char Fluid Bed, Slate CO-fed and Slate in Secondary Reactor Runs	305
Table 99	Calculation of Percentage Difference from 'Model' (No catalyst) Pyrolytic Lignin Content for Non-Catalytic Runs	306
Table 100	Calculation of Percentage Difference from 'Model' (No catalyst) Pyrolytic Lignin Content for Slate Fluid Bed Runs	307
Table 101	Calculation of Percentage Difference from 'Model' (No catalyst) Pyrolytic Lignin Content for Y-Zeolite in Primary Reactor and Char Co-fed Runs	308
Table 102	Calculation of Percentage Difference from 'Model' (No catalyst) Pyrolytic Lignin Content for Char in Secondary Reactor, Char Fluid Bed, Slate Co-fed and Slate in Secondary Reactor Runs	309
Table 103	Viscosity Calculations for EHS17, Stored at 25°C in Viscometer. Temperature of Run 490.79°C. Water Content 6.37 %.	312
Table 104	Calculation of Percentage Difference from 'Model' (No catalyst) Initial Viscosity for Non-Catalytic Runs	313
Table 105	Calculation of Percentage Difference from 'Model' (No catalyst) Initial Viscosity for Slate Fluid Bed Runs	313
Table 106	Calculation of Percentage Difference from 'Model' (No catalyst) Initial Viscosity for Y-Zeolite in Primary Reactor and Char Co-fed Runs	314
Table 107	Calculation of Percentage Difference from 'Model' (No catalyst) Initial Viscosity for Char in Secondary Reactor and Char Fluid Bed Runs	314
Table 108	Calculation of Percentage Difference from 'Model' (No catalyst) Initial Viscosity for Slate Co-fed and Slate in Secondary Reactor Runs	315
Table 109	Line Fit for Initial Viscosity Graphs, Figure 91 and Figure 92	315
Table 110	Calculation of Percentage Difference from 'Model' (No catalyst) AVI and Adjusted AVI for Non-Catalytic Runs	318
Table 111	Calculation of Percentage Difference from 'Model' (No catalyst) AVI and Adjusted AVI for Slate Fluid Bed Runs	319
Table 112	Calculation of Percentage Difference from 'Model' (No catalyst) AVI and Adjusted AVI for Y-Zeolite in Primary Reactor and Char Co-fed Runs	320
Table 113	Calculation of Percentage Difference from 'Model' (No catalyst) AVI and Adjusted AVI for Char in Secondary Reactor and Char Fluid Bed Runs	321

Table 114 Calculation of Percentage Difference from 'Model' (No catalyst) AVI and Adjusted AVI for Slate Co-fed and Slate in Secondary Reactor Runs 322
Table 115 Line Fit for Aston Viscosity Index Graphs, Figure 93 and Figure 94 322
Table 116 Line Fit for Adjusted Aston Viscosity Index Graphs, Figure 95 and Figure 96 323
Table 117 Viscosity and Homogeneity Results for Pyrolysis Liquid from Run LFB46 328

List of Figures

		Page
Figure 1	Two Monomer Repeat Units of Long Chain Cellulose	26
Figure 2	Lignin Monomers (Meier, 1997)	27
Figure 3	The Repeat Units of Beech Wood Lignin (Meier, 1997)	28
Figure 4	Description of Types of Fast Pyrolysis Fluid Modification for Liquid Fuel Production	35
Figure 5	ZSM-5 Framework Structure and Pore System (Diddams, 1997)	51
Figure 6	Petroleum Residual Cracking In A Varying Diameter Compound Catalyst Pore	51
Figure 7	Y-Zeolite Framework Structure Showing a Pore Opening into a Cage (Diddams, 1997)	53
Figure 8	Steps to Prepare Pillared Clay	55
Figure 9	Relationship Between Velocity and Delta Pressure to Find Minimum Fluidising Velocity (Kunii, 1991)	58
Figure 10	IWC Micro-reactor Outline	64
Figure 11	IWC Micro-reactor Collection System (Faix, 1987)	64
Figure 12	Chromatograph Peak Area Minus Blank, Zeolites 1 of 2	68
Figure 13	Chromatograph Peak Area Difference as % of Blank, Zeolites 1 of 2	69
Figure 14	Comparison of the Number of Peaks Resulting from Catalyst Addition to the Pyrolysis Micro-reactor, Zeolites	71
Figure 15	Average GC Peak Area, Zeolites	72
Figure 16	Total Sum of Peak Area Difference as % of Blank Area for Selected Chemicals, Zeolites	73
Figure 17	Sum of Peak Area Difference as % of Blank Peak Area for Selected Chemicals (Absolute Values), Zeolites	74
Figure 18	Average Peak Area Difference as % of Blank Peak Area (Absolute Values), Zeolites	74
Figure 19	To Describe Problem Labelling Levoglucosan Peak - Representation of Overlaid Chromatograph Peaks	76
Figure 20	Hypothetical Trend lines of Peak Area Difference as Percentage of Blank	78
Figure 21	Chromatograph Peak Area Difference as % of Blank as Linear Trendlines 1 of 2	79
Figure 22	Chromatograph Peak Area Difference as % of Blank as Linear Trendlines 2 of 2	79
Figure 23	150 g/h 'Small' Bench Scale Fluidised Bed Fast Pyrolysis Reactor – Commissioning Configuration	83
Figure 24	Detail of Feeder (not to scale)	85
Figure 25	Detail of Reactor (not to scale)	87
Figure 26	Detail of Feed Inlet Tube (not to scale)	88
Figure 27	Cyclone Separator (Coulson, 1991#3)	94
Figure 28	Detail of Liquid Product Collection System- Commissioning Configuration (not to scale)	96
Figure 29	150 g/h Single Product 'Small' Scale Fluidised Bed Fast Pyrolysis Reactor - Experimental Set Up	98
Figure 30	150 g/h Single Product 'Small' Scale Fluidised Bed Fast Pyrolysis Reactor – Experimental Set Up	99

Figure 31	Detail of Davies Double Surface Condenser (not to scale)	100
Figure 32	150 g/h Single Product 'Small' Scale Fluidised Bed Fast Pyrolysis Reactor – Cooling and Liquid Collection System After Running	101
Figure 33	Liquid Product Condensing System- Commissioning Configuration for Heat Transfer Calculations	103
Figure 34	Liquid Product Condensing System- Experimental Configuration for Heat Transfer Calculations (measurements to nearest mm)	105
Figure 35	Catalyst Configurations Showing Reactor and Cyclone	113
Figure 36	Mesh Supporting Catalyst	116
Figure 37	Mesh Plate Restricting Catalyst Escape	117
Figure 38	Secondary Reactor (not to scale)	118
Figure 39	150 g/h Single Product 'Small' Scale Fluidised Bed Fast Pyrolysis Reactor – Including Secondary Reactor System	119
Figure 40	Organic Yield Results from 150 g/h Apparatus Experiments (1 of 2)	139
Figure 41	Organic Yield Results from 150 g/h Apparatus Experiments (2 of 2)	140
Figure 42	200 g/h Pyrolysis Apparatus of Wulzinger (Wulzinger, 1999)	144
Figure 43	200 g/h Pyrolysis Apparatus with Secondary Reactor of Wulzinger (Wulzinger, 1999)	145
Figure 44	Pyrolysis Liquid Yield Results of Wulzinger at 475°C	146
Figure 45	Comparison of Results of Wulzinger to Those Presented in this Thesis (Salter) at 475°C	148
Figure 46	Pyrolysis Liquid Yield Results from Cooke using HZSM-5 on an Alumina Phosphate Binder	150
Figure 47	Percentage Water Content of Pyrolysis Liquids 1 of 2	153
Figure 48	Percentage Water Content of Pyrolysis Liquids 2 of 2	154
Figure 49	Water Content of Pyrolysis Liquid as found by Wulzinger	157
Figure 50	Example Chemicals Occurring in Non-Catalytic Pyrolysis Liquid at Different Temperatures	163
Figure 51	Hydroxyacetaldehyde Production Changes with Catalyst 1 of 2 Amount Found in HPLC of Main Fraction of Liquid	165
Figure 52	Hydroxyacetaldehyde Production Changes with Catalyst 2 of 2 Amount Found in HPLC of Main Fraction of Liquid	166
Figure 53	Levoglucosan Production Changes with Catalyst 1 of 2 Amount Found in HPLC of Main Fraction of Liquid	167
Figure 54	Levoglucosan Production Changes with Catalyst 2 of 2 Amount Found in HPLC of Main Fraction of Liquid	168
Figure 55	Acetic Acid Production Changes with Catalyst 1 of 2 Amount Found in HPLC of Main Fraction of Liquid	169
Figure 56	Acetic Acid Production Changes with Catalyst 2 of 2 Amount Found in HPLC of Main Fraction of Liquid	170
Figure 57	Pyrolytic Lignin Production Changes with Catalyst 1 of 2 Amount Found in Main Fraction of Liquid	172
Figure 58	Pyrolytic Lignin Production Changes with Catalyst 2 of 2 Amount Found in Main Fraction of Liquid	173
Figure 59	Capillary Viscometer	183
Figure 60	Viscosity Change of Pyrolysis Liquid at 25°C	184
Figure 61	Initial Viscosity of Main Pyrolysis Liquid	185
Figure 62	Pyrolysis Liquid Viscosity Results as found by Wulzinger	188
Figure 63	Variation in Viscosity in Pyrolysis Liquid Stored at 25, 50 and 75°C (Hague, 1998#3)	190

Figure 64	Aston Viscosity Index of Pyrolysis Liquid	192
Figure 65	Aston Viscosity Index, Adjusted for Water Content of Pyrolysis Liquid	193
Figure 66	1-2 kg/h 'Large' Laboratory Scale Fluidised Bed Fast Pyrolysis Reactor	200
Figure 67	Change in Initial and Secondary Viscosity of Large Fluid Slate Bed Pyrolysis Liquid, with Time	204
Figure 68	Change in Aston Viscosity Index and Adjusted Aston Viscosity of Large Fluid Slate Bed Pyrolysis Liquid, with Time	204
Figure 69	Change in Water Content of Large Fluid Slate Bed Pyrolysis Liquid, with Time	205
Figure 70	Aston Viscosity Index and Adjusted Aston Viscosity Index of LFB46 Pyrolysis Liquid after 48 Days	206
Figure 71	Aston Viscosity Index and Adjusted Aston Viscosity Index of LFB46 Pyrolysis Liquid after 87 Days	207
Figure 72	Laboratory Scale Apparatus used by Wulzinger (Wulzinger, 1988)	209
Figure 73	Yield Versus Temperature Results from 1 kg/h Apparatus used by Cooke (Cooke, 1999)	211
Figure 74	Chromatograph Peak Area Minus Blank, Zeolites 2 of 2	259
Figure 75	Chromatograph Peak Area Minus Blank, Clays 1 of 2	260
Figure 76	Chromatograph Peak Area Minus Blank, Clays 2 of 2	260
Figure 77	Chromatograph Peak Area Difference as % of Blank, Zeolites 2 of 2	261
Figure 78	Chromatograph Peak Area Difference as % of Blank, Clays 1 of 2	262
Figure 79	Chromatograph Peak Area Difference as % of Blank, Clays 2 of 2	262
Figure 80	Comparison of the Number of Peaks Resulting from Catalyst Addition to the Pyrolysis Micro-reactor, Clays	263
Figure 81	Average GC Peak Area, Clays	264
Figure 82	Total Sum of Peak Area Difference as % of Blank area for Selected Chemicals, Clays	265
Figure 83	Sum of Peak Area Difference as % of Blank Peak Area for Selected Chemicals (Absolute Values), Clays	266
Figure 84	Average Peak Area Difference as % of Blank Peak Area (Absolute Values), Clays	267
Figure 85	Organic Yield Results from 150 g/h Apparatus (Scale 45 – 75 %)	277
Figure 86	Organic Yield Results from 150 g/h Apparatus (Scale 30 – 65 %)	278
Figure 87	Percentage Water Content of Pyrolysis Liquids 1 of 2	279
Figure 88	Percentage Water Content of Pyrolysis Liquids 2 of 2	280
Figure 89	Example Chemicals Occurring in Pyrolysis Liquid from a Slate Fluid Bed at Different Temperatures	310
Figure 90	Example Chemicals Occurring in Pyrolysis Liquid Y-Zeolite Close-Coupled in the Primary Reactor at Different Temperatures	311
Figure 91	Initial Viscosity of Main Pyrolysis Liquid 1 of 2	316
Figure 92	Initial Viscosity of Main Pyrolysis Liquid 2 of 2	317
Figure 93	Aston Viscosity Index of Pyrolysis Liquid, 1 of 2	324
Figure 94	Aston Viscosity Index of Pyrolysis Liquid, 2 of 2	325
Figure 95	AVI Adjusted for Water Content of Pyrolysis Liquid, 1 of 2	326
Figure 96	AVI Adjusted for Water Content of Pyrolysis Liquid, 2 of 2	327
Figure 97	Initial and Secondary Viscosities of LFB46 Pyrolysis Liquid after 48 Days	329
Figure 98	Initial Viscosity of LFB46 Pyrolysis Liquid after 63 Days	329

Figure 99 Initial and Secondary Viscosities of LFB46 Pyrolysis Liquid after 87 Days 330
Figure 100 Percentage Water Content of LFB46 Pyrolysis Liquid after 48 Days, before and after Stability Testing 331
Figure 101 Percentage Water Content of LFB46 Pyrolysis Liquid after 87 Days, before and after Stability Testing 332
Figure 102 Dimensions of Pyrolysis Liquid Storage Vessel for Large Fluid Bed Liquid to be used for Homogeneity Testing (in mm, not to scale) 334
Figure 103 BDH-Y Zeolite: Fresh 335
Figure 104 BDH-Y Zeolite: 1 Use and Regeneration 335
Figure 105 BDH-Y Zeolite: Coked 335
Figure 106 BDH-Y Zeolite: 1 Hour Regeneration 335
Figure 107 BDH-Y Zeolite: 24 Hour Regeneration 336
Figure 108 Fluid Bed Sand: Coked 336
Figure 109 Fluid Bed Sand: 1 Hour Regeneration 336
Figure 110 Fluid Bed Sand: 24 Hour Regeneration 336
Figure 111 Char from Charpot 337
Figure 112 Expanded Slate: Coked 337
Figure 113 Expanded Slate: 1 Hour Regeneration 337
Figure 114 Expanded Slate: 24 Hour Regeneration 337
Figure 115 Char from Charpot 338
Figure 116 Fluid Bed Sand: Coked 338
Figure 117 Fluid Bed Sand: 1 Hour Regeneration 338
Figure 118 Fluid Bed Sand: 24 Hour Regeneration 338
Figure 119 Char from Charpot 339
Figure 120 Char from Filter Paper 339
Figure 121 Grace ZSM-5 Zeolite 339
Figure 122 Char from Charpot 339
Figure 123 Char from Filter Paper 340
Figure 124 Char from Charpot 340
Figure 125 Char from Filter Paper 340
Figure 126 Fluid Bed Sand and BDH-Y Zeolite 340

1 INTRODUCTION

Fast pyrolysis is a moderate temperature (<650°C) thermal process which produces pyrolysis liquid, often known as bio-oil *(Bridgwater, 1991)*. In this thesis, biomass is used as the feed material in the form of pinewood and beechwood. This liquid can be used as a fuel and because of its aqueous nature, it shall be referred to as 'pyrolysis liquid' rather than 'oil' throughout this work.

This Chapter outlines the purpose of modifying pyrolysis liquid, sets the project objectives and outlines the thesis.

1.1 Pyrolysis Liquid

Pyrolysis liquid is a renewable energy source when made from biomass. Its liquid state is advantageous as it can be stored and transported easily *(Bridgwater, 1996)*. The quality of pyrolysis liquid is important for its intended use as a liquid fuel. The use of pyrolysis liquid has been limited by a belief that the quality is inadequate for commercial applications. Biomass-derived pyrolysis liquid is relatively unstable compared to conventional fossil fuels. It changes physically and chemically with time, temperature and exposure to light and air *(Maggi, 1997)*. Quality influencing parameters, such as water content or homogeneity of the liquid, can be modified, however. This can be done by altering the temperature of the reactor, the vapour residence time in the pyrolysis reactor or other physical characteristics of the fast pyrolysis process, such as the method or conditions of liquid collection *(Bridgwater, 1994)*.

This project intends to improve pyrolysis liquid quality. It is therefore necessary to define 'quality' and find the parameters that effect it. As the pyrolysis liquid is so chemically complex, defining the quality in terms of purity or concentration of certain components is difficult. It is however possible to identify physical attributes that are desirable for the designated end use of the product liquid, in this case as a fuel. The most important ones are:

1) Viscosity - A sufficiently low viscosity is needed to facilitate pumping and handling of the liquid or injection through a diesel engine nozzle. A viscosity of less than 20 cS is required to go through an engine *(Leech, 1997)*.
2) Homogeneity - A single-phase liquid is needed so one set of characteristics can be defined for a sample. This would negate the need to agitate the pyrolysis liquid and add 5% methanol before use, as is currently the case.
3) Heating value - The higher the heating value the higher the economic value of the pyrolysis liquid. Pyrolysis liquid has a relatively low heating value around 16 – 18 MJ/kg compared to oil-derived fuels with heating values around 42 – 44 MJ/kg *(Diebold, 1997#2)*. It is inversely proportional to water content. However higher water contents give lower viscosity liquids *(Tiplady, 1996)*.
4) Water content - High water content causes phase separation and reduces the heating value of the pyrolysis liquid.
5) pH value - The acidity of the liquid should not hinder the handling of the material. The more neutral the liquid, the less likely the need for specialist storage drum material, pipework and vessels, personal protective clothing or an expensive hazard accident plan. Un-modified pyrolysis liquid is acidic with a pH of about 3.
6) Instability due to changes in physical properties - This is an important consideration when storing pyrolysis liquid. The age of the liquid should not impact its usefulness. The viscosity of the liquid increases during storage, due to chemical reactions and polymerisation. Phase separation can also occur in high water content liquids that are stored for long periods. Phase separation is also common in pyrolysis liquid greater than around 40-50 % water. If pyrolysis liquid is stored open to the atmosphere and in the light, it can become a solid mass.

   Pyrolysis liquids have a reduced detrimental change if stored in sealed containers at reduced temperatures, preferably under an inert atmosphere *(Oasmaa, 1996)*. Storage under inert gases prevents the absorption of water vapour and reactions occurring between the residual air and the pyrolysis mixture. This, however, increases the complexities of handling and storing the pyrolysis liquid. A solution that changes the liquid itself should therefore be sought.

Pyrolysis liquids contain a large number of different components in small amounts. They are the degradation products of the biomass feed (see Sections 2.1 and 2.1.2 for

more details). Isolation and modification of the main pyrolysis liquid components has been studied *(Hanniff, 1987; Horne, 1992; Katikaneni, 1997)*, but the interaction between all the chemicals contained within the liquid and their modification *in situ* is important. One method to modify the composition of the whole liquid is catalytic vapour phase treatment *(Bridgwater, 1994)*. It is this alternative that has been investigated in the work presented here. (Other methods are discussed in Section 2.3 'Modification of Pyrolysis Liquid'). A promising catalyst has been sought for inclusion in the pyrolysis process, to improve the pyrolysis liquid characteristics. Catalytic processing will be used to reduce the problems of high viscosity, non-homogeneity and instability mentioned above.

1.2 Objectives

The objective of the work presented in this thesis is to explore catalytic modification of the fast pyrolysis process and therefore the pyrolysis liquids it produces. This is to improve the liquid properties and characteristics and thus make it more amenable to utilisation. Whilst describing pyrolysis liquid in Section 1.1, it was shown that it can have a high viscosity, is acidic, unstable and can separate into two phases. These detrimental attributes should be reduced whilst not lowering the heating value below which pyrolysis liquid can not be used as a commercial fuel.

A method of assessing the quality of the pyrolysis liquid is necessarily a secondary objective. This project aims to find the most appropriate parameters and use them to define quality as well as to improve the liquid quality based on that definition. The chosen parameters should therefore be easy to identify and measure, and improvements in them achievable, to allow future use of the quality definition.

The instability primarily manifests itself as an increase in viscosity with time, particularly when the pyrolysis liquid is exposed to heat, light or air. This work therefore aims to address this problem. The reduction of initial pyrolysis liquid viscosity and an improvement in liquid stability will be of particular interest. For this reason, the physical characteristic of the *change* in viscosity with time and/or temperature was chosen. The pyrolysis liquid viscosity changes with time and can

eventually lead to the liquid separating into two phases. This process is complex and not well understood. It is thought to occur by condensation polymerisation.

How the catalysts should be incorporated into the pyrolysis process will also be examined. The resultant pyrolysis liquids from the following configurations of catalyst incorporation will be analysed (see Section 2.5 for more details):

1) Catalyst co-fed with the biomass feed into the pyrolysis process
2) A fluid bed of catalyst in the primary pyrolysis reactor
3) A bed of catalyst close coupled in the pyrolysis process within the primary reactor
4) Addition of a secondary reactor close coupled in the pyrolysis process, that is fed with the vapours from the primary reactor.

Changes in the chemical composition of the modified pyrolysis liquid compared to the raw, un-modified pyrolysis liquid also need to be observed. This will develop an understanding of the chemical source of the instability. The water content of the pyrolysis liquid is important as it influences viscosity (see Chapter 7).

The objectives can be summarised as finding answers to the following questions:

A) What is the best catalyst to produce the best quality pyrolysis liquid?
B) How is 'best quality pyrolysis liquid' defined?
C) Where is the best place in the pyrolysis process to incorporate catalysts?
D) What chemicals within the pyrolysis liquid influence quality?

1.3 Structure of Thesis

The following topics and hypotheses are contained within the Chapters as set out below:

Chapter 2 The history and development of pyrolysis and the upgrading of the pyrolysis liquids, through a review of literature. The hypothesis that catalyst pore size influences the stability of the resultant catalytically-produced pyrolysis liquid is presented here. The relationship between the catalyst pore size and the pyrolysis liquid quality is investigated

throughout the thesis and is initiated in Section 2.4.4 'Zeolite Catalysts' and Section 2.4.5 'Clay Catalysts'.

Chapter 3 Micro-reactor screening of potential catalysts to upgrade pyrolysis liquid.

Chapter 4 Experimental work using small-scale apparatus to produce pyrolysis liquid with and without catalysts.

Chapter 5 Chemical analysis of the liquid pyrolysis product from the experiments described in Chapter 4. Included here is water testing and HPLC analysis.

Chapter 6 Physical analysis of the liquid pyrolysis product from the experiments described in Chapter 4. Included here is viscosity and acidity testing.

Chapter 7 Defines liquid quality using stability testing. The 'Viscosity Index' is used to grade pyrolysis liquids. The hypothesis that the viscosity of pyrolysis liquid decreases with an increased water content of the pyrolysis liquid will be investigated in Chapter 7.

Chapter 8 The scaling up of the process to use 1-3 kg/h apparatus.

Chapter 9 Scanning electron microscope (SEM) techniques are used in the analysis of the catalyst surfaces.

Chapter 10 Conclusions drawn from Chapters 3 to 9 and compared to work described in Chapter 2.

Chapter 11 Recommendations following work on this project.

2 BACKGROUND TO PYROLYSIS LIQUID MODIFICATION

The fossil fuels petroleum, natural gas and coal are currently the industrial world's principal sources of fuel and organic chemicals. However, the environmental effects of these resources are well known and include carbon dioxide emissions contributing to 'the greenhouse effect' and sulphur emissions, which are known to cause 'acid rain'. The search for alternative fuel and energy sources is becoming increasingly intense as petroleum demand increases and environmental awareness intensifies *(Sharma, 1991)*. The pyrolysis of biomass is one source of 'green energy' that is competing for this new market. Being produced from biomass, pyrolysis liquid is a sustainable energy type, unlike fossil fuels. It competes with hydroelectric, wind, geothermal, tidal, solar and other energy production methods. However, biomass is the only renewable source of carbon and the intention is that it will also meet our future organic chemical needs *(Goldstein, 1981)*.

2.1 Biomass Pyrolysis

Pyrolysis can be described as the thermal degradation of biomass in the absence of an oxidising agent or with insufficient oxygen to facilitate full gasification *(Bitowft, 1989)*. At moderate temperatures (400 to 800°C) and around atmospheric pressure (up to 3 bar), pyrolysis liquid, often known as 'bio-oil', is produced *(Grassi, 1992)*. The term 'fast pyrolysis', also known as 'flash pyrolysis', is defined as pyrolysis that employs short vapour residence times (less than 5 seconds and normally 0.2 to 2 seconds) in the heated zone of the apparatus and high reaction rates. (Details of the apparatus used can be found in Chapter 4.) As a consequence, fast pyrolysis produces high to very high yields of liquid (50 to 80 wt%, based on feed). The feed material is rapidly converted to vaporised products, which are immediately quenched in order to avoid secondary polymerisation reactions and thus maximise the yield of liquids and minimise the production of char and gaseous products *(Bridgwater, 1994)*.

Fast pyrolysis to produce pyrolysis liquid can be achieved in several ways, including 'ablative pyrolysis' *(Peacocke, 1991)*; and 'rotating cone pyrolysis' *(Venderbosch, 1997)*. Here the fluid bed process known as the 'Waterloo Fast Pyrolysis Process' *(Scott, 1984, 1987)* will solely be considered. This thesis will concentrate on this

process as the results can be compared to other catalytic modification experiments and the engineering complexities involved with incorporating catalyst to different apparatus is beyond the scope of this project. The scope of the project is constrained by the European Commission contract (contract JOR CT95-0081) for which it was commissioned. The Waterloo Fast Pyrolysis Process has therefore been employed to produce pyrolysis liquid upon which the conclusions presented here are based. The criteria, upon which this process was chosen, are:

a) Low cost - Low relative capital cost due to inexpensive feeding system and a reactor that needs only to withstand atmospheric pressures *(Toft, 1996)*.
b) High liquid yield - The process is designed to maximise liquid to around 70 wt% wet oil on a dry wood basis, as mentioned above.
c) Minimal technical risk - Relatively simple process, proven over many years of use *(Bridgwater, 1991)*.
d) A high feed-to-product energy efficiency - Heating value of 16 to 30 MJ/kg *(Bridgwater, 1991)* shows high energy efficiency based on high yields.
e) Fluid bed fast pyrolysis also has the potential to produce a liquid of a standard to use as a fuel *(Leech, 1997)*.

The intention of this project is not to review the process of pyrolysis, the equipment or operation, as excellent reviews already exists *(Bridgwater, 1991, Diebold, 1997#2; Cooke, 1999)*.

2.1.1 Pyrolysis of Wood

Although many feedstocks can be used for pyrolysis, the most common is woody biomass such as poplar, pinewood, fir, eucalyptus, beechwood and aspen *(Milne, 1997)*. Pinewood and beechwood have been chosen for this project (see Section 4.2).

To be able to start assessing the quality of the fast pyrolysis product, the feed to the process should be understood. Biomass, in this case wood, is an abundant and renewable commodity. It is formed through photosynthesis using chlorophyll and 470 kJ/mole of energy in the form of solar radiation, as in Equation 1 *(Sharma, 1991)*. It is these chemicals that will therefore go on to be the main constituents in pyrolysis liquid.

Ultimately, when the pyrolysis liquid is used as a fuel, the chemicals are converted back to their original form (carbon dioxide and water). This releases the energy from solar radiation minus any energy lost in changing the wood to pyrolysis liquid.

$$CO_2 + H_2O + \text{solar radiation} \rightarrow (CH_2O) + O_2$$

Equation 1

Wood can be categorised in two main groups - softwoods and hardwoods. Hardwood trees are usually broad-leaved and deciduous. Softwoods are normally coniferous or evergreen. Although each species of wood differs chemically, the main constituents are cellulose and hemicellulose (70 – 90 %) and the remainder is lignin. Oxygenated hydrocarbons arise from the degradation of these components *(Bridgwater, 1994)*. Pyrolysis results in the depolymerisation of these wood chemicals through free radical or heterolytic depolymerisation *(Rejai, 1992)*.

Cellulose, shown in Figure 1, has the elemental formula $(C_6H_{10}O_5)_n$. It is a long chain, uniform, glucose polymer with between 700 and 2000 repeating glucopyranose units. The main functional group is the hydroxyl group *(Aabloo, 1995)*.

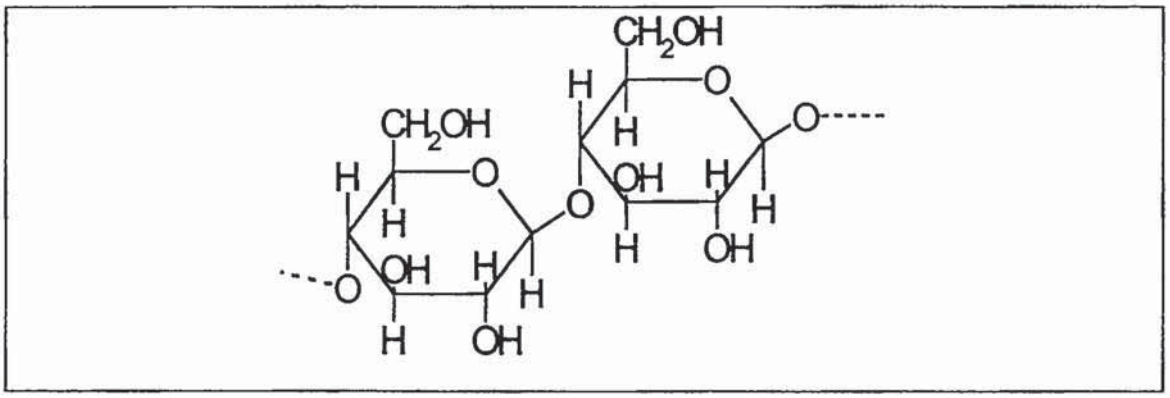

Figure 1 Two Monomer Repeat Units of Long Chain Cellulose

Hemicellulose is much less chemically specific. It has a more branched structure than cellulose and has a mixture of five and six membered carbon rings *(Meier, 1997)*. For pinewood, 65 to 80 % of hemicellulose is galactoglucomannans, which are partially substituted by acetyl groups, and 20 to 35 % of the hemicellulose is arabinoglucuronoxylans *(Theander, 1985)*. Lignin has the empirical formula $C_{10}H_{11}O_2$

and is made up of aromatic rings containing units with three-dimensional, cross-linked, alkoxylated phenolic polymers, as shown in Figure 3 'The Repeat Units of Beech Wood Lignin (Meier, 1997)'. Beech wood is the main wood type used in this project. It can be hydroxyl, guaiacyl or syringyl in type (Figure 2). Lignin, being aromatic, is an important source of useful chemicals *(Sharma, 1991)*. All these constituent chemicals of wood, and their degradation products, should therefore be looked for when examining the chemical composition of pyrolysis liquid.

Figure 2 Lignin Monomers (Meier, 1997)

Figure 3 ***The Repeat Units of Beech Wood Lignin (Meier, 1997)***

(Numbers indicate approximate relative percentage of monomer)

The main pyrolysis reactions are depolymerisation and fragmentation of cellulose and hemicellulose and depolymerisation of lignin. In fast pyrolysis in excess of 450°C depolymerisation and fragmentation are competing pathways. The alkaline inorganic constituents present in biomass promote the fragmentation reaction *(Graham, 1984)*. Depolymerisation involves splitting the polymer into the monomer repeat units, usually breaking a carbon-oxygen bond. It has been hypothesised that the reaction starts with an electron shift between the monomers. Levoglucosan is a major product *(Richards, 1994)*. Fragmentation is the removal of side chains, wholly or in part. It is thought to use an external hydroxyl group. Hydroxyacetaldehyde is a major product and glyoxal, acetol, ethylene glycol, formic acid, methyl glyoxal are also produced *(Scott, 1981)*. The structures of these are shown in Table 1. These products will therefore be tested for in pyrolysis liquid produced in this project (See Section 5). The structures presented in

Table 1 can also be compared to Figure 1 to Figure 3 to show how the raw material becomes the products.

Table 1 Structures of Chemical Products of Wood Pyrolysis

Chemical	Chemical Diameter (Å) Min [a]	Max [b]	Structure
Levoglucosan $C_6H_{10}O_5$	CH_4 3.80	Benzene + ½O_2 4.57	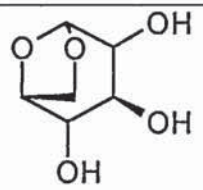
Hydroxyacetaldehyde $C_2H_4O_2$	CH_4 + ½O_2 5.59	2 × CH_4 7.60	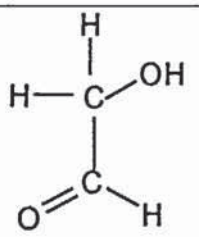
Glyoxal $C_2H_2O_2$	CH_4 + ½O_2 5.59	2 × CH_4 7.60	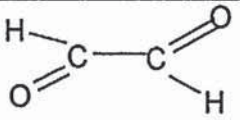
Acetol CH_3COCH_2OH	CH_4 + ½O_2 5.59	3 × CH_4 11.4	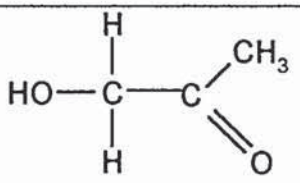
Ethylene glycol $HOCH_2CH_2OH$	CH_4 + ½O_2 5.59	2 × CH_4 7.60	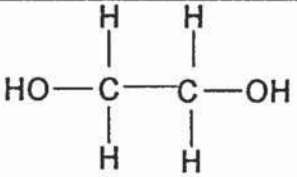
Formic acid HCO_2H	CH_4 + ½O_2 5.59	CH_4 + ½O_2 5.59	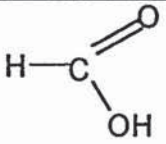
Methyl glyoxal $C_2HO_2CH_3$	CH_4 + ½O_2 5.59	3 × CH_4 11.5	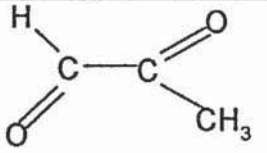

Notes: (a) Diameter of smallest branch (see Section 2.1.2).

(b) Diameter based on main chain of chemical (see Section 2.1.2).

2.1.2 Calculation of Chemical Diameter

It is intended that catalysts be used to modify the chemicals in Table 1. For this reason, the size of the chemicals should be known. This will ascertain if the chemicals will wholly or partly fit into the pores of the chosen catalyst, or alternatively only be able to access the catalytic sites on the external surface of the catalyst, if any exist. Catalyst pores are important as they better control the of size and nature of product molecules as less branched and more molecules that are simple in nature, only, may exit them.

It was not possible to find published estimates or measurements of the chemical diameter. The diameters have therefore been estimated using 'Van der Waal's Excluded Volume and Molecular Diameter Theory' *(Barrow, 1988)*. Equating the structure of the chemical to the size of the components in Table 2 is an extremely rough guide to the chemical diameter. It will indicate if the chemical is much larger or much smaller than the pore diameter, but should not be used when they are a similar size.

To estimate the size of a compound with benzene, the bond length of carbon to carbon bonds in benzene was used. It is 1.39 Å and by trigonometry gives a benzene diameter of 2.78 Å. The results of this crude analysis are shown in Table 1. It shows that many of the chemical products of wood pyrolysis will not fit easily into a 5 Å pore. Lignin and cellulose, the constituents of wood, would not fit wholly into a pore of that size.

Table 2 ***Molecular Size Based on Van der Waal's Second-Virial-Coefficient Data (Barrow, 1988)***

2.2 The Nature of Pyrolysis Liquid

The intention of this project is to improve pyrolysis liquid. The nature of unmodified liquid is therefore reviewed here, so the base upon which to build is known.

One of the intended uses of pyrolysis liquid derived from wood is as a fuel. It would therefore compete with, or substitute, petroleum based liquid fuel products. Pyrolysis liquid is referred to as a carbon dioxide neutral fuel, on combustion only releasing carbon dioxide approximately equal to that taken up by growing the biomass *(Sharma, 1991)*. The fuel has very low sulphur levels, which is beneficial as sulphur present in combustion gases contributes to acid rain. It also does not contain vanadium and nickel *(Rupp, 1991)*. It can therefore be considered 'environmentally friendly' in terms of carbon dioxide recycling and sulphur emissions.

In appearance, pyrolysis liquid is a brown-black, viscous, fuel-oil-like liquid. It is immiscible with conventional hydrocarbon fuels. The water content is up to 30 %, the heating value 15 to 20 MJ/kg and the oxygen content is high, up to 30 %. Pyrolysis liquid has a low pH (around pH3), making it corrosive. Polypropylene and stainless steel should be used for storage and handling *(Bridgwater, 1992)*. It is physically and chemically unstable *(Rupp, 1991; Oasamaa, 1996)*. Thermal deterioration of liquid occurs above 100°C.

Pyrolysis liquid can be compared to petroleum-based products. This is done in Table 3. Three petroleum products have been chosen to show the range of physical properties. The concept of classification of pyrolysis liquid was proposed by Diebold, *(Diebold, 1997)*, but as yet, no ASTM (American Society for Testing and Materials) Boiling Point or Cetane number have been found for pyrolysis liquid. Compared to petroleum fuels, pyrolysis liquid is denser, more viscous, less easy to handle and contains more ash, which can deposit in an engine. These are all poorer qualities than the petroleum fractions *(Rupp, 1991)*. These negative attributes should be considered when defining how the quality of pyrolysis liquid should be improved.

Table 3 Physical Properties of Petroleum and Pyrolysis Liquids

	Motor Gasoline[a]	No. 2 Petroleum Fuel[a]	No. 6 Petroleum Fuel[a]	Pyrolysis Liquid[b]
Fuel Type	Transport fuel	General purpose heating in burners	Heavy oil requiring pre-heating for burning and handling	Static application fuel oil
Density (kg/m^3) @15°C	0.712 - 0.748	0.806 - 0.922	0.934 - 1.064	0.826[c]
Kinematic Viscosity (mm^2/s)	0.4 - 0.6 @38°C	2.0 - 3.6 @38°C 1.9 - 3.4 @40°C	200 - 2000 @38°C	233 @25°C 134 @40°C[d]
Pour Point (°C)	-	-6	-	-23
ASTM Boiling Range (°C)	40 - 225	170 - 145	170 - 500	-
Ash Content % by weight	0	0	0.01 - 0.5	0.1

Notes:
(a) Figures taken from *(Perry, 1984#1)*
(b) Figures taken from *(Bridgwater, 1998)*
(c) Although this is quoted, a number in the region of 1.2 kg/m^3 is thought to be more appropriate *(Solantausta, 1994; Bridgwater, 1991)*.
(d) At 88°C the dynamic viscosity is 230 cP *(Rupp, 1991)*.

Pyrolysis liquid can be exploited in several ways other than as, or in conjunction with, a fuel. These include: as a raw material for speciality chemical production, such as levoglucosan; the glycolaldehyde dimer, hydroxyacetaldehyde; various sugars, as well as some commodity chemicals such as acetic acid, formic acid, methanol and ethanol *(Radlein, 1997)*. The speciality chemicals levoglucosan and hydroxyacetaldehyde are generally present in the highest yields (concentrations of 2-10 wt%). Levoglucosan is an anhydro-sugar with potential uses as a biodegradable polymer or plastic; high value speciality chemicals precursor or low calorie food filler *(Longley, 1994)*. Hydroxyacetaldehyde can be used as a food flavouring and colouring agent and also has possible uses as a tanning agent. It is currently marketed as the major component in

aqueous smoke (or 'barbecue') flavourings *(Stradal, 1996)*. In addition, pyrolysis liquid can be used as a phenol base for resin adhesives *(Diebold, 1998)*.

The end use of the liquid considered here is as a liquid fuel. The main attraction of pyrolysis liquid rather than burning solid biomass is the transportable nature of the liquid. It approximates to the biomass it came from in elemental composition, but has a high energy density and the advantage of de-coupling the conversion and utilisation processes *(Bridgwater, 1994)*.

The functional groups in fast pyrolysis liquids are shown in Table 4 *(Meier, 1997)*. These correspond to the chemicals found in the raw material, wood, as described in Section 2.1.1. When modifying pyrolysis liquid, it is these functional groups that should be considered.

Table 4 Functional Groups in Fast Pyrolysis Liquid

Group Name	**Formula**
Aliphatic hydroxyl	R-OH
Phenolic hydroxyl	Ar-OH
Carboxyl	R-C(=O)-OH
Carbonyl	R-C(=O)-H R-C(=O)-R
Alkenyl	Ar-$(C)_n$-C=C-R

where: R represents a hydrocarbon group
Ar represents an aromatic hydrocarbon group
$(C)_n$ represents a carbon chain with n carbon members

2.3 Modification of Pyrolysis Liquid

As was alluded to in Section 2.1.2, pyrolysis liquid has certain properties that, once improved, would make it more marketable and usable. These properties are described in the Introduction, Section 1, and are: viscosity, homogeneity, heating value, water content and instability.

There are several catalytic and chemical approaches to improving the quality of pyrolysis liquid. They are described in this Section. The nature of the catalysts used will be described in Section 2.4. The methods of applying catalytic and chemical modification are:

1) Modification of the pyrolysis process by addition of catalysts before vapour condensation.
2) Modification of the liquid product by catalytic hydrotreating.
3) Chemical treatment or solvent addition to the pyrolysis liquid product.

These processes are categorised in Figure 4 where mild catalytic modification of pyrolysis vapours, the process explored in this thesis, is highlighted in red. There are no arrows exiting the 'liquid re-vaporisation' box as only 35 % of the pyrolysis liquid can be re-vaporised, which is in itself 75 % of the biomass feed.

There is also an 'internal catalytic effect'. Most biomass contains natural salts in the ash portion that will influence the décomposition products. Since these salts are not easily removed, this catalytic effect becomes part of the simple thermal degradation *(Bridgwater, 1994)*. Inorganic compounds such as potassium, calcium, sodium, silicon, phosphorus and chlorine are the main constituents of the ash in biomass. They particularly catalyse char-forming reactions *(Agblevor, 1996)*. This by-product char may itself have a catalytic effect and influence the biomass decomposition products during pyrolysis.

The processes listed above are now reviewed in Sections 2.3.1 to 2.3.3.

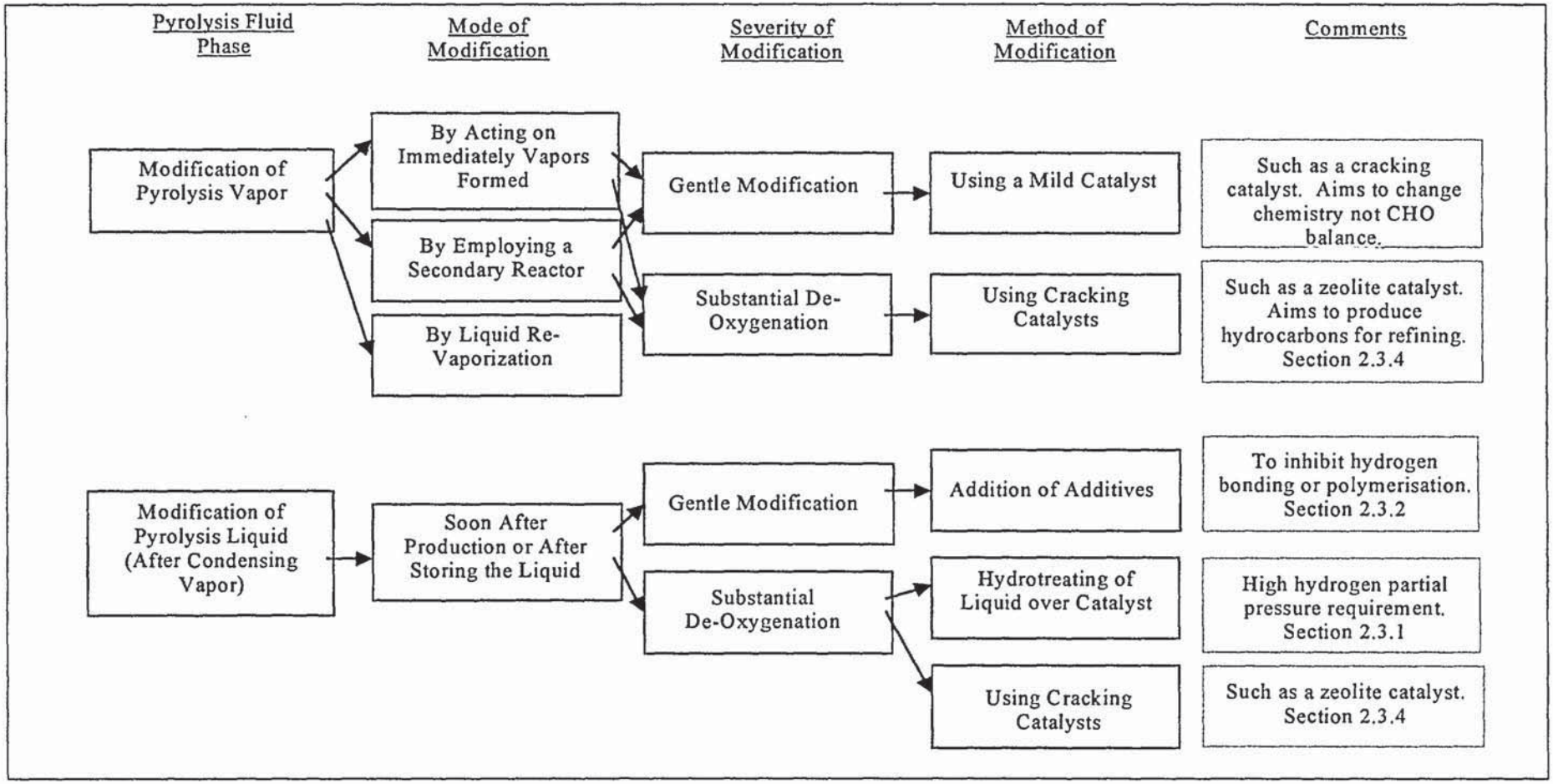

Figure 4 Description of Types of Fast Pyrolysis Fluid Modification for Liquid Fuel Production

2.3.1 Hydrotreating

Hydrotreating is performed on the pyrolysis liquid to form a naphtha-type product by de-oxygenating and creating water, using hydrogen. The product is analogous to a diesel fuel in the boiling range 210 – 410°C *(Sharma, 1991)*. The process of upgrading by hydrotreatment is based on de-sulphurisation technology established in the petroleum industry. It is done at high pressure (70 to 200 bars) to provide a high hydrogen partial pressure. Full hydrotreating involves greater than 99.5 % de-oxygenation and results in a stable water-white product that is miscible with fossil fuels and can be blended or upgraded in a refinery to produce diesel *(Rupp, 1991; Bridgwater, 1994)*. An example of this is the product of hydrotreating pyrolysis liquid being fed into the product stream of the petroleum hydrocracker *(Baldauf, 1997)*. Water readily separates from the hydrocarbon product and is relatively clean. The water also strips out the alkali metals present which is advantageous *(Bridgwater, 1998)*.

The effect of the hydrogen on the transformation of petroleum products can be roughly divided into two processes: hydrotreating and hydro-cracking. In the first case only the carbon-heteroatom bonds are broken and some hydrogenation occurs. In the second case, carbon-carbon bonds are broken *(Churin, 1991)*. The conceptual de-oxygenation reaction is shown in Equation 2 *(Bridgwater, 1998)*.

$$C_6H_8O_4 + 6H_2 \rightarrow 6CH_2 + 4H_2O$$

Equation 2

where $C_6H_8O_4$ is pyrolysis liquid and CH_2 is a naphtha equivalent.

The process typically uses two temperature zones: 250 to 275°C followed by 350 to 400°C. The first temperature zone is for initial stabilisation before the hydrotreating process and is essential to avoid polymerisation *(Churin, 1998; Rupp, 1991)*. Conventional hydrotreating catalysts are used, such as cobalt or nickel molybdenum in oxide or sulphided forms on silica or alumina supports *(Bridgwater, 1994)*. The oxide forms have proved to be less active than sulphided catalyst *(Laurent, 1992)*, but have avoided the problems of product contamination from sulphur. No system has been thoroughly tested for continuous use, but the sulphided nickel molybdenum system has been run for eight days where a substantial deterioration in activity was found. This

was attributed to the attack of water on the catalyst support and a reduction in surface area due to agglomeration *(Rupp, 1991)*. Noble metal supported catalysts are not used as they would be readily deactivated through chemical and physio-chemical processes such as poisoning, sintering and fouling *(Churin, 1998)*.

Batch tests are not very representative for scale-up to commercial scale. Tests in small continuous operating bench scale units were successful with a model compound, but less successful with model feedstocks *(Baldauf, 1997)*.

The hydrotreating process is decoupled from the pyrolysis process, but the economics of using large quantities of high pressure hydrogen (700 l/kg pyrolysis liquid) *(Elliott, 1998)*, together with the high capital cost of a hydrotreating process, prohibit its current commercial exploitation. An alternative to 99 % or more de-oxygenation is to *partially* hydrotreat pyrolysis liquid. This method reduces the hydrogen consumption by 60 %, but the product is undefined *(Bridgwater, 1994)*. Some exploratory work has been done on model compounds *(Churin, 1998)*.

Hydrotreating has been the most fully explored of the upgrading methods. Hydrotreating of biomass derived pyrolysis liquid has been experimented with in the following institutions, Table 5. This table shows the international nature of the work by governmental, university and commercial institutions. Hydrotreatment of model compounds as well as pyrolysis liquid has been explored using catalysts and technology to mimic petroleum refining.

Table 5 Main Institutions Involved with Hydrotreating Pyrolysis Liquid

Institution	Comments	Reference
Battelle Pacific Northwest Laboratory, USA	Sulphided CoMo, NiMo and Y-zeolite with liquefaction and pyrolysis liquids. Fixed bed upflow reactor.	*Elliott, 1987; Elliott, 1988; Baker, 1988*
DMT Fuel Technology, Germany	NiMo with coal liquefaction liquids and biomass pyrolysis liquids.	*Kaiser, 1997*
Imperial College, UK	Hydropyrolysis of wood and lignin.	*Güell, 1994*
Institute for Wood Chemistry, Germany	Hydroliquifaction of wood suspended in oil with C, Mo, Cr, Ni, Pd, Fe in batch autoclave	*Meier, 1988*
National Renewable Energy Laboratory, USA	Sulphided Mo, NiMo with 4-propylguaiacol lignin model compound in trickle-bed reactor.	*Ratcliff, 1998*
University of Compiegne, France	Sulphided CoMo, NiMo and Fe with solvolysis oil and tetralin.	*Elamin, 1994*
University of Chalmers, Sweden	Sulphided NiMo with reduced sodium liquefaction oil in downflow trickle bed.	*Gevert, 1987, 1994*
University of Louvain (UCL), Belgium	Sulphided CoMo, Ni Mo with pyrolysis liquid and tetrahydronaphthalene or carbonyl, carboxylic and guaiacyl in batch autoclave.	*Churin, 1998; 1991; Laurent; 1994#1; #2*
University of Sassari, Italy	Equipment for catalytic continuous bench scale trickle bed reactor for pyrolysis liquids.	*Conti, 1994*
University of Saskatchewan, Canada	CoMo, Ni Mo and Pt with pyrolysis liquid in fixed and trickle bed reactor.	*Sharma, 1991; 1991#2*
Veba Oel, Germany	Commercial catalyst with organic phase of pyrolysis liquid in continuous upflow or downflow reactor.	*Rupp, 1991; Baldauf, 1997*

2.3.1.1 Summary of Hydrotreating Upgrading

Hydrotreating for petroleum refining is widely used commercially. For biomass processing however, it has not progressed commercially because of problems associated with feeding solids into a high pressure reactor, the high cost of large high pressure equipment and the energy needed for gas compression. The large hydrogen requirement (~700 l/kg pyrolysis liquid *(Bridgwater, 1996)*) has, in part, been solved by Marquevich *et al (Marquevich, 1998)*. Hydrogen is produced by catalytic steam reforming of residual streams from biomass conversion. Model compounds such as xylose, glucose

and hemicellulose have been used. Hydrogen yields of 88 % were achieved, but the technique, however, needs considerable refinement.

This project objective is to improve the pyrolysis liquid quality by economic, mild modification of the pyrolysis vapours. Therefore, hydrotreating will not be considered for experimentation.

2.3.2 Chemical Treatment of the Liquid Product

Raw pyrolysis liquid contains a complex mixture of chemicals. Identification and manipulation of those functional groups that create the dynamic nature of the liquid, provides an alternative route to stabilising the liquid after its production. This can be done using selectively reactive chemical reagents.

The instability of pyrolysis liquids is thought to be due to the high quantity of oxygen containing compounds, specifically the chemically reactive carbonyl functions typical of aldehyde and ketone compounds *(Laurent, 1994#2)*. While heating or in air these carbonyls are thought to facilitate polymerisation reactions that yield an overall increase in the viscosity and decrease in the stability of the liquid.

The greatest changes in the viscosity of the pyrolysis liquid occur during the first 2-3 days after liquid production *(Hague, 1998)*. One possible approach to prevent these viscosity increases and stabilise these liquids is by the addition of chemical modifiers to the fresh pyrolysis liquid as it is produced. This has been done by Weekes *(Weekes, 1998)*. The main findings were that phenol was the most favourable chemical in terms of pyrolysis liquid stability and the addition of glycerol, which is a straight chain compound with three alcohol groups, produced a more stable liquid than using simple low series straight chain alcohols. The addition of methanol has previously also been investigated by Diebold, where a stabilising effect was shown *(Diebold, 1997#3)*.

The major problem in upgrading pyrolytic liquids is their poor stability leading to polymerisation of some compounds at high temperatures. Hydrogen donor solvents such as tetralin have been found to improve the stability to some extent, leading to a reduction in coking of the catalyst during hydrotreating *(Sharma, 1991)*. The hydrogen

donor solvent is used to stabilise free radicals by providing a hydrogen source and therefore reducing the tendency of radicals to react with each other to give higher-molecular-weight materials, including coke *(Churin, 1991)*.

The work on this topic is not extensive and although initial results are promising, chemical treatment of the liquid product is considered to be outside the scope of the experimental work presented here.

2.3.3 Catalytic Cracking

Catalytic cracking is extensively used in petroleum refining to improve the Octane number (fuel quality) predominantly of the kerosene cut ($C_{11} - C_{14}$). These long chains are 'cracked' into smaller molecules on a silica-alumina catalyst at temperatures of 400 to 500°C. The major products are light hydrocarbons in the $C_3 - C_5$ range. These small hydrocarbons are then catalytically recombined to yield useful, highly branched $C_7 - C_{10}$ alkanes *(McMurry, 1992)*. See also Section 2.4.3.

This chemistry can be applied to pyrolysis vapours or liquid. Long molecular chains can intertwine and become highly polymeric. Reducing the length of these chains may improve the liquid quality as low molecular weight compounds are generally less viscous than high molecular weight compounds.

Two main groups of catalysts have been used to perform catalytic cracking on pyrolysis vapours: zeolites and clay catalysts. They are both discussed below.

2.3.3.1 Zeolite Catalytic Cracking

The definition of a zeolite and a description of its nature can be found in Section 2.4.4. The process of 'cracking' pyrolysis liquid using this catalyst type is outlined here.

The zeolite catalytic cracking and reforming process is performed at atmospheric pressure to form an aromatic product. Zeolites, particularly ZSM-5, have been investigated in conjunction with biomass upgrading because of their use in petroleum refining (see Section 2.4.4). The temperature of operation is in the region preferred for

optimum oil yields: 450 to 600°C and hourly space velocities of around 2 h^{-1}. The overall stoichiometrics of vapour-phase zeolite cracking of biomass are shown in Equation 3.

$$C_6H_8O_4 \rightarrow 4.6CH_{1.2} + 1.4CO_2 + 1.2H_2O$$

Equation 3

This is a hydrogen-limited reaction with the aromatic product being limited by the availability of hydrogen for aromatics and water formation. Oxygen is rejected as both CO_2 and H_2O. It is suggested that cracking occurs on the catalyst 'surface' and that aromatics are synthesised in the catalyst pores *(Bridgwater, 1994)*.

The zeolite catalyst ZSM-5 was originally developed by Mobil to convert methanol to gasoline *(Chen, 1988)*. It was then tried with cellulose pyrolysis, but there was concern over the problems of coking *(Scahill, 1988)*. Using HZSM-5 (the protonated form of ZSM-5), simultaneous dehydration and decarboxylation occurs in the absence of any reducing gas. The product is in the gasoline boiling range (25 – 200°C) *(Sharma, 1991)* and is of a higher octane than that produced from hydrotreating because of the high yields of aromatics (benzene, toluene and xylene). The mechanism is not simple, in that carbon is deposited on the catalyst, which has to be burned off, as in regeneration in a fluidised catalytic cracking unit. It is however, in principle, possible to modify the zeolite into a bi-functional or multi-functional catalyst to be more selective towards desired products *(Bridgwater, 1992)*. Further details of specific zeolite catalysts can be found in Section 2.4.4.

Catalysts can be integrated in the pyrolysis process either in the main reactor or in a secondary close-coupled reactor *(Rejai, 1992)*. Alternatively catalytic reactions can be decoupled from the pyrolysis process by re-vaporising pyrolysis liquid after production *(Sharma, 1991; Horne, 1994)*. The disadvantage of this is that it allows secondary polymerisation reactions to occur during physical condensation, before the product is modified catalytically. It is also thermally inefficient and increases equipment complexity and cost. Using re-vaporised pyrolysis liquid means that the catalytic action is performed on different chemicals to those immediately created during pyrolysis

before condensation. Work on the re-vaporised liquid will therefore be only an indication of the effect of catalysts on pyrolysis liquid upgrading.

Zeolite cracking of pyrolysis liquid started with the work at Mobil in the 1980's. The following institutions have contributed towards its progression, Table 6. This table shows that ZSM-5 and its hydrogen form, HZSM-5, have been the main focuses of experimentation. Model compounds or re-vaporised pyrolysis liquids have generally been used. The disadvantage of this is that one of the main benefits of catalytic upgrading is not exploited - that it is not necessary to de-couple upgrading from the pyrolysis process.

At the University of Sakatchewan it was found that the nature of the liquid product can be dramatically altered by changing the characteristics and functionality of the catalyst used. For example the products range from mostly aromatic hydrocarbons for zeolite type catalysts (such as HZSM-5) to mostly aliphatic hydrocarbons for amorphous catalysts (such as silica-alumina) *(Katikaneni, 1997).*

Table 6 ***Main Institutions Involved with Catalytic Cracking of Re-Vaporised Biomass Derived Liquids or Model Compounds***

Institution	Comments	Reference
CPERI, Greece	Phenol and methanol in fixed bed reactor with metal sulphates on γ-alumina.	*Samolada, 1995*
INRS (National Institute for Scientific Research), Canada	Model compounds contacted with ZSM-5.	*Hanniff, 1987; Dao, 1998*
Mobil R&D, USA	Development of ZSM-5 with methanol upgrading.	*Chen, 1988*
National Renewable Energy Laboratory (NREL), Department of Energy, USA	HZSM-5 activity during upgrading of model compounds.	*Evans, 1988*
University of Laval, Canada	Low pressure upgrading of re-vaporised vacuum pyrolysis oils with ZSM-5 in a fixed catalyst bed.	*Renaud, 1998*
Universite Catholique de Louvan, Belgium	Characterisation of HZSM-5 during upgrading of re-vaporised pyrolysis liquid.	*Lahousse, 1998*
University of Leeds, Department of Fuel and Energy, UK	ZSM-5 upgrading of model compounds and re-vaporised biomass liquids using a fixed catalyst bed. Addition of steam.	*Horne, 1992, 1996#2*
University of Saskatchewan, Canada	HZSM-5, HY,SAPO-11 molecular sieve, silica-alumina and combinations in a fixed catalyst bed used for upgrading of re-vaporised biomass derived oils. Co-processing with steam and tetralin (hydrogen donor solvent).	*Sharma, 1991; Adjaye, 1994, 1995; Katikaneni, 1997*
VTT (Technical Research Centre of Finland), Finland	Catalyst screening with injection port of GC as a fixed bed catalytic reactor. Pyrolysis is *in situ* with MgO catalyst.	*Leppämäki, 1997*

The results of catalytically upgrading model compounds are helpful in establishing some of the reaction pathways for catalytic pyrolysis. However, only a small proportion of the compounds found in pyrolysis liquid have been studied. Condensed pyrolysis liquids are difficult to vaporise and may thermally degrade to either higher or lower molecular weight components or both *(Johnson, 1998)*. For these two reasons, the superior method of testing catalytic modification of pyrolysis vapour is on-line catalysis

in conjunction with the pyrolysis reactor. Experimentation has also been done in this field and is shown in Table 7.

Table 7 ***Main Institutions Involved with Catalytic Cracking of Freshly Produced Fast Pyrolysis Vapours***

Institution	Comments	Reference
Aston University, Bio-Energy Research Group, UK	Co-feeding of HZSM-5 with biomass for fast pyrolysis. Catalyst concentration study.	*Cooke, 1999*
Institute for Wood Chemistry, Germany	Catalyst screening with injection port of GC as a fixed bed catalytic reactor and off-line. Pyrolysis with zeolites, salts, slate and pumice co-fed and in a secondary fluidised bed.	*Wulzinger, 1998; 1999*
National Renewable Energy Laboratory (NREL), Department of Energy, USA	HZSM-5 activity during upgrading of pyrolysis vapours. Different mixes of pure HZSM-5 and HZSM-5 on a silica binder used in a separate fixed bed downstream reactor. Addition of methanol or steam.	*Evans, 1988; Milne, 1988; Diebold, 1986, 1987, 1988; Scahill, 1988*
University of Leeds, Department of Fuel and Energy, UK	ZSM-5 upgrading using a secondary fixed catalyst bed. Addition of methanol or steam.	*Horne, 1994, 1995, 1995#2, 1996; Williams, 1997, 1998*
University of Waterloo, Canada	Silica-alumina, kalsalite, nickel, HZSM-5 upgrading of hydropyrolysis vapour in a down flow fixed bed secondary reactor.	*Marshall, 1984*

Although catalytic action was applied to freshly produced pyrolysis vapours at the University of Leeds, the method employed to create the pyrolysis vapours was not fast pyrolysis. The vapour residence time used was greater than that used for fast pyrolysis (less than 4 seconds) *(Williams, 1997)*. The results from this institution will therefore not be used for direct comparison with the work presented here, as fast pyrolysis is the method of pyrolysis to be experimented with. These slow pyrolysis vapours are more comparable however than re-vaporised fast pyrolysis vapours.

The National Renewable Energy Laboratory (NREL), USA, formally known as the Solar Energy Research Institute (SERI), has conducted research on catalytic pyrolysis using a fixed bed tubular reactor. This has been done in three ways:

a) A micro-reactor with a secondary reactor containing 1 g of catalyst supported between quartz wool that used helium as the carrier gas *(Milne, 1988; Rejai, 1992)*
b) The slipstream of a vortex reactor to a 100 g catalytic reactor *(Diebold, 1988#2)*
c) The complete stream from a vortex reactor to an 8.5 kg catalytic reactor *(Diebold, 1994)*

The majority of experimental work was carried out on the 1 g fixed catalyst bed screening reactor, but good scalability was suggested by the limited operation of the larger 100 g and 8.5 kg fixed catalyst beds.

ZSM-5 has been used by NREL in the hydrogen or ammonium form and as a fresh, deactivated and regenerated catalyst. In all cases, the catalytic pyrolysis products were assessed on-line using a molecular beam mass spectrometer (MBMS). The results are in the form of mass spectra and the comparison of percentage yields of products based on carbon backbone chain length. Using MBMS on the gas phase of the process did not allow for the secondary and condensation reactions to be observed.

The main parameters investigated by NREL were the temperature, weight hourly space velocity (WHSV) and steam to biomass ratio (S/B). It was found that high yields could be obtained using high WHSVs and low S/Bs. Yields of liquid hydrocarbons of 8 wt% from wood were experienced at 500°C. The overall objective of the work of NREL was to produce hydrocarbon fuel from biomass, preferably in the gasoline range (C_5 to C_{10}). The quality of the pyrolysis liquid was not considered in the same way as it will be in this thesis. NREL found problems with catalyst deactivation due to the coking experienced with the fixed beds used. This should be remembered when designing experiments.

At the University of Waterloo, Marshall used a downflow fixed bed secondary reactor, heated independently of the primary reactor at 300 to 600°C and 505 to 525°C, respectively. The system to produce pyrolysis vapours employed hydrogen as the carrier gas, thus making it hydropyrolysis. This is a different system to the majority of

work being compared, as the regular carrier gas, nitrogen, is inert whereas hydrogen can be part of the pyrolysis reactions. The disadvantage of this is the economics and safety of using hydrogen as discussed when considering hydrotreating (Section 2.3.1).

Marshall compared the following catalysts: Silica-alumina, kalsalite, nickel (impregnated on silica-alumina or kalsalite) and HZSM-5. It was found that the use of silica-alumina encountered severe coking. The use of kalsalite reduced this and the addition of nickel enhanced cracking by providing proton sites. HZSM-5 was found to significantly modify the chemical composition of the resultant pyrolysis liquid by promoting deoxygenation. The run length used was either 15 or 30 minutes and used 9 to 25 g of poplar wood. To gain the mass balance methanol washing was employed. The detrimental effect of this practice is discussed in Section 4.10.1.

The details of how exactly the researchers Cook and Wulzinger incorporated catalysts into the fast pyrolysis process are given Section 4.10, page 142, where they are compared to the work presented in this thesis.

2.3.3.2 Clay Catalytic Cracking

Clay catalysts, which act in a similar way to zeolites (see Section 2.4.5), have also undergone a small amount of experimentation with biomass model compounds. Morrison used acetophenone as a model compound with laponite and montmorillonite clays. No firm conclusions were drawn *(Morrison, 1995)*.

2.3.3.3 Cracking of Gasification Tars

Gasification is a process similar to pyrolysis, performed to produce high gas yields rather than liquid and is sometimes done in conjunction with combustion. A bi-product is the tarry liquid residue. Some work has been done to simulate this tar production by pyrolysis and use catalysts to modify it.

Vassilios and Donnot *(Vassilios, 1990; 1992; Donnot, 1991)* have worked on dolomite in a secondary reactor following the pyrolysis reactor to reduce the tarry portion of the pyrolysis product. Donnot found that dolomite was more catalytically active in a

pyrolysis situation than industrial catalysts such as silico-aluminates. Vassilios used steam in addition to dolomite and reported that naphthalene and tar were reduced in the pyrolysis product. The gaseous yield was increased. The temperature of pyrolysis was 700°C and this was the desired effect. In the case of this report, the aim is to maintain a high liquid product.

2.3.3.4 Summary of Catalytic Cracking Upgrading

The advantage in using zeolite cracking catalysts rather than hydrotreating is the economics of the process. The low pressure, temperatures similar to those preferred for optimum yields of pyrolysis liquid and a close-coupled process make it a desirable process to exploit. Using ZSM5 catalysts, the applicability of catalytic cracking to pyrolysis liquid production has been proven. Further details of both zeolite and clay catalyst used for this purpose are given in Sections 2.4.4 and 2.4.5 below.

2.4 Catalysts

A catalyst is a reaction accelerator. It can affect reaction products by enhancing the speed of one reaction pathway in favour of another. Catalysts may provide an 'acid site' where a proton (H^+) is available to take part in reactions. Alternatively, they have 'base sites' where an electron may take part in reactions. Some catalysts have both acid and base sites. The acid and base sites are often referred to as Brönsted or Lewis sites and are defined in Sections 2.4.1.1 and 2.4.1.2.

Catalysts can also provide a physical surface upon which reactants can come together. Ultimately the chemical composition of a catalyst remains unchanged subsequent to reactions that it has catalysed. The catalysts can, however, change physically or chemically by 'poisoning' or 'blinding' which de-activate the catalyst. These terms are defined in Sections 2.4.1.3 and 2.4.1.4.

2.4.1.1 Brönsted Acid and Base

A 'Brönsted acid' is any substance that donates a proton; a 'Brönsted base' is any substance that accepts a proton *(McMurray, 1992#2)*.

2.4.1.2 Lewis Acid and Base

A 'Lewis acid' is any substance that accepts an electron pair; a 'Lewis base' is any substance that donates an electron pair in forming a covalent bond *(McMurray, 1992#2)*.

2.4.1.3 Catalyst Poisoning

'Poisoning' is when a chemical removes or reduces the catalytic property of the catalyst. This can be done by removing the protons or electrons used for catalytic action. An example of this is heavy metal poisoning of Cobalt Molybdanite hydrofining catalysts used in the refining of hydrocarbon oil products.

2.4.1.4 Catalyst Blinding

'Blinding' of a catalyst, also referred to as 'blanking', is when the pores of a catalyst become blocked or the surface of the catalyst becomes covered, so the catalytic sites are no longer available for reactants. The most common example of this is catalyst 'coking'. This is when carbon deposits are left on the catalyst following reactions. This phenomenon is sometimes also referred to as a type of poisoning. It has been studied with respect to pyrolysis by Donnot *(Donnot, 1991#2)*. Calcium-based catalysts were found to have the longest lifetime and nickel and calcium salt-based catalysts to have the best activity.

2.4.1.5 Catalyst De-Activation

A catalyst can be de-activated by either poisoning or blinding. The activity is reduced by the removal or blocking of active sites. In this circumstance, catalysts can still provide a surface for reactions to occur upon.

2.4.2 Catalyst Variables

There are several variables that should be considered when choosing a catalyst for a particular task. They are:

1) Acid or base sites, or both
2) Acid/base site strength
3) Acid/base site concentration
4) Catalyst chemical composition
5) Catalyst morphology
6) Physical durability of the catalyst
7) Shape selectivity of the catalyst
8) Catalyst interaction with potential sources of de-activation

2.4.2.1 Shape Selectivity

Zeolites are the most common 'shape selective' catalysts. The shape selection refers to the ability of this type of catalyst to select entrance and exit chemicals into or out of its pore structure. Within the pore-structure is where the active catalytic sites are. The selectivity is normally on the basis of size or shape. This is discussed further for zeolites in Section 2.4.4. An example of zeolite use for shape selectivity is in the isomerisiation of naphtha to improve gasoline quality by altering the proportion of benzene in the product.

2.4.3 Catalytic Cracking

'Cracking' refers to the reduction in chain length of hydrocarbon molecules. After initial distillation of crude hydrocarbon oil, many cracking processes occur in a petroleum refinery. Aromatic hydrocarbons formed from biomass pyrolysis have potential applications as fuel components. These aromatic compounds are formed by condensation and cyclisation reactions which occur to a small extent by thermal cracking, but to a larger extent by catalytic cracking *(McMurry, 1992)*. It is therefore proposed that catalysts be added to the pyrolysis process to improve the quality of pyrolysis liquid.

2.4.4 Zeolite Catalysts

Zeolites are alumino-silicates with specific structures. They are crystalline and are made up of silica and alumina tetrahedra that require cations such as sodium (Na^+), ammonium (NH_4^+) or a proton (H^+) to maintain electrical neutrality *(Morrison, 1995)*.

This is because each silicon ion possesses a +4 charge, which is neutralised by four electrons, one from each of the O^{2-} ions, but the aluminium only holds a +3 charge which is 'over-neutralised' by the four electrons surrounding it. The arrangement of the basic alumino-silicate tetrahedra into larger structures differentiates between the types of zeolite.

There are channels running through the three-dimensional crystal lattice and the diameter of them, known as pore size, determines the maximum molecular size of the reactants that may enter and the products that leave. Where the channels within the lattice meet, larger cavities called cages are present. The size of these cages allows molecules to react. If products larger than the pore size are created, they plug up the pores and deactivate the catalyst. Shape-selective zeolites, such as ZSM-5, work by firstly cracking molecules on the Brönsted and Lewis acid sites present on the catalyst surface and secondly by reconstructing smaller molecules in the cages to produce aromatic hydrocarbons. There are many different types of zeolites with pore sizes ranging from 4 to greater than 30 Å and they are used in a variety of catalytic applications in a typical hydrocarbon refinery. In other industries, such as industrial gas production, the main use of zeolites is as adsorbents.

ZSM-5 is the most commonly experimented-with catalyst associated with hydrocarbon processing and biomass pyrolysis. It is an active shape-selective catalyst with pore sizes of 5 Å. This is defined as intermediate between small-pore and large-pore zeolites. This pore size excludes the entry of highly branched molecules with over nine or ten carbon atoms. However, unlike small-pore zeolites, these pores permit the entry of simple aromatic and branched molecules such as benzene and cyclohexane, necessary for their cracking *(Sharma, 1991)*. The framework and pore system are shown in Figure 5. The basic alumino-silicate tetrahedra are arranged to create pentagonal oxygen rings.

ZSM-5 has been shown to convert biomass pyrolysis vapours to a range of aromatic hydrocarbons which have potential applications as fuel components *(Evans, 1998)*.

ZSM-5 zeolite catalyst was originally designed to make aromatic gasoline from methanol. It is now extensively used as an additive to an FCC (fluidised catalytic

cracking) catalyst in petroleum refining to crack heavy oil such as vacuum gas oil. It is used to boost LPG and olefin yields by targeting and cracking specifically the naphtha portion of the oil that has been pre-cracked by the main catalyst. The interaction of different catalysts is shown in Figure 6 *(Stocker, 1997)*. This describes how ZSM-5 is used in a crude oil refinery

Figure 5 ***ZSM-5 Framework Structure and Pore System (Diddams, 1997)***

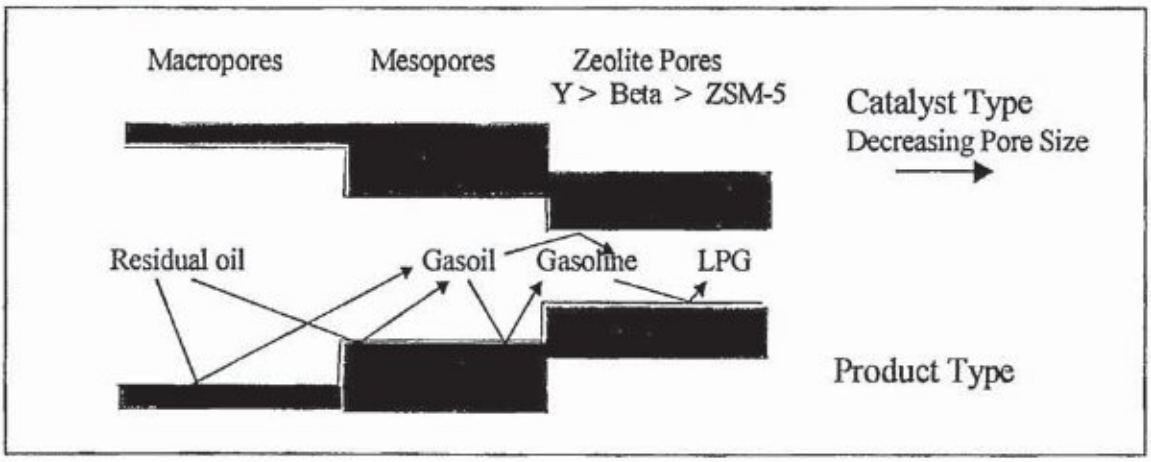

Figure 6 ***Petroleum Residual Cracking In A Varying Diameter Compound Catalyst Pore***

Y-zeolite (faujasite) is also commonly used in the chemical industry. It has a larger pore size (11 Å) and less complicated pore system than ZSM-5. Y-zeolite is compared to ZSM-5 in Table 8 *(Morrison, 1995)* and illustrated in Figure 7 *(Diddams, 1997)*. It is hypothesised in this report that the catalyst pore size influences the stability of the resultant catalytically produced pyrolysis liquid. Y-zeolite will be used to step up in pore size from ZSM-5 at 5 Å to 11 Å.

Y-zeolite (normally in an ultra stable form) is commonly used in FCC to raise the gasoline octane level. It has many acid sites which increase the hydrogen transfer to form many highly branched light iso parafins and light aromatics (particularly when 'G' stabilisation of chemical-hydrothermal treatment, has been used) *(Cartlidge, 1991)*. The main reason for choosing Y-zeolite is that it is a commercially available cracking catalyst.

Table 8 Typical Characteristics of Zeolite Catalysts

Characteristic	**Zeolite ZSM-5**	**Zeolite Y-Zeolite**
Pore Size, Å	5	11
Average Bulk Density, g/ml	0.72	0.61
Pore Volume, ml/g	0.48	0.64
Surface Area, m^2/g	300	440
Sodium Content, %	0.03	0.1
Potassium Content, %	0.01	0.002
Sulphate Content, %	0.01	0.002
Silica / Alumina Ratio	50	11

Figure 7 ***Y-Zeolite Framework Structure Showing a Pore Opening into a Cage (Diddams, 1997)***

2.4.5 Clay Catalysts

Zeolite catalysts are now used as the standard catalyst type in hydrocarbon refineries. Before the development of zeolite catalysts, naturally occurring clay type catalysts were used in petroleum catalytic cracking *(Burch, 1998)*. They are hard wearing, but did not have the flexibility of manipulable pore sizes. Developments in pillaring clays, enabling the pore size to be enlarged to between 5 and 19 Å, make them potentially interesting catalysts in both conventional hydrocarbon and the pyrolysis processes. Acid-treated and cation exchanged montmorillonites have been shown to possess an ability to promote organic reactions as acid catalysts *(Burch, 1988)*. It is hypothesised in this thesis that the catalyst pore size influences the stability of the resultant catalytically produced pyrolysis liquid. Clay catalysts are therefore intended to test this hypothesis by acting as the next pore size up from Y-zeolite, in the range where commercial zeolites are unavailable.

2.4.5.1 Pillared Clay

Clay minerals, either natural or synthesised, are layer silicates, in which the atoms (or ions) are arranged in parallel planes, separated by layers of charge-balancing cations *(Bodman, 1997)*. The increased gallery heights of a pillared clay are created by

exchanging these hydrated cations, for example sodium ions, from between the clay layers with a metal complex. Water is then removed to leave a metal oxide pillar, for example aluminium oxide *(McWhinnie, 1997)*. The steps are illustrated in Figure 8. The random stacking of the layers creates macropores, while the galleries, both pillared and un-pillared are in the micropore range. Pillaring increases gallery heights from around 9 to 19 Å.

Pillared clays were originally designed for use in the petroleum industry to complement zeolites. The problem with zeolite catalysts is the small pore size and the large amount of non-selective pre-cracking. This pre-cracking has to take place before the large residual molecules are reduced to the size capable of diffusing into the very active and selective zeolite component of the catalyst. Although large pore zeolites are theoretically possible (20-30 Å), none have been reported *(Burch, 1998)*. Work on pillared clays, with properties compatible with a petroleum-cracking environment, began in 1974. The use of pillared clays to improve hydrocracking reactivities of coal liquefaction extracts has been investigated *(Bodman, 1997)*. This process is similar to hydrotreating biomass pyrolysis liquids and the catalyst is desired for the same purpose - to produce a more commercially useful liquid. Clays are interesting in this application for their larger and more controllable pore sizes, metal cation effects as well as high temperature stability.

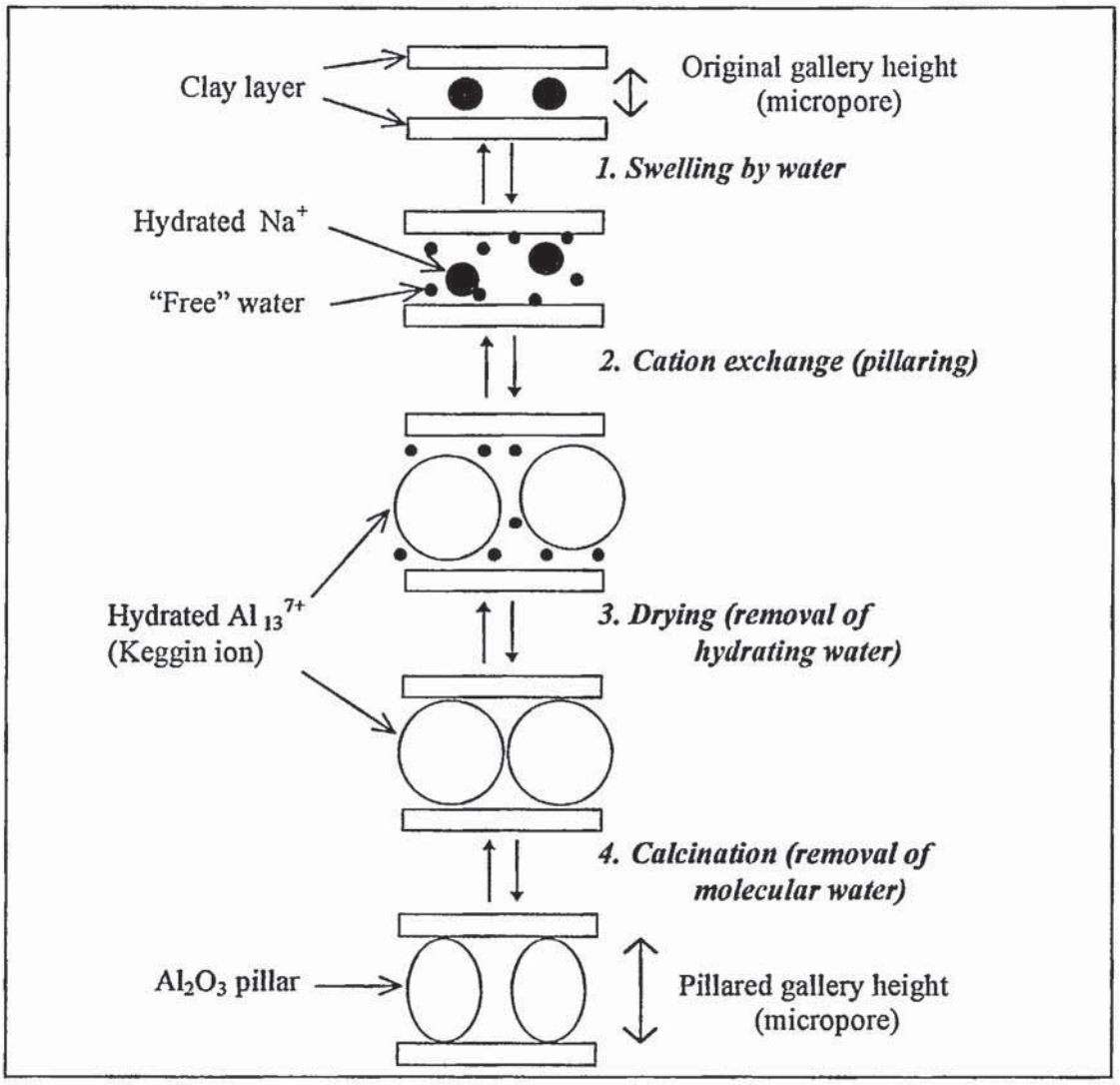

Figure 8 Steps to Prepare Pillared Clay

2.5 Catalyst Addition Technology

The apparatus used and developed for pyrolysis is discussed in Chapter 4. This Section looks at the background to catalyst addition to the pyrolysis process. The options used are described in Section 4.4. The potential arrangements are:

a) Co-feeding biomass and catalyst
b) Fluid bed catalysis
c) Close-coupled in-bed catalysis (fixed or fluid bed)
d) Close-coupled catalyst in a secondary reactor (fixed or fluid bed)

It can be seen that the phenomena associated with both fixed and fluid beds should therefore be understood. They are examined in the following Sections 2.5.1 and 2.5.2.

2.5.1 Fixed Bed Technology

A fixed catalyst bed is the system normally used when a catalyst has a long life (approximately one year). A tubular packed bed in which plug flow is assumed is common. Long tubes reduce end effects and a vessel diameter to particle diameter ratio of greater than 15:1 is preferable to reduce wall effects.

The major problem associated with the use of fixed bed catalysis with biomass pyrolysis is coking. Coking is the deposition of carbon on the catalyst (see Section 2.4.1.4). This is disadvantageous as it blocks catalyst pores and catalytic sites and therefore deactivates the catalyst. This occurrence has been observed at NREL *(Diebold, 1994)* where coking was found to cause rapid catalyst deactivation and non-steady-state reaction conditions.

2.5.2 Fluid Bed Technology

Fluid beds are often used where a catalyst with a short life is being utilised. A short life is regarded as a few seconds long. The advantages of a fluid bed are:

1) Rapid heat transfer
2) Uniform bed temperature (good control of temperature)
3) Good mixing of particles
4) Easy removal or addition of solids (aids catalyst regeneration)
5) Good contact between gas and solid phases (high gas-solid interfacial area)
6) Predictable bed pressure drop characteristics
7) Steady-state operation easily achieved

In contrast, the disadvantages are:

1) Solids entrainment
2) Channelling of the gas phase (dependant on distributor design)
3) Gas velocity is constrained
4) Extra reactor volume is required for solid disengagement
5) Particle attrition and wear on the catalyst surface may occur.

The addition of catalysts to the pyrolysis process has used both fixed and fluid bed technologies. The nature of the fluid bed in the pyrolysis process has not been extensively examined, but work associated with the phenomenon of char removal from the fluidising medium has been researched to a small degree. This section reports some of the theory that will subsequently be needed when designing the incorporation of catalysts into the pyrolysis process (see Section 4.4).

2.5.2.1 Minimum Fluidising Velocity

The minimum fluidising velocity (u_{mf}) is important for determining fluidising conditions and is expressed in Equation 4, the Ergun equation. As the upward velocity of flow of fluid through a packed bed of uniform spheres is increased, the point of incipient fluidisation is reached when the particles are just freely supported by the fluid. The voidage in this condition (e_{mf}) is 0.4 *(Coulson, 1991#2).* The voidage could be expressed more accurately. Values of 0.35 to 0.38 have been considered. The level of accuracy of the other terms in Equation 4, however, negates the need to find e_{mf} to more than one significant figure.

$$u_{mf} = 0.0055 \times [(e_{mf})^3 / (1 - e_{mf})] \times (d_{particle})^2 \times (\rho_{particle} - \rho_{fluid}) \times g / (\mu_{fluid})$$

Equation 4

(See Section 13, 'Nomenclature', on page 234).

The relationship between fluid velocity and delta pressure across the bed is shown in Figure 9. Active bubbling occurs at u_b, when the superficial gas velocity (u_o) is at least six times greater than the minimum fluidising velocity (u_{mf}).

Figure 9 ***Relationship Between Velocity and Delta Pressure to Find Minimum Fluidising Velocity (Kunii, 1991)***

2.5.2.2 Particle Terminal Falling Velocity

The particle terminal falling velocity (u_t) is important for determining entrainment. It is defined as the final steady velocity obtained by a falling single particle in a static fluid. At $u_o = u_t$ the single particle floats on the fluidising fluid upstream, at $u > u_t$ the particle rises with the stream. It depends on particle density, size and shape of the particle and on the viscosity and density of the fluidising fluid. For non-spherical particles it can be calculated only approximately *(Howard, 1989)*. The particles to be calculated in this project shall therefore be assumed to be spherical. The particles first need to be characterised by finding the Reynolds number (Equation 5). They fall into regions *(Coulson, 1991#2)* (Table 9).

$$Re = u d_{particle} \rho_{fluid} / \mu_{fluid}$$

Equation 5

Table 9 Classification of Particles by Reynolds Number and Corresponding Terminal Falling Velocity

Region	Reynolds Number	Characteristic[a]	Terminal Falling Velocity, u_t (m/s)
a	$10^{-4} < 0.2$	Stokes' Law applies, $F = 3\pi\mu_{fluid} d_{particle} u$	$((d_{particle})^2 g / 18\mu_{fluid})(\rho_{particle} - \rho_{fluid})$
b	$0.2 <$ 500 to 1000	Intermediate	-
c	500 to 1000 $< 2\times10^5$	Newton's Law applies, $4F / \pi(d_{particle})^2 \rho_{fluid} u^2 = 0.22$	$[(3d_{particle} \times g / \rho_{fluid})(\rho_{particle} - \rho_{fluid})]^{0.5}$
d	2×10^5	$4F / \pi(d_{particle})^2 \rho_{fluid} u^2 = 0.05$	-

Notes: (a) *(Coulson, 1991)*

If the particles fall into a region where the terminal falling velocity is undefined, then an alternative empirical method is used. This involves the Galileo number (Ga), like the Reynolds number, a dimensionless number (Equation 6).

$$Ga = [(d_{particle})^3 \times \rho_{fluid} \times (\rho_{particle} - \rho_{fluid}) \times g]/(\mu_{fluid})^2$$

Equation 6

The Galileo number has been tabulated against the Reynolds number under terminal falling conditions, where $y = \log_{10}(2Ga/3)$ and $x = \log_{10}(Re_t)$ *(Coulson, 1991#2)*. The terminal falling velocity can therefore be found.

2.5.2.3 Density and Voidage

The work of Wunder compares the fluid bed materials used in pyrolysis *(Wunder, 1999)*. The measurement of particle densities and bulk voidage was done by water displacement. Approximately 50 – 100 ml of bulk material was filled in a 250 ml cylinder and the mass of material found. Equation 7 gives the bulk density.

$$\rho_{bulk} = m_{bulk} / V_{bulk}$$

Equation 7

Sufficient water was then added to obtain an air-bubble-free suspension. Again the mass increase and volume were read. Equation 8 to Equation 10 are then used. These experiments result in the following results, Table 10.

$$V_{particles} = V_{particles+water} - (m_{water} / V_{water})$$

Equation 8

$$\rho_{particles} = m_{particles} / V_{particles}$$

Equation 9

$$\text{Voidage, } e = 1 - (V_{particles} / V_{bulk})$$

Equation 10

Table 10 Physical Properties of Bed Materials and Feed

Particle Type	Bulk Density (ρ_{bulk}), g/cm^3	Particle Density ($\rho_{particle}$), g/cm^3	Voidage (e), cm^3/cm^3
Sand	1.6	2.5	0.3
Slate	0.7	1.9	0.6
Char	0.2	0.6	0.6
Beechwood	0.3	0.8	0.6

2.6 Summary

This project objective is to improve the pyrolysis liquid quality by economic, mild modification of the pyrolysis vapours. Hydrotreating will therefore not be considered for experimentation. Catalytic cracking type experiments, however, will be undertaken. Various modes of operation can be explored including the fluid bed process with catalyst incorporation and a secondary bed reactor (see Section.4.4, 'Incorporation of Catalyst into the Process'). To reduce the number of pyrolysis experiments, preliminary screening of catalysts will be performed (see Section 3). The catalysts in Table 11 are therefore recommended for catalytic micro-reactor screening with the aim of upgrading pyrolysis liquid. The hypothesis that catalyst pore size influences the product of catalytic pyrolysis and therefore the liquid quality will be tested.

Table 11 Catalysts Recommended for Screening Tests

Catalyst	Reason for Choice for Screening
ZSM-5	To compare with the majority of work done previously in the field, mainly on re-vaporised pyrolysis liquid (See Table 6).
ZSM-5 and alumino-silicate mixes	To extend the work of University of Saskatchewan, Canada *(Katikaneni, 1997)* from re-vaporised pyrolysis liquid on a very small scale (Section 2.3.3.1). Also following the work at NREL where different mixes of pure HZSM-5 and HZSM-5 on a silica binder were used *(Diebold, 1986)*.
Y-Zeolite	To extend the work of University of Saskatchewan, Canada *(Katikaneni, 1997)* and to investigate a larger catalyst pore size than ZSM-5.
Clay Catalysts	To extend the work of Morrison *(Morrison, 1995)* and use larger still catalyst pore sizes. (Section 2.3.3.2)

3 CATALYST SCREENING

To improve the quality of pyrolysis liquid, the addition of catalyst in the pyrolysis process is to be utilised. The main apparatus used to trial catalysts in the fluid bed pyrolysis process is a scale of 150 g/h feed. This is described later in Chapter 4. To increase the success of these trials, catalysts have first been screened to estimate their viability of benefiting the experimental program. This will reduce the cost and time taken to do the main catalytic analysis with the 150 g/h apparatus.

Ideally, the desired catalyst would be chosen by knowing:

1) the composition of the raw pyrolysis liquid product,
2) the composition of the desired pyrolysis liquid product,
3) the reactions to enable the raw product to become the desired product, and
4) the catalysts necessary to facilitate that conversion.

This is not possible as:

a) only 40 % of the compounds in the pyrolysis liquid product have been characterised *(Meier, 1997#2)*,
b) the effect of catalyst on all the chemicals present is not known, and
c) the interaction between the different chemicals before and after catalytic action can not be predicted.

Screening will be done in a smaller 'micro-reactor', described below, which is attached to a gas chromatograph for immediate analysis. The small nature of the screening experiments allows them to be performed quickly due to the reduced time of setting them up and the short reaction time. Screening catalysts intended for use in the 150 g/h fluidised bed pyrolysis reactor, aims to:

1) reduce the number of catalysts used in experimentation,
2) ascertain which would be the best catalyst to use, and
3) indicate which chemicals should be analysed for in the product oils.

These screening experiments look at the relative effects of the various catalysts used. The outcome provides a qualitative guide to the results that can be anticipated in the larger scale pyrolysis experiments, although a relationship has not been established to predict exactly what will happen in the larger reactor based on the screening results. This is because of the ratios of catalyst to wood used of approximately 4000:1. Current 150 g/h experimental work uses a ratio of 1:10, weight of catalyst to weight of wood. This is a normal catalyst level for other catalytic applications such as petroleum fluidised catalytic cracking *(Grace, 1996)*.

3.1 Catalyst Screening Apparatus and Experimentation Description

The catalyst screening was done in conjunction with the Institute of Wood Chemistry in Hamburg. Catalyst and wood was supplied by Aston, where the results were analysed. The experimentation was carried out at the IWC where a micro pyrolysis reactor was coupled to a gas chromatograph with flame ionisation detection (FID). A precise amount of wood and catalyst, in the region of 0.2 and 0.5 mg respectively, was used. Pine wood from Union Fenosa in Spain, of a particle size 75-212 μm was used with the zeolite and clay catalysts detailed in Table 12, Section 3.2.

The wood was first dried by placing it in a quartz boat and standing it over phosphorous pentoxide for at least 12 hours. The catalyst and the wood were then intimately mixed and the boat was introduced to the heated interface (Figure 10). The heating coil was started and held at 450°C for the 10 seconds of pyrolysis time. The heating rate of the heating coil was 600°C/s.

A carrier gas, helium, was used to ensure no oxygen was present and that the resulting pyrolysis vapours flowed directly to the GC for analysis. The helium pressure was 2 bar and flowed at 1 ml/min. The vapours were injected into the GC at 250°C and the detector was at 280°C. All experiments were duplicated.

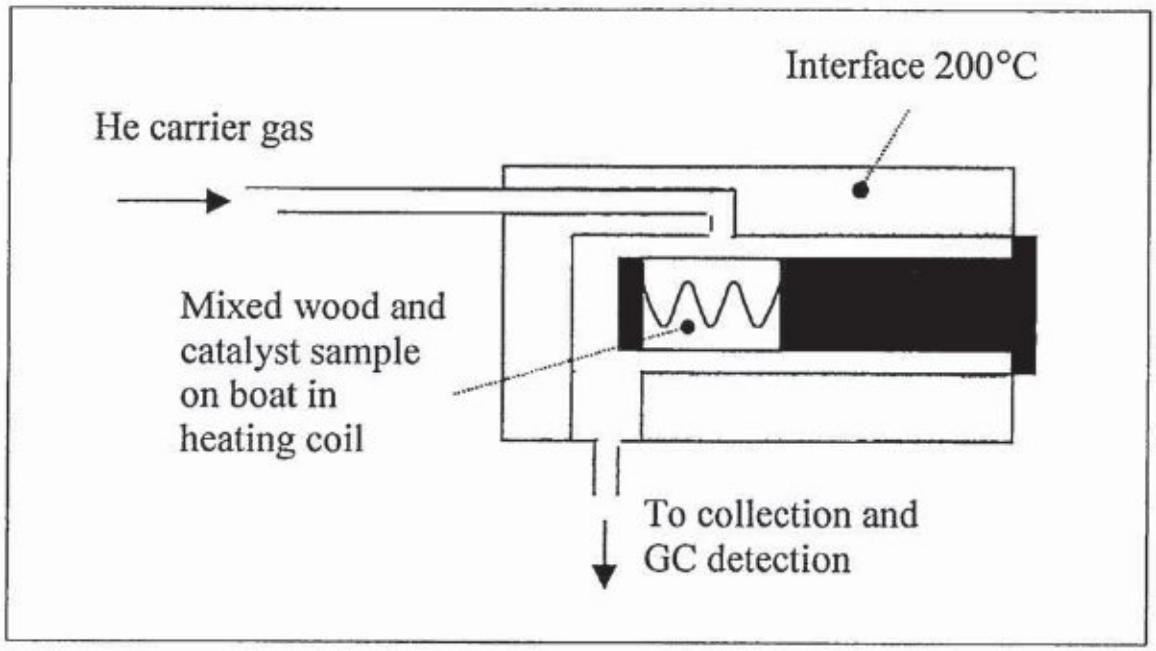

Figure 10 IWC Micro-reactor Outline

Figure 11 IWC Micro-reactor Collection System (Faix, 1987)

3.2 Catalysts Screened

The catalysts shown in Table 12 have been tested using the pyrolysis micro-reactor and GC. They were chosen for their robust nature – being able to withstand pyrolysis

temperatures and friction due to fluidisation, their previous uses and the catalyst pore size.

Table 12 Catalyst Screened in IWC Micro-reactor

Catalyst Code	Pore size / Gallery Height	Description
ZSM-5	5 Å	ZSM-5 zeolite catalyst (SP no. 10-5132.0101) made by Grace Davison. It is 15 % pure on an alumina phosphate binder.
Y	11 Å	Y-zeolite, a hydrogen zeolite clay from BDH with a Y-type structure. Pellet diameter3mm.
FCAT-A, FCAT-B, FCAT-C	5 Å	Fresh catalyst made by Grace Davison. Different mixes of ZSM-5 and alumino-silicate binders.
Equilibrium	5 Å	Equilibriated Grace Davison ZSM-5 catalyst from an FCC unit.
BOD16	12.5 Å	Sodium Montmorillonite clay (un-calcined).
BOD17	12.5 Å	Sodium Montmorillonite clay calcined at 475°C.
BOD18	12.5 Å	Sodium Montmorillonite clay calcined at 525°C.
BOD19	16 Å	Al pillared Sodium Montmorillonite clay(un-calcined).
BOD20	14 Å	Al pillared Sodium Montmorillonite clay, calcined at 490°C.
BOD21	14 Å	Al pillared Sodium Montmorillonite clay, calcined at 525°C.
BOD23	18 Å	Cr pillared Sodium Montmorillonite clay, calcined at 500°C.
BOD24	18 Å	Cr pillared Sodium Montmorillonite clay, calcined at 600°C.

ZSM-5 is a shape selective, medium pore, strong acid zeolite catalyst that has been experimented on by many institutions (see Section 2.3.3). The designed use of this ZSM-5 zeolite catalyst is as an additive to an FCC (fluidised catalytic cracking) catalyst in petroleum refining. It is used when cracking heavy oil such as vacuum gas oil (the fraction closest to bitumen). Its job is to boost LPG and olefin yields by targeting and cracking specifically the naphtha portion of the oil. The temperature of operation of this catalyst depends on the application and chemistry required, but is normally 505 – 540°C in a petroleum FCC. It can, however withstand much higher temperatures, as it does for regeneration.

Y-zeolite is a hydrogen zeolite clay, from BDH, with a Y-type structure. It is a large pore, strong acid zeolite catalyst which has been initially studied by Katikaneni *(Katikaneni, 1997)*. It is supplied in a spherical pelleted form of 3mm. It was chosen because of the large particle size available, to be used in close-coupled catalyst configurations as many zeolites are produced in a much smaller particle size. The larger particle size enables the catalyst to be used in the pyrolysis fluid bed and not be entrained out of the reactor, where it should remain through the duration of the experiment.

The Montmorillonite clay based catalysts, named with the prefix BOD, were made at Aston University and are all experimental. Clay catalysts have previously been used with re-vaporised pyrolysis liquid by Morrison *(Morrison, 1995)*. The pillaring was achieved by the addition of oligomeric polyoxo cation solutions (of the Keggin type) to a clay suspension (see Section 2.4.5 for further details). Six of the eight clays were calcined in a tube furnace under nitrogen flow. Calcination converts hydrated polyoxo cations into stable metal oxide pillars. Prior to calcination, cation insertion is reversible. The calcination process removes both free water (pre-drying) and chemically bound water (calcination).

The temperatures of calcination for plain Montmorillonite clay were based on the temperatures of operation of the pyrolysis reactor. The temperatures of calcination for the metal exchanged pillared clays were taken from literature methods of preparation *(Schoonheydt, 1993; Pinnavaia, 1985)*. The chromium pillared clay was only prepared calcined because of the potential carcinogenic products of reactions with the un-calcined form. If chromium is oxidised in air, a Cr VI is formed which is a hazardous substance.

3.3 Catalyst Screening Results

The raw data are in the form of gas chromatograph traces and corresponding computer-calculated peak area information for each different experiment using a different catalyst. Fifteen runs were done in all, including a run incorporating no catalyst, known as the blank. Occurrence of different chemicals or significantly different concentrations of chemicals indicates the catalytic effect on this screening scale process. This will not be

able to quantify the effect of a catalyst, but will indicate which catalysts may be able to be used to modify the bio-oil product in the 150 g/h fast pyrolysis process. It will also be a sign of what different chemicals to expect and analyse for at this and larger scales, when incorporating catalysts.

The raw data, in the form of chromatograph traces, show the peak retention time of chemicals in minutes and response factor in mVolt seconds. The peaks are compared to a standard and those known, identified. This is done by overlaying the standard, which has been printed on acetate, over the chromatograph with peaks to be identified (see Appendix R, page 341). The retention time at which the peak is produced is then compared to the computer calculation of peak area, from which the peak area of each peak can be found. These results can then be manipulated in a number of ways to predict the best catalyst for producing a more stable pyrolysis liquid.

3.3.1 Manipulation of Screening Information

The raw results are in the form of gas chromatograph traces and corresponding computer-calculated peak area information for each experiment. Fifteen different runs were done in all, including a run incorporating no catalyst, known as the blank. They were all repeated for confirmation and found to be almost identical on repetition.

It is not representative to compare quantitatively the resulting chromatographs from the different runs, as slightly varying amounts of wood were used in each experiment. Although this can be considered when mathematically manipulating the peak areas, it is difficult to account for when visually inspecting the chromatograph traces.

To assess the catalysts, the results have been compared to the blank runs containing only wood and no catalyst. To negate the slightly different amounts of wood used in the 30 runs, the response, in mVolt, has been calculated per unit gram of wood at ambient wetness (approximately 7 % moisture). This comparison to blank runs has been done in two ways (Sections 3.3.1.1. and 3.3.1.2). Sections 3.3.1.3 to 3.3.1.5 then compare the catalytic runs to each other as well as the blank. The results from applying these methods to the screening experiments done are discussed in Section 3.3.3.

3.3.1.1 Chromatograph Peak Area Minus Blank Runs (Method 1)

The first method of comparing catalytic runs is the difference in peak area, per gram of wood compared to the blank run (Figure 12 and Figure 74 to Figure 76, Appendix D, page 259). As the peak area represents the quantity of a certain chemical, this approach enables a single chemical response to be comparatively examined for all the runs. The units of peak area are mVolt seconds.

Although this is a rough guide, it is not wholly satisfactory because peaks from different chemical responses can not be compared. This is because a small peak for one chemical may correspond to a concentration higher than that from a chemical with a large peak. It does however help to identify chemicals that occur when one catalyst is used and not when a different one is used. If, subsequently, a better quality pyrolysis liquid is produced then these graphs will help to identify the chemicals that contribute to stability.

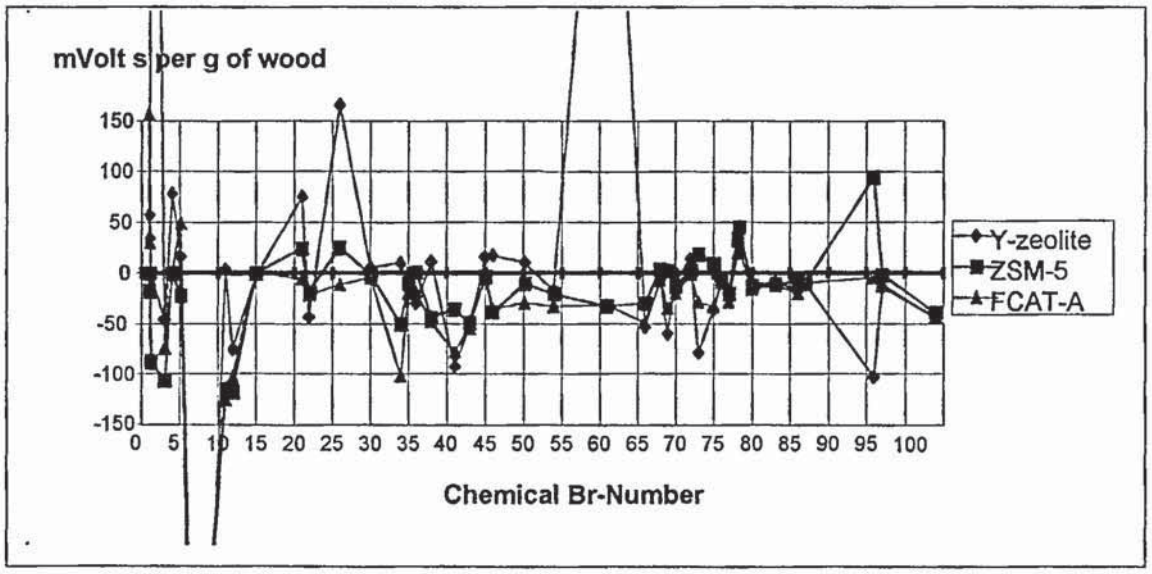

Figure 12 Chromatograph Peak Area Minus Blank, Zeolites 1 of 2

A zero result on this 'chromatograph peak area minus blank' graph indicates that the catalytic response was the same as the non-catalytic one. The data are not continuous and the lines joining the points on the graph are for the purposes of easy identification only.

To improve on this method of analysis, the data should be manipulated to make each chemical response comparable to one another as demonstrated in Section 3.3.1.2.

3.3.1.2 Chromatograph Peak Area Difference as a Percentage of Blank (Method 2)

The second method of comparing the runs to the blank enables better manipulation of the results. It expresses the difference in peak area from the blank, found in the first method, as a percentage of the blank peak for each chemical response (Figure 13 and Figure 77 to Figure 79, Appendix D). The individual chemicals can then be compared to one another. The calculation is Equation 11, where peak area is measured in mVolt seconds.

[(catalyst peak area - blank peak area) * 100 / blank peak area].

Equation 11

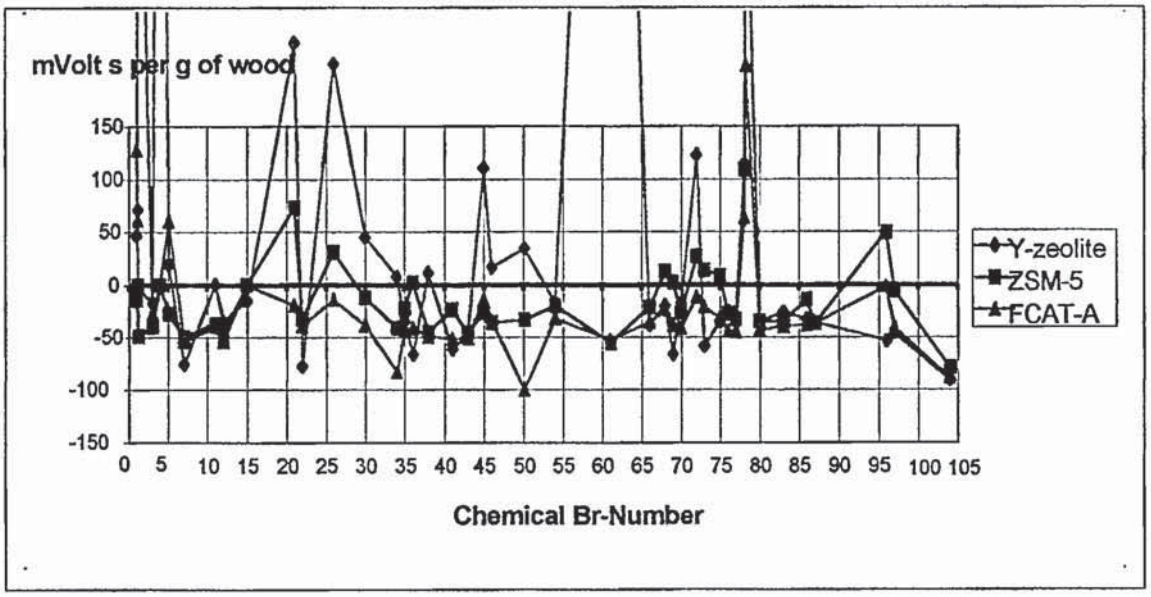

Figure 13 Chromatograph Peak Area Difference as % of Blank, Zeolites 1 of 2

'Chromatograph peak area difference as a percentage of the blank run' shows comparatively how much of each chemical was found. Points above the zero line show how much more of a certain chemical than the non-catalytic run has been detected.

Below the line how much less of a chemical found is shown in terms of a signal strength and length of signal (mVolt seconds).

Sections 3.3.1.1 and 3.3.1.2 describe ways to view the data in a way similar to the original chromatograph. This helps to give an initial impression of the run, but to find the real information gained from the screening experiments, further manipulation is necessary (Sections 3.3.1.3 to 3.3.1.5).

3.3.1.3 Comparison of the Number of Peaks (Method 3)

A simple way to observe the effect of adding a catalyst is to find the number of peaks produced, identified or not. This third method of assessment is shown in Figure 14 and Figure 80 (Appendix D) for zeolites and clays. This indicates the range of chemicals found and highlights differences between the blank run and the particular run being analysed. It could have been found that a pyrolysis liquid with a large variety of chemical compounds or one that is chemically more simple may be more stable. It is hypothesised that a catalyst that produces a larger number of chemical compounds is a more stable one.

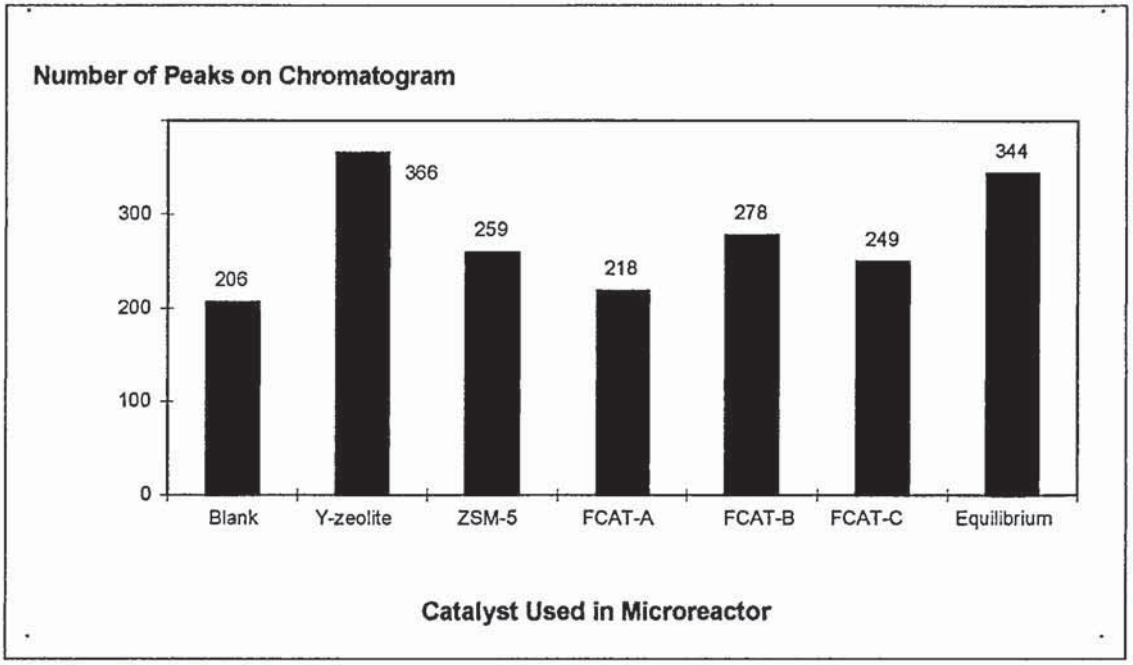

Figure 14 ***Comparison of the Number of Peaks Resulting from Catalyst Addition to the Pyrolysis Micro-reactor, Zeolites***

3.3.1.4 Average GC Peak Area (Method 4)

The average GC peak areas shown in Figure 15 and Figure 81 (Appendix D), have been calculated by summing the areas of the peaks for a run and dividing this by the total number of peaks (Equation 12).

Average GC peak area = Σ_s (area of peak) / Σ_t (peak)

Equation 12

where Σ_s (area of peak) is the sum of selected peak areas and Σ_t (peak) is the total number of peaks.

The peaks used for Σ_s are just those that have been identified and do not remain constant when compared between different catalytic runs. This could be described as 'summing the changing known peaks'. Not all the peaks produced on the chromatograph could be identified, as they were not included in the 'GC standard' of 104 compounds. 'Identified peaks' are therefore those shown in Table 70, 'Identification of Detected Chemicals in Micro-reactor Screening' (268, Appendix D).

This method of analysis shows the amount of known compounds produced per gram of wood, from a particular experiment. It highlights whether it is unknown compounds that are contributing to stability of pyrolysis liquids following catalytic pyrolysis. As the GC standard was developed for non-catalytic runs it is hypothesised that unknown rather than known compounds contribute to stability. A lower result using this method of analysis is therefore an indication of a more stable pyrolysis liquid.

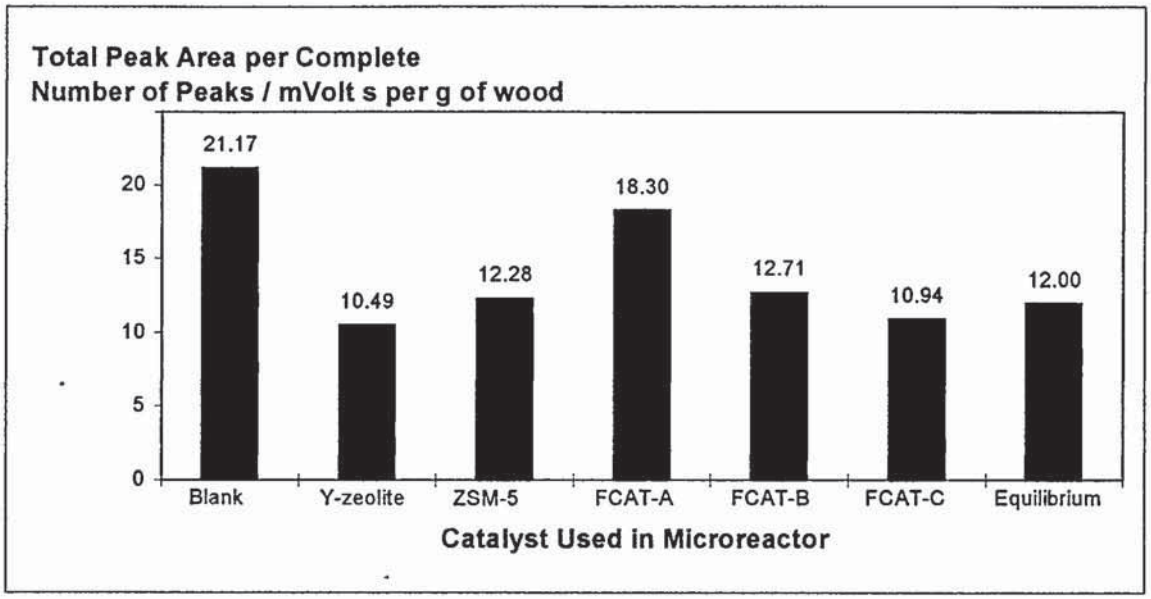

Figure 15 Average GC Peak Area, Zeolites

3.3.1.5 Sum of Peak Area Difference as Percentage of Blank Area (Methods 5 – 7)

Figure 16 and Figure 82, sums of peak area difference as percent of blank peak area for selected chemicals, have been calculated by directional addition (Equation 13, Method 5), whereas the absolute values (Figure 17 and Figure 83) were gained by addition, taking all numbers as positive, regardless of their sign (Equation 14, Method 6).

Sum of peak area difference as percent of blank peak area = Σ_s (Equation 11)

Equation 13

Equation 13, absolute value = Σ_s ($\sqrt{(\text{Equation 11})^2}$)

Equation 14

Method 5 indicates how much more total amount of chemical was found than for the blank run. Method 6 highlights the differences of a run compared to the blank run as a progression to Method 7. It is used because if a run had equal positive and negative differences between it and the blank, a misleading zero value would arise using Method 5.

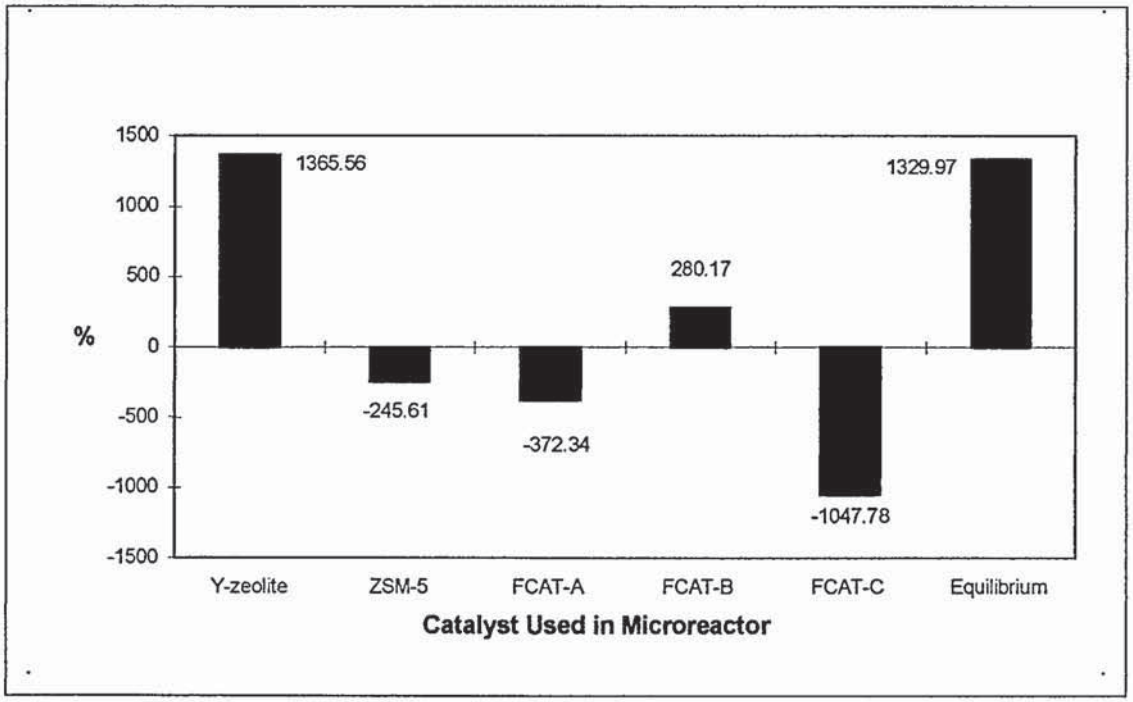

Figure 16 ***Total Sum of Peak Area Difference as % of Blank Area for Selected Chemicals, Zeolites***

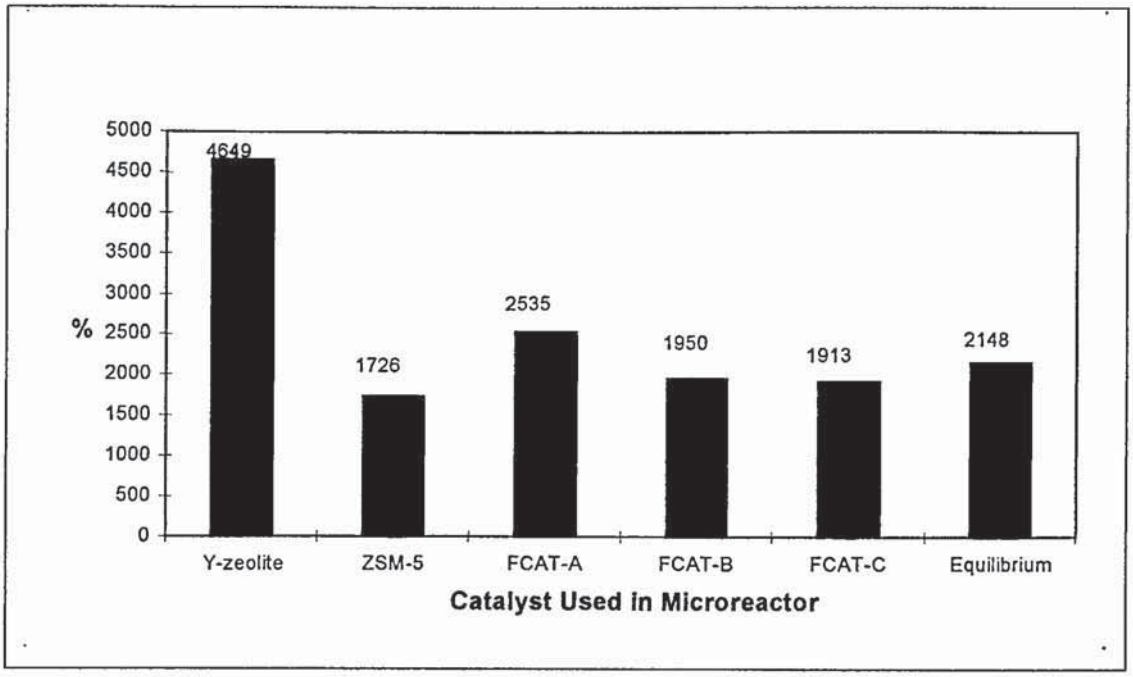

Figure 17 ***Sum of Peak Area Difference as % of Blank Peak Area for Selected Chemicals (Absolute Values), Zeolites***

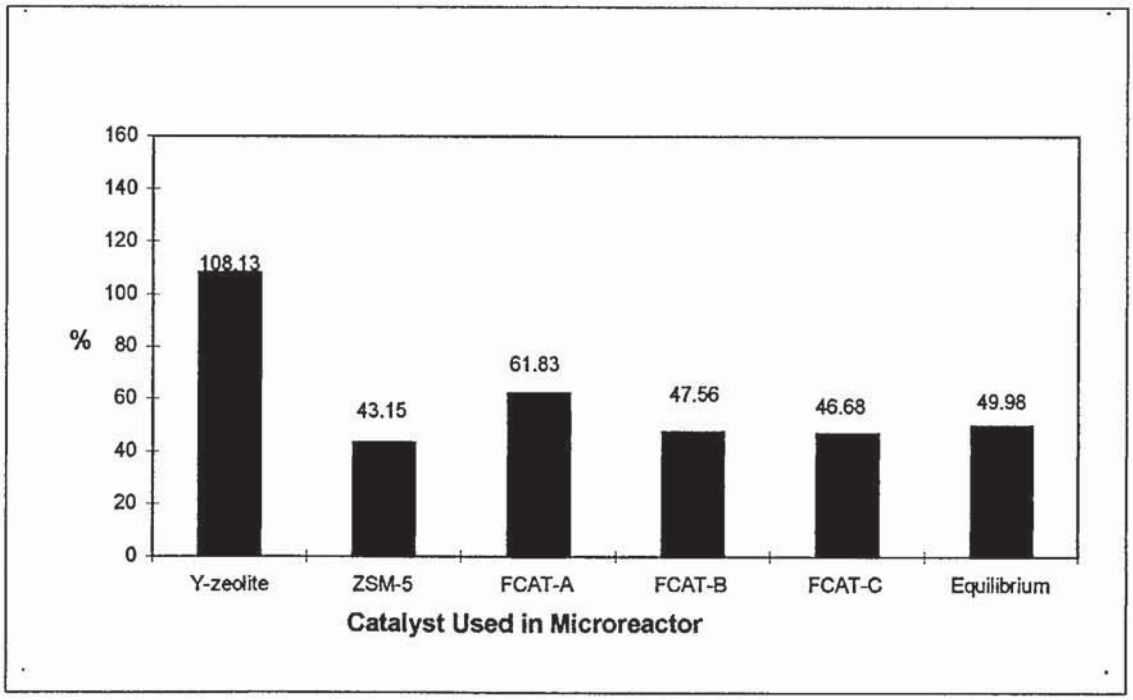

Figure 18 ***Average Peak Area Difference as % of Blank Peak Area (Absolute Values), Zeolites***

The average peak (Figure 18 and Figure 84) has been found by dividing by the number of the *selected peaks* the chromatograph showed for each experimental (Equation 15, Method 7). This shows how different a run is from the blank non-catalytic run. The more different, it is hypothesised, the better.

Average Equation 14 $=\Sigma_s (\sqrt{(\text{Equation 11})^2}) / \Sigma_s$ (peak)

Equation 15

These methods of analysis are ranked in Table 13, Section 3.3.3

3.3.2 Catalyst Screening Assumptions

The numbering of chemicals is taken from the IWC system, using the 'Bremer Number'. Bremer made a standard for analytical pyrolysis. Each spectrum is given a number to help identification of chemicals and for simplifying the comparison of results (see Table 70, Appendix D).

The levoglucosan peak (no. 96) often appeared with a shoulder that was given a separate area by the computer. In this case, the areas of the shoulder and the main peak have been summed and the whole referred to as the levoglucosan peak. This was done for ease of comparison and because it is known that levoglucosan is a large peak which the computer often misinterprets.

Alternatively, the leading peak or the back peak could have been chosen and just this area used. However, as shown in Figure 19, it would be difficult to decide which was levoglucosan and which was the compound with a very similar retention time. It is particularly difficult as the base of the blank peak and the catalytic version are identical. Also, not all the catalytic peaks had a small then large part, some were initially larger then smaller. The assumption that chooses to sum the peaks may be, in effect, summing two different peaks, but they will both be chemically similar to levoglucosan so to keep all the analysis the same the peaks were summed.

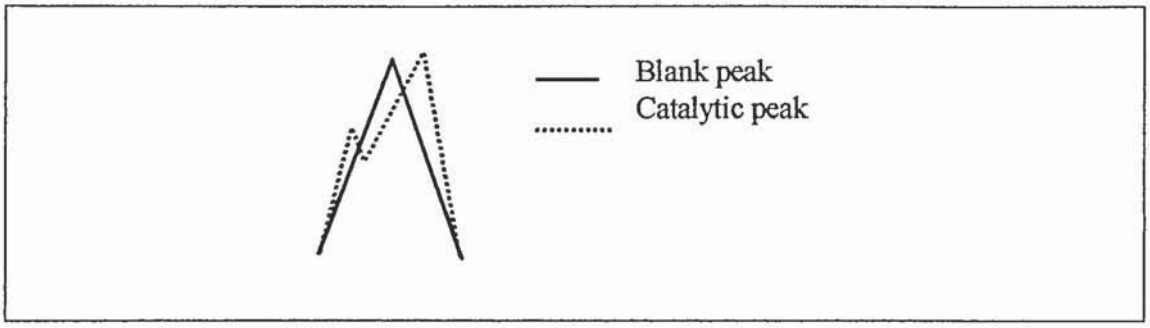

Figure 19 ***To Describe Problem Labelling Levoglucosan Peak - Representation of Overlaid Chromatograph Peaks***

3.3.3 Comparison of Chromatographs from Screening

The most notable results are those of Y-zeolite, BOD16, BOD17 and BOD19. Y-zeolite appears to have the greatest effect on the pyrolysis vapours as a wider variety of chemicals are produced. BOD17 and BOD19 have the opposite apparent effect, as the number of chemicals produced is not known because they appear to be absorbed by the catalyst. BOD16 appears to have no catalytic effect.

Following the manipulation of data as described in Section 3.3.1, the results from each method have been found and the catalysts ranked. 1 was designated the 'best' catalyst according to the method and 14 the 'worst'. For Methods 3 to 7, the results are shown in Table 13.

Table 13 Ranking of Results from Screening Analysis Methods

Catalyst Code (Table 12)	Method 3	Method 4	Method 5	Method 6	Method 7	Sum of Ranks	Order of Ranks
ZSM-5	5	9	10	9	11	44	**10**
Y	1	4	1	1	1	8	**1**
FCAT-A	9	14	11	3	5	42	**8**
FCAT-B	3	10	6	6	8	33	**4**
FCAT-C	7	5	13	7	9	41	**7**
Equilib-rium	2	8	2	5	7	24	**3**
BOD16	11	13	8	10	12	54	**14**
BOD17	13	1	7	13	1	35	**5**
BOD18	6	11	4	11	13	45	**11**
BOD19	14	2	9	14	3	42	**8**
BOD20	4	6	3	2	4	19	**2**
BOD21	8	7	12	8	10	45	**11**
BOD23	10	12	5	12	14	53	**13**
BOD24	12	3	14	4	5	38	**6**

3.3.4 Molecular Weight Hypothesis

It is hypothesised that if more low molecular chemicals are produced and less high molecular chemicals, this can indicate a reduction in viscosity. Viscosity is far more complicated than this, but for straight chain molecules, this is true. On this basis, the effect of catalyst addition can be assessed.

The x-axes of Figure 20 to Figure 22 show the distribution of molecular weights, as indicated by the Bremer Number (see Section 3.3.2). This assumes that the low molecular weights have short retention times and high molecular weights have long retention times. The chemicals are numbered with the Bremer Number (see Table 70, Appendix D.). This corresponds to their retention time and although the x-axis is just the name of the chemicals in number form, it may be regarded as an indication of molecular weight in this analysis.

It therefore follows that a catalytic run with a negative gradient (C, D and E on Figure 20) will give a less viscous pyrolysis liquid than that with a positive gradient (A and B). As a line approaches the origin, the more the run is like the blank run. A negative gradient, which crosses the x-axis (D), is more preferable than one above or below (C or E), as this indicates an increase in low molecular weight chemicals and a decrease in high molecular weight chemicals.

The catalysts producing this negative gradient, in order of significance, are FCAT-A, Y-zeolite, FCAT-C and BOD17. FCAT-A therefore produces the best change in molecular weight distribution and least viscosity, compared to the blank run. It may also produce the least stable pyrolysis liquid as shorter chain lengths polymerise faster, but that will depend on the reactivity of the end chains.

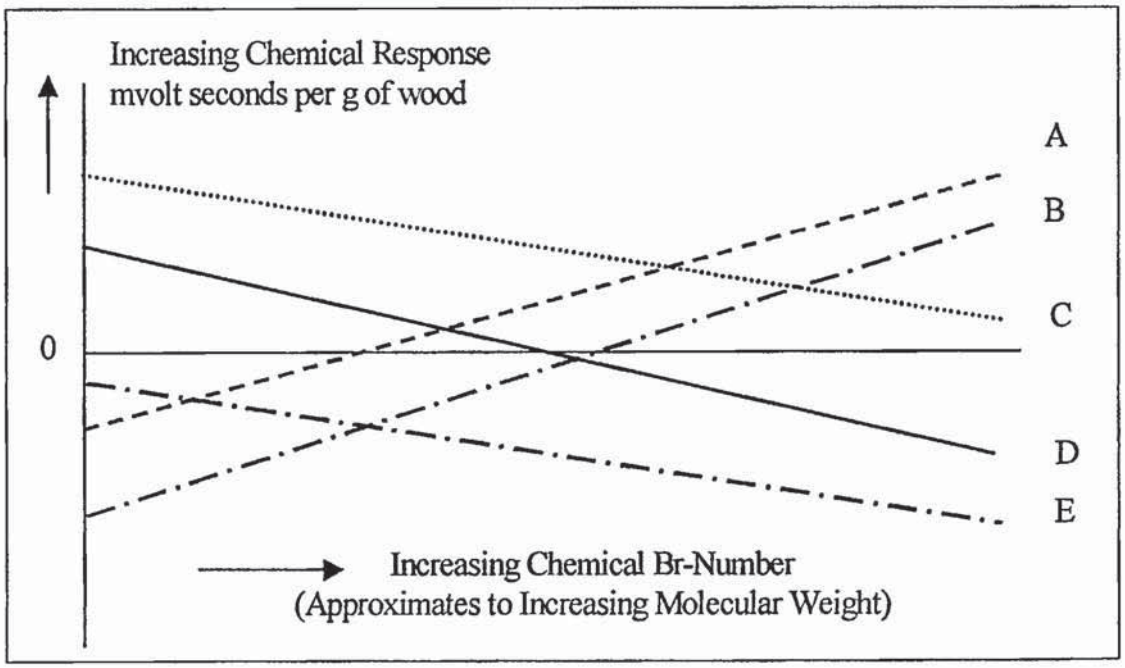

Figure 20 ***Hypothetical Trend lines of Peak Area Difference as Percentage of Blank***

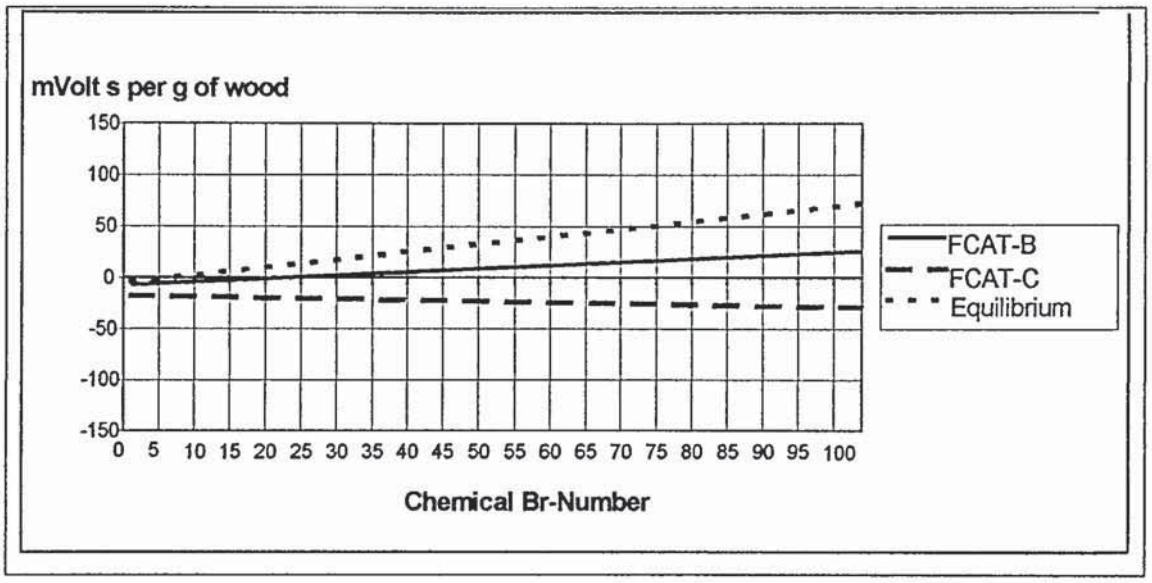

Figure 21 *Chromatograph Peak Area Difference as % of Blank as Linear Trendlines 1 of 2*

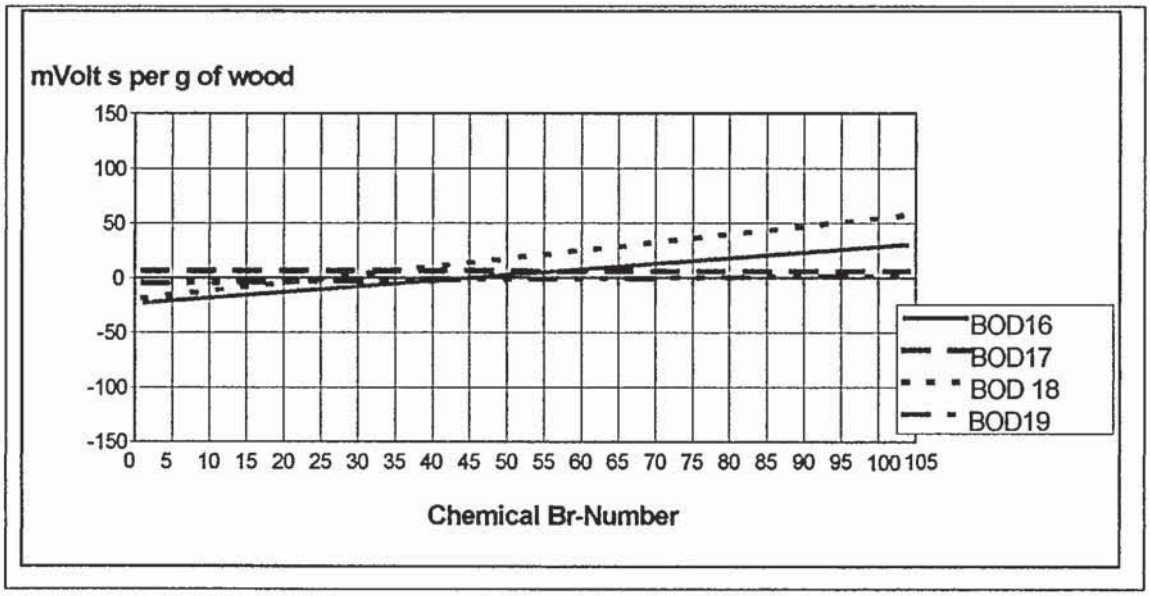

Figure 22 *Chromatograph Peak Area Difference as % of Blank as Linear Trendlines 2 of 2*

It is the quantity of specific chemicals produced in pyrolysis and also screening pyrolysis, that will influence the quality and stability of the pyrolysis liquid. As these chemicals are as yet unknown, another basis for assessing the screening tests and relating them to actual pyrolysis should be found. When pyrolysis using the catalysts

tested here has been done to produce enough pyrolysis liquid for the stability to be found, the significance of the screening tests will be more apparent and future screening will be more meaningful.

Sodium Montmorillonite clay calcined at 475°C (BOD17), un-calcined aluminium pillared clay (BOD19) and the chromium pillared clay, calcined at 600°C (BOD24), have low GC responses showing a small quantity of the selected chemicals produced. This may be due to absorption of the pyrolysis vapours onto the catalyst or to GC error or to few pyrolysis vapours being produced.

The similarity between pillared and un-pillared clays exhibited in BOD18, BOD21 and BOD32, is unexpected. X-ray diffraction analysis of these catalysts confirms they have been pillared successfully. This demonstrates that a change in pore size from 12.5 or 14 to 18 does not effect the chemicals produced in pyrolysis.

3.4 Catalysts Recommended Following Screening Experiments

The recommendations following the screening experiments are summarised in Table 14. The catalyst that performed the best was the Y-zeolite, which had the greatest pore size. If the degree of upgrading is related to pore size then finding a catalyst with an even larger pore size is suggested. This will help more branched molecules to reach the active sites and branching of the final product, reduced. Following the recent work of Wulzinger *(Wulzinger, 1999)*, slate and char should be tried as such a catalyst. Slate was found to be particularly interesting and is described in Section 4.5.3.

Table 14 Screened Catalysts Recommended for Further Testing

Recommended Catalyst	Comments
Y-zeolite	Expected to give the best quality liquid.
Equilibriated ZSM-5	Will help to demonstrate which chemicals are important to stability, although the equilibrated catalyst generally has the higher quantity of a chemical.
BOD20	The most interesting clay, aluminium pillared Sodium Montmorillonite clay, calcined at 490°C

The difficulty in using BOD20 is that it is an experimental non-commercial material. For this reason, commercially available material will be experimented with first in the larger 150 g/h apparatus. Those catalysts used in the main portion of experimentation are described in Section 4.5.

4 EXPERIMENTAL FAST PYROLYSIS

Two scales of fluid bed apparatus have been used for fast pyrolysis. The bench scale, small fluid bed, with a maximum feed rate of 150 g/h has predominantly been used. The larger laboratory scale of 1-2 kg/h has been used for a few specific examples of systems found to be successful on the smaller scale. Details of this reactor can be found in Chapter 8, page 199.

In both cases, the apparatus was configured and operated to derive predominantly the liquid product. Catalytic and non-catalytic experiments were then undertaken, utilising the results of the catalytic screening reported in Chapter 3.

4.1 Apparatus Description

The experimentation using the small fluid bed pyrolysis equipment can be divided into two sections:

1) The preliminary work began to establish that there was an effect on the process from the addition of catalysts. This was done before the screening tests were undertaken, to check the feasibility of catalyst addition to the catalytic pyrolysis process. Existing apparatus was used that followed the work of Hague and Cooke *(Hague, 1998; Cooke, 1999)*. These are referred to as the 'commissioning runs'.
2) The initial use of the apparatus identified shortcomings and problems, which resulted in modifications being made to its set-up. The second section of work utilised these changes. This latter and more substantial portion of work in the modified unit examined that catalytic effect on wood pyrolysis more closely.

Three liquid fractions (along with solid and gaseous products) were gained from each of the preliminary experiments. The number of products collected is determined by the configuration of the cooling and collecting portion of the apparatus (see Section 4.1.1.4). This is the main distinction between the apparatus used for these preliminary tests and those performed thereafter, in which one main product liquid and a small proportion of secondary liquid were collected.

4.1.1 Small Fluid Bed - Commissioning Configuration

The commissioning apparatus configuration is shown in Figure 23. It was of the 'Waterloo Fast Pyrolysis Process' type *(Scott, 1984, 1997).*

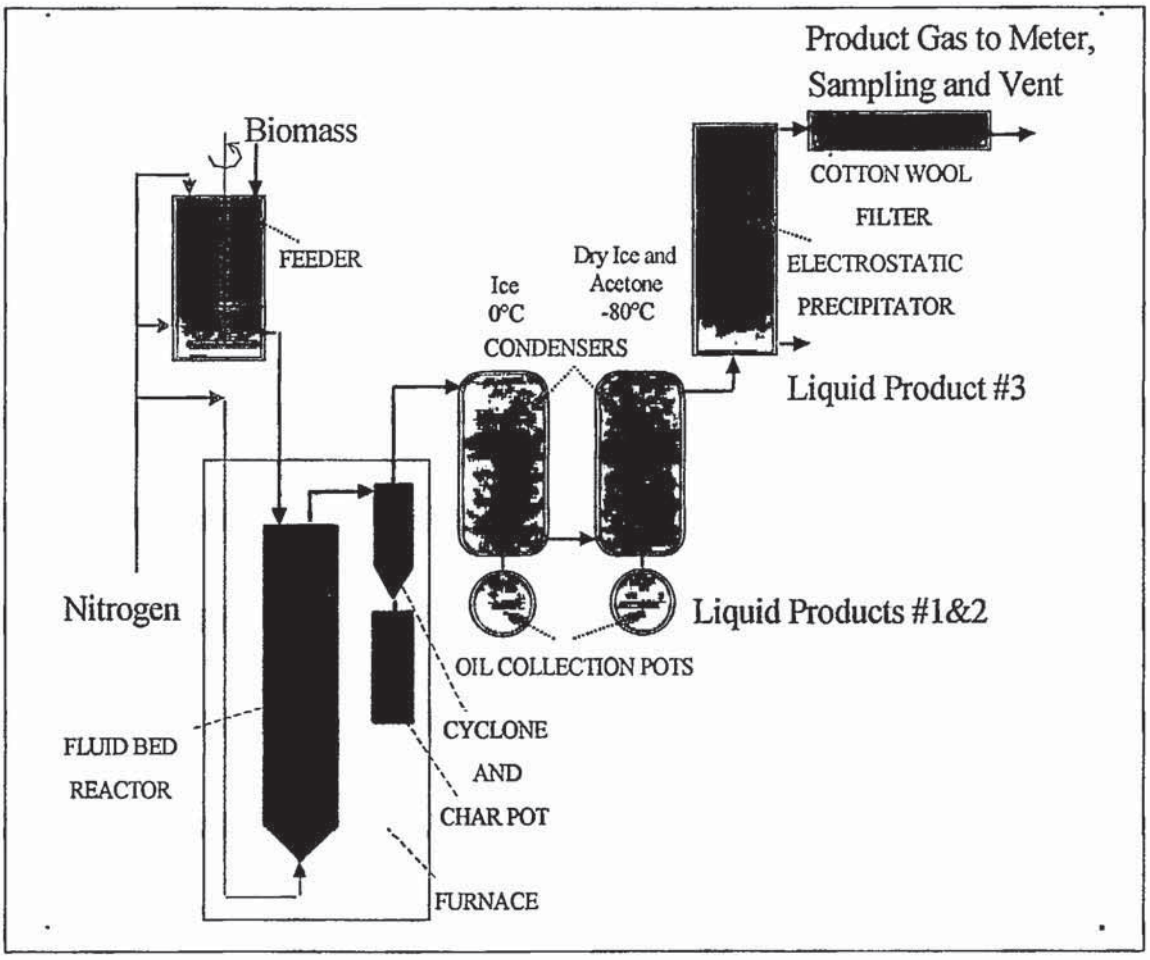

Figure 23 ***150 g/h 'Small' Bench Scale Fluidised Bed Fast Pyrolysis Reactor – Commissioning Configuration***

The initial apparatus used (Figure 23) consists of the following components: the feed system, the reactor, char separation, the liquid product collection system and residual gas handling. The structure and use of these components are described below.

4.1.1.1 The Feed System

A diagram of the feeder system is shown in Figure 24. It supplies approximately 1.5 litres of biomass feed to the reactor. Depending on the density of the feed this is

approximately 150 g. The cylindrical clear Perspex feed hopper (ID 63 mm) is charged from the top and sealed whilst preparing the apparatus. During a run, the level and behaviour of the feed can be observed (due to the clear nature of the feeder). This helps to ensure that mixtures of feed of different colours are fed evenly, red-brown slate and pale beige beech-wood particles for example. The inside of the feeder walls is smooth to enable efficient feeding and to allow easy cleaning which is done by blowing out remaining particles using dry pressurised air.

Biomass is entrained through a 1.7 mm diameter hole in a 3 mm external-diameter, 2 mm inside-diameter 'entraining tube' of stainless steel, which crosses the bottom of the feeder. The dimensions of the tube can be varied, but these diameters were found to be the most successful for the feed types used in this project. The location of the entraining tube is asymmetrically 10 mm from the centre of the cylinder and 25 mm above the bottom, so as not to impede the stirrer. Entrainment occurs because of nitrogen flow through this tube, known as 'entraining nitrogen', and blanketing nitrogen, known as 'feeder top nitrogen'. The latter applies pressure to the particles and the former transports them. The nitrogen is delivered to the feeder using polypropylene tubes. To facilitate entrainment, the feeder is stirred with a bi-paddle agitator. The solid tube paddles, each of 3 mm diameter and 60 mm length are set at right angles to one another. One lies above and one below the entraining tube. The speed at which the stirrer shaft turns can be varied from 83 to 638 rpm. It is normally set at 211, 290 or 365 rpm (this corresponds to settings 1, 1.5 and 2 on a scale between 0 and 10) to give the required feed rate.

The speed of the stirrer, the entraining nitrogen flow-rate and the feeder top nitrogen flow-rate can all be manipulated to alter the flow-rate of biomass to the reactor and the pressure across the feeder. Before using a feedstock, the feeder needs to be calibrated for its particular characteristics, such as particle size and moisture content. The stirrer speed and the feeder top nitrogen flow-rate affect the feed flow-rate the most. As all results are quoted using the *biomass flow-rate* rather than the total feed flow-rate, calibration is most important when using a mixed feed of biomass and catalyst, for example.

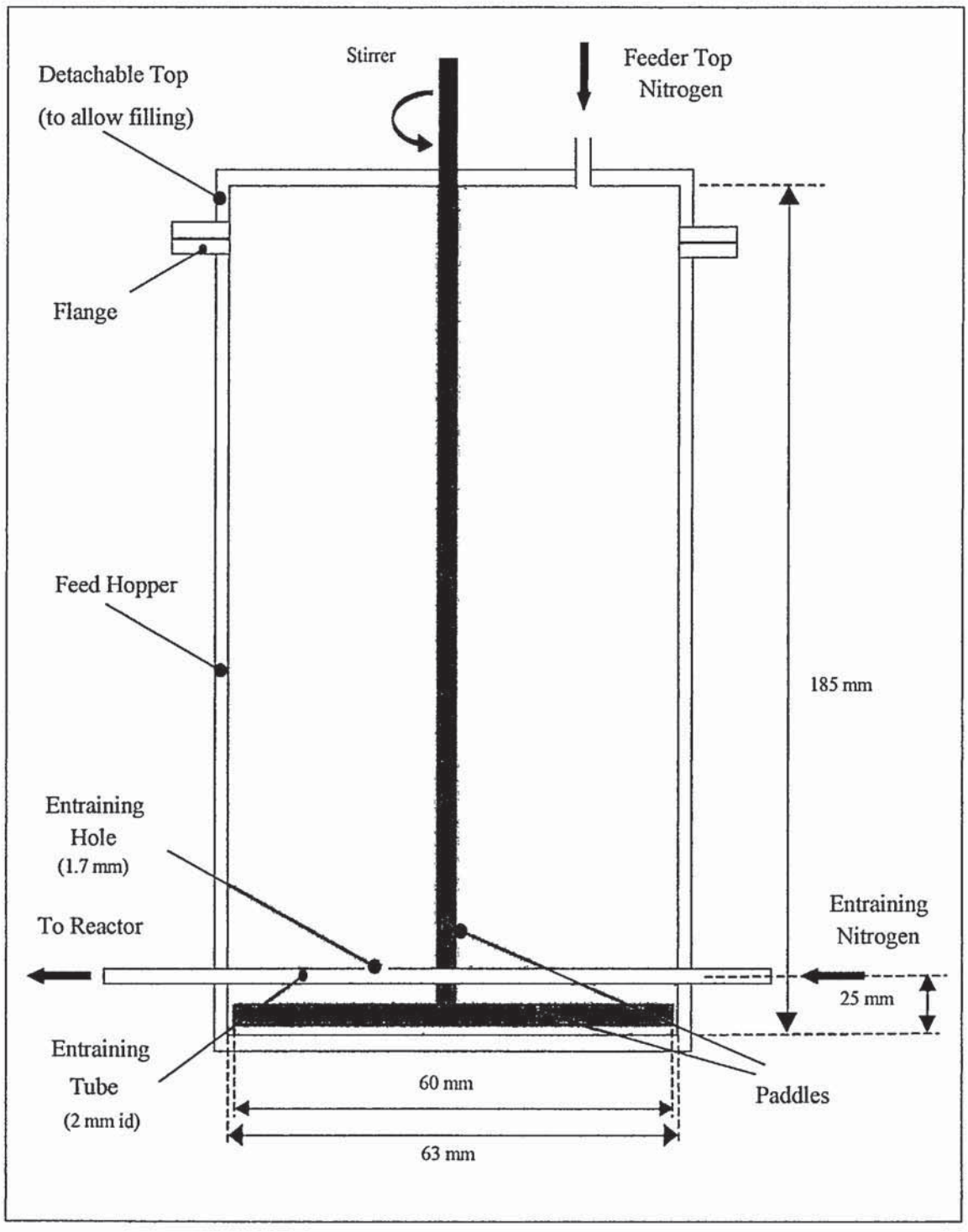

Figure 24 Detail of Feeder (not to scale)

When calculating the feed rate for an experiment, the weight change in the feeder over the length of time the apparatus was operated is used rather than a value found during calibration. This is done to improve accuracy. It therefore takes account of any

fluctuations, such as reduced nitrogen flow due to a slight pressure build up. This could be caused, for example, by a partial blockage such as tube narrowing due to char or tar deposition later in the process, particularly between the reactor and the cooling system. It is still necessary to calibrate the feeder to get an approximate flow-rate, to control it to the desired level during operation.

4.1.1.2 The Reactor

The fluid bed reactor is constructed of 316 stainless steel and has an internal diameter of 39 mm and is 260 mm high from bottom inlet to top. It is described in Figure 25. The top of the reactor can be removed to enable this bed to be changed.

Sand, of particle diameter 355 - 500 μm, is used as the fluid bed medium. 135 g of sand, which before fluidisation has a depth of 8 mm, is used. It is used because of its inert nature, being a silicate. The fluidisation properties are discussed in Section 2.5.2 and below in Section 4.1.1.2.1.

The biomass feed is pneumatically transported down the centre of the bed towards the bottom of the fluidising zone, using nitrogen. The feed tube is not solid as shown in Figure 25, but hollow as in Figure 26. This is to enable cooling of the top of the feed tube using air. This facility was not needed during these experiments, as it is to alleviate blockages that occur predominantly with pre-treated wood and were not a problem with this work.

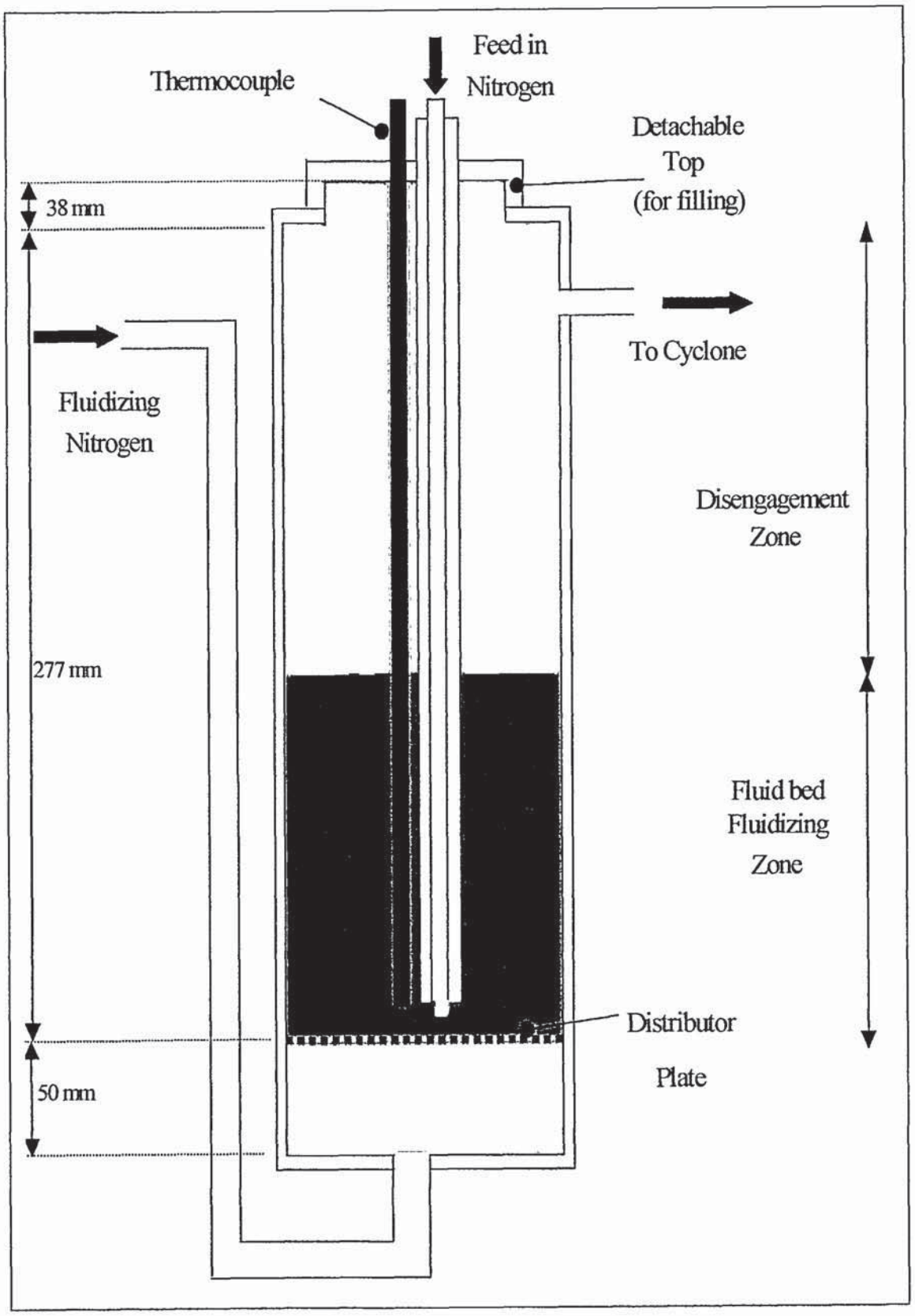

Figure 25 Detail of Reactor (not to scale)

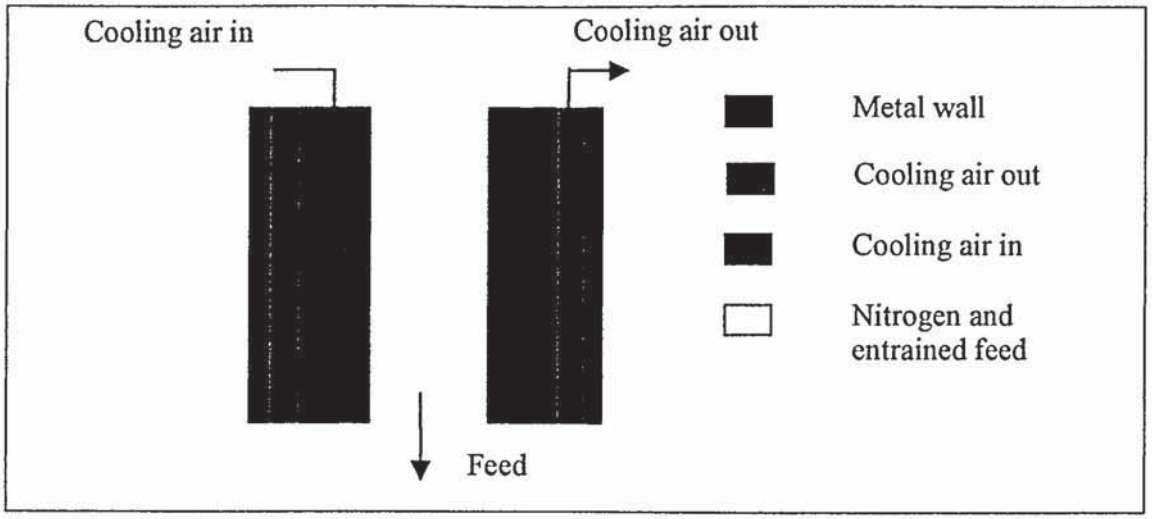

Figure 26 Detail of Feed Inlet Tube (not to scale)

The reactor sits in a furnace. The fluid bed is also heated and fluidised with hot nitrogen, which enters through a 100 μm pore sintered distributor plate, at the bottom of the bed. The nitrogen is heated by passing through the furnace in which the reactor sits. A K-type thermocouple inside the reactor is used to monitor the reactor bed temperature. This temperature is controlled by altering the furnace temperature. The reactor temperature, the furnace temperature and the set point temperature of the furnace are all monitored throughout a run and the set point can be manipulated to produce the desired reactor temperature. To help temperature control and reduce heat losses, the top of the furnace, through which the reactor assembly is suspended, is lagged with glass fibre. The glass fibre wads are covered in metal foil to reduce the 'skin-sensitising' hazard of the glass fibres. Any metal protruding from the furnace is also lagged.

The main body of the reactor is made up of a fluidisation zone and a disengagement zone, which is situated directly above it. It is operated so that the fluidising medium remains in the reactor, but char produced in the pyrolysis reaction is blown out. Upon fluidisation, the sand bed (fluidising medium) expands from a static height of approximately 40 mm to 100 mm.

4.1.1.2.1 Sand Fluidisation and Char Disengagement Calculations

The principles of fluidisation were introduced in Section 2.5.2 'Fluid Bed Technology'. Using Equation 4, (page 57) the minimum fluidising velocity of sand has been found in Table 15. This has been compared to the raw material, beechwood and, in Table 17, char. The calculations have been done at standard temperature and pressure (STP), which is 0°C and 1.013 bara. To find the velocity at which sand stays in the fluid bed and char is removed, the terminal falling velocity has also been found. (Char is tabulated in Table 17.)

Table 15 Fluidising Properties of Reactor Sand and Feed, Calculated at STP

Property	Sand (min)	Sand (av)[a]	Sand (max)	Wood[b] (min)	Wood (av)[a]	Wood (max)
Particle diameter, $d_{particle}$ (m) $\times 10^4$	3.55	4.28	5.00	3.15	4.08	5.00
Particle density, $\rho_{particle}$ (kg/m^3) $\times 10^{-2}$	25.0	25.0	25.0	8.0	8.0	8.0
Minimum fluidising velocity, u_{mf} (m/s)[c]	0.116	0.169	0.231	0.029	0.049	0.074
Bubbling velocity, u_b (m/s)	0.697	1.011	1.383	0.175	0.294	0.442
Reynolds number at u_{mf}	3.31	5.78	9.25	0.73	1.60	2.96
2/3 Galileo number[d]	5646	9861	15776	1261	2730	5043
log(2/3 Ga)	3.75	3.99	4.20	3.10	3.44	3.70
.: log Re_t[e]	2.04	2.17	2.30	1.56	1.84	1.97
.: Re_t	109.7	148.3	199.5	36.5	69.0	94.2
Terminal falling velocity, u_t (m/s)	3.85	4.32	4.97	1.44	2.11	2.35

Notes:
(a) Results based on average particle diameter
(b) Beechwood feed
(c) The following fluid (nitrogen) properties were used:
Density = 1.253 kg/m^3 (from 0.0782 lb/ft^3 at STP *(Perry, 1994#3)* as 1 kg/m^3 = 0.06243 lb/ft^3)
Viscosity = 1.56×10^{-5} kg/m s (from 0.156×10^{-4} Pa.s at 250 K *(Perry, 1994#5)*)
(d) Reynolds number at terminal falling velocity, Equation 6
(e) Tabulated in Coulson *(Coulson, 1991#2)*

The nitrogen velocity was therefore set at 0.5 m/s. This is greater than 0.2 m/s, allowing for all the sand to be fluidised, yet below 1.4 m/s, the minimum velocity at which beechwood would elute from the bed, should it not have reacted. It is below, yet in the region of the sand bubbling velocity (0.7 m/s), ensuring the bed is well mixed, but does not have portions void of particles (bubbles) moving through it. This nitrogen velocity corresponds to a nitrogen flow-rate of 12.7 l/m (the units of the rotameters) as

shown in Table 16. This is similar to the nitrogen flow-rate of 10.5 m/s used by Cooke on the same apparatus *(Cooke, 1999)*.

To ensure that the flow-rate is similar throughout all experiments, the fluidising properties of the proposed alternative fluidisation media should be checked and compared to sand. This is done in Section 4.4.2.

Table 16 Calculation of Nitrogen Flow-rate

Parameter	Value
Nitrogen velocity (m/s)	0.50
Reactor diameter (m)	0.0390
Reactor cross sectional area (m^2)	0.0012
Nitrogen flow-rate at 773 K (m^3/s)	0.0006
Nitrogen flow-rate at 273 K (m^3/s)	0.0002
Nitrogen flow-rate at 273 K (l/min)	12.70

The terminal falling velocity of the char should now be checked to ensure that it is removed from the bed (Table 17).

Table 17 Fluidising Properties of Char Produced in Reactor, Calculated at STP

Property	Char (min)	Char (av)[a]	Char (max)	Char[f]
Particle diameter, $d_{particle}$ (m) $\times 10^4$	3.15	4.08	5.00	1.50
Particle density, $\rho_{particle}$ (kg/m^3) $\times 10^{-2}$	6.00	6.00	6.00	6.00
Minimum fluidising velocity, u_{mf} (m/s)[c]	0.023	0.035	0.055	0.005
Bubbling velocity, u_b (m/s)	0.140	0.212	0.331	0.030
Reynolds number at u_{mf}	0.61	1.14	2.22	0.06
2/3 Galileo number[d]	1038	1936	3780	102
log(2/3 Ga)	3.02	3.29	3.58	2.01
.: log Re_t[e]	1.49	1.35	1.70	0.82
.: Re_t	30.97	50.35	80.72	6.56
Terminal falling velocity, u_t (m/s)	1.19	1.57	2.01	0.54

Notes: (a to e) Notes as Table 15.

(f) Particle diameter that gives a terminal falling velocity approximately 0.5 m/s

It can be seen from Table 17 that at a nitrogen velocity of 0.5 m/s, the char would not be removed from the bed. If a nitrogen velocity of 1.2 m/s were to be used, the nitrogen flow-rate required to produce this would be 30 l/min (Table 18). This is an unexpected result. The char particle size required to elute at 0.5 m/s was therefore calculated to be 1.5×10^{-4} m (Column five, Table 17).

To ascertain the suitable char particle size and therefore whether the wood feed required further grinding and sieving, the system was experimented-with. A flow-rate of 12.7 l/min was therefore used with a feed particle size of 3.15×10^{-4} to 5.00×10^{-4} m, to see if the char was removed at this flow-rate. It was found, by weighing the fluid bed and the cyclone, that the char was removed. It can therefore be concluded that the density of the char particles was found incorrectly (Section 2.5.2.3), *(Wunder, 1999)*.

Table 18 Calculation of Nitrogen Flow-rate

Parameter	Value
Nitrogen velocity (m/s)	1.20
Reactor diameter (m)	0.0390
Reactor cross sectional area (m^2)	0.0012
Nitrogen flow-rate at 773 K (m^3/s)	0.0014
Nitrogen flow-rate at 273 K (m^3/s)	0.0005
Nitrogen flow-rate at 273 K (l/min)	30.4

4.1.1.3 Char Separation

Also included in the furnace is the cyclone, through which the reactor products pass in order to be separated, and the char pot, used to collect the char. The diameter of the cyclone on entry is 25 mm. Like the reactor, the cyclone and char pot are constructed of 316 stainless steel.

Solid particles larger than 10 μm *(Sinnott, 1993)*, mainly char, are removed by the cyclone and collected in the char pot. The char has similar dimensions to the biomass particles from which it came (Table 15). No cyclone is 100 % efficient, but the efficiency is dependent on the diameter of the particles to be retained. Above particle diameters of 75 μm, the grade efficiency is practically 100 %, it is approximately 95 % at particle diameters of 45 μm, then the efficiency drops off dramatically to 10 % for 5 μm particles. The terminal falling velocity of the smallest particle that the cyclone will retain, is given by Equation 16 and Table 19 *(Coulson, 1991#3)* as 0.42 m/s. Without knowing the char density it is not possible to back calculate the smallest char particle, but 0.42 m/s corresponds to a diameter less than half the smallest wood particle size.

$$u_{t,\,dmin} = (0.2\times(A_i)^2 d_o \rho_{fluid}\, g) / [\pi Z d_t G]$$

Equation 16

Table 19 Numbers used for Calculation of Terminal Falling Velocity of the Smallest Particle Retained by Cyclone, Calculated at STP

Symbol	Parameter	Value
A_i	Cross sectional area of gas inlet (m^2)	1.227×10^{-4}
d_o	Diameter of outlet (m)	1.25×10^{-2}
ρ_{fluid}	Density of nitrogen[(a)] (kg/m^3)	1.253
Z	Length of cyclone (see Figure 27) (m)	7.5×10^{-2}
d_t	Diameter of cyclone body (see Figure 27) (m)	2.5×10^{-2}
G	Mass flow-rate of nitrogen[(a)] (see Section 4.1.1.2.1) (kg/s)	7.5×10^{-4}
$u_{t,\,dmin}$	The terminal falling velocity of the smallest particle which the cyclone will retain (m/s)	0.42

Notes: (a) Assume the nitrogen and pyrolysis vapours approximate to nitrogen properties

Figure 27 Cyclone Separator (Coulson, 1991#3)

4.1.1.4 The Liquid Product Collection System

The vapours, gases and aerosols then pass, by means of a transfer arm, to the liquid product collection assembly. This transfer section is insulated to minimise deposition of

char and tarry liquid before product collection. Pyrolysis vapours begin to condense below 400°C and could cause blockages that would halt operation.

The three-fraction liquid product system (shown in Figure 28) consists of two glass finger condensers and an electrostatic precipitator (EP). Glass is easy to clean and enables the vapours to be viewed. A reduction in observed vapour flow-rate or the cessation of vapour production are early indicators that something is wrong with a run and is therefore a safety feature.

The first condenser contains ice at 0°C and the second, dry ice at –80°C and acetone, to provide good contact between the dry ice and the condenser walls. The approximate internal surface area of each condenser in contact with the cooling medium is 3.15×10^4 mm^2. The internal diameter of each condenser is 45 mm; the curved portion at the bottom is a hemisphere and the internal length up to the hemispherical portion is 200 mm. This is compared to an improved cooling system in Section 4.1.2.1.

The product leaving the cyclone is in the form of condensable vapours, aerosols and non-condensable gases. The heavy ends of the condensable vapours are collected in the first condenser and the light ends and water in the second.

A round bottom flask attached below each of the condensers, known as oil pot 1 and oil pot 2, collects the liquid that runs down the inside of the condenser and can be removed after operation. The electrostatic precipitator (EP) has a tap on the base, allowing the liquid product remaining in the EP bottom, to be drained out after a run.

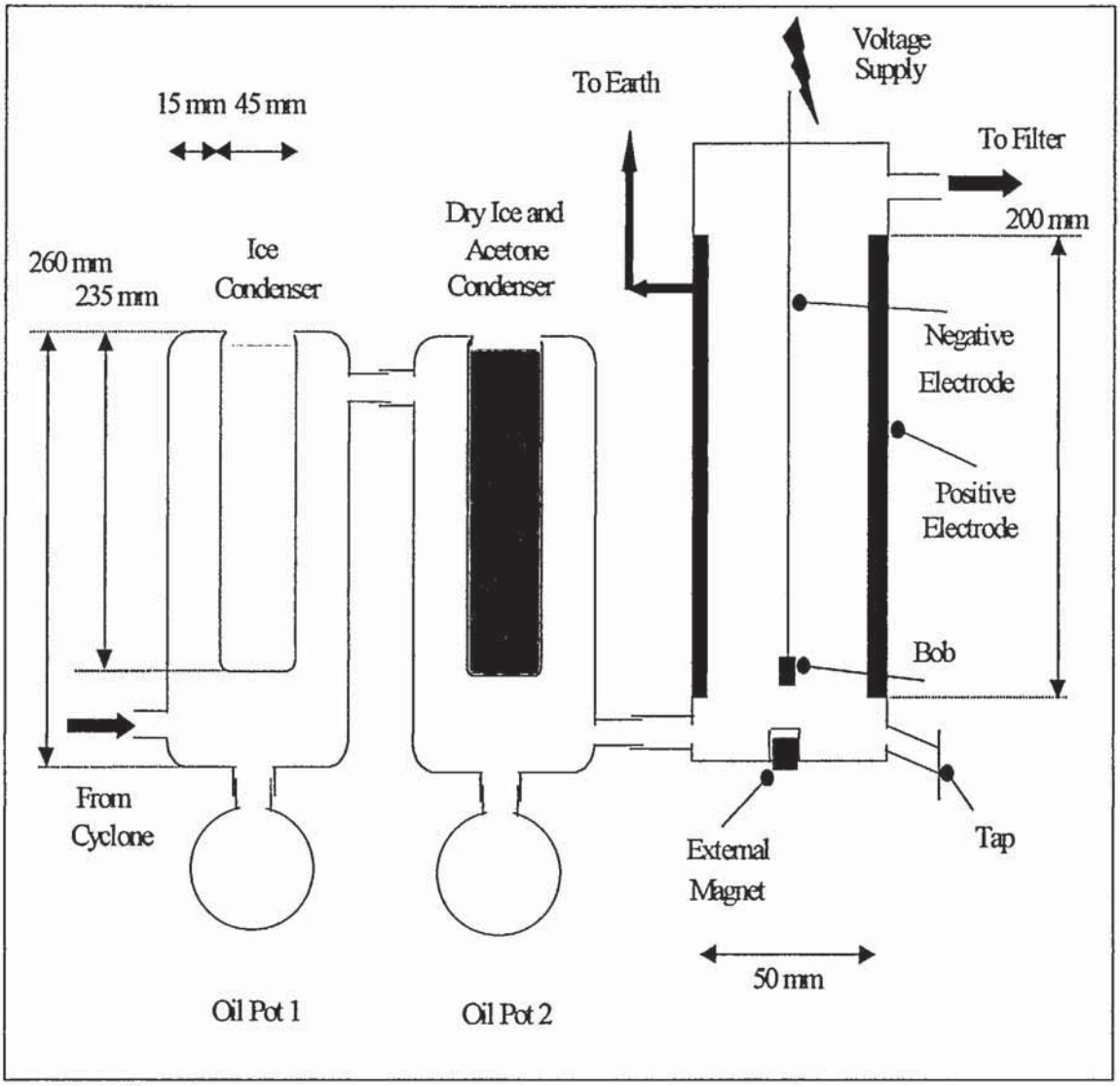

Figure 28 ***Detail of Liquid Product Collection System- Commissioning Configuration (not to scale)***

The EP is used to capture aerosols and particulates from the vapours. A significant portion of the liquid product would be captured in and eventually block the subsequent cotton wool filter, if the EP did not prevent these aerosols exiting with the gases. Within the 50 mm diameter glass housing of the EP is a circumferential metal tube which acts as a positive collection electrode. Hanging down the centre is a thin metal wire, weighted with a bob and held in position with an external magnet. This acts as the negative electrode and carries 15 kV. The aerosols become negatively charged due to the presence of ions in the space between the electrodes. They are attracted to the metal

tube, where they give up their charge, coalesce and run as a liquid to the bottom of the EP.

The voltage of the negative electrode should be high enough to remove all aerosols from the vapours, but low enough so that arcing does not occur between the electrodes, which would eliminate the electrostatic effect. The level was manipulated to 15 kV, which achieved both of these criteria successfully and all the vapours exited the EP aerosol free. This was confirmed by no discoloration or weight change in the cotton wool filter (Section 4.1.1.5).

4.1.1.5 Residual Gas Handling

The cotton wool filter protects the gas meter from condensable gases, particularly water, and particulates, especially char, in the event of the EP failing. The volume of gas exiting the apparatus is measured with a gas meter, then vented through the laboratory extraction system. As the mass of gas is needed for the mass balance the temperature of the gas into the gas meter is also measured. The type and quantity of each gas produced is also needed. An off-take allows samples of the product to be taken, by hand pumping the vented gas into small gas collection bombs. These were then sampled and then analysed after the experiment using gas chromatography. This is described in Section 4.7.2, Gas Chromatography.

4.1.2 Small Fluid Bed - Experimental Configuration

The apparatus described above was subsequently modified by the author, to collect a single liquid product and improve the mass balance closure. The production of a single liquid was necessary because of the unsuccessful re-mixing of the product liquids from the two oil pots and the electrostatic precipitator, which failed to become a homogeneous liquid on reintroduction with one another. As the amount of liquids collected (approximately 5 ml, 2 ml and 10 ml respectively) was unhelpfully small, physical and chemical testing of them was limited. Having a single resultant pyrolysis liquid enables testing to be done on a more substantial, single sample. Thus a greater number of tests can be done and they need not be repeated on three different liquid fractions. This altered apparatus is described in Figure 29. A photograph of the

apparatus is shown in Figure 30. It is shown set up ready to use, with some of the aluminium foil-covered insulation removed for improved viewing.

The details of the experimental configuration remain the same as the commissioning configuration in the areas of the feed system, the reactor and char separation. A description of the liquid product collection system and the residual gas handling, the changed areas of the apparatus, follows.

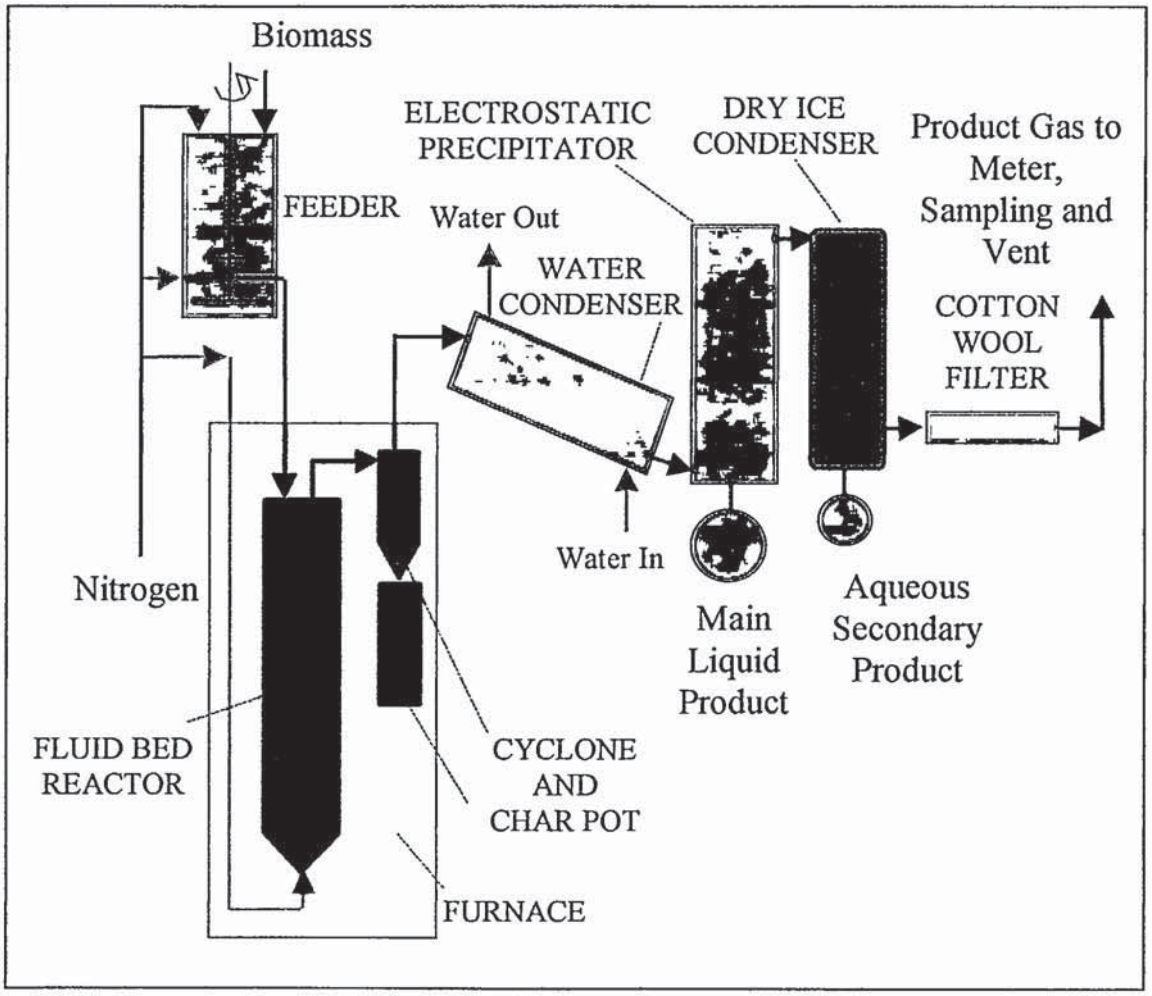

Figure 29 ***150 g/h Single Product 'Small' Scale Fluidised Bed Fast Pyrolysis Reactor - Experimental Set Up***

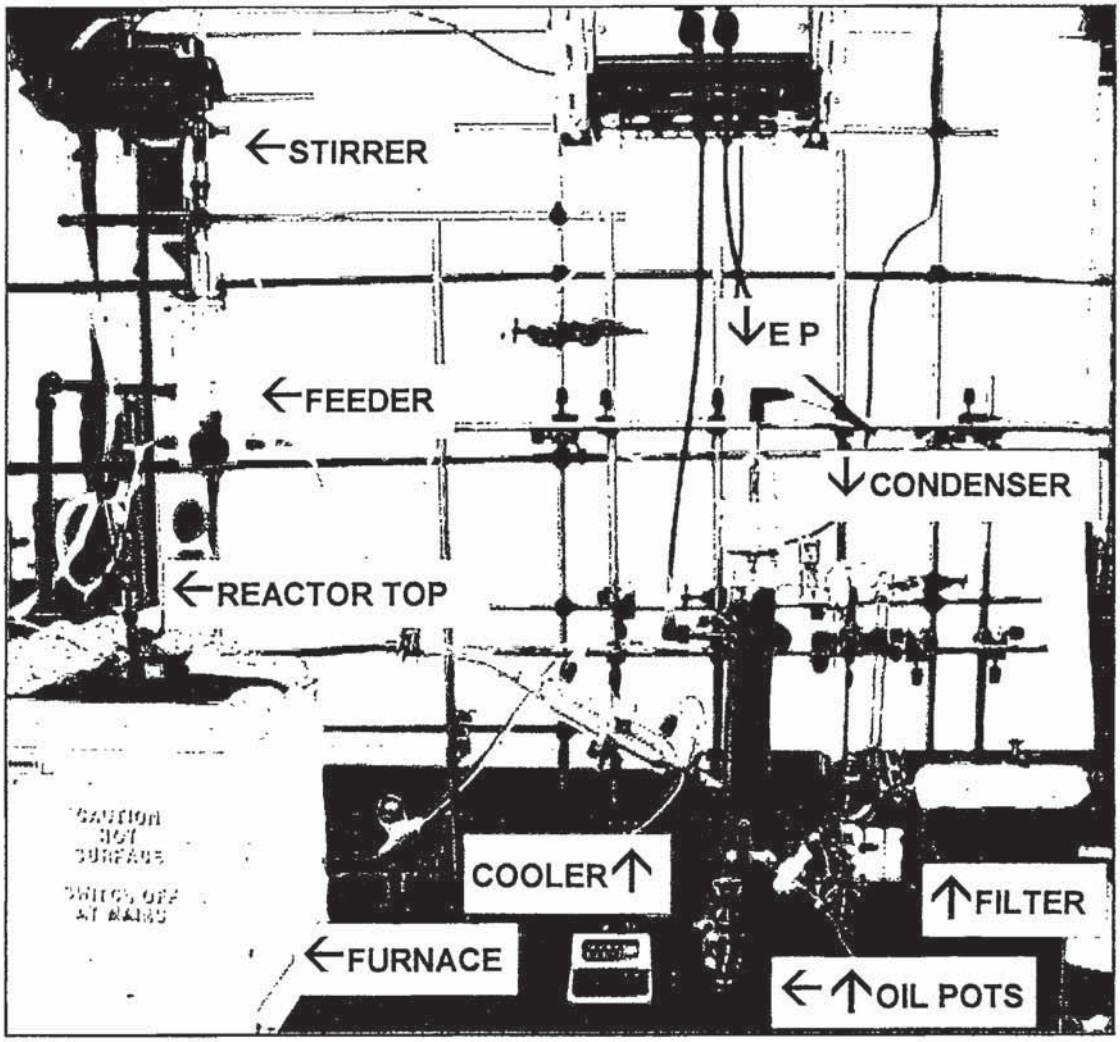

Figure 30 ***150 g/h Single Product 'Small' Scale Fluidised Bed Fast Pyrolysis Reactor – Experimental Set Up***

4.1.2.1 The Liquid Product Collection System

Attaining a single product liquid was achieved by allowing the condensed liquid to flow into the bottom of the electrostatic precipitator, rather than being collected separately. In the bottom of the EP the condensed liquids combine with those draining down it that have been electrostaticaly precipitated. The resultant liquid is then collected in a detachable oil pot beneath.

To facilitate liquid flow to the electrostatic precipitator, a 'Davies type' double surface condenser, mounted sloping at 60°, was used to replace the two finger condensers in the previous configuration. This design of condenser was chosen because of the high

contact area between cold and hot process sides, but with a low tortuosity of flow paths. Although a condenser, such as a 'Liebig type' condenser may have a greater contact area between cold and hot process sides, the helical design presents many contact points for char or tarry liquid to be deposited. A 'Davies double surface' type condenser is therefore less prone to blockages and considerably easier to clean (Figure 31). The internal surface area is 1.7×10^{-2} m^2 *(Fischer, 1997)* which compares to 3.15×10^{-2} m^2 in the commissioning configuration. This is compensated for by having a flowing rather than the static cooling medium.

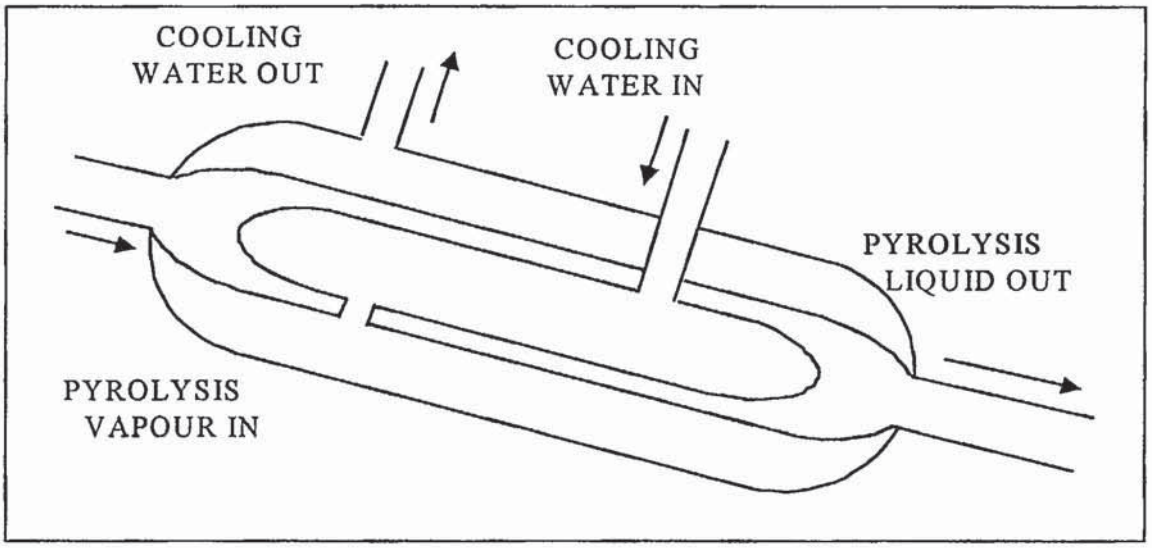

Figure 31 Detail of Davies Double Surface Condenser (not to scale)

The cooling-side liquid used in the condenser was tap water. Although ample cooling could be provided by a dedicated chiller unit, trials were done using tap water to reduce the cost of the process and make potential scale-up more economically viable. A 15°C water flow-rate in the region of 1 - 2 l/min was found to provide sufficient cooling to allow the electrostatic precipitator to work effectively. To test the temperature at which the main liquid product was collected, a series of experiments were done with a thermocouple introduced in the electrostatic precipitator. (These runs are named EHS20 to EHS26). The thermocouple was located between the exit from the condenser and the entrance to the oil pot. It was found that this flow-rate of water could achieve product vapour/aerosol temperatures between 23 - 35°C. The average temperature was 29°C.

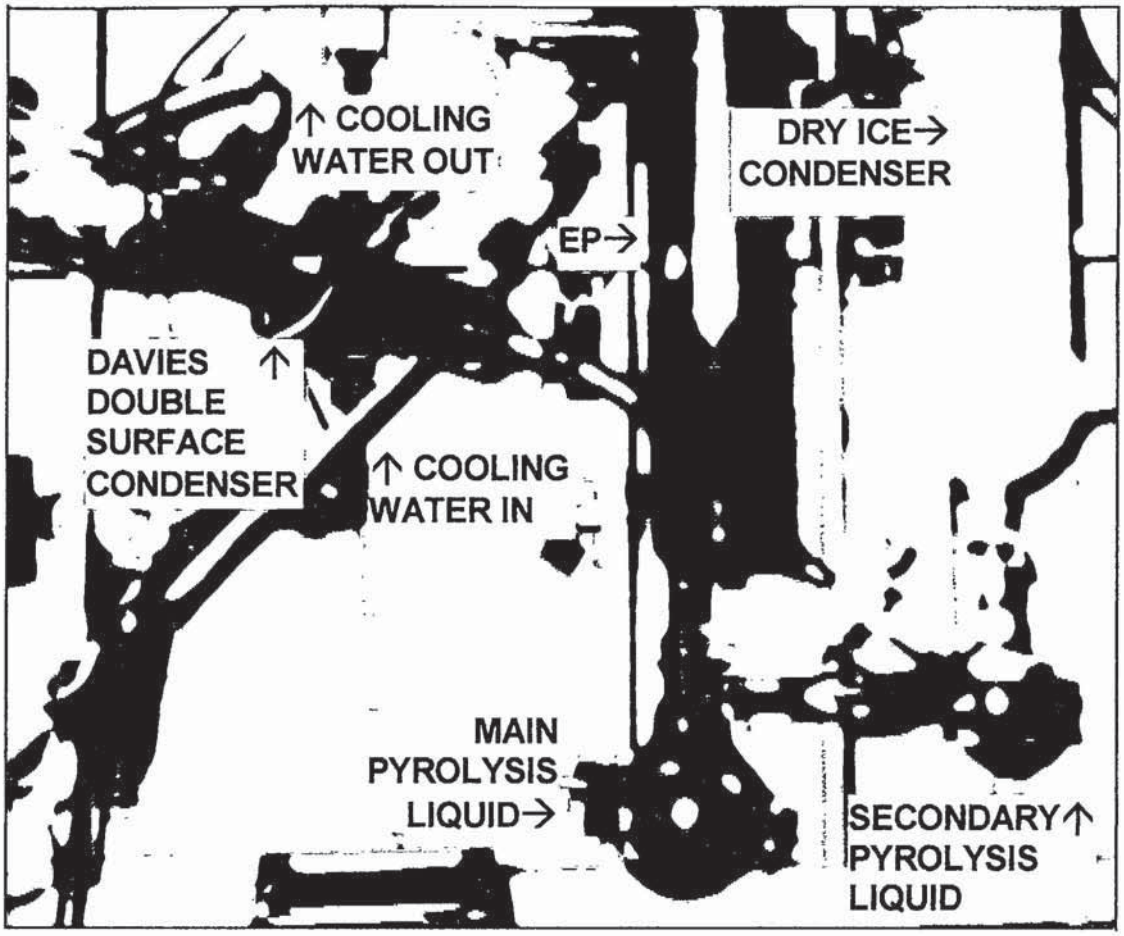

Figure 32 ***150 g/h Single Product 'Small' Scale Fluidised Bed Fast Pyrolysis Reactor – Cooling and Liquid Collection System After Running***

Using the new condenser for cooling the process no longer contained an element of cooling below 0°C (previously supplied by the dry ice–acetone condenser). The cotton wool filter was having to absorb water and aqueous substances that would have previously been collected prior to the cotton wool filter in the apparatus. Cotton wool is used dry from the oven and acts as a physical barrier. This could have become a limiting factor to the process - a run would have to be terminated before the cotton wool was saturated so no damage would be done to the gas meter. For this reason a dry ice–acetone finger condenser was added to the process after the electrostatic precipitator. This element only collects a small amount of liquid (9 wt% of liquid collected). It is thought of as a secondary liquid and it enables the length of time an experiment proceeds for, to be unlimited by saturation of the cotton wool filter. The secondary liquid is collected and analysed in the same way as the main liquid, only for

completeness of the mass balance. It represents the fraction of the product that would normally be recycled and/or vented in a full-scale system. The cooling and liquid collection system is shown in Figure 32.

4.1.2.2 Design of Condenser

To estimate the cooling desired for the 'new' condenser, the heat removed in the commissioning set up was calculated. At the start of the run, the heat transfer load, Q, is calculated using Equation 17, assuming that the method of heat transfer is conduction. As the ice and dry ice are continually topped up, it is assumed that this heat transfer profile is consistent throughout the experimental run.

$$Q = (k_G / x_G) \times A_T \times (T_{hot} - T_{cold})$$

Equation 17

Equation 17 can be applied to both condensers to calculate the total heat load of the cooling system. The inlet and outlet temperatures (T_{Pin} and T_{Pout}, see Figure 33) are 500 and 36°C respectively, but the intermediate temperature, T_{Pmid} is unknown and is estimated to be 300°C. The thermal conductivity of borosilicate glass is 1.1 W/m K *(Perry, 1984 #4)* and the thickness of the apparatus walls is 0.5 mm. The area of heat transfer is 3.15×10^4 mm^2. The heat load for the two condensers combined is Equation 18 giving 60.98 kW. This is based on the change in temperature only and does not account for the change in pyrolysis product phase. To do this the specific heat capacity of pyrolysis liquid would have to be found. This method is therefore only to be a guide to help select a correctly sized condenser and water flow-rate.

$$Q = (1.1 \times 3.15\times10^{-2} / 5\times10^{-4}) \times [(500 - 0) + (300 - (-80))] = 60.98 \text{ kW}$$

Equation 18

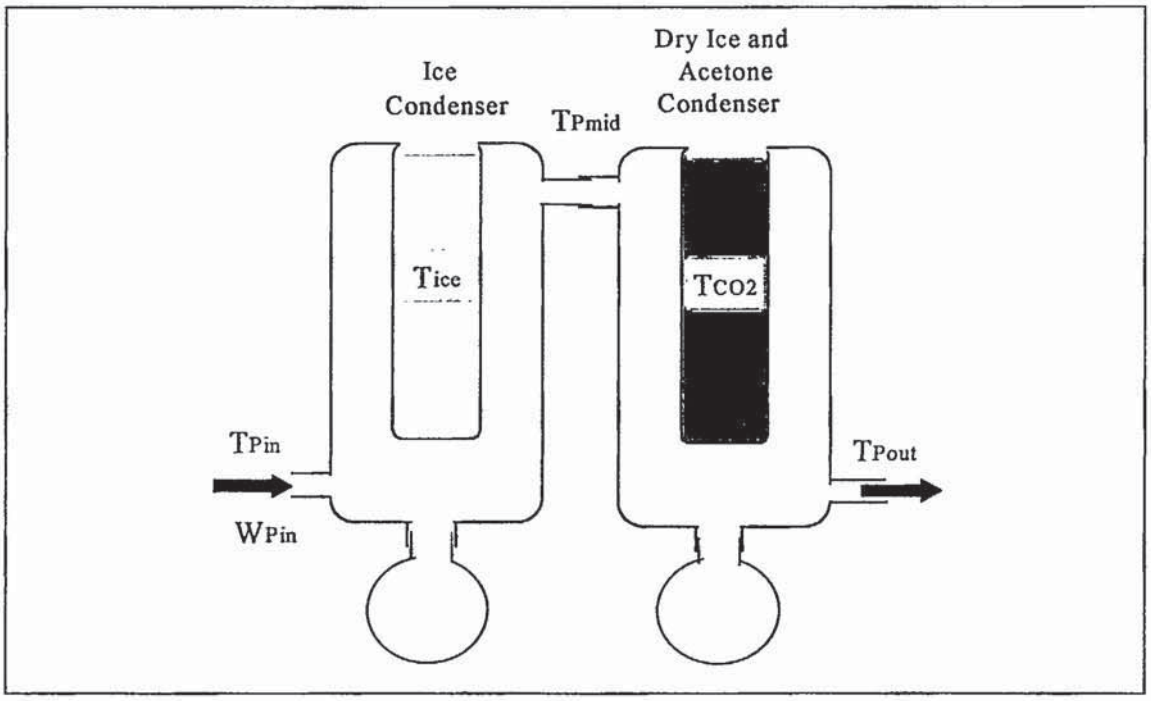

Figure 33 ***Liquid Product Condensing System- Commissioning Configuration for Heat Transfer Calculations***

To find the corresponding flow-rate of water in the single product system, Equation 19 and Equation 20 have been used. The positions of the temperature points are shown in Figure 34.

$$Q = W_W \times Cp_w \times \theta_{lm}$$

Equation 19

$$\theta_{lm} = [(T_{Pin} - T_{Wout}) - (T_{Pout} - T_{Win})] / \ln[(T_{Pin} - T_{Wout}) / (T_{Pout} - T_{Win})]$$

Equation 20

The outlet temperature of the water is unknown and has been estimated as 2°C greater than the inlet temperature of 15°C. At 15°C, the specific heat capacity of water is 4.186 kJ/kg K *(Rogers, 1988)*. The pyrolysis liquid exit temperature was measured as 36°C when the inlet temperature was 500°C. This gives a log mean temperature difference of 147.3 K (Equation 20). The mass flow-rate of water was found to be 0.0989 kg/s (Equation 21). This corresponds to a volumetric flow-rate of 5.80 l/min (Equation 22), where the density of water (ρ_W) at 15°C is 0.01704 bar which corresponds to 1704 N/m^2 *(Rogers, 1988)*.

$$W_W = 60984 / \{4.186\times10^3 \times [(500 - 17) - (36 - 15)] / \ln[(500 - 17) / (36 - 15)]\}$$
$$= 0.0989 \text{ kg/s}$$

Equation 21

$$F_W = W_W / \rho_W = 0.0989 / 1704 = 5.80\times10^{-5} \text{ m}^3/\text{s} = 5.80 \text{ l/min}$$

Equation 22

To check that the flow in the condenser is turbulent, the Reynolds number (Re) has been calculated (Equation 23 to Equation 25, Table 20 and Figure 34). A value less than 2000 shows the flow to be lamina and the heat transfer is not as efficient under these conditions. It was found that at all positions in the condenser, at a flow-rate 0.0989 kg/s, the flow regime was turbulent.

$$Re = (\rho_W u l) / \mu_W$$

Equation 23

$$u = W_W / \rho_W s$$

Equation 24

$$Re = (W_W l / s) / \mu_W$$

Equation 25

Table 20 Calculation of Tube Flow Area at Different Condenser Positions

Position in Condenser	Calc for flow area, s	Value for d (m)	Result for s (m^2)	Character-istic length, $l^{(a, b)}$	Re No.	Turbulent / Laminar
Entrance and exit (tube)	$\pi d^2 / 4$	5×10^{-3}	1.96×10^{-5}	$l = d$	33213	Turbulent
Inner section (tube)	$\pi d^2 / 4$	11×10^{-3}	7.85×10^{-5}	$l = d$	16577	Turbulent
Outer section (annulus)	$\pi(D^2-d^2)/4$	25×10^{-3} 18×10^{-3}	3.01×10^{-4}	$l = D - d$	3028	Turbulent

Notes: (a) *(Butterworth, 1977)*

(b) d is diameter or inner diameter. D is outer diameter

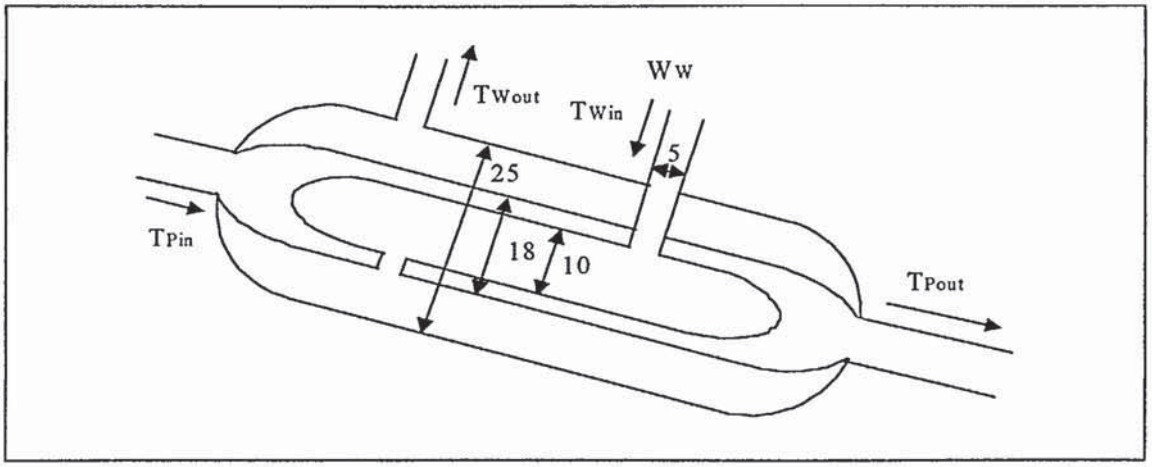

Figure 34 ***Liquid Product Condensing System- Experimental Configuration for Heat Transfer Calculations (measurements to nearest mm)***

4.1.2.2.1 Comparison of Heat Transfer Design to Actual Condenser Operation

Assumptions were made during the design of the single condenser. On operating the condenser that was designed, the outlet temperature can be measured and the heat transfer re-calculated to confirm the assumptions. A cooling water flow-rate of 2 l/min at 15°C was found to result in an exit temperature of 29°C, when the inlet temperature was 500°C. A 2°C increase in cooling water temperature across the condenser was confirmed. Using Equation 19 and Equation 22, the heat transfer load was found to be 91.166 kW (θ_{lm} = 132.4 K, W_W = 0.1645 kg/s). This result can be used in three ways:

1) The assumption of the intermediate temperature in the commissioning configuration is correct. The heat associated with the change in pyrolysis product phase (heat of condensation) is therefore (60.98 – 91.166), that is -30 kW.
2) The assumption of pyrolysis heat of condensation being zero is correct. The intermediate temperature in the commissioning configuration is therefore 735.5°C. This was found using the Excel 'goal seek' tool and shows that the initial estimate was low at 300°C.
3) The difference in heat load is a combination of the intermediate temperature being lower and some energy being used for the heat of condensation. This is the most realistic answer, but is not quantifiable. With the difference in design and operation being so small, this has little impact.

The mass flow-rate used in operation does not differ from the design so resulting in a turbulent flow regime.

4.1.2.2.2 Estimation of Heat Transfer Coefficient

The quantification of the designed condenser with operation allows the heat transfer coefficient, U, to be calculated using Equation 26. It was found to be 11.06 kW/m^{2}K (Equation 27).

$$Q = U \times A_T \times (T_{hot} - T_{cold})$$

Equation 26

$$Q = 91.166 \times 10^3 / (1.7 \times 10^{-2} \times (500 - 15))$$

Equation 27

4.1.2.3 Residual Gas Handling

In addition to the changes to the product collection assembly, the method of analysing the product gases was upgraded. A dedicated on-line gas chromatograph was installed. It sampled the gas continuously and could give detailed compositions of the product gases throughout the experimental run. (See Section 4.7.2, Gas Chromatography, for further details)

4.2 Biomass Feed, Preparation and Handling

Two biomass feedstocks have been used in this project:

1) Pinewood (*Pinus Sylvestris*). Pine is a coniferous softwood tree, known for its gummy resin. It was supplied by Union Electrica Fenosa of Spain and was used because pinewood had previously been found to be a successful feed for this apparatus and followed on from previous work *(Cooke, 1999)*. It was chosen by the partners in the European Commission funded project 'contract JOR CT95-0081' for whom this work was undertaken. Pinewood was used for the commissioning runs and micro-reactor screening only.
2) Beechwood (*Fagus Sylvestris*), from 'J. Rettenmaier and sons' in Germany, was used when the partners in the European Commission funded project changed the

species of wood to be used. This makes the work directly comparable with the closest piece of work being undertaken elsewhere, that of Wulzinger in Hamburg, Germany *(Wulzinger, 1999)*. The same supplier of wood of the same size and moisture content was used. Beechwood was used for the experimental runs.

The resultant pyrolysis liquids from pinewood and beechwood have previously been found to be chemically similar *(Meier, 1997#2)* and are shown in Table 21. The results from each wood type can therefore be compared.

Table 21 ***GC Analysis of Pinewood and Beechwood Fast Pyrolysis Liquids (Meier, 1997#2)***

It was necessary to double-grind and double-sieve the pinewood. A Fritsch cutting mill with a 500 µm screen was used to grind the wood. Grinding the wood twice reduced the number of 'needle' shaped particles. Needle-shaped particles, although they have one side that will fit through the screen used for sieving, have the drawback that their rectangular nature means they are larger than the screen size when orientated differently. This causes problems with the feeder and reactor feed tube, which can be reduced by double-grinding the wood as this reduces the length of needle-shaped particles and makes them closer to square in shape. The beechwood was prepared by the supplier to have the desired particle size and shape.

It was not necessary to dry either wood before pyrolysis as they were both found to have an acceptable 4 to 9 % water content (the limit being 10 %) (See Section 4.6).

4.3 Apparatus Operation

4.3.1 Preparation

The reactor is set up by first applying anti-seize compound to the steel 'Swagelok' joints between reactor top and body, char-pot and cyclone and cyclone top and tube-ex-cyclone. These component parts are then weighed. 135 g of clean, acid washed, furnace dried dry sand (particle diameter 355 - 500 μm,) are added into the reactor body. A wire rod is inserted into the reactor top feed tube before fitting top and body together to prevent the feed tube being blocked with sand. All components are screwed together and closed tight with a spanner. The complete reactor is weighed and placed in the furnace. It is then insulated around the reactor top and between the cyclone and the cooling system.

All glassware is clean and oven-dried. Glass-glass joints are greased with vacuum grease and the glass joint to the metal socket with 'Silver Goop'. The cotton wool filter is packed with oven-dry cotton wool. All glassware is weighed, assembled and clamped in place, ball and socket joints are held tight with metal clips.

To operate the apparatus, the feeder is first calibrated so that it feeds at a rate between 50-150 g/hr. The feeder is then weighed.

4.3.2 Start Up

If using the on-line GC apparatus to monitor the exit gas composition, it is heated up at least one hour before a run starts and calibrated before commencing the run. The reactor furnace is switched on and the set point reactor temperature, to which the furnace temperature controls, is input. The heat-up time is typically one hour.

When the reactor has reached operating temperature a small flow-rate of fluidising nitrogen is put through it to ensure uniform heating. The wire rod blocking the feed tube is kept in at this point. Dry-ice and acetone are put in the secondary condenser (and ice is put in the first condenser when a finger condenser is being used as in the pre-modification set-up). When the reactor temperature has re-equilibrated, the nitrogen

flow is turned off, the wire removed from feed tube and the feed tube connected from the reactor to the feeder. The feed tube will now not be blocked by sand as there will not be fluidising nitrogen in the bed without a flow down the feed tube.

The following are turned on: the water supply to the first condenser (in post-modification set-up); the electrostatic precipitator (EP); the entraining nitrogen first, followed by the fluidising nitrogen and the feeder top nitrogen. If using the on-line GC apparatus, it can be started once the experimental condition flow-rates have been established. When the GC is steady and the base line is satisfactory, the stirrer can be started. At this point, the time and the gas meter reading are noted. Biomass should now be feeding into the fluid bed and smoke-like vapour should be visible in the condenser.

The following are recorded at regular intervals: the furnace set point, the furnace temperature, the reactor temperature, the feeder pressure drop, the reactor pressure drop and gas meter readings. This is done using the 'results proforma' shown in Appendix B (see also Table 22). The marked reading error on the pressure gauges ('pressure drop across feeder' and 'pressure drop across fluid bed') is due to vibration of the indicating needle during reading measurement.

During the run, it may be necessary to add more dry ice to the condensor. The EP voltage and amperage, the temperature into the gas meter, the nitrogen flow-rates and the degree of saturation of the cotton wool filter are also periodically checked.

Table 22 Readings Taken Throughout an Experimental Run

Parameter	Example Reading[a]	Frequency of Reading	Accuracy of Reading
Time from start of experiment	1 minute	0-20 minutes, every minute, then every 5 minutes	± 5 seconds
Time of day at start	15:40	Once	± 15 seconds
Time of day at end	16:20	Once	± 15 seconds
Reactor temperature	449°C	As time, 0-20 minutes, every minute, then every 5 minutes	± 0.5°C
Furnace temperature	463°C	As time, above	± 0.5°C
Furnace set point temperature	460°C	As time, above	± 0.5°C
Pressure drop across feeder	34 inches of water	As time, above	± 2 inches of water
Pressure drop across fluid bed	29 inches of water	As time, above	± 2 inches of water
Volume of gas passed through gas meter	38167 dm^3	As time, above	± 0.5 dm^3
Entraining nitrogen flow	1.5 l/min	Every 10 minutes	± 0.1 l/min
Feeder top nitrogen flow	1.2 l/min	Every 10 minutes	± 0.05 l/min
Fluidising nitrogen flow	10.0 l/min	Every 10 minutes	± 0.5 l/min
Stirrer speed	1.25 graduations	Once	± 0.25 graduations
Cooling water flow-rate out	1800 ml per 89.36 seconds	Once	± 10 ml ± 0.05 seconds
Cooling water temperature	22°C	Once	± 0.5
EP voltage	7 kV	Once	± 0.25 kV
EP amperage	0.01 mA	Once	± 0.002 mA

Notes (a) Figures taken from run named 'EHS42'

4.3.3 Problems

If during the run the feed tube becomes blocked, all gas flows are turned off, the clock stopped and the gas meter reading noted down. Once the pressures have dropped to zero the flexible tube is removed from the reactor top and any biomass removed from it. Any biomass removed is weighed so that it can be accounted for in a mass balance. It may also be necessary to use a wire rod to clean the feed tube to remove any charred feed. The reactor is then restarted as per start up, noting gas meter and time readings.

4.3.4 Shutdown

To stop the run, the feed to the reactor is halted by turning off the stirrer. The time and gas meter reading are noted, the furnace switched off and the fluidising nitrogen stopped before the feeder top and entraining nitrogen flows are stopped. The apparatus is left to cool, normally overnight, by inserting the rod down the reactor feed tube (this prevents sand blocking the feed tube while no feeding nitrogen is flowing) and restarting the fluidising nitrogen at a low flow for a few hours. This is then stopped and the apparatus sealed with bungs. It is best to separate the glass ball from the metal socket (between the transfer arm from the cyclone and the condenser arm to the condenser) as heavy residue can sometimes stick these together.

4.4 Incorporation of Catalyst into the Process

There are four conceptual reactor configurations that can be used to incorporate catalyst into fluid bed pyrolysis equipment. These are illustrated in Figure 35 below and are:

A) 'Co-feeding' biomass and catalyst, either separately in a dual feeding mode or in a mixed feed into the pyrolysis fluid bed. This simulates a fluidising catalytic cracking (FCC) unit such as those used to refine crude oil, where the catalyst is regenerated and recycled.

B) Including catalyst as the whole or part of the fluidising bed - 'in-bed'. This is equivalent to an FCC unit that runs until the catalyst is 'spent'. The catalyst may be subject to rapid coking deactivation or poisoning. This mode of operation can also be used to find the point at which regeneration of a catalyst would be necessary by running for different lengths of time and examining the catalyst

activity. This can be done using standard reactants that produce a known yield with a fully active catalyst. The surface area or pore size can also be examined using BET (Brunauer, Emmet and Teller equation for multilayer adsorption) *(Allen, 1997)* and SEM (Scanning Electron Microscopy).

C) 'Close-coupled' in-bed reactions where the catalyst is held in the fluidising zone of the reactor using a mesh plate or cage.

D) Utilising a 'close-coupled' catalyst in a secondary reactor with either a fixed or fluid bed. This can be orientated vertically or horizontally. This is an alternative method of incorporating catalyst, although similar to C), the catalyst is in the system after char removal. The use of a secondary reactor has the advantage of temperature control that is independent of the first reactor.

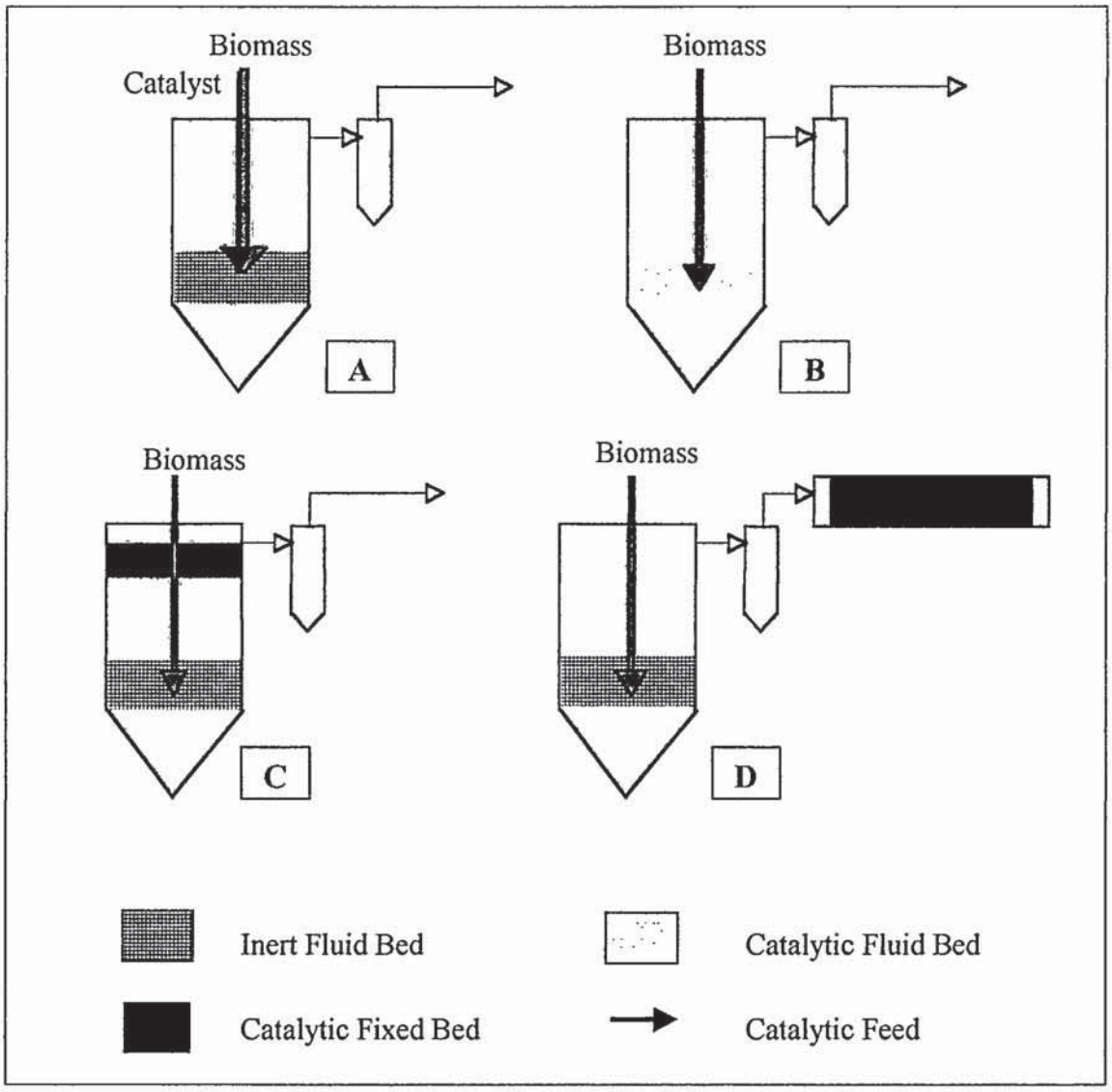

Figure 35 Catalyst Configurations Showing Reactor and Cyclone

4.4.1 Co-Feeding Biomass and Catalyst

Experimentation in this mode needed a uniform feed of the catalyst and biomass mix. The first catalyst tried was ZSM-5 (see Section 4.5) during the commissioning runs. It had a particle size of 212 - 75 μm. It was found to be necessary to grind the wood to the size of the ZSM-5 zeolite catalyst to ensure a uniform distribution of both wood and catalyst in the feed. If this was not done, the catalyst preferentially entrained and a consistent feed of wood and catalyst in the correct ratio could not be achieved. This feeding phenomenon was studied by using trial mixtures of the wood and catalyst at different particle sizes, collecting, rather than pyrolysing the resulting fed mixture, and

assessing the amounts of wood and catalyst accumulated. Only visual assessments could be made because other methods, such as adding the mixture to water so the wood floated and the catalyst sank, were found to be unsuccessful. The clear-walled feeder enabled the different coloured wood and catalyst to be observed. When larger particle sizes of wood were tried, layering of wood and catalyst occurred and the catalyst would move towards the bottom of the feeder faster.

Later experiments used catalyst where the particle size could be specified. In these instances, the catalyst and wood were ground to the same size of 315 to 500 μm.

4.4.2 Replacement of Fluidising Medium by Catalyst

To replace the fluidising medium of the reactor, the fluidising properties of the replacement particles should be known or found. The volume and particle size can be altered to ensure that both fluidisation occurs and char particles are disengaged and blown out of the reactor. To compare one experiment with another, the space velocities of the reacting particles should be kept in the same region. It was found that if particles had similar, but not identical properties, then the *volume* of the fluid bed should be held constant. The fluid bed equations in Section 2.5.2 have been used to predict the fluidisation characteristics of the catalytic pyrolysis components. They are shown in Table 15, Section 4.1.1.2.1 and Table 23. It can be seen that a nitrogen velocity of 0.5 m/s is suitable, but a small proportion of the char will be removed with the char that is created in the reactor. This is because the terminal falling velocity of the fine particles (0.26 m/s) is below 0.5 m/s. This was experimented with to ascertain whether it was necessary to sieve the char before using it in the fluid bed. It was found, however, that loosing the fine particles of the fluidising medium, in this instance, made a negligible difference, so removing them by sieving was not necessary.

Table 23 Fluidising Properties of Fluidising Medium Replacement Materials, Calculated at STP

Property	Slate (min)	Slate (av)[a]	Slate (max)	Char (min)	Char (av)[a]	Char (max)
Particle diameter, $d_{particle}$ (m) $\times 10^{-4}$	3.15	4.08	5.00	1.00	4.50	8.00
Particle density, $\rho_{particle}$ (kg/m^3) $\times 10^2$	19.0	19.0	19.0	6.0	6.0	6.0
Minimum fluidising velocity, u_{mf} (m/s)[c]	0.070	0.116	0.175	0.002	0.045	0.141
Bubbling velocity, u_b (m/s)	0.417	0.698	1.051	0.013	0.268	0.848
Reynolds number at u_{mf}	1.76	3.81	7.03	0.02	1.62	9.08
2/3 Galileo number[d]	2998	6490	11988	30	2756	15484
log(2/3 Ga)	3.48	3.81	4.08	1.48	3.44	4.19
.: log Re_t[e]	1.84	2.04	2.24	0.32	1.77	2.30
.: Re_t	69.02	109.65	172.19	2.11	59.02	199.53
Terminal falling velocity, u_t (m/s)	2.73	3.35	4.29	0.26	1.63	3.11

Notes: (all) Notes as Table 15, page 90.

4.4.3 Close-Coupled In-bed Catalyst

A catalyst can be used in this mode in two ways:

1) It can be held in a cage in the disengagement zone of the reactor to prevent it either falling into the fluidising zone of the reactor or escaping from the top of the reactor.
2) The fluidising properties of the catalyst can be utilised:
   a) For a catalyst with a minimum fluidising velocity less than that of the fluidising medium (sand), it can be supported on a mesh plate, providing that the fluidising velocity is less than that of its minimum fluidising velocity (see Figure 36).
   b) Alternatively, for a catalyst with a minimum fluidising velocity greater than that of sand, it can be prevented from exiting the reactor by a mesh plate, providing that the fluidising velocity is greater than that of its minimum

fluidising velocity and the height at which it would fluidise is higher than the top of the reactor. (See Figure 37)

The advantage of using a plate rather than a cage is because of the ease of insertion into the reactor top. Because the neck of the reactor is smaller than the body, a flexible plate can be inserted at an angle and orientated correctly once it is in the desired place. It is held in place by pressure on the reactor walls by the turned up edges of the plate.

When designing a fixed bed or catalyst cage, the easy removal of char should be considered as a build up of char would both blind the catalyst and cause an increased pressure drop. The mesh size of the plate or cage should be as large as possible while still supporting or holding the catalyst in the correct place. In these experiments, a stainless steel mesh of 1 mm diameter holes and 0.3 mm diameter wire was chosen for ease of cutting, manipulation durability and char removal.

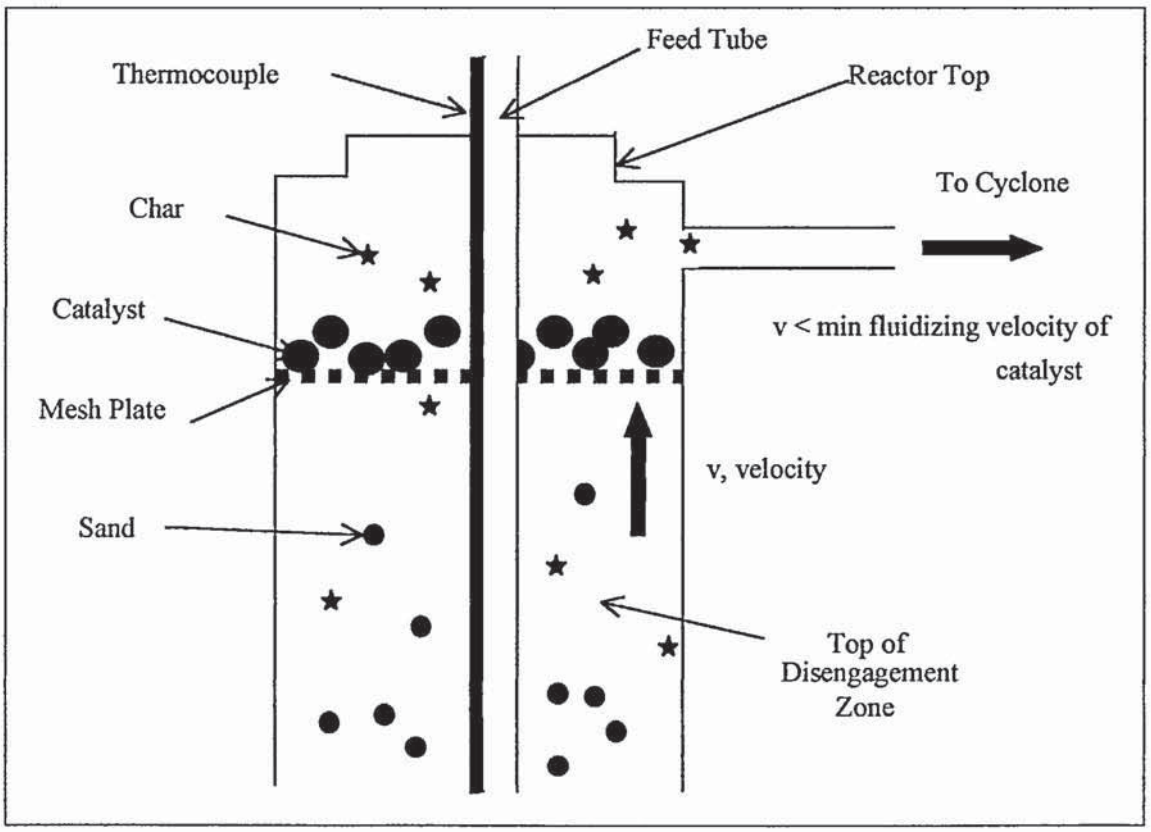

Figure 36 Mesh Supporting Catalyst

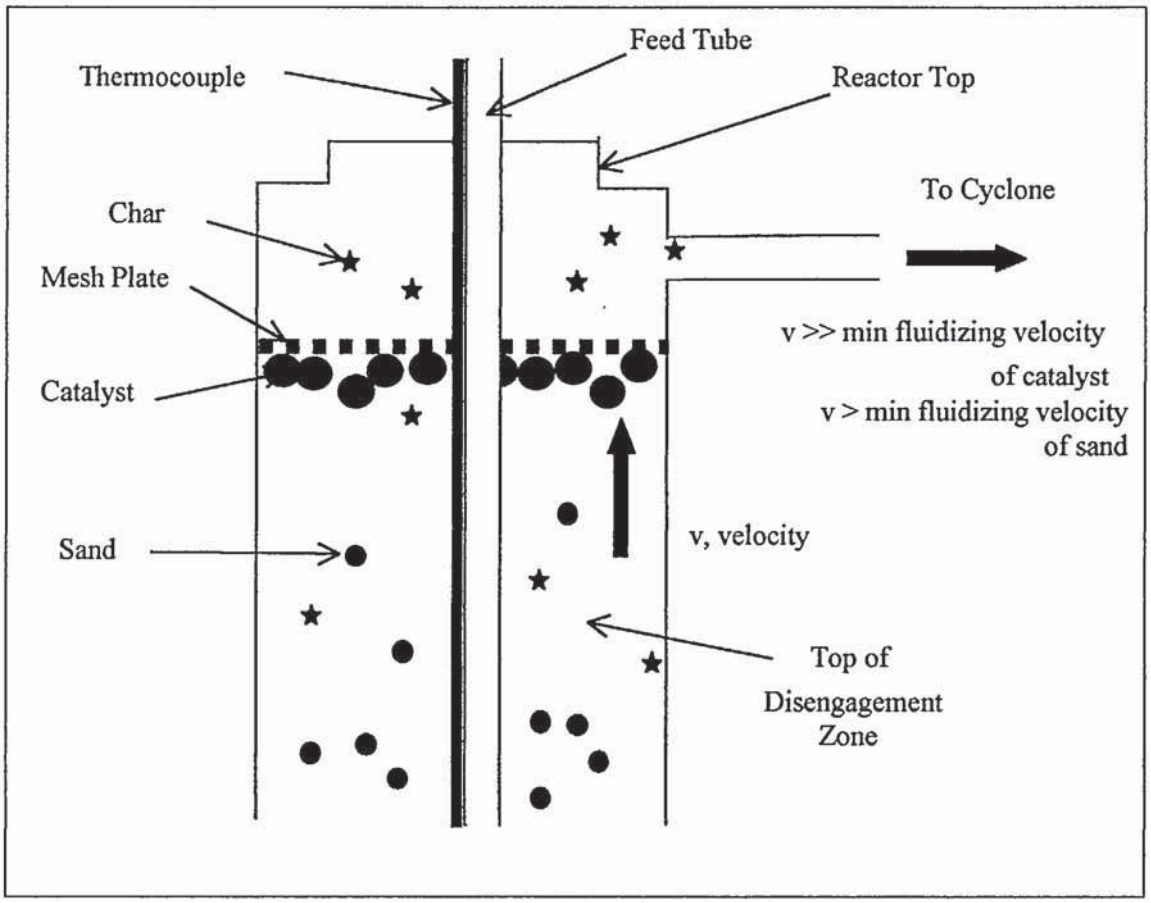

Figure 37 Mesh Plate Restricting Catalyst Escape

4.4.4 Close-Coupled Catalyst in a Secondary Reactor

The incorporation of a catalyst, close-coupled in a secondary reactor, can be achieved in several ways. The variables include:

1) The orientation of the reactor (horizontal or vertical).
2) The heating method of the secondary reactor. This can be either separate to the primary reactor or included in the primary reactor furnace.
3) The catalyst state in the reactor, either fluidised or packed.

A horizontal reactor with a separate heating source or a vertical reactor included in the existing furnace, both with a packed bed of catalyst, are the most practical combinations that can be achieved. The first of these options was tried and is shown in Figure 38. The reactor temperature at the entrance to the secondary furnace and at its exit, as well

as the furnace set point temperature, were monitored throughout the experimental runs of this type. The maximum furnace set point was 800°C. This produced an average furnace temperature of 780°C. This resulted in an average reactor entrance temperature of 330 - 420°C and exit of 400 - 530°C, depending on the exit temperature from the primary reactor. The reactor used was a stainless steel tube of id = 15 mm, od = 19 mm.

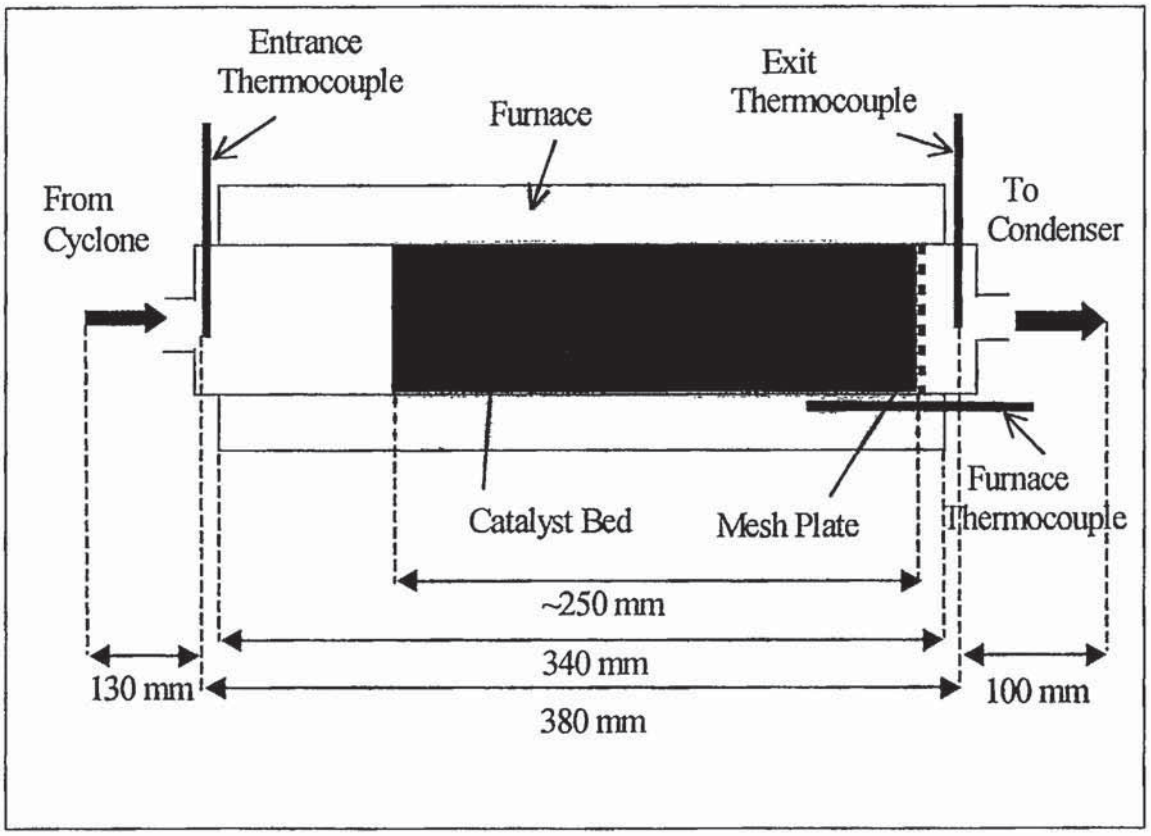

Figure 38 Secondary Reactor (not to scale)

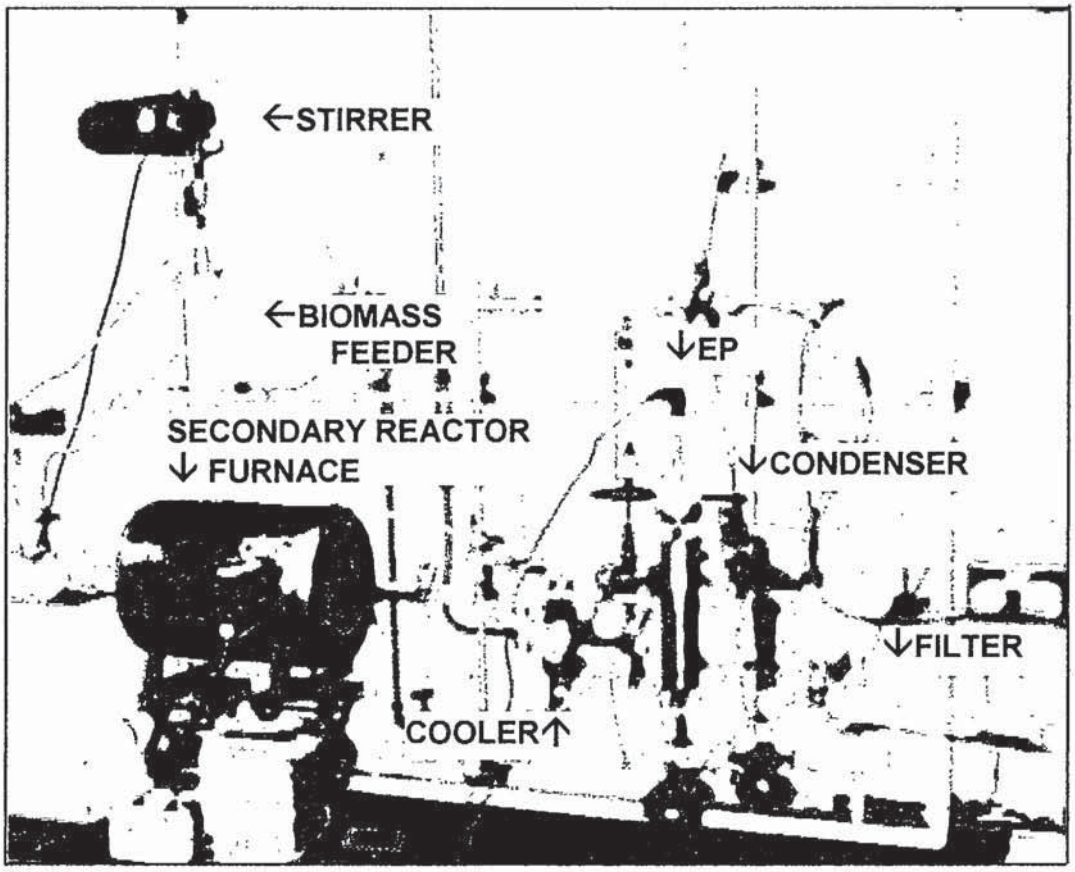

Figure 39 *150 g/h Single Product 'Small' Scale Fluidised Bed Fast Pyrolysis Reactor – Including Secondary Reactor System*

4.5 Catalysts Used in the Apparatus

Screening and evaluation of catalysts (see Sections 2.6 and 3) enabled the following catalysts to be chosen for testing using the 150 g/h fast pyrolysis apparatus. All the potential variables of their use are shown in Table 24:

Table 24 Catalysts and Potential Configurations of Use in150 g/h Fluid Bed

Catalyst Code[a]	Description	Possible Configurations of Use
ZSM-5	Grace Davison zeolite	Co-fed
Y	BDH Y-zeolite	Close-coupled in primary or secondary reactor. Ground for co-feeding.
Slate	Thermally-expanded slate	Replacing inert sand fluid bed or close-coupled in secondary reactor.
Char	Wood char from charpot of non-catalytic experiments	Replacing inert sand fluid bed, close-coupled in secondary reactor, also co-feeding smaller particle sizes.

Notes: (a) Code refers to catalysts described in Table 12, page 65.

Details of the catalysts are given in Sections 2.4.4 and 3.2. They are summarised below with their mode of inclusion.

4.5.1 ZSM-5

ZSM-5 zeolite catalyst (SP no. 10-5132.0101) made by Grace Davison is 15 % pure on an alumina phosphate binder. It has a structured pore size of 5 Å. The co-fed ZSM-5 was used with pine wood in the commissioning runs, before catalyst screening had been performed (Section 3), based on work by Cooke *(Cooke, 1999)*. As more effective catalysts were found through screening, further modes of operation were not pursued, particularly because of the small particle size of the ZSM-5 product making other modes of incorporation impossible.

A comparison of the properties of ZSM-5 and Y-zeolite can be found in Table 8, Section 2.4.4, 'Zeolite Catalysts'.

4.5.2 Y-Zeolite

Y-zeolite is a hydrogen zeolite clay, from BDH, with a Y-type structure and pore size of 11Å. Y-zeolite was initially tested using pinewood during the commissioning runs then more extensively tested using beech wood following the positive screening results reported in Section 3.4.

4.5.3 Slate

Thermally-expanded slate was initially used to replace the inert sand as the fluidising medium. Slate is a metamorphic rock that splits into thin layers. It is a silicate. It has an orderly arrangement in parallel planes of minute flaky minerals such as chlorite, $(Mg, Fe, Al)_6(OH)_8(Si, Al)_4O_{10}$. It was formed by pressure on a clay over a goelogically-long time *(Goss, 1972)*.

A single batch of slate was prepared together with the IWC by grinding, sieving and heating in a furnace. This was used for this project and at the IWC to provide a direct comparison. The comparative results can be found in the resulting report *(Meier, 1998#2)*.

The particle size was 315 to 500 μm with randomly positioned and sized pores. The designed use of the slate in this form is as a plant pot soil top decoration although it can have many uses in other forms, such as for roof covering. In its pre-ground state, pore size was up to 1 mm. The pore volume is about 90 %, the particle density is 1.70 g/cm^3. It is easily ground to the desired particle size. It is chemically neutral, heat resistant to 1100°C and resistant to extremes of pH. The detailed chemical composition is not available.

Slate was incorporated into the pyrolysis process as a replacement for the inert fluidising medium. Following fluidisation experiments *(Wunder, 1999)*, the sand was replaced by slate of an equal volume.

4.5.4 Char

The char that was used to co-feed with the biomass was taken from previous non-catalytic beech wood experiments on the small fluid bed. The contents of the small fluid bed char pot were used. This had a particle size of 150 - 500 μm.

The char used in the secondary reactor and to replace the fluid bed in the small apparatus was produced in the large fluid bed (see Chapter 8). Because of the larger feed size, the char particle size is larger than that collected from the small apparatus. It

is approximately 100 - 800 μm, but is difficult to determine precisely by sieving because of the oblong nature of the particles.

4.6 Experimental Description

There are several process variables that have been considered:

1) feed type, size, shape, moisture and flow-rate,
2) reactor temperature,
3) condensing temperature,
4) vapour residence time in hot zone of apparatus, and
5) catalysts - zeolites, clays, cracking catalyst, slate,

The following operating conditions were chosen:

1) Two feedstocks were used, pinewood initially for commissioning runs and beechwood for the main portion of the experiments (see section 4.2). The change was due to a group decision with the other members of the European contract, with which this work is associated. The two types of wood are chemically similar and the chemical composition of the resulting pyrolysis liquid should not vary greatly. The size of beechwood chosen was 315 to 500 μm. This particle size feeds easily into the small apparatus and is in a range that is supplied by the manufacturer so as to reduce grinding and sieving before each experiment as was necessary with the pinewood used in the earlier experiments. The fine particles, (particularly below 50 μm, but preferably below 200 μm) need to be removed to prevent blockages in the feed tube. The fine particles can become agglomerated due to static charging. Feeding with the smaller sized particles used for the commissioning runs is described in Section 4.2 - Biomass Feed, Preparation and Handling and Section 4.4.1 - Co-Feeding Biomass and Catalyst.

   The shape of the wood particles was also defined by the preparation of them. The pinewood was ground twice to reduce needle shaped particles. With the beechwood, this was not necessary as the manufacturer's preparation produced a more spherical particle shape. The exact moisture of the wood was tested for each

experiment for mass balance purposes. It has to be below 10 % for pyrolysis and the supplied moisture of both the beech and pinewood (4 to 9 %) was found to be in the desired range.

The feed flow-rate is determined by process limitations. The greatest quantity of liquid product is desired to gain enough product for testing purposes, so the maximum feed rate is appropriate. Although the apparatus is rated to 150 g/h, when co-feeding, the catalyst must be considered along with the biomass. A biomass flow-rate of 100 g/h was therefore chosen. The intended length of each run was set at 60 minutes. This is long enough for the experiment to achieve steady operation for a reasonable time and for sufficient liquid to collect. It is also appropriate for the size of feeder – enabling a single filling to be made so as not to stop the run to top-up the feeder. It is also convenient as preparation for running an experiment and cooling it down results in a day's work and does not necessitate over-night or unattended running which would have safety implications.

Parameters associated with the feed have therefore been chosen as constants in the experiments.

2) Two temperatures of operation were originally used for comparison of experimental runs, 475 and 508°C. Wulzinger *(Wulzinger, 1999)* of the Institute of Wood Chemistry in Hamburg (IWC), Germany found the first temperature maximised liquids production and Cooke *(Cooke, 1999)* of Aston University in Birmingham, using the same apparatus as that described in Section 4.1.1, found she obtained maximum liquids at 508°C. Although these maximum liquid-yield temperatures were established for non-catalytic systems, catalytic systems were initially assumed to have a similar optimum temperature as a basis to commence experimentation. Other systems are reviewed in Chapter 2.

Subsequent experiments done post-commissioning used a range of temperatures. The variation of temperature was used to establish the 'organic liquid yield peak' from which the optimum temperature of operation can be found. This peak, which ascertains at what temperature the maximum product can be gained, is useful in assessing pyrolysis liquid production method secondarily after liquid quality. The

reactor temperature was varied between 450 and 550°C in steps of 25°C, for a set of experimental runs on each catalyst. The 'organic liquid yield peak' could then be compared to an average peak obtained by Toft *(Toft, 1996)*. This empirical peak was obtained by collecting experimental data from many fast pyrolysis results, operating non-catalytically, using a variety of biomass feedstocks. This is a useful comparison to gauge whether work is giving a realistic result that can be transferred to other technologies and systems.

The temperature of the reactor will therefore be a variable between experiments.

3) The design of the water-cooled condenser determines the flow-rate in the range 10-20 l/min to maintain the desired vapour temperature (see Section 4.1.2.2). When considering scale-up of the process, the most economic system would have the cooling medium the closest to ambient temperatures. This should be balanced with 'capturing' the greatest number of vapours. The vapour temperature is therefore fixed.

4) The vapour residence time in the hot zone of apparatus could be varied by altering flow-rates and feed-rates. For the purposes of reducing the number of different experiments, it will not be examined in this work and shall therefore stay constant at 0.5 ± 0.2 seconds.

   The vapour residence time, also known as total hot space residence time, is one of the parameters which define the experiments and allow comparison between differing sets of apparatus. It is the time that the pyrolysis vapours spend in the reactor system and is therefore indicative of the extent of secondary reaction that may occur. It is calculated using the volumetric throughput of the reactor system divided by the volume of the reactor (above the distributor) minus that of the fluidising medium, the volume of the cyclone and transfer arm up to the first point of cooling.

5) The choice of catalyst is necessarily an experimental variable. Details of the catalysts used can be found in Section 4.5.

Table 25 and Table 26 give a summary of the experimental pyrolysis runs carried out:

Table 25 Summary of Commissioning Run Variables, (Three Product)

Catalyst	Configuration	Temperatures, °C
None	Sand bed, 135 g	475, 508
ZSM-5	10 % co-fed	475, 508
Y-zeolite	Close coupled in 1ry reactor, 10 g	508
Y-zeolite	10 % co-fed	508

Table 26 Summary of Experimental Run Variables, (Single Product)

Catalyst	Configuration	Temperatures, °C
None	Sand bed	450, 475, 500, 525, 550
Slate	Fluid bed	450, 475, 500, 525, 550
Slate	Co-fed	475, 500, 525
Slate	Secondary reactor	500
Y-zeolite	Close coupled in primary reactor	450, 475, 500, 525, 550
Char	Fluid bed	475, 500, 525
Char	Co-fed	450, 500, 525
Char	Secondary reactor	450, 500, 525, 550

4.7 Pyrolysis Product Analysis Techniques

The liquids and gases from the pyrolysis reactions are collected, measured, weighed and analysed to produce a mass balance for the experiment. The water contents of the product liquids are found and the aqueous fractions are chemically analysed by high-pressure liquid chromatography. The composition of the gas product is found by gas chromatography.

4.7.1 Karl Fischer Water Testing

The Karl Fischer coulometric method used to establish the water content of the pyrolysis liquid is accurate at low water contents and is the accepted standard method of establishing the water content of pyrolysis liquid. A Mitsubishi, model CA-20, KF coulometer was used and is accurate to 0.1 wt%. It is less time consuming and simpler

than a volumetric method which uses large quantities of solvents. It does not need re-calibrating frequently. The disadvantage is that pyrolysis liquid with very high water contents and/or viscosity needs dilution before testing. A small sample of raw pyrolysis liquid is weighed and diluted with a known weight of methanol of known water content. There are however potential reactions between the pyrolysis liquid and some of the solvent, methanol, used. This method of using a diluent was still used, as it is an established method of testing for water content and widely used in this field.

4.7.2 Gas Chromatography

Early gas analysis for runs EHS01 to EHS11 was carried out by batch samples in bombs and batch analysis after the run was complete. Normally four samples per hour were taken. From run EHS16 onwards, an on-line GC was used which samples the gas every five minutes and an average taken for the entire run. Runs EHS12 to EHS15 were used to establish the validity of the new GC system by using it and manually taking bomb samples. Table 27 shows the differences found between the average gas results. The manual system shows inconsistencies, particularly in the methane result. The automatic system is able to detect larger amounts of hydrogen, carbon monoxide, ethylene and propylene. Not only being automated is more reliable, but also the actual GC apparatus used for detection was different and was dedicated to the pyrolysis apparatus in the case of the automatic system.

Table 27 Comparison of Gas Sampling Systems

Average Gas (% in sample)	EHS13 Bomb[a]	EHS13 Auto[b]	Difference as %of Auto	EHS14 Bomb[a]	EHS14 Auto[b]	Difference as % of Auto
Hydrogen	0.310	0.709	56	0.317	0.670	53
Carbon monoxide	0.000	2.194	100	0.062	1.384	96
Carbon dioxide	0.071	3.432	98	6.494	4.120	-58
Methane	6.954	0.327	-2027	0.046	0.164	72
Ethane	0.044	0.014	-214	0.000	0.005	100
Ethylene	0.011	0.068	84	0.025	0.035	29
Propane	0.020	0.000	-0	0.000	0.005	100
Propylene	0.000	0.412	100	0.006	0.016	63
n-Butane	0.005	0.000	-0	0.000	0.000	0
n-Butene	0.000	0.000	0	0.000	0.000	0

Notes: (a) Manually taken gas sample, average of three bomb samples

(b) Automated sampling system

4.7.2.1 Use of In-line Gas Chromatography Equipment

An off-take from the gas vented from the pyrolysis apparatus during an experimental run is periodically sampled by the gas chromatography equipment and analysed. The equipment used is a Series 610 gas chromatograph, with VALCO sample collection and column switching facility. The computer control uses UNICAM software. The molecular sieve column analyses for hydrogen and carbon monoxide using argon as the carrier gas. The HayeSep column uses hydrogen carrier gas to analyse for carbon monoxide, carbon dioxide, C_1 and C_2 hydrocarbons when using a four-minute analysis. C_3 and C_4 hydrocarbons may also be analysed when using a longer, eight-minute, analysis time. Two separate thermal conductivity detectors are used, but displayed simultaneously in a single trace.

The sample gases against which the system is calibrated are shown in Table 28.

Table 28 Calibration Gas Standards

Constituent	% gas by volume '1.5 %' sample[(a)]	% gas by volume '7 %' sample[(b)]
n-Butane	1.52	7.12
Propane	1.57	7.27
Propene	1.69	7.79
Ethane	1.70	7.65
Ethene	1.58	7.11
Carbon dioxide	1.49	7.29
Carbon monoxide	1.43	6.65
Methane	1.47	6.81
Hydrogen	1.55	6.83
Nitrogen (by difference)	86.00	35.48

Notes: (a) So named because of the components being approximately 1.5 % each in nitrogen.

(b) Components approximately 7 % each in nitrogen.

Argon and Hydrogen are used as the carrier gases. The following settings are used on the GC (Table 29).

Table 29 Temperature and Time Settings for GC

Setting	Level
Detector	130°C
Injector	100°C
Automatic Valco valves oven	100°C
Column	120°C
Run time	4.6 seconds

The minimum heat up time is one hour for stabilisation. The flow of gas to be tested, from the apparatus, is set at to 30 ml/min and is pumped at a pressure of 0.2 psi. The computer plots the results and calculates the volume of each gas by comparing the signal to the standard results, using a computer package known as the '4880 program'

produced by UNICAM. (See Section 4.8.1 for more details of the equations used to do this.)

4.8 Small Fluid Bed Pyrolysis Mass Balance

For both apparatus configurations, the 'commissioning runs' and the 'experimental runs', mass balances were undertaken. They were used to determine the ratio of product types (char, liquid and gas) and ascertain the accuracy of the runs by calculating the 'mass balance closure'.

Following operation of both configurations, the apparatus is allowed to cool and the product liquids drain into the oil pots. The condensers are externally dried so that the only weight increase is due to internal liquid. This is done using a small amount of methanol and pressurised air to evaporate any liquid off the outside of the glass, due to condensation of air-borne water vapour onto it and the liquid held in the finger condensers. The 'complete system' is weighed, dismantled and the individual components weighed. These are compared and investigated if they do not match. The results proforma shown in Appendix B (page 253) is filled in as this is done, for each experiment. This shows where the breaks in the apparatus are made for weighing the 'complete system' as it is not possible to find the mass of the feed system, the reactor system and the collection system together.

The difference in mass before and after the experiment in reactor components is classed as char. The difference in the glassware weights is a combination of oil, char and water, the ratios of which are subsequently ascertained. The difference between initial and final gas meter readings is the total volume of gas and from GC analysis, the volume of pyrolysis gases can be determined.

For the single product 'experimental runs', the first portion of liquid from the oil pot beneath the EP is stored at room temperature and used for physical property testing. The remaining half of this liquid and that from the second condenser is stored separately in the fridge for chemical analysis by HPLC (High Rerformance Liquid Chromatography) and KF (Karl Fischer Coulometer) analysis. (See Section 4.7.1) For

the commissioning runs the three products are stored and analysed separately, when sufficient is collected.

In both cases, all other glassware is rinsed using ethanol and the washings filtered using a pre-dried and pre-weighed filter paper, to separate char. The washings are collected in a pre-dried and pre-weighed flask so it is possible to calculate the mass of ethanol used to wash the liquids. Ethanol was chosen as a solvent because of potential reactions with methanol and pyrolysis liquid, but low enough volatility so it remains with the pyrolysis liquid in the stoppered flask. When all liquids have been removed from the glassware (condensers, EP, oil pots, cotton wool and cotton wool filter), the filter paper is oven dried. The flask of ethanol washings and the dry filter paper, which contains the char from the liquids, is weighed. The results proforma shown in Appendix B (page 253) is also filled in during this weighing process.

The moisture content of the feed is calculated by drying three samples in the oven at 105°C for at least 6 hours until the mass is constant (usually 28 to 52 hours). The moisture content of the liquid products, the washings and the ethanol must also be determined. The mass balance can then be calculated on a moisture free basis.

4.8.1 Mass Balance Calculation Development

Mass balances were computed for each run to determine the proportion of each product produced and also to estimate the accuracy of each experimental run. The calculations were developed from those performed by the inventors of the 'Waterloo Fast Pyrolysis Process' *(Scott, 1987)*. All results are quoted on a dry wood feed basis.

The dry wood-fed basis can be calculated by multiplying the average percent moisture on wet wood basis by the difference in the mass of feeder before and after the run, minus the catalyst fed and taking this from the wet wood fed (the difference in the mass of feeder before and after run minus the catalyst fed). The catalyst fed is found by the percent catalyst in the feed multiplied by the mass of wet wood and catalyst fed. This assumes that the wood and catalyst are fed in the exact ratio that they were mixed together in. This could be checked by analysing the residue of feed in the feeder. By comparing the ash remaining after burning the residue from a non-catalytic run and the

ash and catalyst remaining from a wood-catalyst mix, the catalyst levels in the wood can be found. With a low percentage of catalyst (10 %), it was not possible to do this accurately.

The amount of organic liquid produced by the run is found by taking the total water found in the liquids from the total amount of liquid found. The mass of total liquid recovered is the difference in glassware mass before and after the experiment, minus the mass of char collected found by difference in filter paper before and after filtering the liquid-char-ethanol mix. This method was used for the single product system and assumes that the micro char in the oil is negligible and classed as liquid. Therefore the total amount of char that leaves the reactor system (those components in the furnace - reactor, cyclone, char pot and transfer tube) is found in the residue liquid, used for filtering. This assumption agrees with the method used by Wulzinger *(Wulzinger, 1999)*.

The three product system used previously, employs the same assumption as Cooke *(Cooke, 1999)*. In this instance, the mass of total liquid recovered is the difference in glassware before and after the experiment minus the mass of char in the pre-filtered liquid. This mass of char cannot be measured directly and is calculated by the mass of char collected, found by difference in filter paper before and after filtering liquid-char-ethanol mix, as a percentage of the mass of what has been filtered. What has been filtered is the mass of liquid and char in glassware minus the mass of liquid poured into sample jars and kept separately. The assumption made in this case is that the char in the liquid product is equal to that in the residue oil used for filtering. This is a poor assumption and was changed for the experimental runs.

The char found in the total process must also include that collected elsewhere, other than in the glassware. The mass of char and catalyst found in reactor, char pot and transfer tube, including coking of the sand is found by difference in mass of those items. The mass of catalyst fed is taken from this. If the catalyst travels past the cyclone, then it is still included in this equation as it sticks to the glassware and is washed off with ethanol and trapped in the filter paper, where it is classed with the char. This assumes that no catalyst contaminates the product liquid. To confirm this the liquid could be filtered. Filtering the liquid without solvents (which would destroy the usefulness of the

sample) is extremely difficult and even if achieved it would be difficult to differentiate between char and catalyst, although comparing catalytic and non-catalytic experiments would be possible. Dissolving a small amount in methanol and filtering was tried, but when such small amounts are in question it was impossible to attain an accurate answer. This has negligible effect on the final mass balance result.

To find the proportion of water generated by the experiment, the mass of water in the oil pots plus the mass of water in the liquid residue on the glassware, should be found. The liquid residue on glassware is, however, mixed with the ethanol used to wash it off. The percent of water in samples (including the ethanol washings) is analysed using Karl Fischer coulometric titration techniques. The mass of water in the oil pots is therefore the mass of liquid in the oil pot multiplied by the percent water in the sample. The rest of the water is found by the mass of water in oil ethanol mix minus the mass of water in ethanol.

The locations of the products found are summarised in Table 30.

Table 30 Location of Pyrolysis Products (Both Configurations)

Product	Location	How Measured
Char	Char pot	Mass difference
Char	Reactor body	Mass difference
Char	Liquid residue on glassware	Filtration of ethanol washings
Micro char	Liquid product	Not measured and counted as liquid
Water	Liquid product	Karl Fischer titration
Water	Liquid residue on glassware	Karl Fischer titration of ethanol washings and ethanol
Organics	Liquid product	Mass of liquid minus mass of water
Organics	Liquid residue on glassware	Mass of liquid residue minus mass of water and ethanol
Gas	Vent	Gas meter and gas chromatography

To find the mass of pyrolysis gases produced, from the gas chromatograph compositions, the percentage volume of each individual gas (methane, carbon dioxide, ethene, ethane, hydrogen, propene, propane, carbon monoxide and n-butane) is

multiplied by the total volume of gas produced and its density at 20°C *(Perry, 1984#3)*. The percent of each gas in the sample is computed using averages taken from two standard samples, A and B, containing component gases at 1 % and 7 % (See Table 28) and using Equation 28.

$$\left[\left(\text{GC area} \times \frac{\%\text{ in standard A}}{\text{standard A GC area}}\right) + \left(\text{GC area} \times \frac{\%\text{ in standard B}}{\text{standard B GC area}}\right)\right] \div 2$$

Equation 28

This assumes that the gases exit at 20°C. The measured temperature has been found to be 15°C. Assuming ideal gas behaviour where P is pressure, V is volume and T is temperature in Kelvin, Equation 29 applies:

$$P_1V_1 / T_1 = P_2V_2 / T_2$$

Equation 29

If the pressure is assumed to be constant and 0°C is 273 K, then the percentage difference, x, between the volumes when the temperature is accounted for is found by Equation 30 and Equation 31:

$$(V_2 - V_1) = x\% \times V_1 / 100$$

Equation 30

$$100 \times (V_1 / V_1) \times ([(273+16) / 273+20)]-1) = x\% = 1.4\ \%$$

Equation 31

The actual volume difference due to the temperature discrepancy is therefore very small and will not affect the results.

4.8.2 Errors Associated with Mass Balance Calculations

The mass balances achieved are subject to errors from experimental variable fluctuations such as temperature, feed rates and gas flow-rates. This has been estimated to find the degree of confidence in the final mass balance results. The accuracies quoted in Table 31 are those that can be gained during actual experimental conditions. They

take into consideration the accuracy of the apparatus quoted by the manufacturers and what fluctuations, if any, occur during operation.

Table 31 Accuracy of Apparatus

Apparatus	Measurement	Accuracy
Balance 1	Mass of apparatus	± 0.005 g
Balance 2	Mass of reactor	± 0.05 g
Balance 3	Mass of samples for Karl Fischer water titration	± 0.00005 g
Rotameter 1	Entraining nitrogen flow	± 0.1 l/min
Rotameter 2	Feeder top nitrogen flow	± 0.05 l/min
Rotameter 3	Fluidising nitrogen flow	± 0.5 l/min
Pressure gauge 1	Pressure drop across feeder	± 2 inches of water[(a)]
Pressure gauge 2	Pressure drop across fluid bed	± 2 inches of water[(a)]
Thermocouple	Fluid bed temperature	± 0.5 °C
Controller	Furnace temperature	± 0.5 °C
Positive displacement gas volume meter	Product gas volume	± 0.00005 m^3
Gas Chromatograph	Product gas analysis	± 0.05 %

Notes (a) High error due to pressure fluctuations giving rise to inaccurate reading

The accuracies in Table 31 were then used in conjunction with the mass balance calculations to compute an error on the mass balance results *(Roberts, 1999)*. These are shown in Table 32. The final mass balance results should be considered accurate to a margin or 0.8 % above or below the final result obtained. This shows that errors do not make an impact on the results.

Table 32 Calculated Mass Balance Errors

Component	Error (%)
Gas	± 4.2
Organics	± 0.5
Char	± 1.4
Water	± 3.2
Total	**± 0.8**[(a)]

Notes (a) The total is not simply the sum of the percentage errors because of the relative weights of each component.

4.9 Discussion of Mass Balance Results

Table 33 and Table 71 to Table 75 (Appendix E, page 270), show a complete set of results from the small fluid bed pyrolysis apparatus. They are displayed in temperature order for each different catalytic set of experiments. Primary is represented by '1ry' and secondary by '2ry'. The figures shown in italics are those not used for further calculations, normally because of poor mass balance closures or a problem during experimentation. A poor closure is one of less than 86 % or more than 104 %. This is because of a closure less than 100 % can be ascribed to losses whilst a closure grater than 100 % is not an actual possibility.

Those not used for further calculations are runs numbered EHS18, 19, 26 and 48. The first three of these have been replaced by runs numbered EHS33, 21 and 31 respectively. Runs numbered EHS24, 28, 47 and 49 have closures between 85 and 93 % and should be treated with a degree of circumspection. EHS24 and 28 have been repeated and are runs EHS29 and 32. It was not necessary to repeat EHS47 and 49 as they belonged to sets of experiments that produced low liquid yields and results of less interest. The exact reason for the poor runs could not be found. That is why repeats of them were necessary, but no modifications to apparatus or method could be made.

Table 33 ***Runs on 150 g/h Apparatus, Beech Wood Feed, No Catalyst***

Run no.	EHS	*18*	33	50	16	17	21	*19*	22	23	20	42
Catalyst type		-	-	-	-	-	-	-	-	-	-	-
Av. Run Temp (°C)		*452*	453	475	478	491	501	*502*	523	523	549	447
Run time (min)		*38*	45	45	51	42	46	*63*	42	46	29	38
Flow-rate (g/h)		*112*	133	133	101	123	112	*54*	118	104	146	113
Hot space residence time (s)		*0.51*	0.54	0.52	0.62	0.51	0.50	*0.56*	0.47	0.48	0.45	0.56
Product Yield (%)	**gas**	*12.0*	15.0	14.2	10.1	14.0	16.3	*16.8*	18.6	17.0	25.2	11.9
	organics	*75.3*	59.1	61.0	71.7	64.3	63.2	*56.9*	63.5	60.3	54.5	64.2
	char	*15.0*	11.8	12.1	11.6	10.7	9.5	*9.3*	10.4	8.7	7.6	11.5
	water	*7.4*	8.2	13.6	8.0	6.4	6.5	*2.0*	8.6	7.4	11.9	8.0
	liquids	*82.7*	67.3	74.6	79.7	70.7	69.7	*58.9*	72.1	67.7	66.4	72.2
Closure (%)	**wood in**	***109.8***	**94.0**	**100.9**	**101.4**	**95.4**	**95.5**	***85.0***	**101.1**	**93.4**	**99.1**	**95.5**

The results have been compared to 'empirical data'. This was calculated using equations derived by Toft *(Toft, 1996)*. The empirical Toft eqation was obtained by using a large number of results from several institutions using various equipment configurations and a variety of woody biomass feedstocks. It was found that reaction temperature is the single most significant influence on the liquid yield. Equation 32 to Equation 35 were used to describe the percentage of products gained through pyrolysis (organic liquid, gas, char and water). Differentiating Equation 32 gives the maximum yield of 64.9 % at 502°C.

$$\text{Organics \%} = -16.4 \times 10^{-6} (T)^2 + 0.0164 (T) - 3.47$$

Equation 32

$$\text{Gas \%} = 8.06 \times 10^{-6} (T)^2 - 0.0071 (T) + 1.64$$

Equation 33

$$\text{Char \%} = 8.60 \times 10^{-6} (T)^2 - 0.0099 (T) + 2.95$$

Equation 34

$$\text{Water \%} = -4.70 \times 10^{-6} (T)^2 - 0.0049 (T) + 1.20$$

Equation 35

where T = Reaction temperature, °C

On using these equations, it was found that Equation 35 yielded a negative result. This is assumed to be an error which could not be corrected by simply changing the sign of the result. The empirical water content was therefore found by difference using Equation 32 to Equation 34, assuming 100 % closure.

Examining the organic yield results from pyrolysis experiments allows these experiments to be compared with previous work in this field. It is also a useful way of comparing catalytic and non-catalytic runs with one another. In addition, the temperature giving the maximum organics yield can be found. After examining the quality of the resultant pyrolysis liquid, the amount of organic product gained should be considered as well as the temperature at which this is achieved.

The organic yield results, found in Table 33 and Table 71 to Table 74, have been plotted to find the 'organic yield peak' and temperature at which the maximum liquid is

produced. This is displayed in Figure 85 and Figure 86 (Appendix F, page 277). A second order polynomial line has been used to connect the points based on catalyst type and position in apparatus. Although the overall mass balance result of EHS33 appeared satisfactory, the graph of liquid yield showed that it did not fit the general trend. It was therefore repeated as EHS50. Both results have been displayed for comparison. Those results mentioned above as having been disregarded and shown in italics in Table 33 are not included in the graphs.

Simplified versions of these graphs are shown in Figure 40 and Figure 41. The equations yielded from them are Equation 36 to Equation 43. The closeness of line fits are displayed in Table 34 as R^2 values. The R^2 values are calculated by the Microsoft Excel program, in which the graphs were drawn. A value of one indicates a perfect fit.

The non-catalytic experiments have a similar peak to the correlated empirical data. This means that the results gained here can be compared with standard pyrolysis results from other pieces of apparatus. It indicates that no particularly unusual phenomenon are occurring in these experiments. Only the slate fluid bed produces results that are in a similar yield-temperature region as the empirical and non-catalytic experiments. The use of slate as a fluid bed does in fact reduce the temperature at which the maximum liquid yield is found from 490 to 475°C. This result is not repeated when slate is co-fed. At the slate co-fed organic peak of 500°C, there is a satisfactory yield, but it is much lower than the empirical yield at all other temperatures. This is shown by the larger gradient (positive and negative) that produces the peak (Figure 41). A slate secondary reactor gave a very poor yield result of 43 % organics at 503°C.

The shape of the organic yield curve for Y-zeolite is very similar to the empirical result, but the percentage yield is reduced by approximately 6.5 %. Y-zeolite has been shown on both graphs for comparison, as has the empirical curve.

The results using char as a catalyst are difficult to compare, as they do not follow the characteristic organic yield graph shape. The char secondary reactor is most definitely the worst configuration (as the slate secondary reactor was for the slate configurations). Co-fed char and the char fluid bed are similar to themselves and in the region of the

non-catalytic experiments in the 450 to 500°C temperature range. After this point the yield from the char fluid bed configuration dramatically decreases.

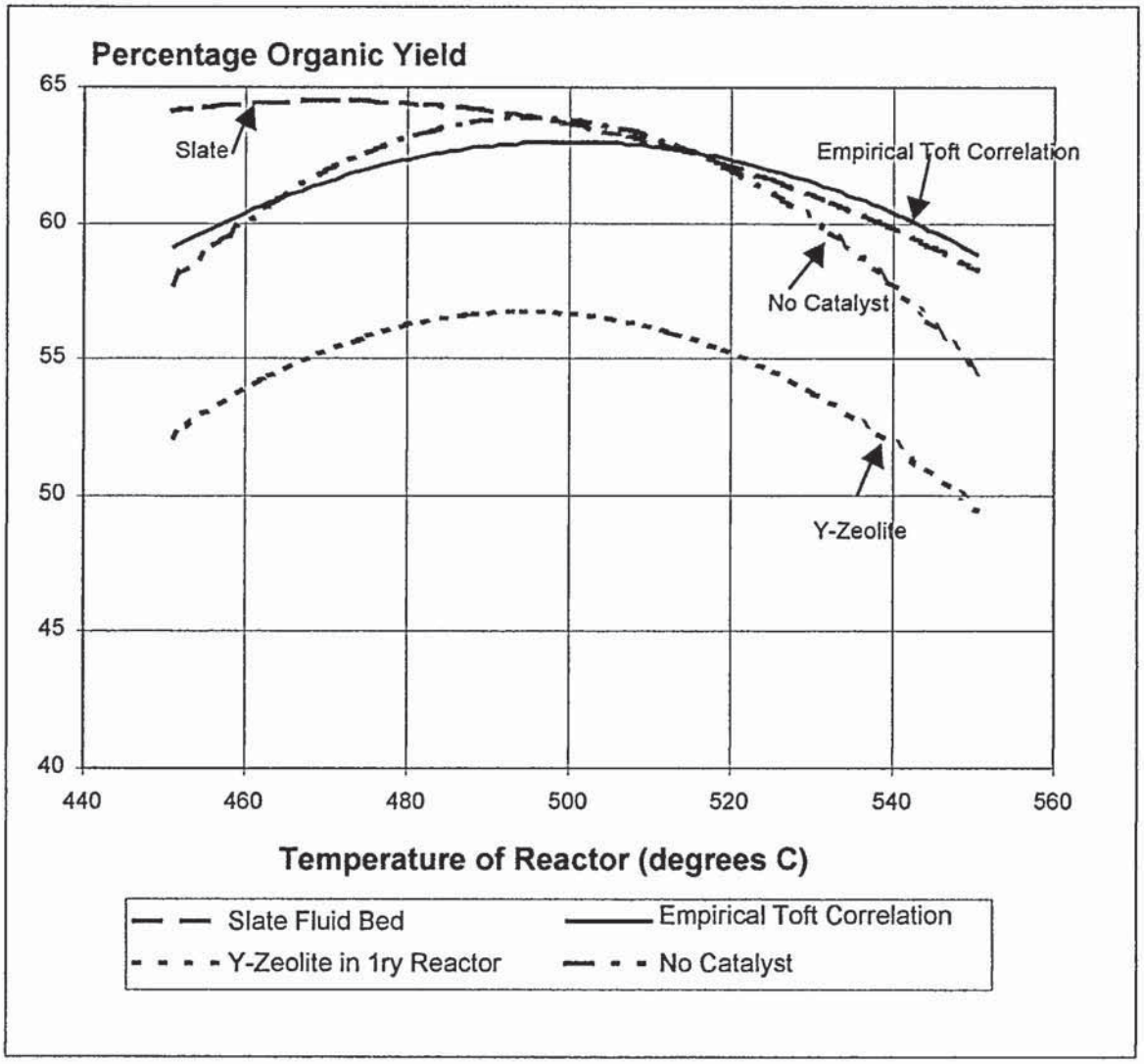

Figure 40 Organic Yield Results from 150 g/h Apparatus Experiments (1 of 2)

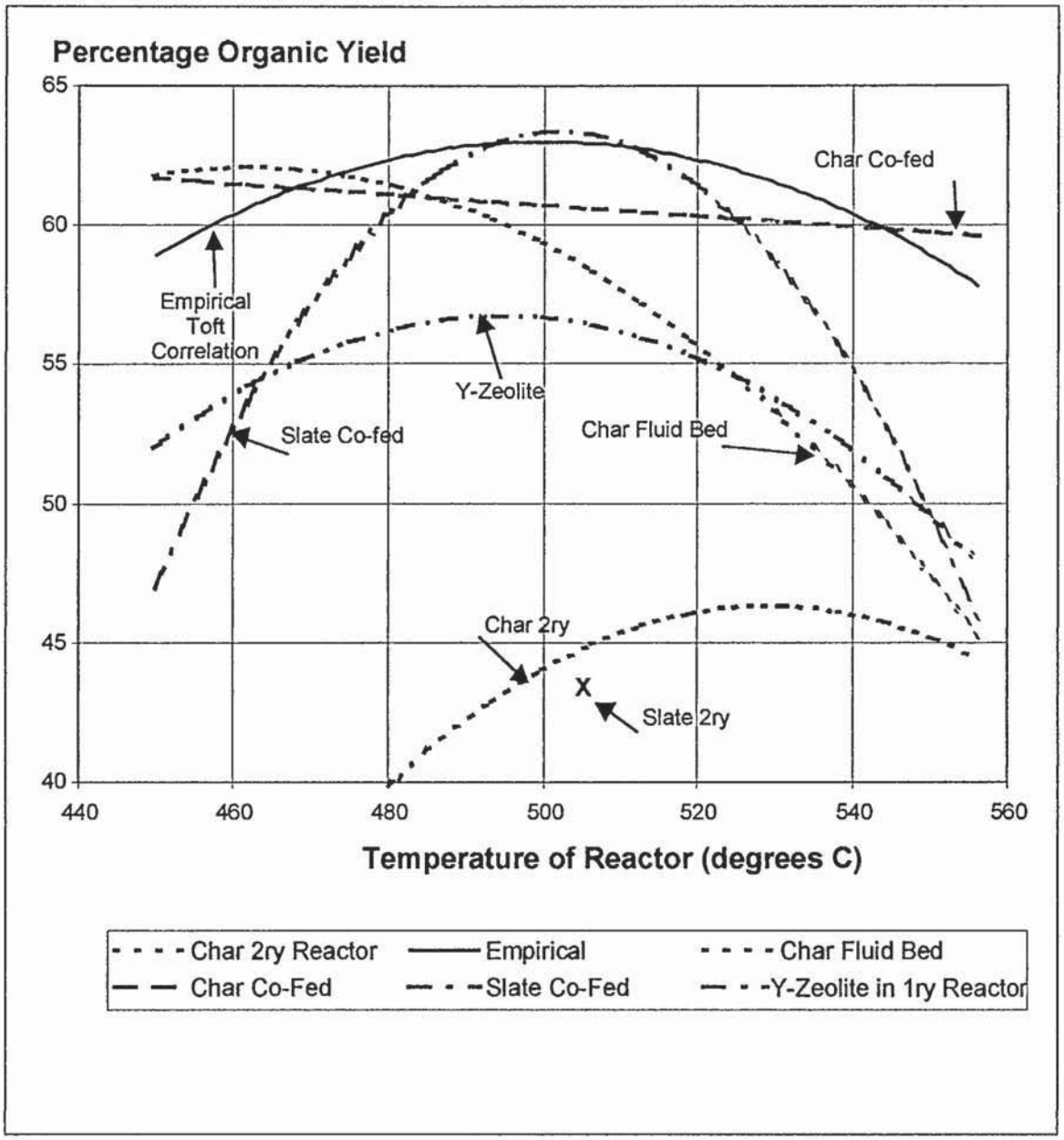

Figure 41 Organic Yield Results from 150 g/h Apparatus Experiments (2 of 2)

Empirical Organics % $= -0.0000164\ (T)^2 + 0.0164\ (T) - 3.47$

Equation 36

No catalyst Organics % $= -0.0031\ (T)^2 + 3.0534\ (T) - 692.39$

Equation 37

Slate fluid bed Organics % $= -0.001\ (T)^2 + 0.9198\ (T) - 151.98$

Equation 38

Y-zeolite in 1ry Organics % $= -0.0024\ (T)^2 + 2.3283\ (T) - 519.33$

Equation 39

Char in 2ry Organics % $= -0.0027\ (T)^2 + 2.816\ (T) - 699.16$

Equation 40

Char fluid bed Organics % $= -0.0019\ (T)^2 + 1.77\ (T) - 347.13$

Equation 41

Char co-fed Organics % $= -0.00195\ (T) + 70.441$

Equation 42

Char co-fed Organics % $= -0.006\ (T)^2 + 6.0471\ (T) - 1455$

Equation 43

Where T = Reaction temperature, °C

Table 34 R^2 Values for Equation 36 to Equation 43

Catalyst	R^2 Value	Equation No.
Empirical	(1.000)[(a)]	Equation 36
No catalyst	0.857	Equation 37
Slate fluid bed	0.815	Equation 38
Y-zeolite in 1ry	0.933	Equation 39
Char in 2ry	0.998	Equation 40
Char fluid bed	1.000	Equation 41
Char co-fed	1.000	Equation 42
Slate co-fed	1.000	Equation 43

Notes (a) This is from an equation used to draw the curve and can only return an R^2 value of 1.

To look at the accuracy of the results and compare it to the expected accuracy of ± 0.8 %, the results of the non-catalytic runs were analysed in Table 35 *(Roberts, 1999)*. This shows a standard deviation of 6.8, which is acceptable for these experiments.

Table 35 Variation of Experimental Results

Experimental Run	Closure (%)
EHS16	101.4
EHS17	95.4
EHS18	109.8
EHS19	85.0
EHS20	99.1
EHS21	95.5
EHS22	101.1
EHS23	93.4
EHS33	94.0
Arithmetic Mean	**97.2**
Sample Standard Deviation	**6.8**

4.10 Comparison of Mass Balance Results to Wulzinger and Cooke

As highlighted in Chapter 2, two other researchers have experimented with the incorporation of catalysts in fast pyrolysis. The differences in experimentation and a comparison of the mass balances will be undertaken here.

4.10.1 Experimental Comparison with Wulzinger

Wulzinger of the Institute of Wood Chemistry also used the Waterloo type fast pyrolysis apparatus to incorporate catalysts in the pyrolysis process (Figure 42). In a similar way to this project, he also developed a system to replace the two condenser system (described in Section 4.1.1.4). He did this by incorporating a Liebig cooler, cooled with ethanol at –15°C. To replace the cotton wool filter in the Aston set-up, he used a washing bottle system of methanol in which to dissolve the residual vapours. Methanol was also used to wash any residual liquid from the apparatus on completion of an experiment and it would be then combined with the main product. To find the

amount of liquid yielded, the methanol was driven off by rotary evaporation at 40°C and under a vacuum of 200 mbar. There are a number of disadvantages of this method:

1) it can not be guaranteed the methanol does not react with the pyrolysis liquid,
2) the portion of the pyrolysis liquid evaporates before methanol, is removed,
3) a portion of pyrolysis liquid evaporates close after methanol, may be lost,
4) methanol may be left in the pyrolysis liquid, boosting its proportion in the mass balance and reducing its viscosity,
5) washing the equipment so well and including this in the product can not be included in commercial scale up, where the residue on the apparatus would not be removed by a continuous process.

When the secondary reactor is incorporated (Figure 43), it is positioned vertically, unlike in this project which used the secondary reactor positioned horizontally.

With the set of experiments performed by Wulzinger, no variation in temperature was used and the reactor temperature was constantly 475°C. The feed rate was variable, not constant, at 80 to 200 g/h. The experimental run length was half that used at Aston, at thirty minutes. Having a shorter run time means less of the run is done under steady-state conditions and a greater proportion of the time is a start-up type mode. Whether this influences the end result is unknown.

The calculation method to find the mass balance is identical to that described in this report, except in one feature. This is the method of finding the percent gas yield. This is found by difference, making the total closure to 100 %. This means it is not possible to assess the accuracy of an experiment by using the percentage closure.

Figure 42 200 g/h Pyrolysis Apparatus of Wulzinger (Wulzinger, 1999)

Figure 43 ***200 g/h Pyrolysis Apparatus with Secondary Reactor of Wulzinger (Wulzinger, 1999)***

4.10.2 Mass Balance Comparison with Wulzinger

Wulzinger has reported the percentage yield obtained by using catalysts in the pyrolysis system. The catalysts either replace the fluid bed, are close coupled in the primary reactor, or in the secondary reactor. As the feed rate rather than the temperature is held constant, the liquid yield has been plotted for the different experiment types, against feed rate (Figure 44).

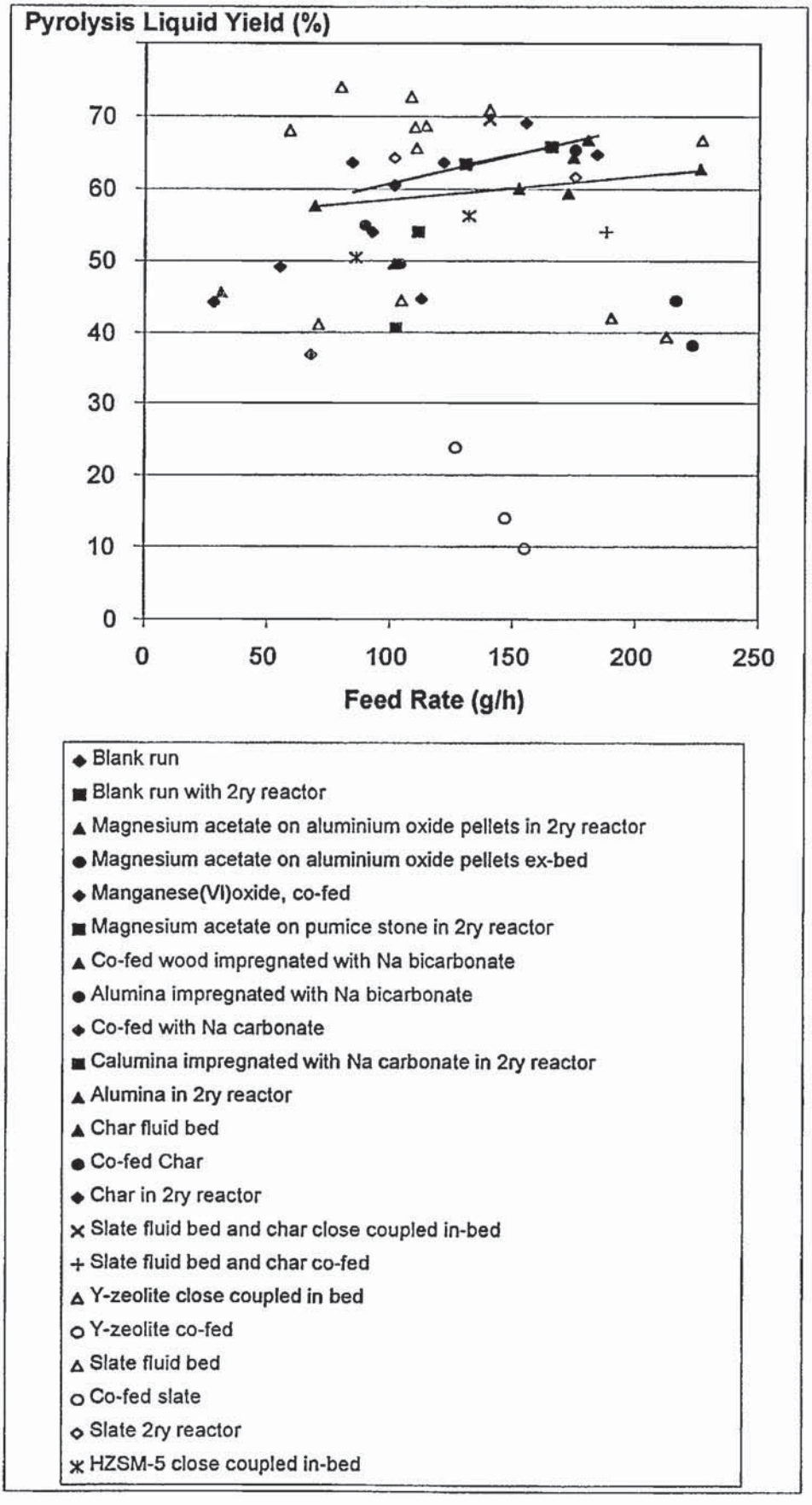

Figure 44 Pyrolysis Liquid Yield Results of Wulzinger at 475°C

It can be seen that only slate improved the yield of liquid compared to the blank runs. Unlike the results reported in this project, Y-zeolite does not have a beneficial effect on liquid yield. The slate results range to higher percentage liquid yields than in this report (approximately 75 % compared to 65 %) and there is greater difference between the slate and the blank non-catalytic runs. The results however should be compared relatively as shown by Figure 45. The non-catalytic pyrolysis liquid yield of Wulzinger is not as great as that of the empirical, while the blank run marked 'Salter' is of the same magnitude. This may be due to water being lost during rotary evaporation as described in Section 4.10.1. Had the organic yield rather than the pyrolysis liquid yield (organics plus water) been quoted, then the results may have been more comparable. This does however highlight the problem of methanol addition and removal.

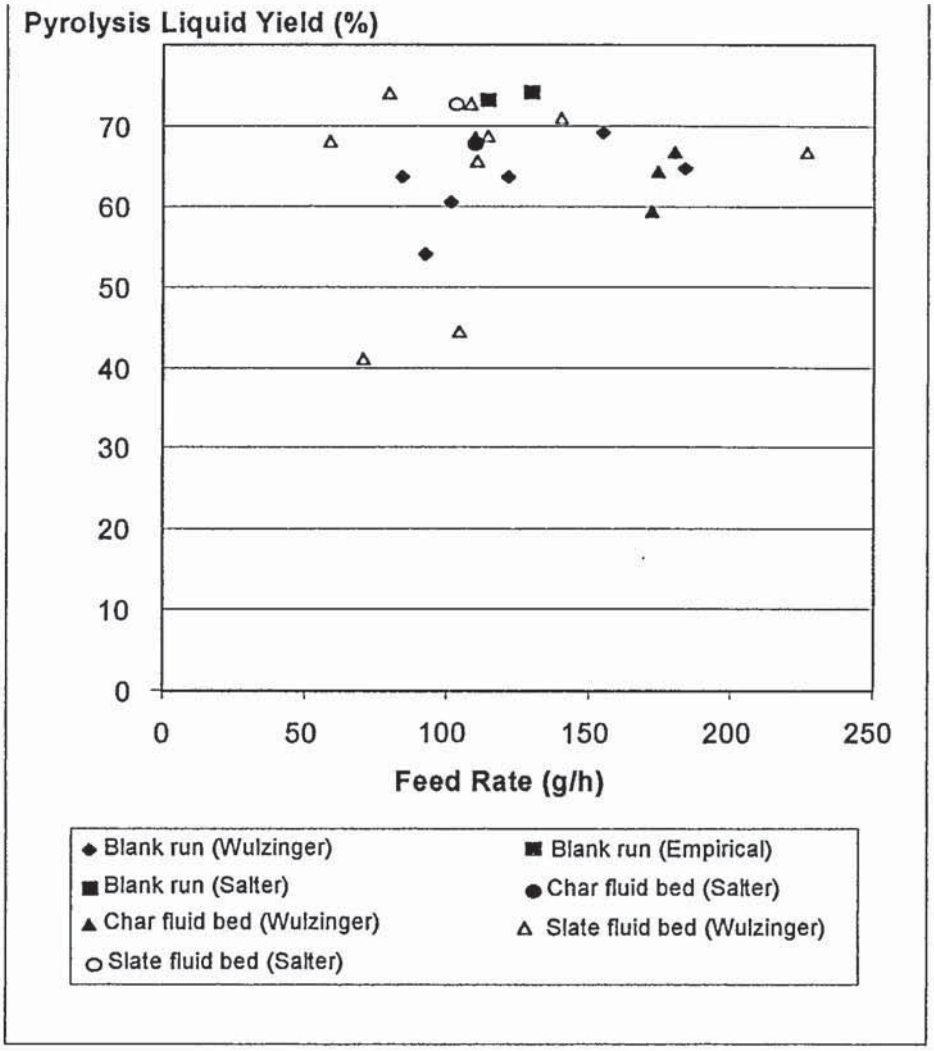

Figure 45 ***Comparison of Results of Wulzinger to Those Presented in this Thesis (Salter) at 475°C***

4.10.3 Experimental Comparison with Cooke

Cooke of Aston University worked prior to the work described in the bulk of this report. The set-up of the apparatus was as the commissioning configuration described in Section 4.1.1. Two finger condensers and an electrostatic precipitator were used producing three products that were then combined, rather than a single product as in this project. The gas was sampled intermittently and analysed at a later date rather than the continuous monitoring that was performed in this project.

In this project a variety of catalysts were used in different configurations. Cooke experimented with HZSM-5 on an alumina phosphate binder in co-feeding mode, in varying proportions to the wood feed.

4.10.4 Mass Balance Comparison with Cooke

The calculation of the mass balance for the work by Cooke is almost identical to the calculation done in this report. It differs in the accounting of char. This project assumes that micro char in the pyrolysis liquid is negligible and all the char is filtered out in the filter paper. Cooke assumed that there was the same proportion of char in all liquids as was found in the liquid remnant in condensers. This is thought to be false as the chary, tarry product that remains in the condensers is not representative of the liquid product that is found in the oil pots.

The results of Cooke *(Cooke, 1999)* have been plotted. Figure 46 shows the pyrolysis liquid yield at various reactor temperatures with varying proportions of catalyst. It can be seen that the non-catalytic points do not have the classic yield-temperature curve as demonstrated by the empirical formula and supported by this project (Section 4.9). The yield for all the runs is approximately the same, showing that HZSM-5, in 25 % or 50 % proportions to the wood feed, does not impact the proportion of liquid produced.

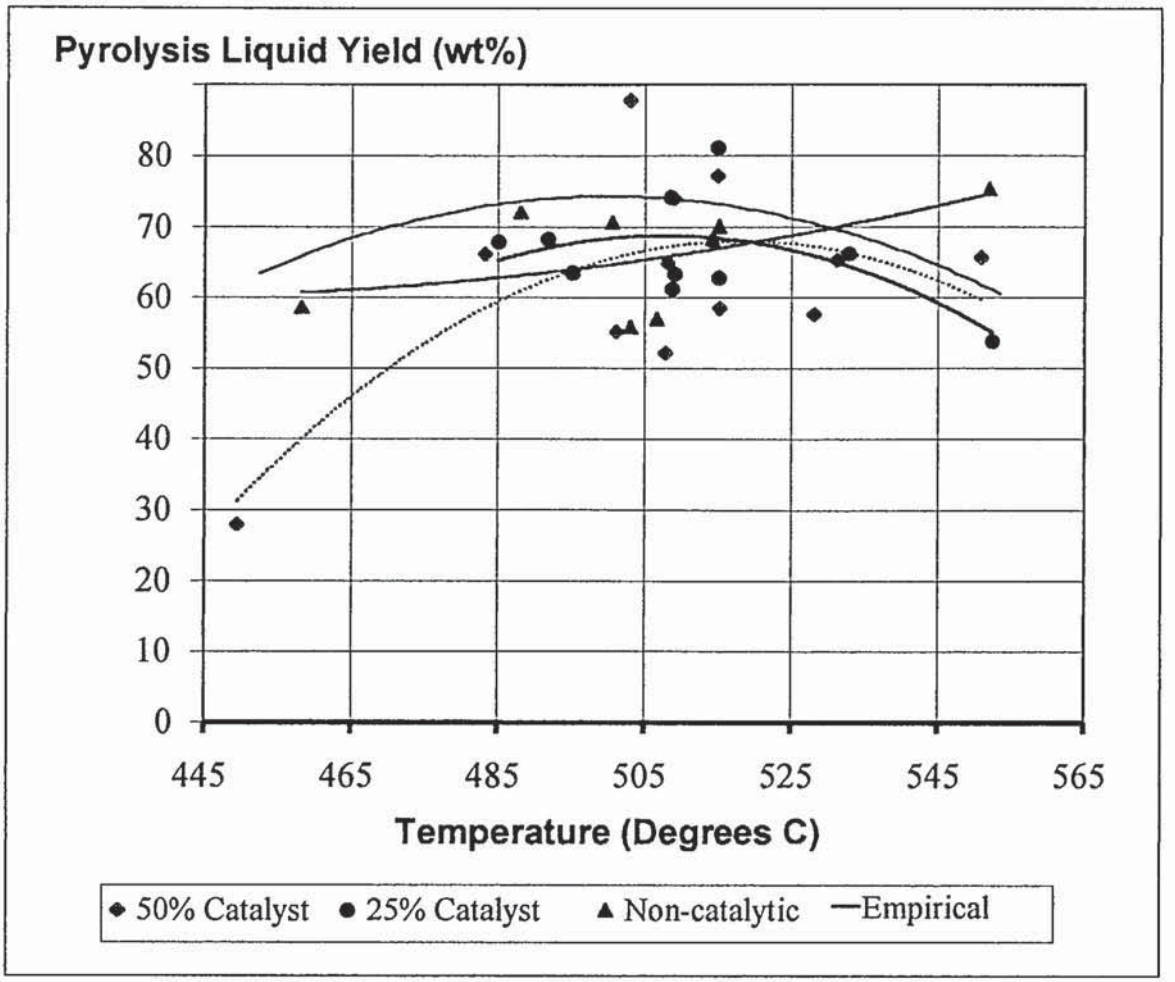

Figure 46 ***Pyrolysis Liquid Yield Results from Cooke using HZSM-5 on an Alumina Phosphate Binder***

5 CHEMICAL ANALYSIS OF THE LIQUID PYROLYSIS PRODUCT

To have a better understanding of the liquid product and define it more fully, it needs to be chemically analysed. On a simple level, the moisture content gives an initial indication of the quality and viscosity of liquid. It is believed that the higher the water content the lower the viscosity *(Tiplady, 1996)*. More detailed high performance liquid chromatography (HPLC) can begin to define the chemical composition of the liquid. These techniques are described in this Chapter. The aim of composition analysis is to compare the chemical changes in the liquid with the way it was made (type of catalyst, configuration and temperature) and the resulting stability (see Chapter 7).

5.1 Water Content

To complete the mass balance associated with each experimental pyrolysis run, the amount of water in the product liquid is found. This is also a parameter that is useful when assessing the pyrolysis liquid. A full description of the method of Karl Fischer water analysis used can be found in Section 4.7.1. The percentage water content is found of a pyrolysis liquid sample, which has been stored at 4°C following production and cooling, until preparation, no more than 10 minutes before water testing.

The water content of pyrolysis liquid has been linked to viscosity *(Tiplady, 1996)*. As the water content increases, so the viscosity falls. This hypothesis will be explored in this Section. The purpose of examining the water content in this study is to see if that is also true for catalytically produced liquids and to examine the relationship between water content and stability.

5.1.1 Water Content Results

The raw data for the water content of the pyrolysis products can be found in Section 4.9, but is examined in more detail here. The comparison between the type and position of catalyst used, the average temperature of the reactor during the experiment and the percentage of water in the resulting pyrolysis liquid is shown in Figure 87 and Figure 88 (Appendix G, page 279). The points on these graphs have had a straight line drawn

through them to help to see their groupings, but not to indicate that they are linked linearly. Table 76 (Appendix G, page 281) then displays the closeness of fit of the linear representations by expressing the 'R^2 values'. Poor linear correlations were drawn and the results have therefore been looked at more closely. It is believed that Figure 47 and Figure 48 are more representative of the relationship between water content, temperature and catalyst used. The first shows the overall trend of the three main experimental sets, slate catalyst bed, no catalyst addition and inclusion of Y-zeolite in-bed. The small amount of scatter can be see in Figure 87 (Appendix G, page 279). The line for results when no catalyst is used is included in Figure 48 for reference. In this graph, the sets of experiments have fewer points and linear representations are not able to be made.

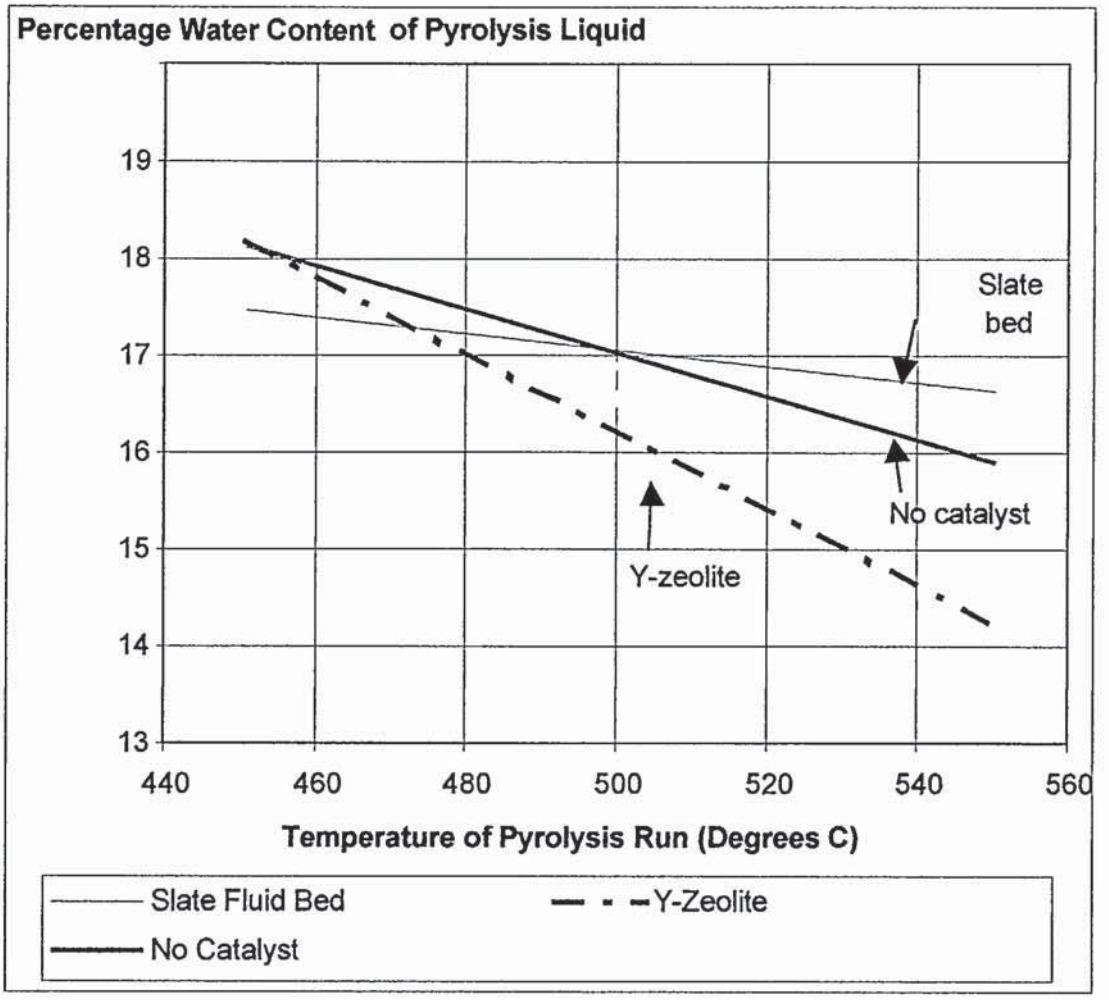

Figure 47 Percentage Water Content of Pyrolysis Liquids 1 of 2

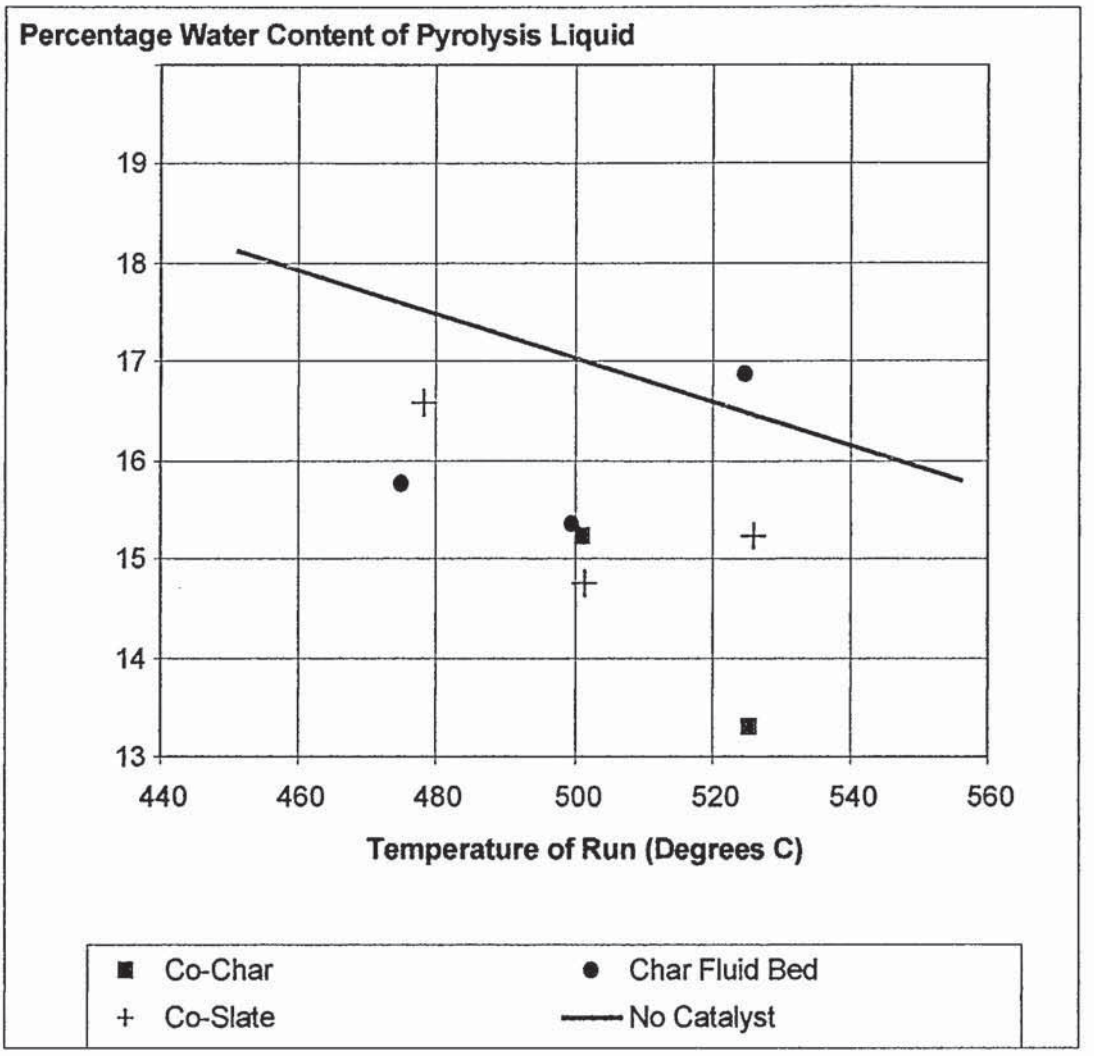

Figure 48 Percentage Water Content of Pyrolysis Liquids 2 of 2

5.2 Discussion of Water Content Results

Several factors are known to effect the water content of pyrolysis liquid. The water content of the pyrolysis liquid is a function of vapour concentration at the point of condensation in the pyrolysis process; gas flow-rate when produced and most importantly the temperature at which the pyrolysis liquid is collected. These factors have been kept constant while producing the pyrolysis liquid, to enable a direct comparison between the pyrolysis liquids produced with different catalysts in different configurations.

The poor R^2 values (Table 76) confirm the non-linear nature of the relationship between catalyst type, temperature of pyrolysis and percentage water content of the pyrolysis liquid. Co-fed char has a value of one because of the limited number of points (two) and the good fit of using char in the secondary reactor should be disregarded because of the spurious point at 450°C. Only Figure 47 has enough data points for each set of conditions. Figure 48 is for comparison to see if any remarkable results can be found from the conditions that have not been studied in as much detail. In most cases, the addition of a catalyst reduces the water content of the resulting pyrolysis liquid. Between 450°C and 500°C, those runs containing Y-zeolite, a slate fluid bed and no catalyst, produce liquid of a similar water content. Above 500°C, Y-zeolite runs produce more water than slate which has more than non-catalytic runs (see Figure 47). The percentage water content, however, is not greatly different, particularly when the scatter of points is considered (Figure 87).

To bring the water data together numerically rather than assessing it graphically, the percentage difference between each water content result and a 'model' result has been calculated. The model result is the equation of the straight line of the non-catalytic percentage water results. This is Equation 44. The individual results are shown in Table 77 to Table 81 (Appendix G). They are summarised in Table 36 where the average for each type of catalyst system is shown. The results have been ranked to show the pyrolysis liquid with the greatest percentage water content at the top and the least at the bottom of the table.

$$y = -0.0223x + 28.2$$

Equation 44

where y = Percentage water content of pyrolysis liquid

x = Temperature of pyrolysis run

Table 36 ***Average Percentage Difference between Pyrolysis Liquid Water Content and 'Model' Water Content (Ranked)***

Catalyst System	Average Percentage Difference between Water Content and Model (%)
Slate secondary bed	-18.08[a, b]
Slate fluid bed	-0.65
No catalyst	0.10
Y-zeolite in-bed	3.83
Char secondary reactor[c]	5.80
Char fluid bed	6.02
Co-fed slate	8.80
Co-fed char	14.95

Notes: (a) Negative result indicates more water contained in pyrolysis liquid than non-catalytic run.

(b) Result taken from a single experimental run.

(c) Run EHS45 excluded from average due to spurious result.

It is difficult to relate the water content to catalyst activity as it can be seen that, how the incorporation of the catalyst is achieved, is also a factor. This is illustrated by pyrolysis liquid produced with co-fed slate having considerably less percentage water then slate in the secondary bed or a fluid bed of slate in the primary reactor runs. These results will be compared to stability results to assert the hypothesis that better quality pyrolysis liquids have a higher percentage of water contained within them.

5.2.1 Water Content Comparison with Wulzinger

As discussed in Section 4.10, Wulzinger of the IWC has performed experiments in a similar manner to those done for this project. The method of water analysis is identical and the results are briefly compared here. Figure 49 shows the variety of catalysts used, their configuration of incorporation and the water content of the pyrolysis liquid produced, is plotted against the feed rate of wood to the pyrolysis reactor.

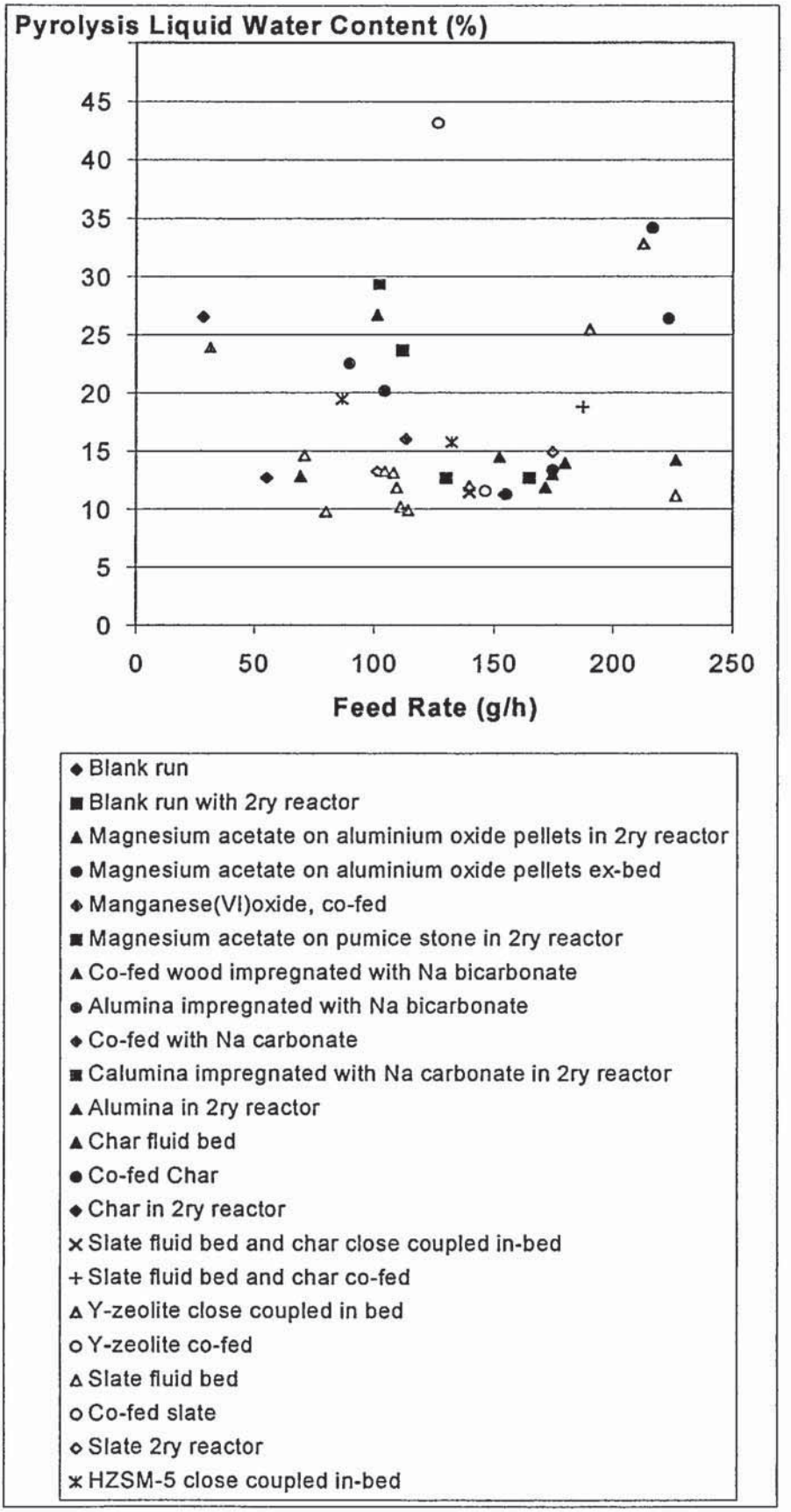

Figure 49 Water Content of Pyrolysis Liquid as found by Wulzinger

It is difficult to compare accurately the water contents found by Wulzinger because of the wide amount of scatter in the results. Wulzinger generally found slightly less water in the blank runs than found in this project, but at a feed rate of 100 g/h, a great deal more water was found. Generally, the Y-zeolite runs have a particularly high water content, a results not duplicated in the work for this project. The slate results, however, are very similar.

5.3 High Performance Liquid Chromatography

The main chemical analysis technique used was high performance liquid chromatography (HPLC). Currently, it is only the aqueous phase of the liquid product that can be analysed. No method has been developed to look at the complicated composition of the whole pyrolysis liquid by HPLC.

The aqueous phase is obtained by adding 4 g of mobile phase (sulphuric acid and water) to 2 g of pyrolysis liquid, shaking, and then centrifuging for 5 minutes at 4000 revs/min. The tarry portion phase separates and settles at the bottom of the sample vial. The aqueous layer is separated and filtered using an Acrodisc PTFE 0.2 μm filter. HPLC is subsequently performed on the aqueous fraction. Therefore, if changes in composition occur in the water insoluble lignin-based phase (the remaining pyrolysis liquid) they will not be detected. The HPLC testing of the aqueous phase is therefore only an indication that changes in the product composition may have occurred. In general, the aqueous phase contains sugars, aliphatic acids, alcohols, ketones and aldehydes.

The HPLC system is based on a Unicam Crystal 200 quaternary gradient pump and a refractive index detector, Gilson 132. The mobile phase used is H_2SO_4 0.005M at a constant concentration. The Biorad cation exchange column used is Aminex HDX-87H, 300 × 7.8 mm.

The pyrolysis liquid samples for HPLC testing, like the liquids for water analysis, are stored at 4°C between collection and testing. Testing occurs three to six days after production of the liquid. The low temperature and the short time before sample testing

ensures that the sample liquids are chemically the same as those produced and ageing of the liquid is not a factor.

5.3.1 High Performance Liquid Chromatography Results

The weight percent of each chemical detected on a dry wood-fed basis has been tabulated and graphed according to catalyst used and temperature of the pyrolysis reaction. These are shown in Table 37 (page 160) and Table 84 to Table 87 (Appendix H) and in Table 38 (page 161) and Table 88 to Table 91 (Appendix H) respectively. The samples from the main fraction of the liquid, obtained from the bottom of the electrostatic precipitator, and the secondary liquid, trapped by the dry ice condenser, have been considered separately. 'r' indicates that a sample has been re-analysed. Re-analysis was necessary when a satisfactory result was not achieved. This was often due to the apparatus being switched off for a period of time and difficulty attaining a consistent base line when it was re-started.

The results for two chemicals, hydroxyacetaldehyde and levoglucosan, have been emboldened in the tables. This is because they are the most significant chemicals in pyrolytic wood decomposition (see Section 2.1.1).

Although both the main liquid and the secondary liquid have been analysed, the main liquid is of most interest. The secondary liquid, as mentioned before, is collected for completeness of the mass balance. If a particularly interesting HPLC result is found then this might be a reason to collect the secondary liquid, other than for mass balance purposes. No chemicals of particular significance or quantity were found in the secondary liquid. Should there have been, this may have led to deliberately fractionating the product liquid specifically for chemical synthesis.

Table 37 HPLC Analysis - Main Fraction of Liquid, Wt% on Dry Wood Basis of Chemicals Found and Pyrolytic Lignin, No Catalyst

Run No	EHS - No Catalyst	42	33	50	16	17	21	22	23	20
	Av. Run Temp (°C)	**447.3**	**453.1**	**475.4**	**477.6**	**490.8**	**500.8**	**522.9**	**523.0**	**549.2**
CB	Cellobiose	0.00	0.00	0.09	0.00	0.00	0.00	0.00	0.00	0.00
G	Glucose	0.01	0.27	0.45	0.30	0.26	0.00	0.00	0.00	0.16
F	Fructose	0.00	1.03	0.00	0.00	0.00	0.00	0.00	0.00	0.00
GX	Glyoxal	3.59	0.02	6.36	0.15	0.17	0.02	0.01	0.02	0.02
HA	**Hydroxyacetaldehyde**	**23.72**	**20.17**	**22.39**	**18.49**	**20.62**	**15.77**	**17.73**	**18.80**	**14.99**
LG	**Levoglucosan**	**4.62**	**3.01**	**4.21**	**5.06**	**4.56**	**1.74**	**1.85**	**1.96**	**2.50**
FD	Formaldehyde	4.93	2.29	4.57	2.89	3.15	1.06	1.44	1.72	2.20
FC	Formic Acid	0.00	4.01	0.00	4.60	4.50	2.00	2.11	3.02	2.72
HOAc	Acetic Acid	5.35	4.55	5.34	3.86	4.01	3.27	3.41	4.12	4.40
A	Acetol	2.66	2.85	3.46	1.09	1.15	1.00	0.99	0.96	1.25
BL	Butyrolactone	5.37	0.00	0.00	0.00	0.00	0.00	0.00	0.00	0.00
FUA	Furoic Acid	0.00	0.18	0.00	0.00	0.00	0.00	0.00	0.00	0.00
BEL	2-Buten-1-ol	0.23	0.00	0.36	0.00	0.00	0.00	0.00	0.00	0.00
FUE	2(5H)-Furanone	0.00	0.00	0.00	0.60	0.46	0.49	0.00	0.39	0.33
	Pyrolytic Lignin	2.16	3.22	5.28	3.53	3.39	2.63	3.44	1.88	1.67

Table 38 ***HPLC Analysis - Secondary Fraction of Liquid, Wt% on Dry Wood Basis of Chemicals Found and Pyrolytic Lignin, No Catalyst***

Run No	EHS - No Catalyst	42	33	50	16	17	17r	21	22	23	20
	Av. Run Temp (°C)	**447.3**	**453.1**	**475.4**	**477.6**	**490.8**	**490.8**	**500.8**	**522.9**	**523.0**	**549.2**
F	Fructose	0.78	0.00	0.82	0.00	0.00	0.00	0.00	0.00	0.00	0.00
GX	Glyoxal	0.00	0.08	0.00	0.00	0.00	0.00	0.00	0.00	0.00	0.00
X	Xylitol	3.23	0.27	4.21	0.00	0.00	0.00	0.00	0.00	0.00	0.00
HA	**Hydroxyacetaldehyde**	**4.32**	**0.56**	**6.86**	**0.95**	**0.13**	**0.84**	**3.16**	**0.78**	**0.98**	**0.51**
LG	Levoglucosan	0.30	0.04	0.51	0.10	0.00	0.00	0.00	0.00	0.00	0.00
LA	Lactic Acid	0.00	0.00	0.00	0.00	0.00	0.11	0.00	0.00	0.00	0.00
FD	Formaldehyde	4.53	0.65	7.54	1.40	0.19	0.82	3.43	1.00	1.08	0.77
FC	Formic Acid	0.00	0.25	0.00	0.50	0.09	0.34	0.00	0.00	0.00	0.00
HOAc	Acetic Acid	3.34	0.46	4.65	0.61	0.16	0.69	2.23	0.62	0.65	0.58
A	Acetol	1.03	0.16	1.40	0.17	0.03	0.21	0.60	0.21	0.19	0.12
MeOH	Methanol	2.11	0.28	3.22	0.31	0.00	0.31	1.23	0.34	0.35	0.35
MCPD	Cyclopentanedione	0.00	0.00	0.12	0.00	0.00	0.00	0.00	0.00	0.00	0.00
BEL	2-Buten-1-ol	0.00	0.00	0.02	0.00	0.00	0.00	0.00	0.00	0.00	0.00
FUE	2(5H)-Furanone	0.00	0.00	0.00	0.00	0.00	0.00	0.00	0.02	0.02	0.00
	Pyrolytic lignin	0.26	0.02	0.02	0.02	0.02	0.01	0.03	0.02	0.01	0.01

5.3.1.1 Comments on the Occurrence of Chemicals

It is the intention to correlate the occurrence and non-detection of these chemicals to the stability of the pyrolysis liquid to try to find which chemicals either stabilise or destabilise the liquid. This is done in Chapter 7.

To initially assess the results of HPLC analysis, the occurrence of chemicals can be examined. Table 93 and Table 94 (Appendix H) look at this using a tick to represent when a particular chemical is found in the majority of experiments under the conditions stated in Table 92 (Appendix H). A cross, therefore is where the chemical has not been identified in the stated set of pyrolysis liquids. Table 93 looks at the main fraction of pyrolysis liquid and Table 94 the secondary liquid. Points have been emboldened and repeated to highlight unusual or notable results.

It can been see that, excepting glucose (which does not occur) and fructose (which does occur) in the main fraction of the liquid, the same chemicals occur in the liquid from the slate fluid bed as in the non-catalytic liquid. The only other configuration when glucose is not produced is when a slate secondary reactor is employed. Fructose is also produced in the system that includes Y-zeolite in the primary reactor. These could be significant chemicals if the configurations associated with them are found to be related to stability.

Hydroxyacetaldehyde, levoglucosan, formaldehyde, acetic acid and acetol are all found in the main pyrolysis liquid for every catalytic and non-catalytic configuration. Pyruvic acid, lactic acid and crotonaldehyde have not been detected in the main liquid or the secondary liquid, excepting lactic acid in the secondary liquid when char is co-fed. Methanol is not found in any main liquids. Cellobiose, glucose, fructose, butanol and furanone have not been detected in any secondary liquids.

Glyoxal is not detected in only the slate secondary bed configuration when to find it in the main liquid is the standard result. Glyoxal is only found in the secondary liquid when Y-zeolite has been close coupled in the primary reactor or with a char secondary reactor.

5.3.1.2 Quantities of Chemicals Found

As well as the simple occurrence of chemicals in the pyrolysis liquid, the relative amounts of individual chemicals will be related to liquid stability (see Chapter 7). For each catalytic configuration, the chemicals produced can be plotted against temperature of pyrolysis. Examples of these are shown in Figure 50, Figure 89 and Figure 90 (Appendix J). Hydroxyacetaldehyde is not shown as it is produced in a much greater quantity (~20 %).

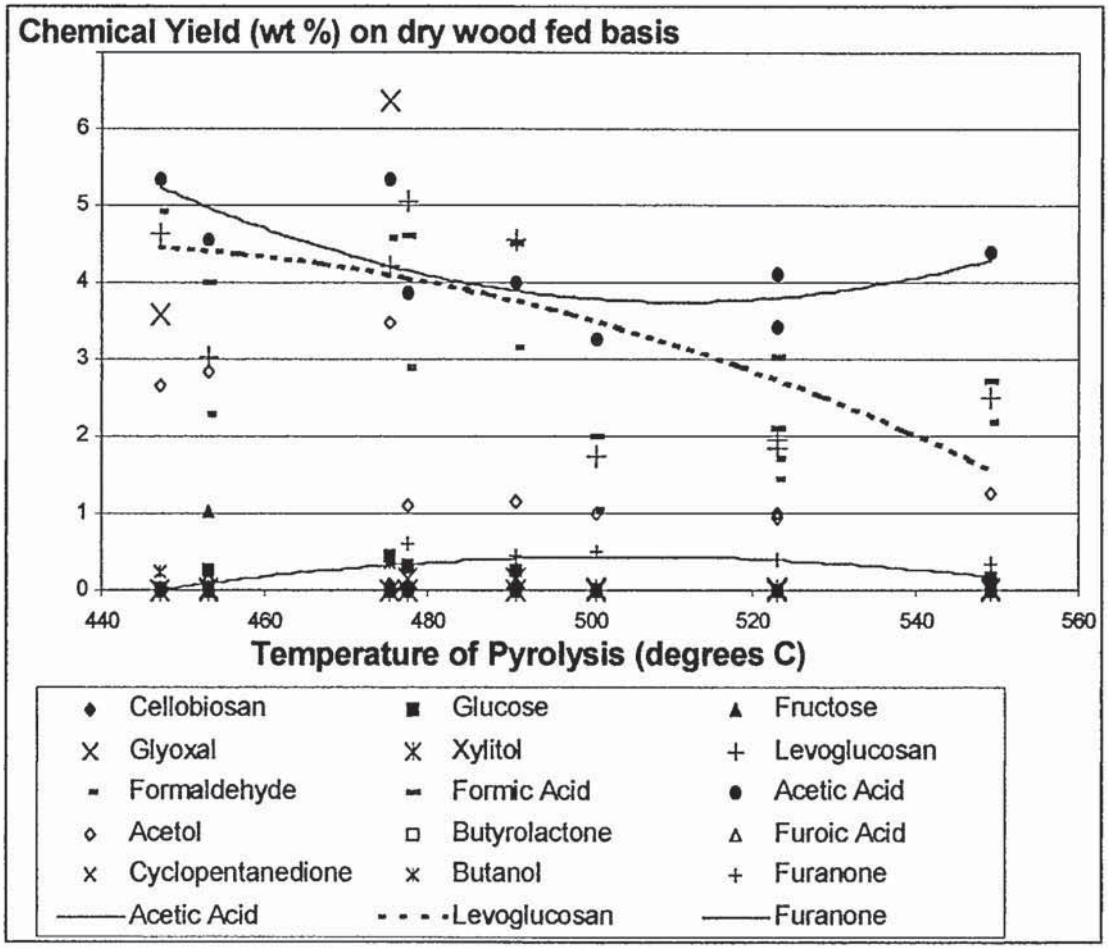

Figure 50 Example Chemicals Occurring in Non-Catalytic Pyrolysis Liquid at Different Temperatures

It is difficult to analyse and compare the different catalytic configurations when all the chemicals are considered. Individual chemical results have therefore been used in conjunction with both the temperatures of pyrolysis and catalytic systems. For the three

main sets of experiments, with no catalyst, slate fluid bed and Y-zeolite in the primary reactor, the quantities of hydroxyacetaldehyde, levoglucosan and acetic acid, the three main indicative chemicals, have been graphed, Figure 51, Figure 53 and Figure 55. Subsequent catalyst systems have also been graphed, Figure 52, Figure 54 and Figure 56. Hydroxyacetaldehyde and levoglucosan are found in the greatest quantities in pyrolysis liquid and are significant because they have been previously extracted and exploited as individual chemicals (see Section 2.1.2).

5.3.1.3 Hydroxyacetaldehyde Results

Figure 51 and Figure 52 show the percent yield of hydroxyacetaldehyde on a dry wood-fed basis for the various catalyst configurations. Slate catalyst as the fluid bed has the effect of slightly decreasing hydroxyacetaldehyde amounts in the aqueous component of the main liquid compared to no catalyst. Y-zeolite in the primary reactor produces a greater reduction in hydroxyacetaldehyde.

Table 39 shows the R^2 values for Figure 51 and Figure 52. In each case, a second order polynomial curve fit was chosen to link the points. The results have been compared to model results in Section 5.4.1.

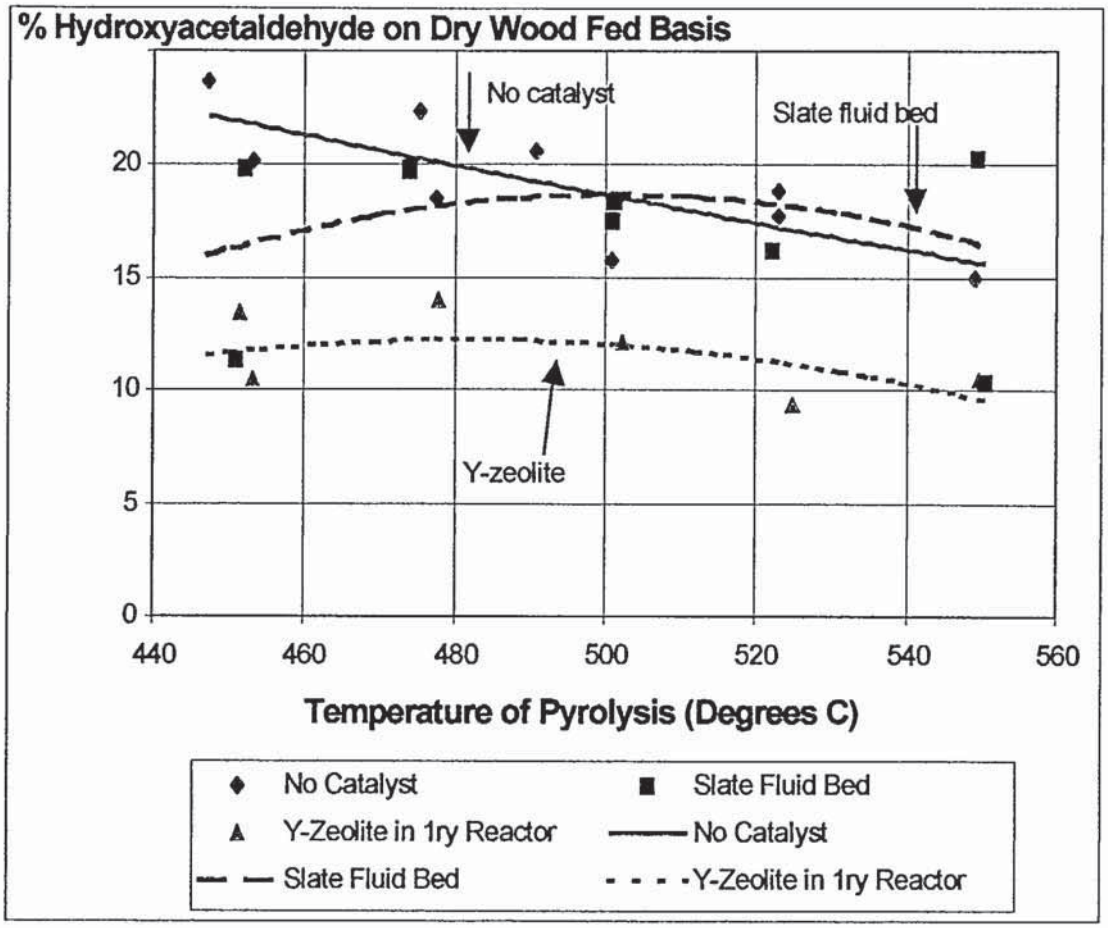

Figure 51 ***Hydroxyacetaldehyde Production Changes with Catalyst 1 of 2 Amount Found in HPLC of Main Fraction of Liquid***

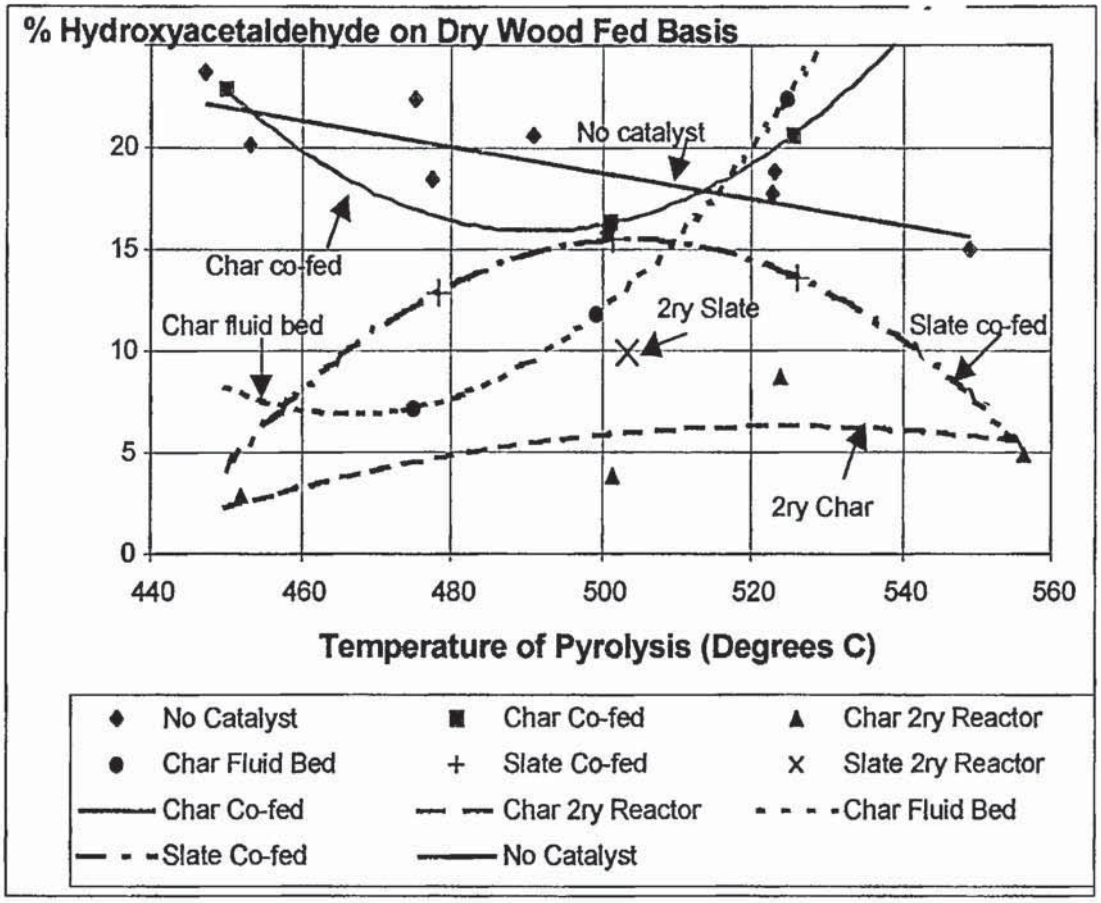

Figure 52 *Hydroxyacetaldehyde Production Changes with Catalyst 2 of 2 Amount Found in HPLC of Main Fraction of Liquid*

Table 39 *Line Fit for Hydroxyacetaldehyde Graphs, Figure 51 to Figure 52*

Experiment Set	No. Points	Chosen Line Type	R^2 Value	Alternative Line Type	R^2 Value
No Catalyst	11	Polynomial (2^{nd} order)	0.566	Linear	0.565
Y-Zeolite	7	Polynomial (2^{nd} order)	0.255	Linear	0.144
Slate Fluid Bed	10	Polynomial (2^{nd} order)	0.075	Linear	0.001
Char 2^{ry} Reactor	4	Polynomial (2^{nd} order)	0.461	Linear	0.288
Co-Fed Char	3	Polynomial (2^{nd} order)	1.000	Linear	0.267
Char Fluid Bed	3	Polynomial (2^{nd} order)	1.000	Linear	0.954
Co-Fed Slate	3	Polynomial (2^{nd} order)	1.000	Linear	0.070

5.3.1.4 Levoglucosan Results

Figure 53 and Figure 54 show the percent yield of levoglucosan on a dry wood-fed basis for the various catalyst configurations.

Table 40 shows the R^2 values for Figure 53 and Figure 54. A mixture of third order and second order polynomial curve fits were chosen to link the points. This was based on the number of points available and the closeness of fit of the points. The results have been compared to model results in Section 5.4.1.

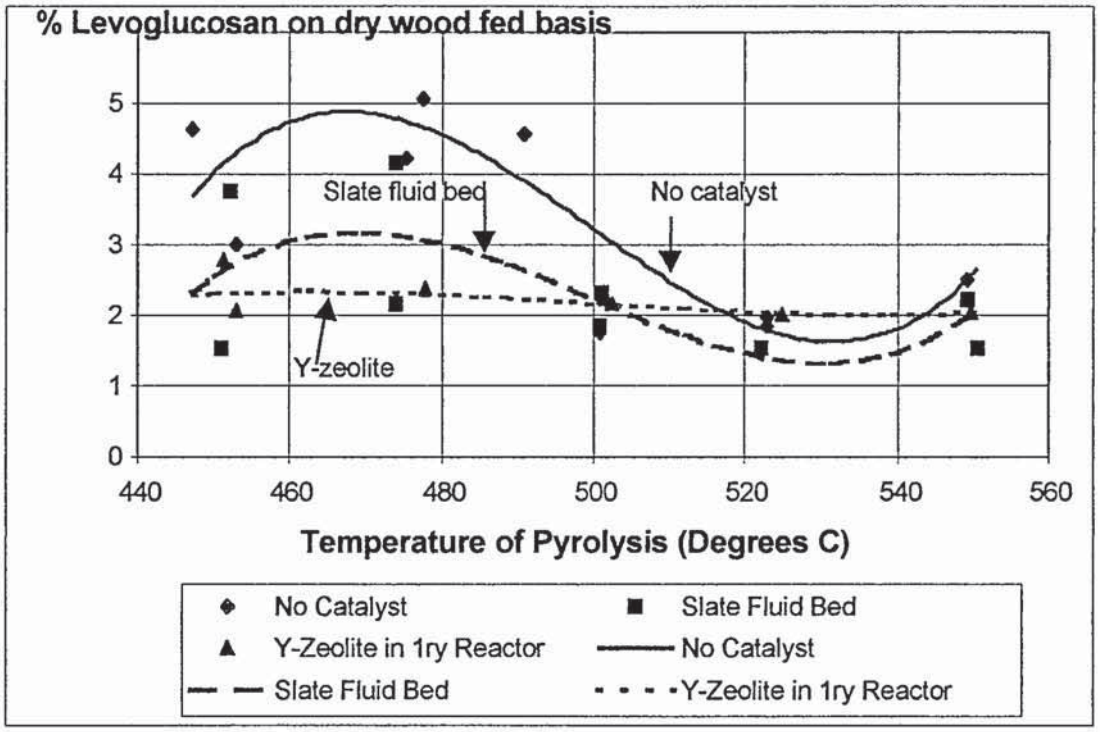

Figure 53 ***Levoglucosan Production Changes with Catalyst 1 of 2 Amount Found in HPLC of Main Fraction of Liquid***

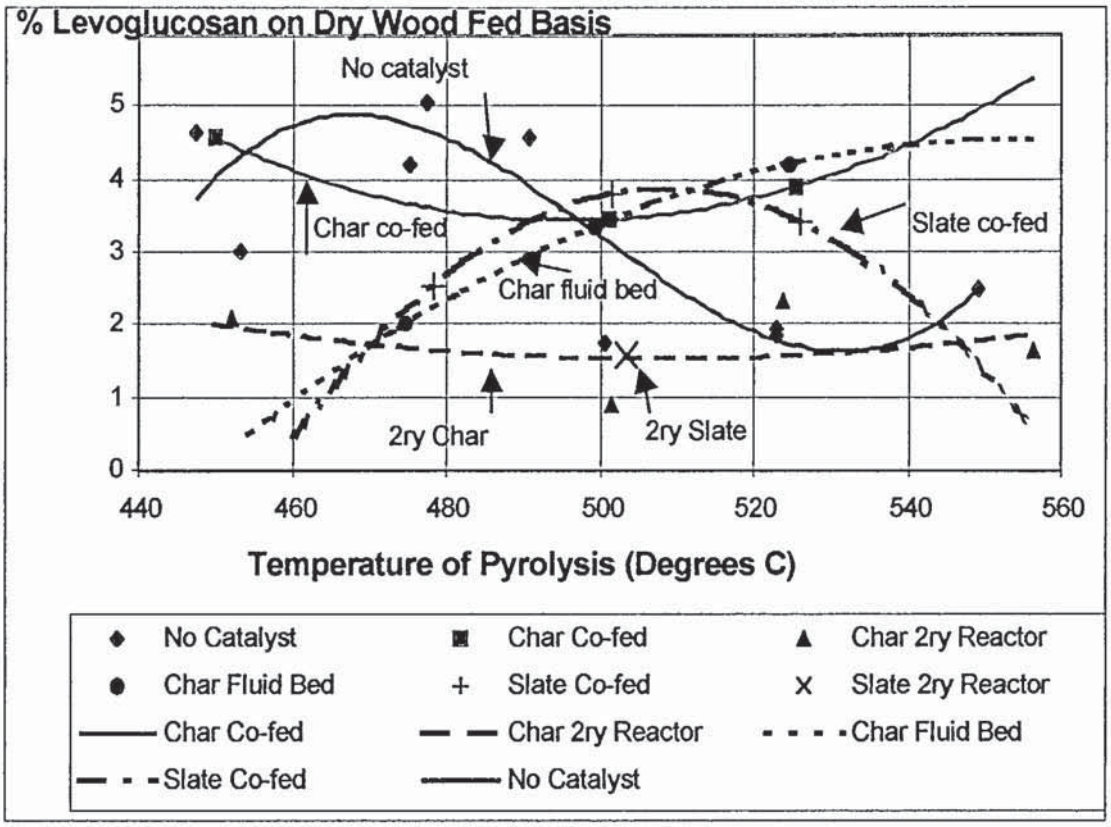

Figure 54 *Levoglucosan Production Changes with Catalyst 2 of 2 Amount Found in HPLC of Main Fraction of Liquid*

Table 40 *Line Fit for Levoglucosan Graphs, Figure 53 to Figure 54*

Experiment Set	No. Points	Chosen Polynomial	R^2 Value	Alternative Polynomial	R^2 Value
No Catalyst	11	3rd order	0.669	2nd order	0.421
Y-Zeolite	7	3rd order	0.356	2nd order	0.193
Slate Fluid Bed	10	3rd order	0.225	2nd order	0.208
Char 2ry Reactor	4	2nd order	0.1176	3rd order	1.000
Co-Fed Char	3	2nd order	1.000	3rd order	1.000
Char Fluid Bed	3	2nd order	1.000	3rd order	1.000
Co-Fed Slate	3	2nd order	1.000	3rd order	1.000

5.3.1.5 Acetic Acid Results

Figure 55 and Figure 56 show the percent yield of acetic acid on a dry wood-fed basis for the various catalyst configurations. The results are similar in pattern to those of levoglucosan.

Table 41 shows the R^2 values for Figure 55 and Figure 56. A mixture of third order and second order polynomial curve fits were chosen to link the points. This was based on the number of points available and the closeness of fit of the points. The results have been compared to model results in Section 5.4.1.

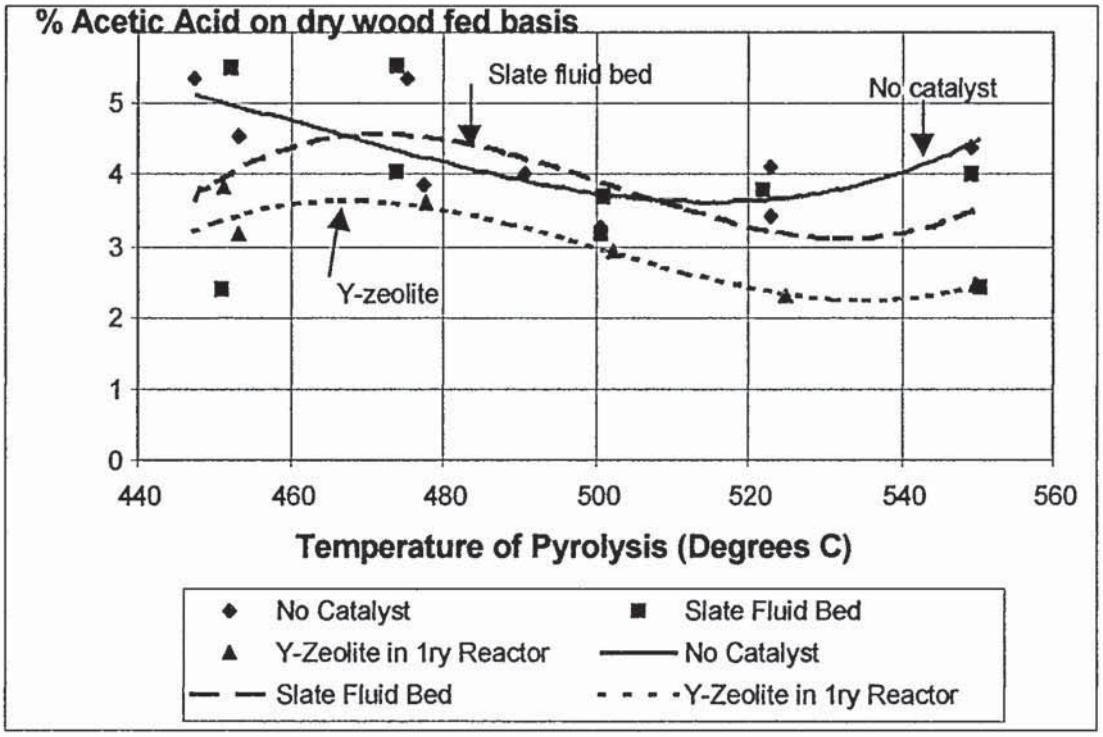

Figure 55 ***Acetic Acid Production Changes with Catalyst 1 of 2 Amount Found in HPLC of Main Fraction of Liquid***

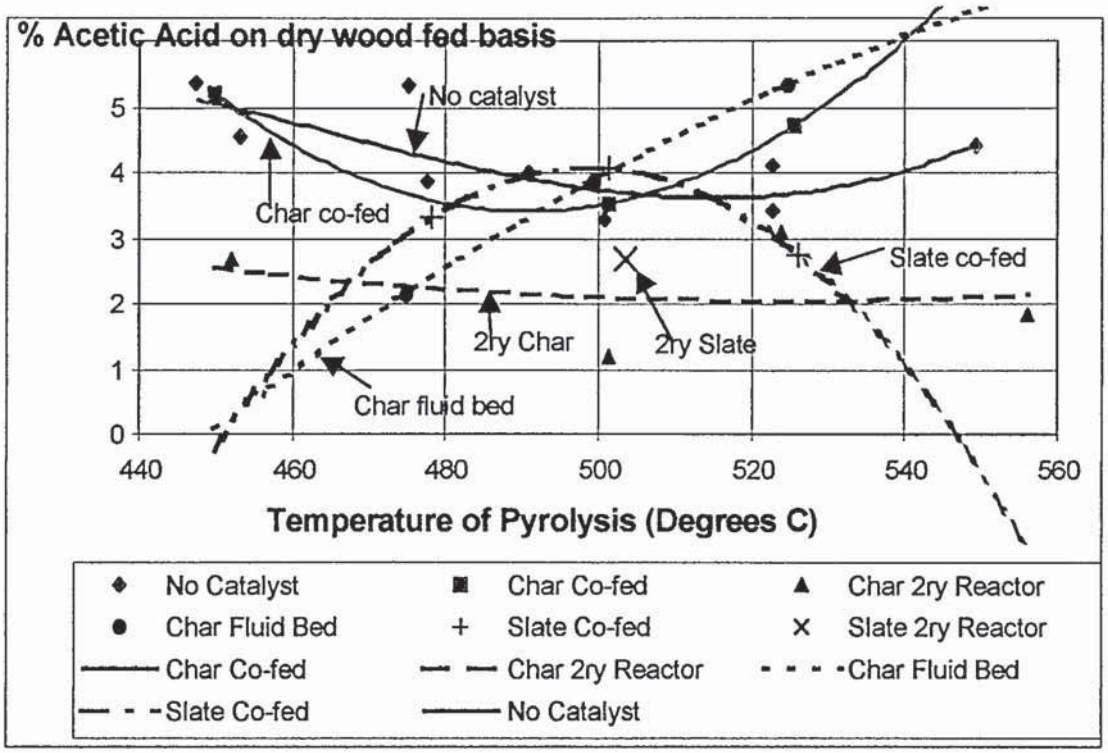

Figure 56 ***Acetic Acid Production Changes with Catalyst 2 of 2 Amount Found in HPLC of Main Fraction of Liquid***

Table 41 ***Line Fit for Acetic Acid Graphs, Figure 51 to Figure 52***

Experiment Set	No. Points	Chosen Polynomial	R^2 Value	Alternative Polynomial	R^2 Value
No Catalyst	11	3rd order	0.5432	2nd order	0.5197
Y-Zeolite	7	3rd order	0.8142	2nd order	0.6831
Slate Fluid Bed	10	3rd order	0.1752	2nd order	0.0986
Char 2ry Reactor	4	2nd order	0.0644	3rd order	1.000
Co-Fed Char	3	2nd order	1.000	3rd order	1.000
Char Fluid Bed	3	2nd order	1.000	3rd order	1.000
Co-Fed Slate	3	2nd order	1.000	3rd order	1.000

5.3.1.6 Lignin Results

Figure 57 expresses the quantity of pyrolytic lignin found in the three main sets of experiments, with no catalyst, slate fluid bed and Y-zeolite in the primary reactor.

Figure 58 displays the remaining catalytic configurations and the quantity of pyrolytic lignin at different pyrolysis temperatures. The curves are particularly interesting to examine alongside the organic yield results (Figure 40 and Figure 41) as the peaks themselves and the relationships between the different catalytic systems is similar. This indicates that the temperature of pyrolysis determines the amount of pyrolytic lignin produced which then affects the organic yield of the experimental run. This phenomenon is independent of catalytic system.

There is one anomaly, however. This occurs at 475°C for Y-zeolite, slate fluid bed, no catalyst and char fluid bed. For all these systems the percentage of lignin yielded does not fit in with the predicted curve and also is not similar to the organic yield results. It is difficult to assign this to experimental error as these runs were not done at a particular time together and there is nothing to distinguish them from other experiments, apart from the temperature at which they were done. This is discussed further in Section 5.4. A run at 475°C was not performed for the other catalytic systems so this phenomenon can not be checked in all systems. This phenomenon can be used to examine the effect of pyrolytic lignin on stability separately from organic yield or other parameters that simply follow the same trend as it does not follow the general temperature trend at 475°C. This is done in Chapter 7.

Table 42 shows that with a third order polynomial equation, the lines for no catalyst, Y-zeolite and slate fluid bed have some scatter, but fit the general trend. With fewer points, it is more difficult to analyse the alternative modes of operation.

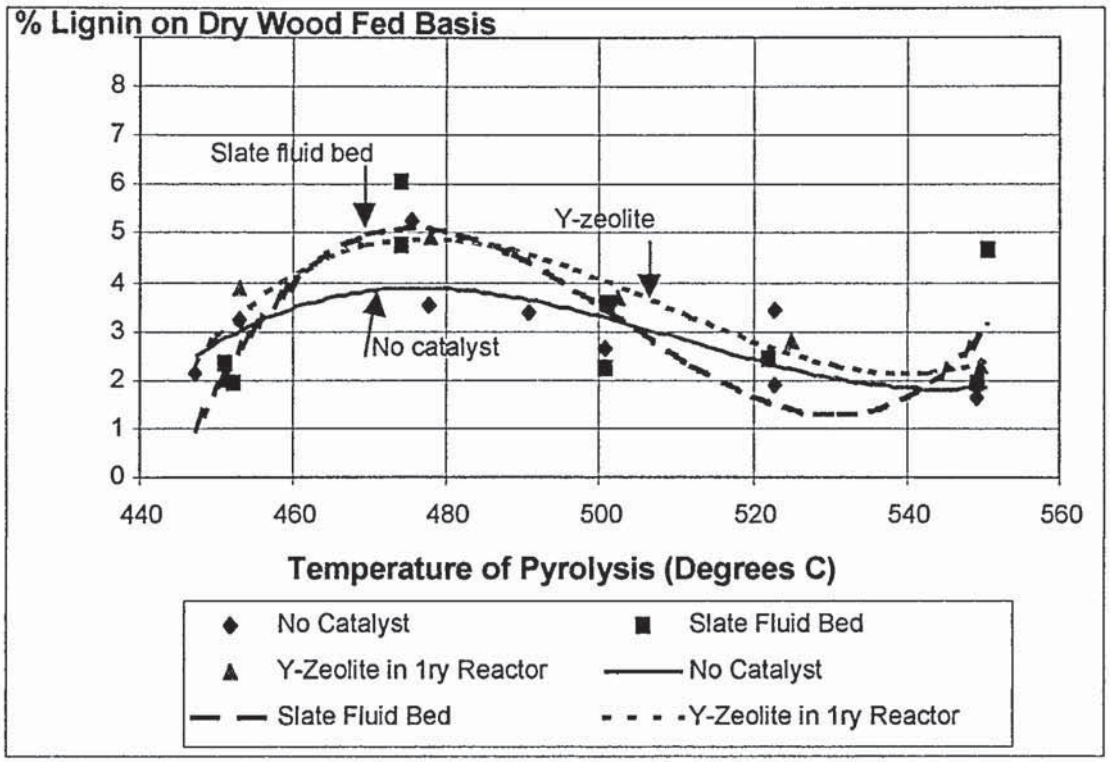

Figure 57 ***Pyrolytic Lignin Production Changes with Catalyst 1 of 2 Amount Found in Main Fraction of Liquid***

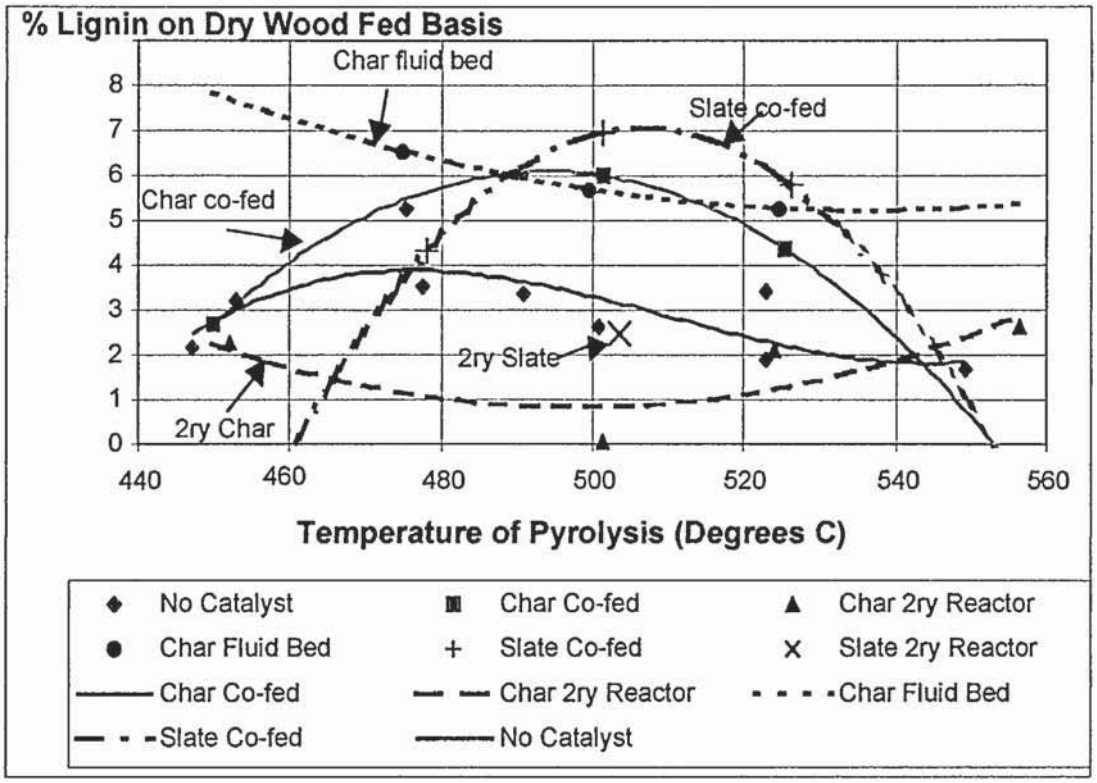

Figure 58 ***Pyrolytic Lignin Production Changes with Catalyst 2 of 2 Amount Found in Main Fraction of Liquid***

Table 42 ***Line Fit for Graphs Lignin, Figure 57 to Figure 58***

Experiment Set	No. Points	Chosen Polynomial	R^2 Value	Alternative Polynomial	R^2 Value
No Catalyst	11	3rd order	0.567	2nd order	0.445
Y-Zeolite	7	3rd order	0.701	2nd order	0.448
Slate Fluid Bed	10	3rd order	0.616	2nd order	0.105
Char 2ry Reactor	4	2nd order	0.639	3rd order	1.000
Co-Fed Char	3	2nd order	1.000	3rd order	1.00
Char Fluid Bed	3	2nd order	1.000	3rd order	1.000
Co-Fed Slate	3	2nd order	1.000	3rd order	1.000

5.4 Discussion of Liquid Product Chemical Analysis Results

There are three main purposes for examining the chemical composition of the liquid resulting from catalytic and non-catalytic pyrolysis:

1) To correlate chemical occurrence with stability.
2) To look for high quantities of a particular chemical that would be suitable for extraction.
3) To understand the effect of different types of catalyst and their mode of operation on the degradation mechanisms.

The addition of any catalysts to the system does not yield any chemical in a significantly higher quantity than the non-catalytic configuration. No chemical therefore satisfies criterion 2). Criterion 1) will be examined in further detail in association with stability results in Section 7.2. The results of the effect of catalyst and configuration are summarised below for hydroxyacetaldehyde, levoglucosan and lignin in Sections 5.4.1 and 5.4.2.

Criterion 3) can be answered by the relative amounts of hydroxyacetaldehyde and lignin produced. The results from HPLC analysis show that the proportion of hydroxyacetaldehyde yielded compared to levoglucosan is high. From Section 2.1.1, this would indicate that cellulose fragmentation rather than depolymerisation is the predominant decomposition pathway.

5.4.1 Hydroxyacetaldehyde, Levoglucosan and Acetic Acid Results

To bring the hydroxyacetaldehyde, levoglucosan and acetic acid data together numerically rather than assessing it graphically, the percentage difference between each chemical content result and 'model' results, have been calculated, similarly to the water content results (see Section 5.2). The model result is the equation of the second order polynomial line of the non-catalytic percentage hydroxyacetaldehyde, levoglucosan or acetic acid result. This is Equation 45 for hydroxyacetaldehyde, Equation 46 for levoglucosan and Equation 47 for acetic acid.

$$y = 0.00006x^2 - 0.1243x + 65.621$$

Equation 45

where y = Percentage hydroxyacetaldehyde content of pyrolysis liquid (wt% on dry wood-fed basis)

x = Temperature of pyrolysis run

$$y = -0.0002x^2 + 0.1847x - 35.414$$

Equation 46

where y = Percentage levoglucosan content of pyrolysis liquid (wt% on dry wood-fed basis)

x = Temperature of pyrolysis run

$$y = -0.0004x^2 - 0.3792x + 100.57$$

Equation 47

where y = Percentage acetic acid content of pyrolysis liquid (wt% on dry wood-fed basis)

x = Temperature of pyrolysis run

The individual results are shown in Table 95 to Table 98 (Appendix H). They are summarised in Table 43, Table 44 and Table 45 where the average for each type of catalyst system is shown. The results have been ranked to show the pyrolysis liquid with the greatest percentage specific chemical content at the top and the least at the bottom of the table. The result for the non-catalytic system indicates how robust the model is. For levoglucosan and acetic acid, where the average percentage difference between the non-catalytic runs and the non-catalytic model is large, the model is not a good representation of the actual result due to the scatter of points around the model.

The acetic acid results and those of levoglucosan are similar and are not thought to be individually significant. For this reason, the levoglucosan results only will be considered further.

Table 43 ***Average Percentage Difference between Pyrolysis Liquid Aqueous Fraction Hydroxyacetaldehyde Content and 'Model' Hydroxyacetaldehyde Content (Ranked)***

Catalyst System	Average Percentage Difference between Hydroxyacetaldehyde Content and Model (%)
Co-fed char	-5.20[(a)]
No catalyst	-1.03
Slate fluid bed	4.00
Char fluid bed	22.89
Co-fed slate	23.41
Y-zeolite in-bed	40.33
Slate secondary bed	45.78
Char secondary reactor	70.74

Notes: (a) Negative result indicates more hydroxyacetaldehyde contained in pyrolysis liquid than non-catalytic run.

Table 44 ***Average Percentage Difference between Pyrolysis Liquid Aqueous Fraction Levoglucosan Content and 'Model' Levoglucosan Content (Ranked)***

Catalyst System	Average Percentage Difference between Levoglucosan Content and Model (%)
Co-fed char	42.04
No catalyst	48.89
Co-fed slate	52.18
Char fluid bed	52.85
Slate fluid bed	65.05
Y-zeolite in-bed	67.65
Char secondary reactor	73.06
Slate secondary bed	77.20

Table 45 ***Average Percentage Difference between Pyrolysis Liquid Aqueous Fraction Acetic Acid Content and 'Model' Acetic Acid Content (Ranked)***

Catalyst System	Average Percentage Difference between Acetic Acid Content and Model (%)
Co-fed char	60.10
No catalyst	62.28
Slate fluid bed	66.27
Char fluid bed	66.35
Co-fed slate	69.63
Y-zeolite in-bed	72.60
Slate secondary bed	75.68
Char secondary reactor	81.18

5.4.2 Lignin Results

Lignin yields vary from 0 to 7% in the main liquid product on a dry wood-fed basis. The trend of the lignin produced generally mimics that of the percentage organic yield, as would be expected. An anomaly has however been observed at a pyrolysis temperature of 475°C and can be seen when the percentage of lignin is calculated as a percentage of the percentage organic yield using Equation 48:

$$\text{Lignin ratio} = \frac{\%\ \text{lignin} \times 100}{\%\ \text{organic yield}}$$

Equation 48

The lignin ratio has been calculated for those catalyst systems that include an experiment at 475°C and is shown in Table 46. It can be seen that for the non-catalytic, slate fluid bed and Y-zeolite close coupled in the primary reactor configurations, this phenomenon occurs. There is not sufficient data to confirm that this is true for the char fluid bed also. As it happens in the non-catalytic configuration as well as others it is not significant in terms of stability, but may be interesting to examine in the future (see Section 12.4.1).

Table 46 Comparison of Organic Yield and Lignin Percentage Production

No Catalyst											
Run Number, EHS	**33**	**50**	**16**	**16r**	**17**	**17r**	**21**	**22**	**23**	**20**	**42**
Av. Run Temp (°C)	453	**475**	477	477	490	490	500	522	522	549	447
Organic Yield %	59.06	61.02	71.67	71.67	64.33	64.33	60.90	63.50	60.32	54.52	64.20
Lignin Yield %	3.22	5.28	3.53	3.53	3.39	3.39	2.63	3.44	1.88	1.67	2.16
Lignin Ratio	5.45	**8.65**	4.93	4.93	5.28	5.28	4.33	5.42	3.11	3.06	3.36
Slate Fluid bed											
Run Number, EHS	**31**	**40**	**25**	**25 r**	**24**	**29**	**27**	**28**	**28**	**32**	
Av. Run Temp (°C)	450	452	**473**	**473**	500	501	522	549	549	550	
Organic Yield %	63.70	64.01	65.23	65.23	58.56	64.69	59.93	52.59	52.59	58.97	
Lignin Yield %	2.32	1.94	6.05	4.77	2.26	3.57	2.41	1.92	1.92	4.66	
Lignin Ratio	3.64	3.03	**9.28**	**7.31**	3.86	5.51	4.02	3.66	3.66	7.91	
Y-Zeolite											
Run Number, EHS	**39**	**34**	**34**	**35**	**36**	**37**	**38**				
Av. Run Temp (°C)	451	453	453	**477**	502	525	549				
Organic Yield %	51.85	62.15	62.15	57.24	55.75	54.43	49.84				
Lignin Yield %	1.99	3.88	3.88	4.90	3.67	2.77	2.29				
Lignin Ratio	3.84	6.25	6.25	**8.56**	6.59	5.09	4.59				
Char Fluid Bed											
Run Number, EHS	52	49	51								
Av. Run Temp (°C)	**474**	499	524								
Organic Yield %	61.77	59.45	54.65								
Lignin Yield %	6.55	5.71	5.28								
Lignin Ratio	**10.61**	9.60	9.66								

The percentage difference between each pyrolytic lignin content result and a 'model' result, has been calculated. The model result is the equation of the second order polynomial line of the non-catalytic percentage lignin result. This is Equation 49.

$$y = -0.0005x^2 + 0.5162x - 121.43$$

Equation 49

where y = Percentage lignin content of pyrolysis liquid (wt% on dry wood-fed basis)

x = Temperature of pyrolysis run

The individual results are shown in Table 99 to Table 102 (Appendix H). They are summarised in Table 47 where the average for each type of catalyst system is shown. The results have been ranked to show the pyrolysis liquid with the greatest percentage lignin content at the top and the least at the bottom of the table. The results for char are

very different depending upon the configuration of incorporation. This shows that the method of adding the catalyst is important. When comparing this to the slate results, it can be seen that the configuration is important for each chemical, but not in the same way. Co-feeding is the best method for slate, but the worst for char.

Table 47 ***Average Percentage Difference between Pyrolytic Lignin Content and 'Model' Lignin Content (Ranked)***

Catalyst System	Average Percentage Difference between Lignin Content and Model (%)
Char fluid bed	48.78
Co-fed slate	50.64
Co-fed char	61.15
Y-zeolite in-bed	68.68
Slate fluid bed	71.09
No catalyst	71.88
Slate secondary bed	78.90
Char secondary reactor	83.72

5.4.3 Summary of Discussion of Liquid Product Chemical Analysis Results

HPLC analysis has found that a great many chemicals can be identified in the pyrolysis liquid. The levels of these chemicals have been studied. The relationship between the type of catalyst configuration used to produce the liquid and the temperature of production has been examined. This study concludes that the level of individual chemicals is not significant. This, however, is untrue for the level of lignin found in the liquid during preparation of the pyrolysis liquid for HPLC analysis. Lignin levels appear to be connected with pyrolysis liquid stability and this relationship is examined in more detail in Section 10.6.2.

6 PHYSICAL ANALYSIS OF THE LIQUID PYROLYSIS PRODUCT

6.1 Viscosity Testing

The majority of viscosity testing has been done using capillary viscometers. Initially a Haake rotary viscometer was used, but was quickly superseded for the reasons given below (Section 6.1.1). All viscosities that have been graphed have been found by capillary viscometry.

6.1.1 Haake Rotary Viscometer

The disadvantage of the Haake rotary viscometer is that a 15 ml sample is necessary. This sample size is too large to be produced using the small fluid bed over a reasonable time period, such as one hour. During testing using a Haake viscometer, the pyrolysis liquid is exposed to the air, altering the controlled conditions and resulting in a loss of volatiles. Shear is also applied to the pyrolysis liquid and may change it permanently, not making the sample suitable for re-testing.

6.1.2 Capillary Viscometry

Capillary viscometers were used to measure the kinematic viscosity of the liquid pyrolysis product. 'Miniature suspended level' viscometers were employed. They use 3 ml samples of pyrolysis liquid, which is more suitable for the small amounts of pyrolysis liquid produced in an hour's run (typically) using the 150 g/h pyrolysis apparatus. The pyrolysis liquid can be stored in the water bath, in the actual capillary viscometers, at the conditions set. This storage *in situ* for testing avoids the pyrolysis liquid cooling on removal from the water bath. They are therefore a better method of viscosity measurement, for this application, than the Haake viscometer.

The kinematic viscosity, μ, ($mm^2/s \equiv$ centiStokes) of the liquid was calculated from a mean measured flow time, t, (seconds) using the formula in Equation 50.

$$\mu = Ct$$

Equation 50

C is the calibration constant which is unique to each viscometer and applies when the flow time is not less than 200 seconds. The calibration of the viscometers uses the kinematic viscosity of distilled water at 20.00°C of 1.0038 mm^2/s. They have been guaranteed to 95% confidence by the PSL Calibration Laboratory *(PSL Calibration Laboratory, 1998)*.

C is in the region of 0.01 $(mm^2/s)/s$ and has the advantage of being independent of temperature for this type of viscometer.

6.1.3 Procedure for Use of Capillary Viscometers

Each miniature suspended level viscometer covers a limited range. The apparatus should therefore be chosen to match the viscosity of the liquid. Normally a 'number 4' viscometer is appropriate for pyrolysis liquid stored at room temperature for 24 hours. A 'number 5' is generally used following storage at an elevated temperature.

Testing can not be performed immediately after the end of the run as the apparatus and product liquid is still hot and time needs to be allowed for the liquid to flow down into the product collection vessels. An exact time between being made and tested must be maintained as the viscosity of the oil is constantly changing. The pyrolysis liquid changes most significantly in the first 24 hours after production. For this reason the viscosity is not measured immediately but allowed to establish a degree of consistency. A standard time span of 24 hours it therefore taken to ensure uniformity.

1) At the end of an experimental run producing pyrolysis liquid, the time of day is recorded and the pyrolysis liquid remains in the apparatus until it has reached room temperature and collected in the collection vessels. It is then stored at room temperature. Between 17 and 20 ml of liquid is stored in a 25 ml sample jar with screw lid. To maintain consistency, the first oil poured from the oil pot (oil pot one) is always used for viscosity testing.

2) 24 hours after the end of the experimental run, approximately 6 ml of the liquid is poured into the capillary viscometer and left to stand in a water bath at 25°C for 10 minutes to equilibrate.
3) The vent is blocked with a bung (see Figure 59) and a pipette filler is used to draw the liquid up the capillary above the second marked line, ensuring no air bubbles are trapped in the capillary.
4) The pipette filler and bung are removed and the liquid level is allowed to fall. The time taken for the liquid to move between the two manufacturer marked lines is recorded to the nearest one-hundredth of a second.
5) The liquid is allowed to run out of the capillary into the reservoir completely before steps 3 and 4 are repeated until results are within acceptable viscometer limits. This changes with the viscometer constant calculated by the manufacturer *(PSL Calibration Laboratory, 1998)*.

The viscometers are cleaned using acetone and left to dry. They are never oven-dried or heated.

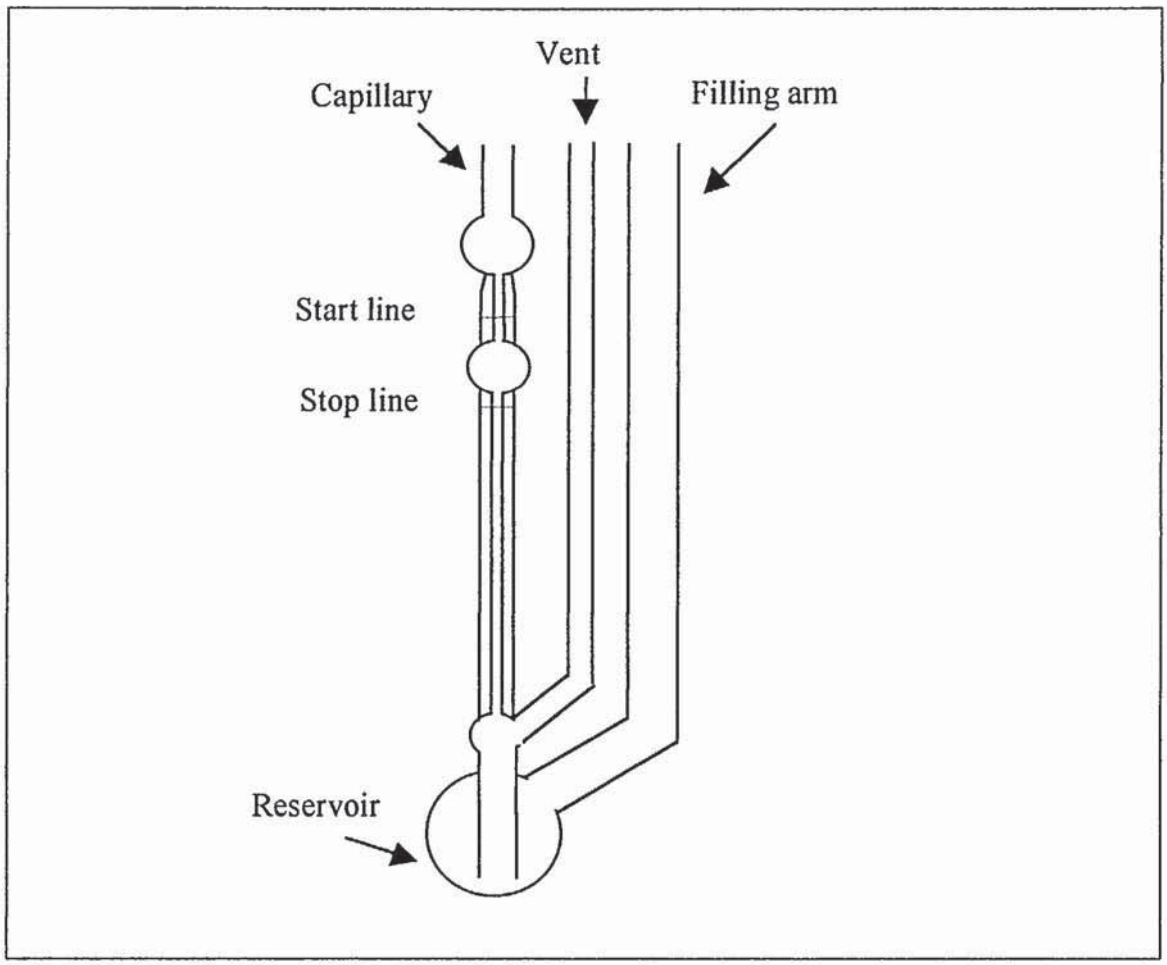

Figure 59 Capillary Viscometer

6.2 Viscosity Testing Results

6.2.1 Single Test Over Extended Time Period

To observe the change in viscosity, the viscosity of a sample was examined over time. The liquid used was from run number EHS17. The temperature of the pyrolysis run was 490.8°C and the water content of the resulting oil was 6.37 %. The liquid was stored at 25°C in a viscometer in a temperature controlled water bath. Periodically the viscosity was measured using the procedure in Section 6.1.3. The results are shown in Table 103, in Appendix K and plotted in Figure 60. Each point on the graph represents the average kinematic viscosity found at that time.

Figure 60 shows the increase in viscosity of the pyrolysis liquid over time from 58 to 108 mm^2/s over a 28-day period. This illustrates that if a pyrolysis liquid were to be

used commercially that it would not be possible to store it currently and have the same liquid come out of storage as went into storage. It is primarily this effect that is being tackled by the addition of catalyst in processing of pyrolysis liquid.

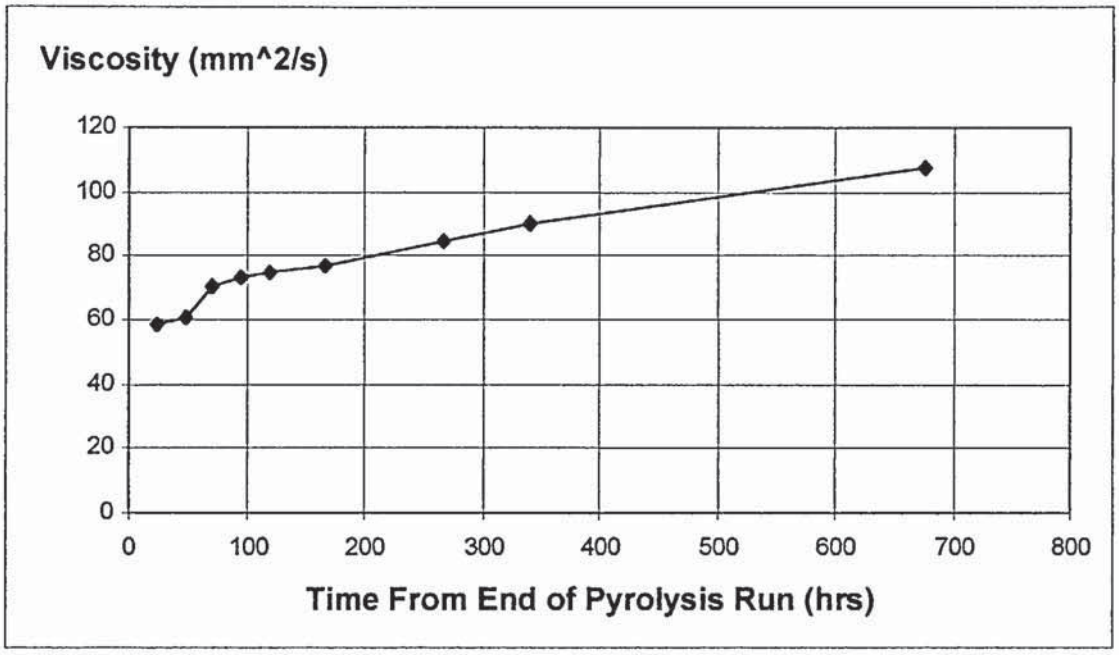

Figure 60 Viscosity Change of Pyrolysis Liquid at 25°C

6.2.2 Initial Viscosity

The viscosity of all the pyrolysis liquids produced was found, twenty-four hours after the end of the run. This is termed 'initial viscosity' and is plotted in Figure 91 and Figure 92, Appendix L. For the no catalyst configuration, the slate fluid bed and Y-zeolite close coupled in the primary reactor, the results are summarised in Figure 61. Slate used as a fluid bed reduces the viscosity of the liquid to a greater extent than Y-zeolite, but both produce a more favourable result than without any catalyst. Of the remaining catalyst systems, only slate in the secondary reactor significantly reduces the viscosity of the pyrolysis liquid. There is only one result for this, but at 504°C, the viscosity is 24 mm^2/s. This compares to 58 mm^2/s for an equivalent liquid produced non-catalytically and 53 mm^2/s with a slate fluid bed in the primary reactor.

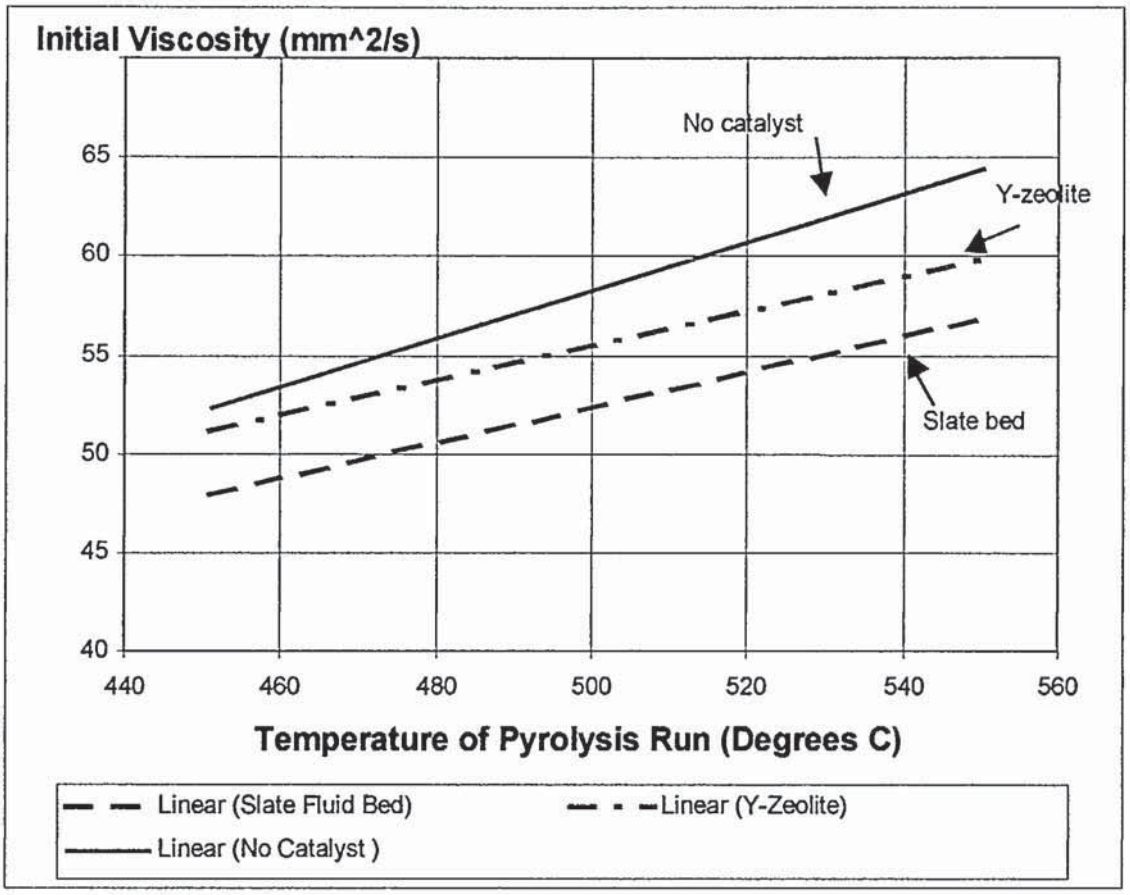

Figure 61 Initial Viscosity of Main Pyrolysis Liquid

The initial viscosity in nearly every case increases with the average run temperature. The exception is the liquid produced with co-fed char, for which there are only two points to compare, the first of which is particularly high. This result is not thought to be significant and can be verified with further experimental runs. The initial viscosity for pyrolysis liquid produced with a char fluid bed is similar to that with no catalyst. The liquid produced with a secondary char bed, starts with a low viscosity at the lower range of temperatures, but increases rapidly with temperature and is greater than the non-catalytic liquid initial viscosity above 515°C. The phenomenon of viscosity change is discussed further in Section 7.1.

6.3 Discussion of Initial Viscosity Results

To compare the initial viscosity results to those from chemical analysis, the catalyst types and modes of operation have been ranked in a similar way using a model for

comparison. The model result is the linear equation of the non-catalytic initial viscosity result. This is Equation 51.

$$y = 0.1222x - 2.7822$$

Equation 51

where y = Initial viscosity of pyrolysis liquid (mm^2/s)

x = Temperature of pyrolysis run

The individual results are shown in Table 104 to Table 108 (Appendix K). They are summarised in Table 48 where the average for each type of catalyst system is shown. The results have been ranked to show the pyrolysis liquid with the lowest average initial viscosity at the top and the highest (worst) at the bottom of the table.

For the maximum organic yield temperature, around 480 to 500°C, the percentage difference between the initial viscosity of liquid from each catalytic system and the model initial viscosity has been ranked. This is shown in Table 49. Looking at these results show that the liquid from the pyrolysis run at the maximum organic yield temperature is indicative of the average result.

Table 48 Average Percentage Difference between Initial Viscosity of Pyrolysis Liquid and 'Model' Initial Viscosity (Ranked)

Catalyst System	Average Percentage Difference between Initial Viscosity and Model (%)
Slate secondary bed	58.45
Y-zeolite in-bed	11.86
Char fluid bed	3.71
Slate fluid bed	1.03
Co-fed slate	-0.61[(a)]
No catalyst	-1.81
Char secondary reactor	-2.37
Co-fed char	-27.08

Notes: (a) Negative result indicates higher initial viscosity of pyrolysis liquid than non-catalytic run.

Table 49 ***Percentage Difference between Initial Viscosity of One Pyrolysis Liquid and 'Model' Initial Viscosity at Maximum Organic Yield Temperature (Ranked)***

Catalyst System	Run No.	Percentage Difference between Initial Viscosity and Model (%)	Temperature of Corresponding Pyrolysis Run (°C)
Slate secondary bed	55	58.45	503.53
Y-zeolite in-bed	35	3.78	477.91
Slate fluid bed	29	7.08	501.08
Char fluid bed	49	-2.07	499.43
No catalyst	17	-2.07	490.79
Co-fed slate	53	-0.53	501.49
Co-fed char	57	-20.92	501.33
Char secondary reactor	-	-	-

6.4 Comparison of Viscosity Results to Wulzinger

As highlighted in Chapter 2, two other researchers have experimented with the incorporation of catalysts in fast pyrolysis (Wulzinger and Cooke). Wulzinger additionally observed the viscosity of the resultant pyrolysis liquid. The results are shown in Figure 62.

Y-zeolite appears to reduce substantially the viscosity of the pyrolysis liquid as demonstrated by this report, but the inclusion of slate in the pyrolysis process either has the same viscosity results as the blank non-catalytic run or increases the viscosity. The variation in results, however, is large. The overall range that the viscosity is measured in is lower than the viscosities measured in this report. This may be the effect of the potential inclusion of methanol in the pyrolysis liquid, as discussed in Section 4.10.

One catalyst that has not been tested in the project described in this report, γ-alumina, appears to have a positive effect on the viscosity of the pyrolysis liquid. Co-feeding char also shows a reduction in viscosity as demonstrated in this report.

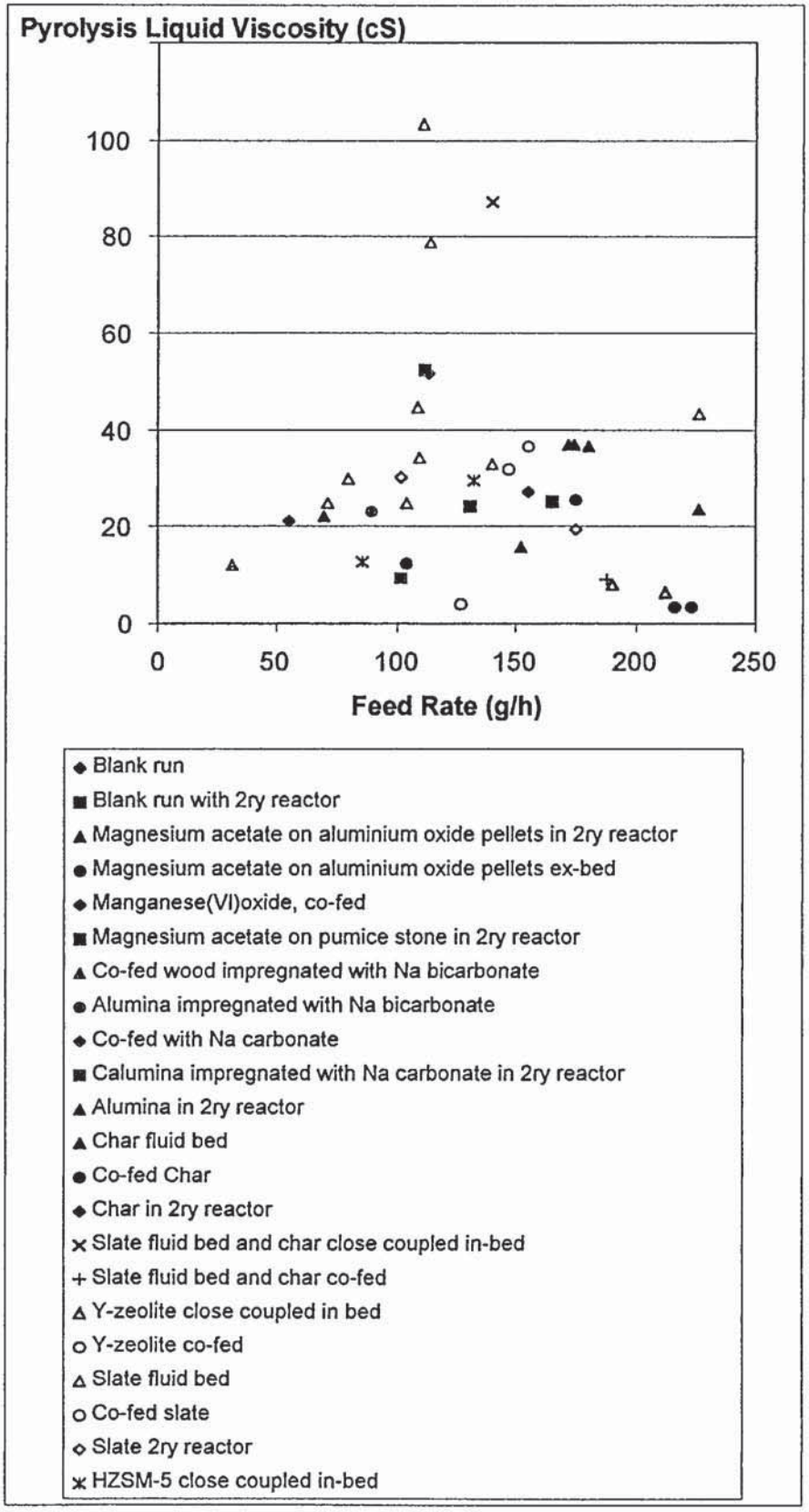

Figure 62 Pyrolysis Liquid Viscosity Results as found by Wulzinger

7 LIQUID PRODUCT QUALITY TESTING

To test the quality of pyrolysis liquid it is first necessary to define 'quality'. A low viscosity, high heating value and neutral pH, in conjunction with stability is desirable. The properties of pyrolysis liquid have been studied in previous chapters, but the change in these properties will be looked at here.

Viscosity of pyrolysis liquid has been found to increase with time at room temperature (Section 6.2.1), apparently due to the presence of acids in the aqueous phase *(Churin, 1990)*. A study of the change in liquid viscosity and associated parameters, such as water content, has therefore been carried out.

7.1 Stability Testing

Stable pyrolysis liquid is desirable as this indicates a better quality liquid. Several properties change with time, but the most significant and measurable is viscosity. The 'Aston Viscosity Index' (AVI) has been developed as a measure of the stability of pyrolysis liquid. The technique has been established as a standard against which the result of experimentation can be judged and the most appropriate catalyst or stabilising chemical can therefore be evaluated. When comparing the qualities of pyrolysis liquids, viscosity is one of the indicative parameters. The change in viscosity with time also indicates the stability of the liquid. Other parameters that should be taken into account when considering pyrolysis liquid quality are water content and heating value. As the water content is linked to viscosity they should always be considered together. The water content can also indicate the heating value of the pyrolysis liquid.

7.1.1 Stability Testing Development

Viscosity change is used to find the viscosity index, an indication of stability. Capillary viscometry (see Section 6.1) was used to establish the 'Aston Viscosity Index' (AVI). It uses raised temperatures to accelerate ageing of the pyrolysis liquid and to therefore asses liquid stability. It was developed following a study of the effect of storage temperature on pyrolysis liquid viscosity *(Hague, 1998#3)*. Three temperatures, 25, 50 and 75°C were used to store pyrolysis liquid for viscosity and water content testing (Figure 63). It was found that pyrolysis liquid was most stable with respect to viscosity

when stored at 25°C since it has the flattest curve. This temperature was chosen as the reference temperature at which all liquid would be tested. A direct comparison could therefore be made between liquids stored at different temperatures. This is also convenient, as it is an acceptable temperature at which to hold a water-bath.

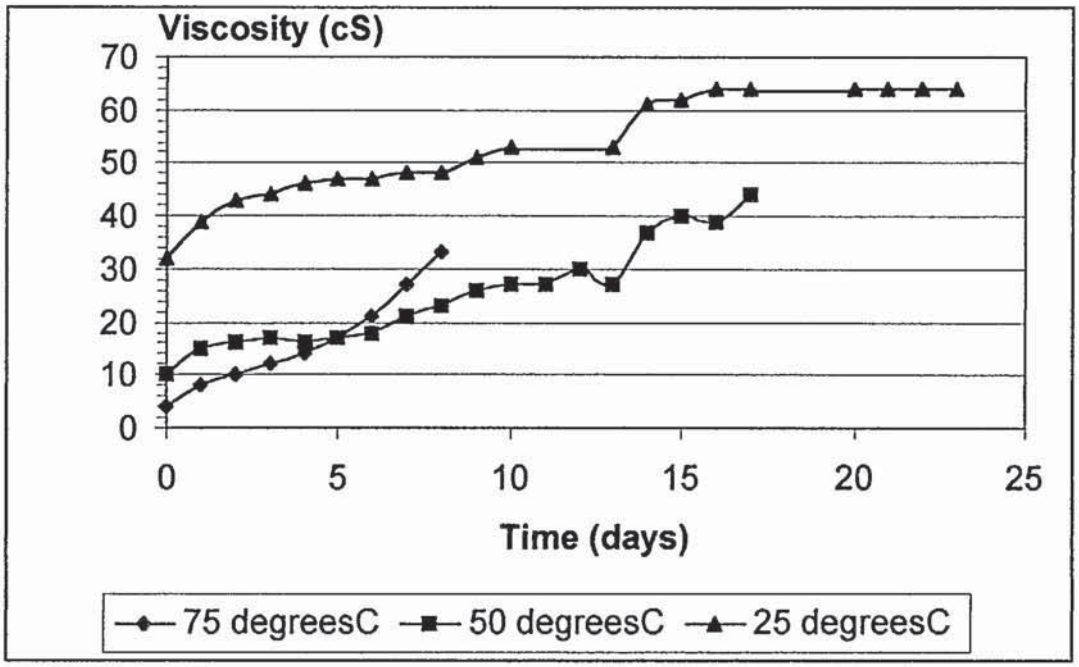

Figure 63 ***Variation in Viscosity in Pyrolysis Liquid Stored at 25, 50 and 75°C*** *(Hague, 1998#3)*

7.1.1.1 Aston Viscosity Index

AVI has been used to provide a measure of stability by finding the relative change in viscosity with time. Pyrolysis liquid is tested at 25°C by capillary viscometry, 24 hours after production, having been stored at room temperature. This is μ_{t1}, the initial viscosity (as found in Section 6.2.2), in Equation 35, below. The stability of each pyrolysis liquid is tested at a specific time after production. An exact time between being made and tested must be maintained as the viscosity of the oil is constantly changing. The pyrolysis liquid changes most significantly in the first 24 hours after production. For this reason the viscosity is not measured immediately but allowed to establish a degree of consistency.

The liquid is then stored for a further 24 hours at 75°C and the viscosity is re-tested at 25°C (μ_{t2}). The AVI is the relative change in viscosity, as calculated by Equation 52.

$$AVI = (\mu_{t2} - \mu_{t1})/ \mu_{t1}$$

Equation 52

The lower the number is, the more stable the pyrolysis liquid. A zero result indicates no viscosity change. This test represents approximately two and a half months at room temperature, depending on the pyrolysis liquid. Its advantage is that only 48 hours is required for a test, rather than prolonged ageing tests.

7.1.2 Procedure For Pyrolysis Liquid Stability Testing

It has been found that the difference between storing at room temperature and a constant 25°C is not significant. The pyrolysis liquid is kept at room temperature, a temperature at which the least change in viscosity will occur. It is stored in opaque polypropylene jars to reduce the effect from changes due to UV light and air.

The viscosity apparatus used is identical to that described in Section 6.1.2, as is the first part of the procedure – Steps 1) to 5) in Section 6.1.3. The remaining steps are described here.

6) The liquid in the viscometer is returned to the sample jar, sealed, and put into a water bath at 75°C. It is left here for 24 hours exactly.
7) On removal from the 75°C water bath, steps 2 to 5 are repeated using the 25°C water bath as before.
8) Equation 52 is then used to calculate the AVI.

7.2 Stability Results

The results of initial viscosity testing are displayed in Section 6.2. The water content of the pyrolysis liquids should also be considered with the stability and are shown in Section 5.1.1. The results of stability testing are in Appendix M. Figure 93 and Figure 94 (Appendix N) have been plotted from this information. The most significant of these results is the AVI of slate and Y-zeolite displayed against AVI of blank runs using no

catalyst (Figure 64). Here it is shown that using a slate fluid bed or Y-zeolite close-coupled in the primary reactor produces a liquid that is more stable than that produced with no catalyst. Above a 500°C pyrolysis run temperature, the slate fluid bed liquid has a lower AVI than the Y-zeolite liquid. AVI, like initial viscosity, increases with the temperature of the pyrolysis run. All the configurations are compared in Section 7.3.1.

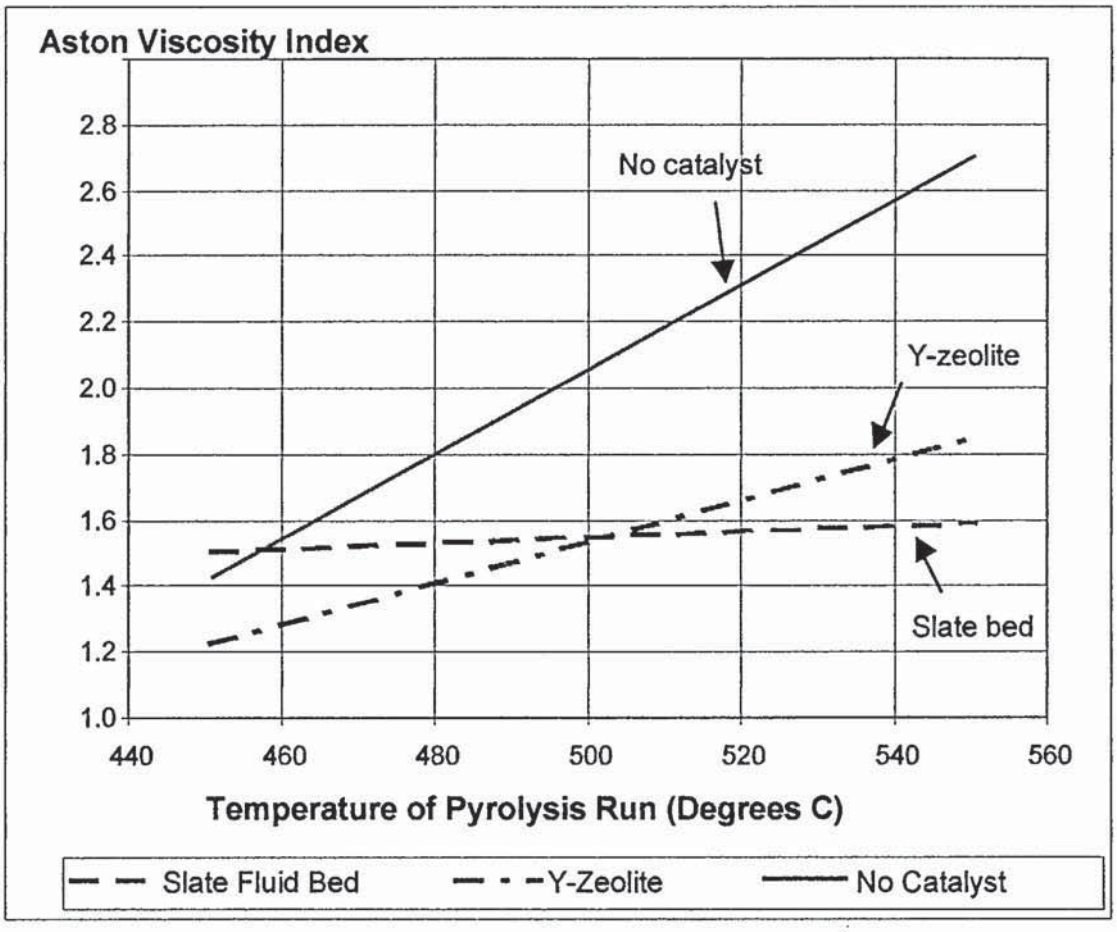

Figure 64 Aston Viscosity Index of Pyrolysis Liquid

7.2.1 Adjusted Aston Viscosity Index

It is hypothesised that water content effects the viscosity and stability of pyrolysis liquid. Therefore, to relate stability and water content, an adjusted version of the AVI has been formulated. It accounts for the water content and takes 20 % as the standard amount of water contained in the pyrolysis liquid by using Equation 53. The multiplier, 2, is used following stability experimentation *(Hague, 1998#3)*.

'Adjusted AVI' = AVI-(2*AVI*((20-H2O)/20))

Equation 53

The results of this can be found in Appendix N, Figure 95 and Figure 96. They are summarised here in Figure 65 for the three main catalyst configurations. This shows that about a pyrolysis run temperature of 490°C, that a slate fluid bed is the best way to produce stable pyrolysis liquid and that below that temperature, Y-zeolite close coupled in the primary reactor is more effective. This effect is more pronounced than the non-adjusted AVI as the slate fluid bed result decreases rather than increase with temperature. All the configurations are compared in Section 7.3.2.

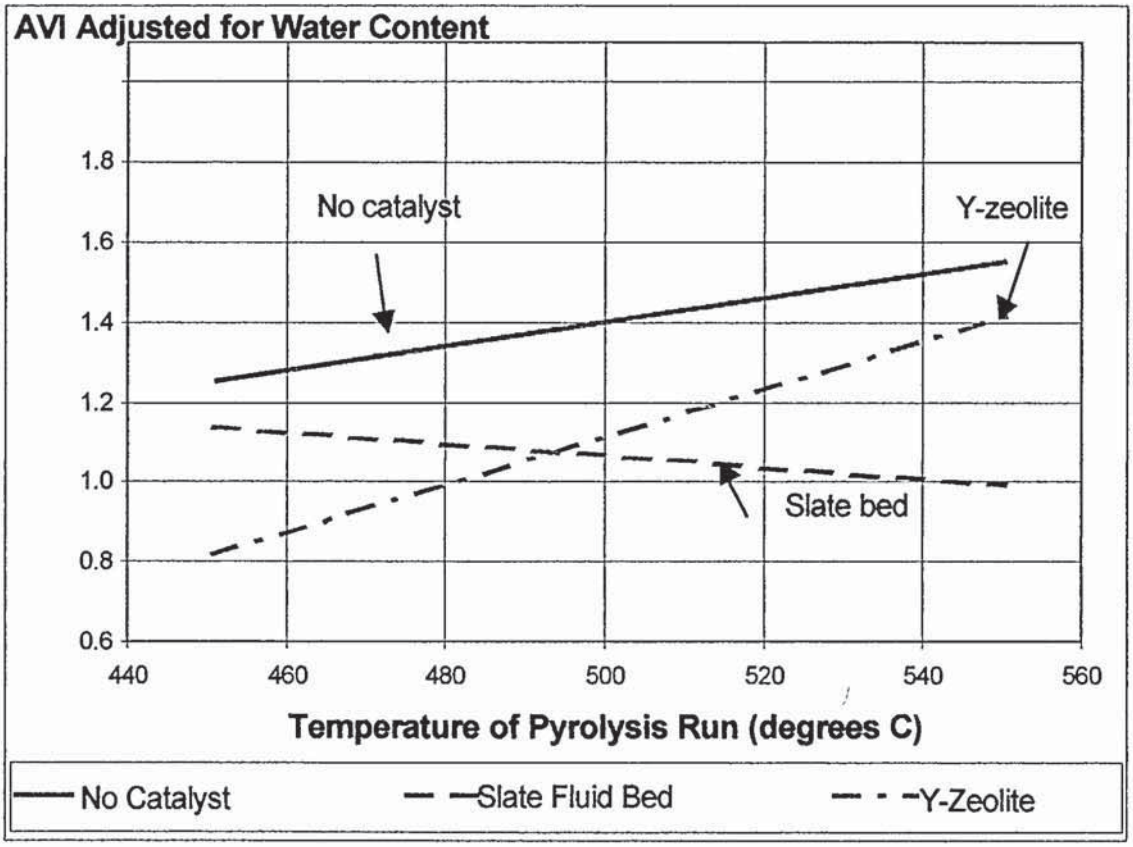

Figure 65 Aston Viscosity Index, Adjusted for Water Content of Pyrolysis Liquid

7.3 Discussion of Stability Results

7.3.1 Modelling and Ranking of AVI Results

To be able to rank the stability results, the percentage difference between each AVI result and a 'model' result, has been calculated. The model result is the linear equation of the non-catalytic AVI result. This is Equation 54.

$$y = 0.0129x - 4.3874$$

Equation 54

where y = Aston Viscosity Index of pyrolysis liquid
x = Temperature of pyrolysis run

The individual results are shown in Table 110 to Table 114 (Appendix M). They are summarised in Table 50 where the average for each type of catalyst system is shown. The results have been ranked to show the pyrolysis liquid with the lowest (best) AVI at the top and the highest at the bottom of the table. The results for the pyrolysis liquids collected at the maximum organic yield temperature are shown in Table 51. The result for no catalyst highlights the inaccuracy of this method

Table 50 ***Average Percentage Difference between Pyrolysis Liquid AVI and 'Model' AVI (Ranked)***

Catalyst System	Average Percentage Difference between AVI and Model (%)
Char fluid bed	40.01
Co-fed char	35.67
Y-zeolite in-bed	22.00
Slate fluid bed	17.73
Slate secondary bed	-1.43
Char secondary reactor	-1.76
Co-fed slate	-4.57
No catalyst	-4.80

Notes: (a) Negative result indicates a higher AVI pyrolysis liquid than non-catalytic run.

Table 51 Percentage Difference between AVI of One Pyrolysis Liquid and 'Model' AVI at Maximum Organic Yield Temperature (Ranked)

Catalyst System	Run No.	Percentage Difference between Initial Viscosity and Model (%)	Temperature of Corresponding Pyrolysis Run (°C)
Y-zeolite in-bed	35	40.46	477.91
Co-fed char	57	32.39	501.33
Char fluid bed	49	32.34	499.43
Slate fluid bed	29	31.46	501.08
No catalyst	17	29.13	490.79
Slate secondary bed	55	-1.43	503.53
Co-fed slate	53	-3.08	501.49
Char secondary reactor	-	-	-

7.3.2 Modelling and Ranking of Adjusted AVI Results

Similarly to the AVI results, the percentage difference between each adjusted AVI result and a 'model' result, has been calculated. The model result is the linear equation of the non-catalytic AVI result. This is Equation 56.

$$y = 0.003x - 0.0862$$

Equation 55

Where y = Adjusted Aston Viscosity Index of pyrolysis liquid

x = Temperature of pyrolysis run

The individual results are shown in Table 110 to Table 114 (Appendix M) with the AVI calculations. They are summarised in Table 52 for the AVI adjusted for water content, where the average for each type of catalyst system is shown. The results have been ranked to show the pyrolysis liquid with the lowest adjusted AVI at the top and the highest (least stable) at the bottom of the table.

Table 52 ***Average Percentage Difference between Pyrolysis Liquid Adjusted AVI and 'Model' Adjusted AVI (Ranked)***

Catalyst System	Average Percentage Difference between Adjusted AVI and Model (%)
Co-fed char	57.97
Char fluid bed	48.15
Y-zeolite in-bed	29.48
Slate fluid bed	20.83
Co-fed slate	16.10
No catalyst	-8.48
Char secondary reactor	-13.61
Slate secondary bed	-50.71

Notes: (a) Negative result indicates a higher adjusted AVI pyrolysis liquid than non-catalytic run.

Table 53 ***Percentage Difference between Adjusted AVI of One Pyrolysis Liquid and 'Model' Adjusted AVI at Maximum Organic Yield Temperature (Ranked)***

Catalyst System	Run No.	Percentage Difference between Initial Viscosity and Model (%)	Temperature of Corresponding Pyrolysis Run (°C)
Co-fed char	57	48.21	501.33
Char fluid bed	49	47.20	499.43
Y-zeolite in-bed	35	47.06	477.91
Slate fluid bed	29	34.31	501.08
No catalyst	17	32.20	490.79
Co-fed slate	53	28.12	501.49
Slate secondary bed	55	-50.71	503.53
Char secondary reactor	-	-	-

7.3.3 Aston Viscosity Index Error Analysis

An error analysis was carried out on the Aston Viscosity Index calculations using the same method as for the propagation of errors for the mass balance closure results (see

Section 4.8.2) *(Roberts, 1999)*. The suspended level viscometer has an accuracy of ± 0.35 %. The errors associated with viscosity testing are shown in Table 54. The AVI is accurate to ± 0.72 %. The adjusted AVI is only accurate to ± 5.92 % because of the water testing associated with it.

Table 54 Errors Associated with Viscosity Testing

Parameter	Error (%)
Initial Viscosity	± 0.35
Secondary Viscosity	± 0.35
Aston Viscosity Index	± 0.72
Adjusted Aston Viscosity index	± 5.92

7.4 Acidity Testing

One of the detrimental parameter of pyrolysis liquid is the low pH. A limited study was undertaken to analyse the acidity of the liquid, before and after stability testing. A '713 pH meter' from Metrohm was used with a '6.0228.00' probe, which measures between 0 and 14 pH at 0 to 80°C. It was found that the liquid was consistently 3.6 pH at 20°C, before stability testing and 3.4 to 3.2 pH at 20°C, when removed from the 75°C water bath after 24 hours. The uniformity of this result shows that the acidity of the liquid was not effected by catalyst type, but increases with the age of the liquid. The increase is equivalent to an increase of 0.2 to 0.4 pH in two months.

7.5 Summary of Discussion of Liquid Product Quality Testing

This chapter has examined the properties of the pyrolysis liquids when produced by different methods, incorporating the catalysts described in Section 4.5. An attempt has been made to define some properties, particularly physical properties, as critical to the quality and stability of the liquid, such as viscosity and the Aston Viscosity Index.

Both the type of catalyst and the mode of incorporation were found to influence the AVI. The four most stable liquids, as measured by the AVI, were produced by: a char fluid bed in the primary reactor, char co-fed in to the primary reactor, Y-zeolite close coupled in the primary reactor and a slate fluid bed in the primary reactor. The use of a secondary bed resulted in a less stable liquid.

The relationship between the viscosity and AVI results and other properties, such as chemical composition of the pyrolysis liquid, is developed in Section 10.6.

The acidity of the liquid is one parameter that is detrimental to the quality of the pyrolysis liquid. It was found not to be influenced by the incorporation of catalysts into the fast pyrolysis process.

8 CATALYTIC PYROLYSIS PROCESS SCALE UP

In order to confirm the conclusions drawn from experimentation using 150 g/h apparatus, a larger apparatus was used.

8.1 Large Fluid Bed Apparatus Description

This is used for producing larger amounts of pyrolysis liquid. It has been fully described previously *(Hague, 1998#2)*. The dimensions given here are approximate. The large (1 kg/h) fluid bed apparatus is similar in layout to the 150 g/h fluid bed pyrolysis apparatus described in Chapter 4, but wood is screw fed using a pair of screws and entrained using nitrogen into the reactor. The feed wood is simply entrained in the smaller scale apparatus. The large fluid bed is shown in Figure 66. The 300 mm diameter feeder is calibrated prior to running and set to deliver a certain feed rate, which can be altered during the run if necessary.

Fluidising gas to the particle bed is electrically preheated by three heaters whose temperatures are controlled. A band heater is used around the reactor, positioned around the bed wall for additional heat. The reactor is 150 mm in diameter and 480mm long. The product vapours and entrained particles then pass through a 50 mm diameter cyclone. The top of the particle collection beneath, known as the char pot, is kept at 400°C using a band heater around the top to prevent condensed organic vapours and char sticking and blocking the solids exit from the cyclone. The apparatus is also lagged to reduce this phenomenon. To improve the efficiency of the char removal, a second 50 mm diameter cyclone has also recently been added.

The liquid product is collected in a quench system using octane as the quench liquid to provide good contact but give a completely immiscible second phase in the product that can be readily separated. Octane is inert, does not absorb water from the product and has a low volatility. This is unlike the collection system on the smaller apparatus, described in Sections 4.1.1.4 and 4.1.2. The quench-unit has disc and donut internals for good contacting and a jacket of re-circulating refrigerant. The refrigerant is passed through a chiller, which cools the liquid to –1.5°C. The diameter of the quench vessle is 200 mm and it is 1 m high.

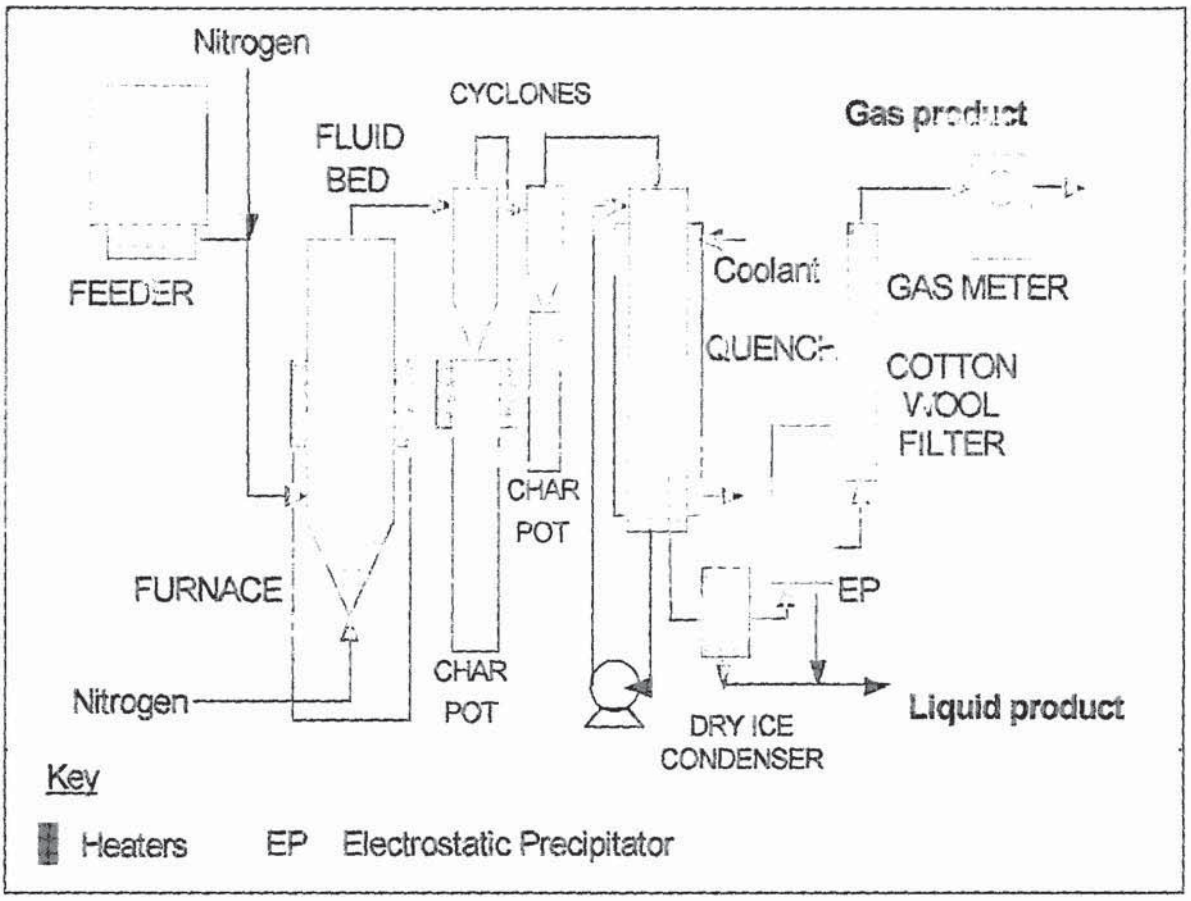

Figure 66 *1-2 kg/h 'Large' Laboratory Scale Fluidised Bed Fast Pyrolysis Reactor*

Exit gases from the quench column contain a significant quantity of aerosols and volatiles. An electrostatic precipitator is included in the system to improve the removal of aerosols from the gas and recover as liquid product. This has a diameter of 200 mm and a height of 110 m. Further cooling and collection is carried out in a dry ice/acetone condenser at around –80°C. Residual persistent aerosols are removed in the cotton wool filter before the remaining gases are metered and vented. An off-take of product gas is piped to a GC for continuous analysis every five minutes in the same way as the 150 g/h reactor (Section 4.1.2.3).

All measured temperatures are recorded automatically every 20 seconds by a computerised data logger. Differential and gauge pressure measurements are recorded at approximately five-minute intervals throughout a run. After running, it is necessary

to separate the pyrolysis liquid from the octane. All liquids collected are placed in a separating funnel where the pyrolysis liquid can be drained off. This process is not necessary with small fluid bed experiments as no quench liquid is used.

8.2 Large Fluid Bed Apparatus Operation

Slate, being one of the successful catalysts resulting from small fluid bed experiments, has been incorporated into the operation of the large fluid bed. The complete inert sand bed was replaced with one of thermally-expanded slate. Following fluidising experiments using slate and char collected from previous runs, the satisfactory conditions were found. These conditions enable slate to form a bubbling bed and remain in the fluidising zone of the reactor whilst char is entrained out of the reactor. Testing was done initially at ambient temperatures in glass apparatus allowing the type of bed flow to be viewed. Hot testing was then carried out using the actual large fluid bed with a glass top to the reactor. Nitrogen flow-rates to create a well-mixed bed were determined.

The best slate particle size was found to be 500 to 850 μm. The smallest size is fixed by the size of the holes in the nitrogen distributor at the bottom of the fluid bed, which are 500 μm in size. This compares to a slate particle size of 315 to 500 μm in the 150 g/h fluid bed and a sand particle size of 355 to 500 μm. In the large fluid bed, the sand size is normally 500 to 833 μm.

The mass of slate added was 450 g, which is the corresponding volume to the 1 kg of sand normally used as the fluid bed. The reactor temperature used was 475°C, which is the temperature at which maximum organic yields were found using the small fluid bed apparatus with a slate fluid bed.

A comparative non-catalytic run was also performed. On completing the experiment, it was found that char had built up in the primary reactor and may have been acting as a catalyst, close coupled in the primary reactor. The char would have occupied the freeboard area of the reactor, above a standard sand fluid bed. The char particle size was difficult to determine because of its rod shape nature, but was in the region of 100 to 800 μm. The mass balance closures are shown below in Table 55. Previous non-

catalytic runs can however be used for comparison and are described in Section 8.6, 'Scale-Up Comparison with Cooke'.

Table 55 Large Fluid Bed Results

Run Name	LFB45	LFB46
Description	Non-catalytic run with char build-up in primary reactor	Slate fluid bed in primary reactor
Run Temperature, °C	488	486
Run Time	3 hrs, 15 mins	3 hrs, 19 mins
Gas % Yield	16.0	17.8
Organics % Yield	41.1	52.0
Char % Yield	18.1	14.2
Water % Yield	18.9	11.2
Liquids % Yield	60.1	63.2
% Closure	94.1	95.2

8.3 Large Fluid Bed Stability Results

On comparing the large fluid bed, with slate incorporated, to the small fluid bed apparatus, the results were found to be favourable. The viscosity results are displayed in Table 56. The AVI was found using the method described in Section 7.1.1.1.

Table 56 Comparison of Large and Small Fluid Bed Stability Results

Run Name	LFB46	EHS25
Reactor Scale	Large Fluid Bed	Small Fluid Bed
Catalyst Configuration	Slate Fluid Bed	Slate Fluid Bed
Run Temperature, °C	486	474
Water Content, %	15.4	18.9
Initial Viscosity, mm^2/s	34.6	48.3
Secondary Viscosity, mm^2/s	64.4	102.4
AVI	0.86	1.12
Adjusted AVI	0.99	0.47

The large fluid bed pyrolysis liquid is even more stable and lower in viscosity than expected based on the small fluid bed results. This is despite having a lower percentage water content, which indicates that the large fluid bed liquid may beneficially have a higher heating value. This shows that the larger scale apparatus magnifies positive effects of the catalyst incorporation. This can be confirmed by the comparison of non-catalytic experiments. This was not possible due to ongoing apparatus re-design. The build up of char negates the use of run LFB45 for this purpose.

8.3.1 Change of Stability with Time

Due to the larger quantities of pyrolysis liquid produced by the large fluid bed, there was sufficient sample to monitor the change in initial viscosity, and stability with time. Figure 67 shows that the viscosity increase with time has not been halted by the replacement of the sand fluid bed by slate in the pyrolysis process. This is confirmed by the AVI and adjusted AVI in Figure 68. These indicators reduce with time, showing that the pyrolysis liquid is becoming more stable. This may be a function of the water content (Figure 69) which reduces over the life of the pyrolysis liquid, as shown. If this test were to be continued for another 12 weeks, the equilibrium point at which the pyrolysis liquid stops changing may be found. Comparing these graphs confirms that the use of the AVI and Adjusted AVI are satisfactory methods for assessing the stability of pyrolysis liquid.

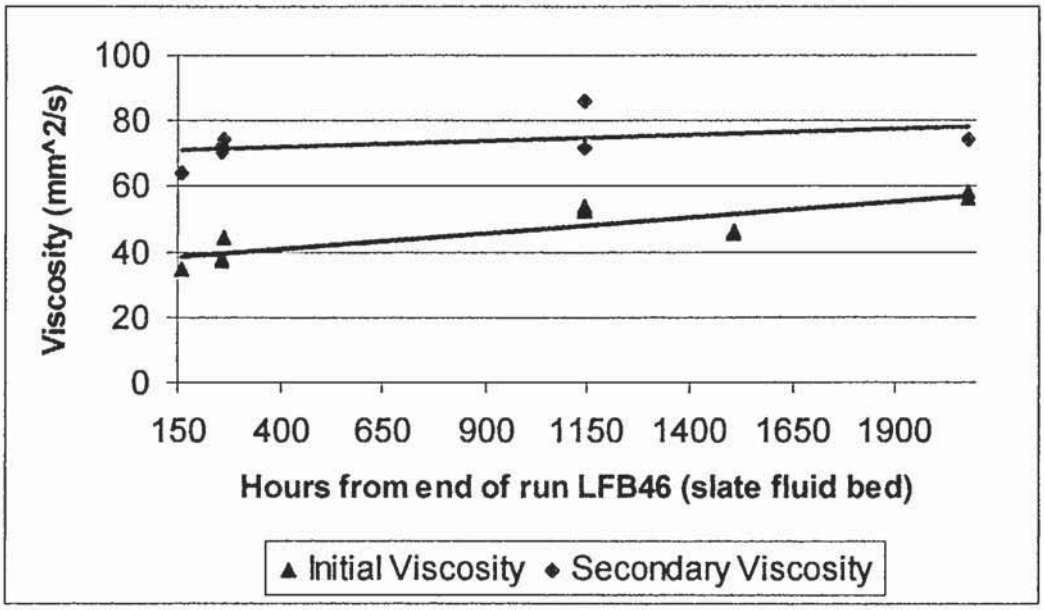

Figure 67 *Change in Initial and Secondary Viscosity of Large Fluid Slate Bed Pyrolysis Liquid, with Time*

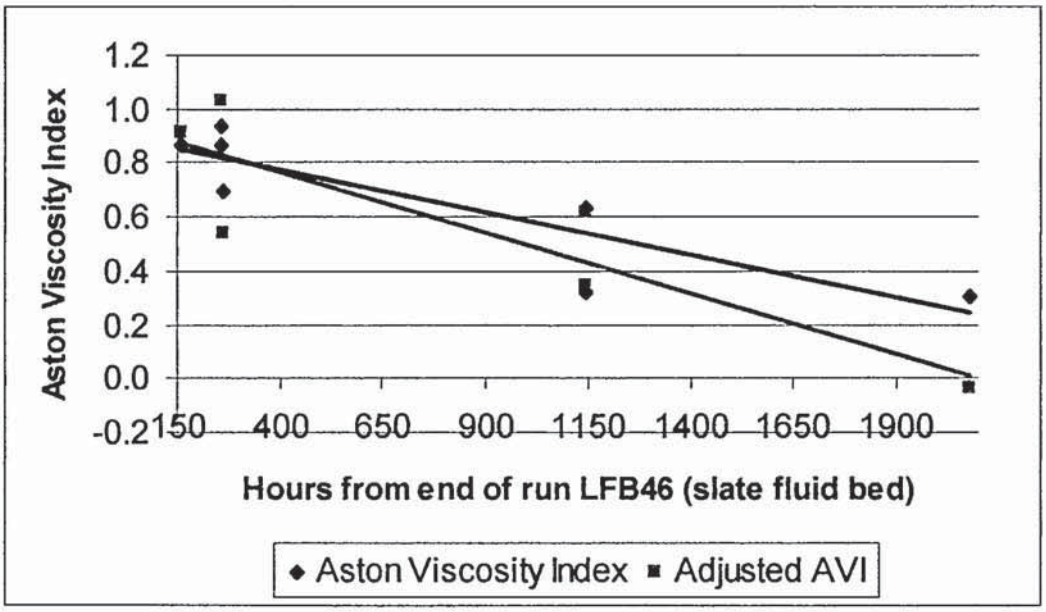

Figure 68 *Change in Aston Viscosity Index and Adjusted Aston Viscosity of Large Fluid Slate Bed Pyrolysis Liquid, with Time*

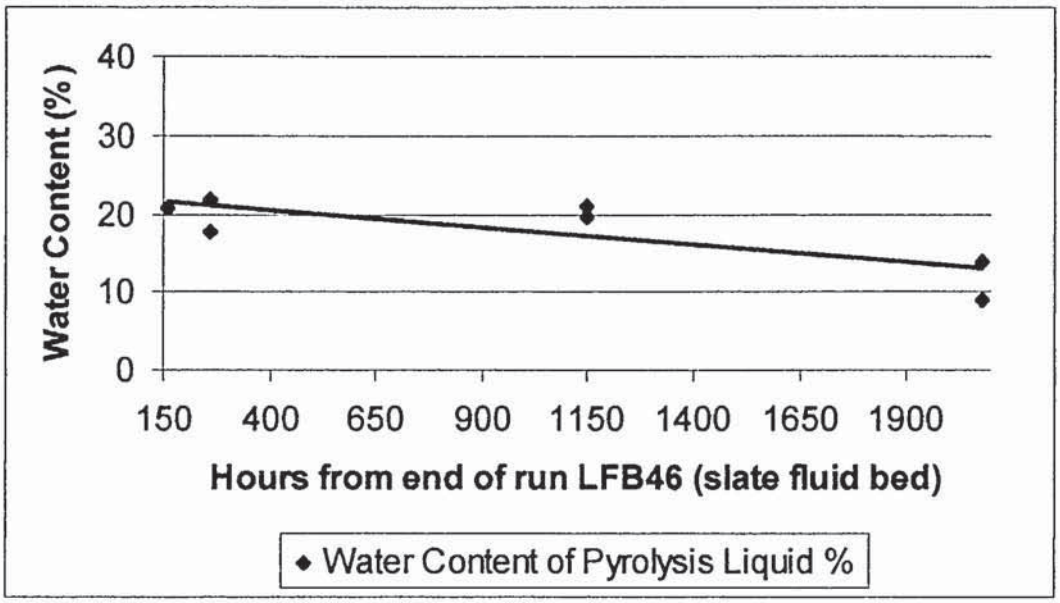

Figure 69 *Change in Water Content of Large Fluid Slate Bed Pyrolysis Liquid, with Time*

8.4 Large Fluid Bed Homogeneity Testing

To look at the homogeneity of the pyrolysis liquid produced, the way in which viscosity and water testing was done, was modified. This type of testing could not be done on the small samples produced from the bench scale apparatus. The viscosity and water content were found for the following samples. The procedure for testing this is described in Appendix P.

1) liquid taken from the top portion of the sample,
2) liquid taken from the middle portion of the sample,
3) liquid taken from the bottom portion of the sample,
4) liquid taken from the sample once well shaken.

No visible phase separation had occurred, and testing from different depths in this way showed that within the limits of the analysis technique, the liquid was not truly homogeneous and changed over 12 weeks. The results are shown Figure 70 and Figure 71, and Figure 97 to Figure 101 in Appendix P, page 328.

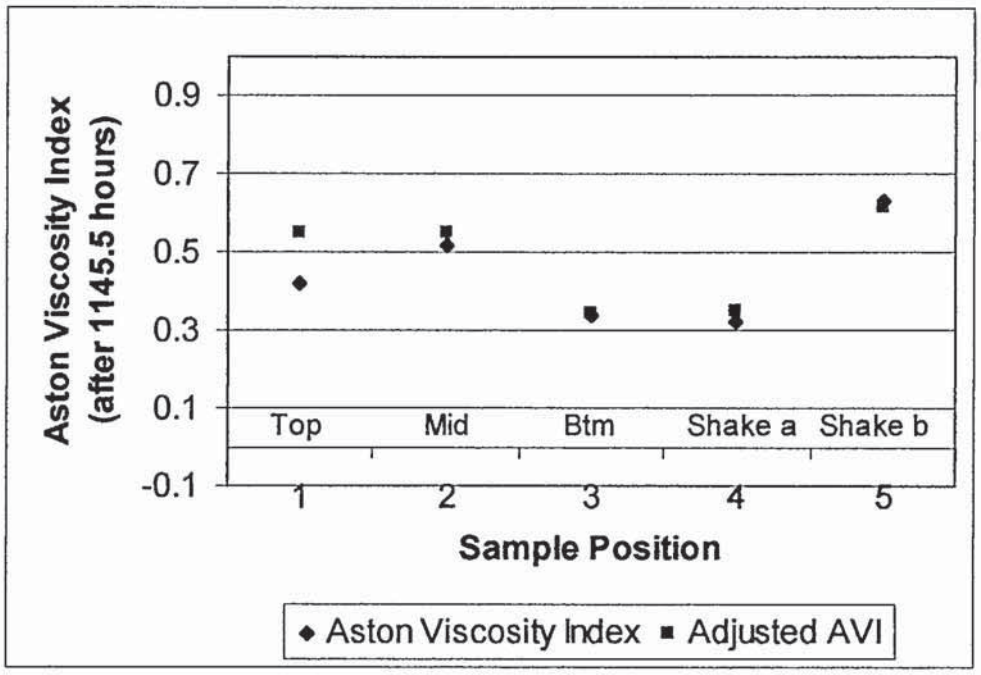

Figure 70 ***Aston Viscosity Index and Adjusted Aston Viscosity Index of LFB46 Pyrolysis Liquid after 48 Days***

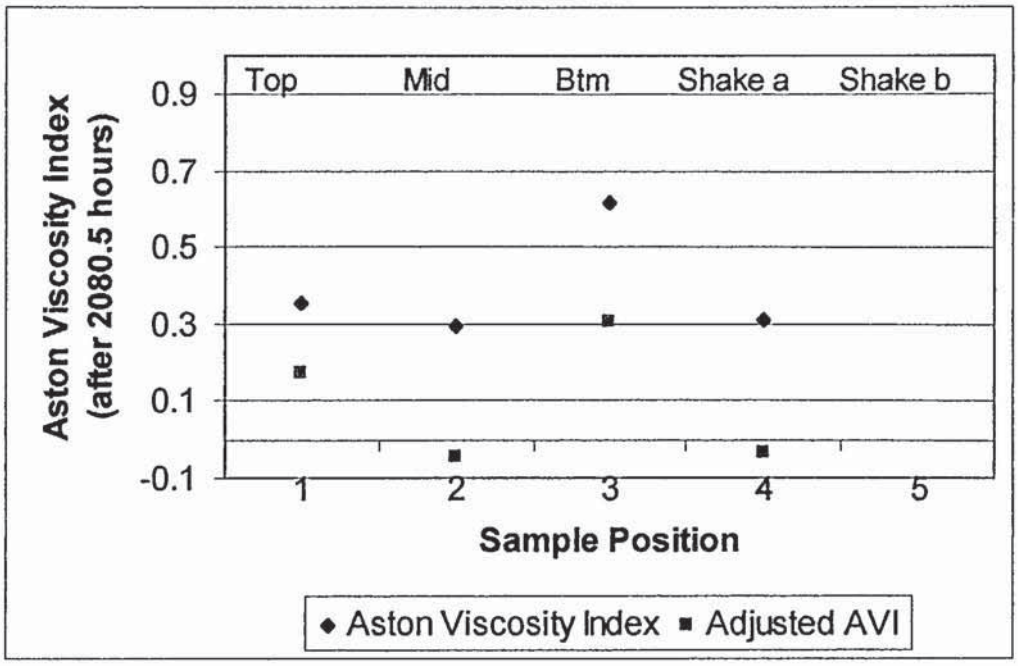

Figure 71 ***Aston Viscosity Index and Adjusted Aston Viscosity Index of LFB46 Pyrolysis Liquid after 87 Days***

It is hypothesised that any microfine char in the liquid would settle towards the bottom of the pyrolysis liquid. This may cause localised differences in the pyrolysis liquid, causing it not to be entirely homogeneous. This could be by the simple presence of char, but also there may be a catalytic effect similar to that shown by the addition of char to the configuration of the small fluid bed pyrolysis apparatus. This is supported by the AVI of the bottom portion of the liquid changing directionally opposite to the top and middle of the sample. While they get more stable, the bottom of the liquid gets less stable and increases the water content. It is not possible to compare the shaken sample as this potentially contains liquid from all three sections: top, middle and bottom. This difference in the shaken sample can be explained by the non-uniformity of the liquid.

8.4.1 Pyrolysis Liquid Filtration

This result indicates that the presence of microfine char is beneficial to slate fluid bed produced pyrolysis liquid, initially, but should be removed between 48 and 87 days after production. The optimum time for this could be found by further homogeneity testing, as described in Appendix P, using a shorter time interval between testing. Methods of

filtration should also be investigated. It is not possible to filter pyrolysis liquid through a filter medium under atmospheric pressure. One method is to use a solvent to dilute the liquid. This method is used by Wulzinger *(Wulzinger, 1999)*, where methanol is the diluent. The disadvantage of this is that no reaction between the pyrolysis liquid and the diluent can not be guaranteed and is a further variable which should be understood through experimentation and chemical analysis.

An alternative method of filtration is 'hot filtration' *(Diebold, 1994#2)*. This method uses either flexible ceramic bags or sintered incoloy as the filter. The pyrolysis vapours are heated to at least 450°C to allow them to be filtered. This extends the residence time of the product at high temperature, which causes cracking. This therefore produces a lower percentage yield of liquid. There is also the cost of further processing associated with the process.

The higher cost and the poorer liquid yield should be balanced against the potential storage improvements of eliminating the char, but may also have to take account of a higher initial viscosity. By using the Aston Viscosity Index, this could be a topic for further research. The desired storage time and end use of the pyrolysis liquid may influence the method of production and the inclusion of post-production treatment.

8.5 Scale-Up Comparison with Wulzinger

In addition to the work described in Section 4.10.1, the work of Wulzinger included a scaled-up experiment that incorporated slate as the fluid bed material *(Wulzinger, 1998)*. Slate was the most promising result from the bench scale experimentation (200g/h). The laboratory scale apparatus is shown in Figure 72.

The results showed that the resulting pyrolysis liquid was chemically comparable to un-catalysed runs, however the viscosity was lower. It was not stated by how much and the stability was not measured. The presented results are shown in Table 57.

Table 57 ***Experimental Conditions and Results from the Laboratory Scale Apparatus of Wulzinger (Wulzinger, 1998)***

Figure 72 ***Laboratory Scale Apparatus used by Wulzinger (Wulzinger, 1988)***

8.6 Scale-Up Comparison with Cooke

Working on the same apparatus as described in Section 8.1, Cooke tested pine wood in the 1 kg/h laboratory scale apparatus at Aston *(Cooke, 1999)*. Between her experimentation and that described in Section 8.2, the following changes were made:

1) a second cyclone added
2) an electrostatic precipitator included
3) the quench column cooled using liquid chilled to –1.5°C rather than cold water

Despite that, the results are very similar (Table 58, Figure 73). It appears that the inclusion of slate or char at Aston or slate at IWC slightly lowers the yield of pyrolysis liquid compared to the non-catalytic experiments of Cooke. This is the opposite to the results found in the 150 or 200 g/h apparatii at Aston and IWC, respectively, that show the pyrolysis liquid yield to increase slightly with the inclusion of slate or char.

Figure 73 ***Yield Versus Temperature Results from 1 kg/h Apparatus used by Cooke (Cooke, 1999)***

Table 58 Results from 1 kg/h Reactor at Aston Reported by Cooke

Run Temperature (°C)	449	476	514	525	562
Vapour Residence Time (s)	1.06	1.29	1.19	1.05	1.13
Gas % Yield	12.7	12.7	15.4	16.4	23.8
Organics % Yield	46.2	55.9	59.4	54.1	39.7
Char % Yield	24.8	15.8	10.1	14.4	19.9
Water % Yield	11.9	11.6	12.4	14.8	13.7
Liquids % Yield	58.1	67.5	71.8	68.9	53.3
% Closure	95.6	96.1	97.3	99.7	97.0

9 CATALYST REGENERATION AND SCANNING ELECTRON MICROSCOPY

Using a Scanning Electron Microscope (SEM) to view catalysts used, and the char or coke produced from running the pyrolysis apparatus, is useful to deduce what physically happens to the catalyst surface during an experiment. The final location in the apparatus of the catalyst following pyrolysis may also be ascertained by examining product char samples for catalyst. The SEM technique can also be used to evaluate the degree of regeneration achieved by putting used catalyst in the furnace to burn off the coke deposits. These reasons for analysis have been included alongside the list of samples for which micrographs were obtained. (Table 59) 'Regen' represents those catalysts analysed to ascertain the effect of heating in a furnace to remove combustibles, especially coke. 'Locate' indicates the char, coke and catalyst samples used to find where the catalyst used ends up on completion of a pyrolysis experiment using the small fluid bed at Aston.

Table 59 Source of Samples for Scanning Electron Microscope Images

No.	Sample	Run from which taken	Preparation	Reason for analysis
01	BDH-Y zeolite catalyst	-	Fresh unused	Regen
02	BDH-Y zeolite catalyst	EHS07[a]	Once used and furnace heated	Regen
03	BDH-Y zeolite catalyst	EHS39[b]	Coked	Regen
04	BDH-Y zeolite catalyst	EHS39	Coked + 1 hour furnace	Regen
05	BDH-Y zeolite catalyst	EHS39	Coked + 24 hour furnace	Regen
06	Fluid bed sand	EHS39	Coked	Regen
07	Fluid bed sand	EHS39	Coked + 1 hour furnace	Regen
08	Fluid bed sand	EHS39	Coked + 24 hour furnace	Regen
09	Char from charpot	EHS39	-	Locate
10	Thermally-expanded slate	EHS40	Coked	Regen
11	Thermally-expanded slate	EHS40	Coked + 1 hour furnace	Regen
12	Thermally-expanded slate	EHS40	Coked + 24 hour furnace	Regen
13	Char from charpot	EHS40	-	Locate
14	Fluid bed sand	EHS42[c]	Coked	Regen
15	Fluid bed sand	EHS42	Coked + 1 hour furnace	Regen
16	Fluid bed sand	EHS42	Coked + 24 hour furnace	Regen
17	Char from charpot	EHS42	-	Locate
18	Char from filter paper[d]	EHS42	-	Locate
19	Grace Davison ZSM-5 zeolite catalyst	-	Fresh unused	Locate
20	Char from charpot	EHS08[a,e]	-	Locate
21	Char from filter paper[d]	EHS08	-	Locate
22	Char from charpot	EHS09[a,f]	-	Locate
23	Char from filter paper[d]	EHS09	-	Locate
24	Fluid bed sand and BDH-Y zeolite catalyst	EHS38	Sand contaminated with co-fed catalyst + 24 hour furnace	Locate Regen

Notes:
(a) EHS07, 08 and 09 used pine wood whilst the rest used beech wood
(b) Catalyst from primary reactor
(c) EHS42 is a non-catalytic run
(d) Filtrate from ethanol washings of glassware
(e) EHS08 co-fed Grace Davison ZSM-5 zeolite catalyst
(f) EHS09 co-fed crushed BDH-Y zeolite catalyst

9.1 Scanning Electron Microscopy Results

In the case of BDH-Y zeolite regeneration, fresh zeolite appears to be less flat and therefore have a slightly larger surface area than the regenerated catalyst. After twenty-four hours of furnace heating, the surface appears more smooth. Both coked and catalyst that has spent one hour in the furnace, still appear to have the high surface area of the fresh catalyst. Using the furnace to regenerate the catalyst therefore appears to damage the catalyst surface. A reduction in the activity of the catalyst has, however, not been observed in the experimental pyrolysis work. BDH-Y catalyst, when removed from the reactor is black with coking. When it is fresh or after twenty-four hours of regeneration, it is white. After only one hour of regeneration there is still a hint of greyness. It is therefore recommended that the optimum time for regeneration is less than twenty-four hours, to avoid damage to the surface, and greater than one hour (in the region of two hours) to remove all the coke. Additionally, there is no evidence that The catalyst ends up in the char pot (see Figure 111, 'Char in Charpot' in Appendix Q, page 337).

When thermally-expanded slate is used as the fluidising medium, coke appears to build up around the pores rather than blocking or covering them. The surface is therefore more smooth after regeneration when the coke has been burned off. This result agrees with work done by Lahousse et al. on zeolites *(Lahousse, 1998)*. They found that the access for the reactant to the zeolite particles seems very free and the coke present in the sample does not seem to be formed in the zeolite agglomerates. Also, if any slate is lost from the fluid bed, it was not detected in the char in the char pot (see Figure 115, Appendix Q).

Char in the char pot was found to be of a completely different nature to that collected from the filter paper as can be seen from Figure 119 and Figure 120 (Appendix Q). It was also discovered that co-fed ZSM-5 does not get trapped by the cyclone, but is found in the char in the filter paper. It is therefore in the liquid and char remaining on the glassware. This will impact the further development of this pyrolysis technology if small particle size ZSM-5 is to be used as a catalyst. It is also not certain where the catalytic reactions are occurring. Although it is unlikely, because of the temperatures, there is a possibility that catalysed reactions may still occur in the product liquid.

10 Summary of Discussions

The results and discussions from Chapters 3 to 9 are brought together in this Chapter:

10.1 Catalyst Screening

There was excellent comparison between pyrolysis results from the micro-reactor when they were repeated, showing accuracy of results. The lack of difference between the results from the wood and sodium montmorillonite run and the blank non-catalytic run showed that this catalyst had not affected the pyrolysis reactions. The most promising catalyst to use in larger scale pyrolysis was found to be Y-zeolite, although slate and char were not tested using the screening method.

The results have been ranked and are shown, in order, in Table 60. The hypotheses set up in Chapter 3 are examined in Section 10.1.1.

Table 60 Ranking of Results from Screening Analysis Methods

Order of Ranks[a] (Most promising first)	**Catalyst Code** (Table 12)	**Catalyst Pore Size** (Table 12)
1	Y	11 Å
2	BOD20	14 Å
3	Equilibrium	5 Å
4	FCAT-B	5 Å
5	BOD17	12.5 Å
6	BOD24	18 Å
7	FCAT-C	5 Å
8	FCAT-A	5 Å
8	BOD19	16 Å
10	ZSM-5	5 Å
11	BOD18	12.5 Å
11	BOD21	14 Å
13	BOD23	18 Å
14	BOD16	12.5 Å

Notes (a) Results taken from Table 13

10.1.1 Catalyst Screening Hypotheses

In Chapter 3, several hypotheses were set up to assess the catalyst screening. Following that screening and subsequent fluid bed pyrolysis, those hypotheses should be re-examined. They are listed below:

a) Unknown rather than known identifiable compounds contribute to stability.
b) The more chemically different a pyrolysis liquid is from the blank non-catalytic pyrolysis liquid, the more stable it is.
c) A more stable pyrolysis liquid contains a larger number of chemical compounds than a less stable one.
d) A more stable pyrolysis liquid has more low molecular chemicals and less high molecular chemicals.
e) The larger the catalyst pore size, the more stable the resultant pyrolysis liquid.
f) Screening using the micro-reactor technique can predict the most promising catalyst in the bench scale apparatus.

10.1.1.1 Unknown and Identifiable Compounds

No specific chemicals were found that related to stability. The hypothesis that unknown rather than known identifiable compounds contribute to stability is therefore probably true, but has not been proven.

10.1.1.2 Chemical Difference from Blank Run

Comparing the degree of chemical difference of a pyrolysis liquid produced with a catalyst to that produced with no catalyst, can be seen in Table 61 to be a useful tool in predicting the most stable liquid. Although the order is not exact, it does predict the most stable liquid correctly and there is not a large degree of difference in the rest.

Table 61 Degree of Chemical Difference to Blank Run Compared to Stability

Method 7[a, b] Order of Ranks	Catalyst Code (Table 12)
1	Y
1	BOD17
3	BOD19
4	BOD20
5	FCAT-A
5	BOD24
7	Equilibrium
8	FCAT-B
9	FCAT-C
10	BOD21
11	ZSM-5
12	BOD16
13	BOD18
14	BOD23

Overall Order of Ranks[b] (Most promising first)	Catalyst Code (Table 12)
1	Y
2	BOD20
3	Equilibrium
4	FCAT-B
5	BOD17
6	BOD24
7	FCAT-C
8	FCAT-A
8	BOD19
10	ZSM-5
11	BOD18
11	BOD21
13	BOD23
14	BOD16

Notes (a) 'Method 7' described in Section 3.3.1.5.

(b) Results taken from Table 13

10.1.1.3 Number of Chemical Compounds

Using the simple method of counting the number of peaks produced by chromatograph analysis also predicted the most promising catalyst to be Y-zeolite. Table 62 shows that like the degree of chemical difference analysis (Section 10.1.1.2), the order is not exactly correct. In this case, although good, this method is not quite as successful as comparing the degree of chemical difference of a pyrolysis liquid produced with a catalyst to that produced with no catalyst.

Table 62 Degree of Chemical Difference to Blank Run Compared to Stability

Method 3[a, b] Order of Ranks	**Catalyst Code** (Table 12)
1	Y
2	Equilibrium
3	FCAT-B
4	BOD20
5	ZSM-5
6	BOD18
7	FCAT-C
8	BOD21
9	FCAT-A
10	BOD23
11	BOD16
12	BOD24
13	BOD17
14	BOD19

Overall Order of Ranks[b] (Most promising first)	**Catalyst Code** (Table 12)
1	Y
2	BOD20
3	Equilibrium
4	FCAT-B
5	BOD17
6	BOD24
7	FCAT-C
8	FCAT-A
8	BOD19
10	ZSM-5
11	BOD18
11	BOD21
13	BOD23
14	BOD16

Notes (a) 'Method 3' described in Section 3.3.1.3.

(b) Results taken from Table 13

10.1.1.4 Ratio of Low Molecular Chemicals to High Molecular Chemicals

Predicting a more stable pyrolysis liquid using the premise that it has more low molecular chemicals and less high molecular chemicals is more difficult that the other predictive methods described in Chapter 3. It was less successful in predicting the most stable liquid, but may be an indication of the liquid with the lowest initial viscosity. Further testing would be necessary to establish this. It could be done by bench scale production of pyrolysis liquid using ZSM-5 on alumino-silicate binder, and sodium montmorillonite clay calcined at 475°C, followed by initial viscosity and AVI measurement.

Table 63 ***Ranking of the Catalysts used to Produce Pyrolysis Liquid High in Low Molecular Weight Compounds***

Order of Ratio of Low to High Molecular Weights[a]	Catalyst Code (Table 12)
1	FCAT-A
2	Y
3	FCAT-C
4	BOD17

Notes (a) See Section 3.3.4.

10.1.1.5 Catalyst Pore Size

Table 60 shows the most promising catalyst and compares this to their pore size. It can be seen that stability is not a function of pore size. Although Y-zeolite, the highest ranked catalyst, has a large pore size, catalysts of all sizes can be found throughout the Table 60.

10.1.1.6 Pre-Screening for Bench Scale Pyrolysis

The use of the micro-reactor to pre-screen catalyst for bench scale pyrolysis successfully found Y-zeolite as a promising catalyst that performed very well in the larger scale testing. The hypothesis associated with this system, however, should be refined so this micro scale testing can be used as the sole method of experimentation, bypassing the need to use the bench scale apparatus.

10.2 Pyrolysis Heat Transfer During Condensation

Calculations on the pyrolysis apparatus commissioning configuration cooling system yielded the design of the experimental single product condenser and the following results (Section 4.1.2.2):

1) In the commissioning system, the exit temperature of the pyrolysis product after the secondary finger condenser was found to be 36°C when the inlet temperature of the vapours to the primary condenser was 500°C.

2) In the same system as 1), the intermediate temperature was calculated to be 300°C between the ice condenser at 0°C and the dry ice condenser at –80°C.
3) The newly designed single product condenser used to replace the system in 1) and 2) was found to require a 2 l/min cooling water flow-rate. This was when the cooling water temperature was 15°C in and 17°C out, the pyrolysis product temperature was 500°C in and 29°C out and the surface area for heat transfer was 1.7×10^{-2} m^2. This cooling water flow-rate corresponds to 0.15 kg/s and a turbulent flow regime.
4) The heat transfer coefficient, U, for the condenser in 2) was found to be 11 kW/m^2K.

10.3 Mass Balance Analysis

10.3.1 Empirical Comparison

To compare the pyrolysis results found whilst undertaking this project with other projects, empirical results were used that incorporated results from other systems of varying types and sizes and using a variety of feedstocks. These empirical results were derived from Toft *(Toft, 1996)*. The non-catalytic experiments from this project, when plotted, have a similar organic yield peak shape and the maximum occurs at the same temperature as the empirical data. This means that the results gained here can be compared with standard pyrolysis results from other work using alternative pieces of apparatus. It indicates that no particularly unusual phenomenon are occurring in these experiments and confirms the validity of the results and approach.

Only the experiments where the fluid be has been replaced by a slate fluid bed, produce results that are in a similar yield-temperature region as the empirical and non-catalytic experiments (maximum of 64 % organic yield at 490°C). The use of slate as a fluid bed does in fact reduce the temperature at which the maximum liquid yield is found from 490 to 475°C. This result is not repeated when slate is co-fed. At the slate co-fed organic peak of 500°C, there is a satisfactory yield, but it is much lower than the empirical yield at all other temperatures. The slate secondary reactor gave a very poor yield result of 43 % organics at 503°C.

The shape of the organic yield curve for Y-zeolite is very similar to the empirical result, but the percentage yield is reduced by approximately 6.5 %.

The results using char as a catalyst do not follow the characteristic organic yield graph shape. The char secondary reactor is the worst configuration (as the slate secondary reactor is for the slate configurations). Co-fed char and the char fluid bed are similar to themselves and in the region of the non-catalytic experiments in the 450 to 500°C temperature range. After this temperature point, the yield from the char fluid bed configuration dramatically decreases.

10.4 Liquid Product Chemical Analysis

The percentage of water, hydroxyacetaldehyde, levoglucosan and lignin in the pyrolysis liquid was found to be linked to the following variables:

1) the temperature of the experiment
2) the catalyst used
3) the mode of its use

10.4.1 Pyrolysis Liquid Water Content

It was hypothesised, based on previous work, that the viscosity of pyrolysis decreases with increased water content. It was found that this was a rough indication, but does not always follow. The catalyst configuration that produced the pyrolysis liquid with the highest water content, slate in the secondary reactor, was found to have the lowest viscosity. Also, the catalyst configuration that produced the pyrolysis liquid with the lowest water content, co-fed char, was found to have the highest viscosity. However, the other catalyst configurations did not follow that pattern as shown in Table 64, below.

10.4.2 High Performance Liquid Chromatography

Section 2.1.1 showed that the major product from cellulose depolymerisation is levoglucosan and the major product from cellulose fragmentation is hydroxyacetaldehyde. The results from HPLC analysis show that much more

hydroxyacetaldehyde is produced compared to levoglucosan. This indicates that cellulose fragmentation rather than depolymerisation is the predominant decomposition pathway. The relationship between hydroxyacetaldehyde, levoglucosan and lignin with initial viscosity and stability is examined in Section 10.6.2.

10.5 Liquid Product Physical Analysis

Capillary viscometry was found to be a satisfactory method of finding the kinematic viscosity of pyrolysis liquid. The viscosity of the pyrolysis liquid was measured twenty-four hours after the end of the pyrolysis experiment. This found that the following were all variables that effected the viscosity result:

1) the temperature of the experiment
2) the catalyst incorporated
3) the mode of its incorporation

The slate secondary bed, the Y-zeolite close-coupled in-bed and the char fluid bed were found to give the lowest initial viscosity product. However, only one experiment with a slate secondary bed was performed and further testing is recommended to confirm this result. The initial viscosity is compared to stability in Section 10.6.

10.6 Small Fluid Bed Pyrolysis Product Stability

The stability of the pyrolysis liquid was also found to depend on the following variables:

1) the temperature of the experiment
2) the catalyst incorporated
3) the mode of its incorporation

To find the cause of the stability change, the results from chemical and physical analysis can be compared to the stability results. This is done in Table 64. The pore size of the catalyst had no effect on the stability of the pyrolysis liquid, both in the screening experiments and in the larger scale experimentation.

Table 64 Ranked Properties of Pyrolysis Liquid Compared to Stability Expressed as Aston Viscosity Index

Rank	Water Content (Greatest Amount First)[a]	Hydroxyacetaldehyde Content (Greatest Amount First)[b]	Levoglucosan Content (Greatest Amount First)[c]	Lignin Content (Greatest Amount First)[d]	Initial Viscosity (Lowest First)[e]	Stability (Lowest AVI First)[f]	Catalyst Pore Size (Largest First)
1	Slate secondary bed	Co-fed char	Co-fed char	Char fluid bed	Slate secondary bed	**Char fluid bed**	Char
2	Slate fluid bed	No catalyst	No catalyst	Co-fed slate	Y-zeolite in-bed	**Co-fed char**	Slate
3	No catalyst	Slate fluid bed	Co-fed slate	Co-fed char	Char fluid bed	**Y-zeolite in-bed**	Y-zeolite
4	Y-zeolite in-bed	Char fluid bed	Char fluid bed	Y-zeolite in-bed	Slate fluid bed	**Slate fluid bed**	
5	Char secondary reactor	Co-fed slate	Slate fluid bed	Slate fluid bed	Co-fed slate	**Slate secondary bed**	
6	Char fluid bed	Y-zeolite in-bed	Y-zeolite in-bed	No catalyst	No catalyst	**Char secondary reactor**	
7	Co-fed slate	Slate secondary bed	Char secondary reactor	Slate secondary bed	Char secondary reactor	**Co-fed slate**	
8	Co-fed char	Char secondary reactor	Slate secondary bed	Char secondary reactor	Co-fed char	**No catalyst**	

Notes (a) Taken from Table 36 (b) Taken from Table 43 (c) Taken from Table 44
(d) Taken from Table 47 (e) Taken from Table 50 (f) Taken from Table 52

10.6.1 Comparison of Stability to Initial Viscosity

Using Table 64, the stability of pyrolysis liquid produced using different catalyst configurations, found by the Aston viscosity index, can be compared to the initial viscosity of the pyrolysis liquid, found by capillary viscometry. The results are similar with two notable exceptions (colours refer to arrows in Table 64):

1) When char is co-fed, it produces the most viscous liquid, but a stable one.
2) The use of a secondary reactor containing slate produced the least viscous pyrolysis liquid, but the stability of this liquid was mediocre compared to the other results.

10.6.2 Comparison of Stability and Initial Viscosity to Chemical Production

When examining the chemicals in the differently produced pyrolysis liquids and comparing them to the viscosity and stability results, Table 64 shows that there is no link between either hydroxyacetaldehyde or levoglucosan and the stability or viscosity of the liquids that contain them. Lignin, however, is an excellent indicator of the stability of the pyrolysis liquid. With the exception of the pyrolysis liquid produced by co-feeding slate, the more lignin in the pyrolysis liquid, the more stable the liquid is.

10.7 Scale -Up of Bench Scale Pyrolysis

The work of Wulzinger *(Wulzinger, 1999)* found also that slate as a fluid bed configuration successfully improved the quality of the resultant pyrolysis liquid. The scaling up of the bench scale process to laboratory scale was therefore tested at both Aston and the Institute for Wood Chemistry. The results however, were promising, but not conclusive from either institution. Further work is therefore recommended to confirm the benefits of using a slate fluid bed in large-scale apparatus.

10.8 Follow-Up of Objectives

The objectives of this thesis were set as the following questions. They will be reviewed in this Section.

A) What is the best catalyst to produce the best quality pyrolysis liquid?

B) How is 'best quality pyrolysis liquid' defined?
C) Where is the best place in the pyrolysis process to incorporate catalysts?
D) What chemicals within the pyrolysis liquid influence quality?

10.8.1 How is 'Best Quality Pyrolysis Liquid' Defined?

The pyrolysis liquid with the greatest stability, the lowest initial viscosity and the highest heating value (indicated by low water content) is defined as the pyrolysis liquid of the best quality. The amount of liquid yielded also influences the 'best' liquid as the end use of the pyrolysis liquid is as a fuel and the most economically produced liquid is desirable. All these factors should be balanced.

10.8.2 What is the Best Catalyst to Produce the Best Quality Pyrolysis Liquid?

The best quality pyrolysis liquid was produced using a char fluid bed. However, if the economics of high yielding yet good quality liquid are taken into account, the slate fluid bed is the best. The third best catalyst configuration is the inclusion of Y-zeolite close coupled in the primary reactor.

10.8.3 Where is the Best Place in the Pyrolysis Process to Incorporate Catalysts?

The quality of the pyrolysis liquid was found to be influenced by the catalyst type and the location of its inclusion, in combination. For the slate catalyst, the following configurations are in the order in which they produce the best liquid, best first:

1) Catalyst in the primary reactor as the fluid bed medium
2) Catalyst in the secondary reactor
3) Catalyst co-fed into the primary reactor

10.8.4 What Chemicals within the Pyrolysis Liquid Influence Quality?

The lignin content of the pyrolysis liquid greatly influences the stability of the liquid and therefore affects the liquid quality. No other chemical alone could be identified as having a direct effect on the pyrolysis liquid quality.

11 CONCLUSIONS

The most important conclusions are:

1) Quality of pyrolysis liquid is defined by (in order of importance):
   a) High stability, defined by a low Aston Viscosity Index
   b) Low initial viscosity
   c) High heating value, defined by low water content
   d) High liquid yield

Not all these are compatible and a balance must be met which is why they should be considered in this specific order.

2) The quality of the pyrolysis liquid formed using the following systems, is the best of those tested (best first):
   a) Slate fluid bed in the primary reactor replacing fluidising medium
   b) Char fluid bed in the primary reactor replacing fluidising medium
   c) Y-zeolite fluid bed in the primary reactor replacing fluidising medium

3) The use of a slate fluid bed is the only system that does not reduce the organic yield when compared to the non-catalytic system. It also reduces the temperature at which the maximum yield is found from 490 to 475°C, which is economically desirable for power consumption. This is an excellent result and is an additional reason why the use of slate is a successful finding.

4) The most promising catalyst screened, Y-zeolite, was also successful when tested in the 150 g/h scale reactor. It was surpassed only by slate and char in fluid bed mode, which were not pre-screened. The success of Y-zeolite confirms that screening in a micro-reactor, attached to a GC is a valid method for pre-screening.

5) With the exception of the pyrolysis liquid produced by co-feeding slate, the more lignin in the pyrolysis liquid, the more stable the liquid is (the lower the AVI). The lignin content of the pyrolysis liquid greatly influences the stability of the liquid

and therefore affects the liquid quality. This unexpected results shows that promoting lignin production improves the pyrolysis liquid quality.

6) The use of the secondary reactor, containing catalyst, dramatically reduces the organic yield of the system from an average of 56 to 64 %, down to an average of 44 to 46 %.

7) In producing quality pyrolysis liquid, the order of the modes of catalyst incorporation is (best first):
   a) Primary reactor bed replacement
   b) Secondary reactor
   c) Co-feeding catalyst

8) A new cooling system for the 150 g/h pyrolysis apparatus was designed, built and successfully operated.

9) The comparison with empirical data was found to be good and confirms the validity of the experimental results and approach.

10) Capillary viscometry was successfully used to find the kinematic viscosity of pyrolysis liquid.

11) The decrease of pyrolysis liquid viscosity with increasing water content did not always occur when comparing pyrolysis liquid produced by different methods. Water content therefore can not be used as a measure of relative viscosity. It can only be used when comparing pyrolysis liquid formed in the same mode with the same catalyst.

12) The proportion of hydroxyacetaldehyde produced compared to levoglucosan indicates that cellulose fragmentation rather than depolymerisation is the predominant decomposition pathway in producing pyrolysis liquid catalytically.

12 RECOMMENDATIONS

Following the studies undertaken in this thesis, recommendations have been made for the continuation of this work. They comprise of:

a) Modifications to the addition of catalysts in the fast pyrolysis process
b) Additions and changes to the current process
c) Improvements to the current apparatus and experimentation techniques
d) Examination of pyrolysis liquid chemistry.

12.1 Catalyst Recommendations

12.1.1 Scaling

To confirm the effect of the slate fluid bed is still valid in scaled-up apparatus, further stability testing of non-catalytic pyrolysis liquid from the larger scale is recommended for comparison.

12.1.2 Mode of Operation

To confirm if the modes of operation for a particular catalyst always effects the result in the same order, further testing of Y-zeolite in different configurations and slate in the 'close coupled in primary reactor' mode is recommended. This would result in the three 'best' catalysts being tested in all modes (co-feeding, fluid bed in primary reactor, close-coupled in primary or secondary bed).

12.1.3 Catalyst Mixes

In the work of Katikaneri *(Katikaneri, 1997)* very different results were found when catalysts were mixed, compared to the use of a single catalyst. It is therefore suggested that combinations of the catalysts tested in this report be tried. The aim should shift from not just pyrolysis liquid stability, but include increasing the heating value and therefore the commercial value. It is suggested that this is possible by slate catalytic pyrolysis with HZSM-5 combined. It is hypothesised that this would act similarly to catalytic cracking of hydrocarbon oil, where HZSM-5 is added to the standard catalyst. It may be found that the slate stabilised the pyrolysis vapours and HZSM-5 acts on a

small proportion of them to increase the heating value, analogous to raising the Octane number of petroleum oil.

12.1.3.1 Catalyst Modes

Mixing of catalyst types could be achieved not only by straight mixing, but by combining modes of operation. For example, a system with a catalytic fluid bed in the primary reactor could incorporate a secondary reactor with a different catalyst.

12.1.4 Catalyst Regeneration

The slate catalyst is believed to be subject to rapid coking. It is suggested that the point at which the slate catalyst requires regeneration be found. That is, when the catalyst should be regenerated. Including catalyst as the whole or part of the fluidising bed - 'in-bed', is equivalent to an FCC unit that runs until the catalyst is 'spent'. This mode of operation can also be used to find the point at which regeneration of a catalyst would be necessary by running for different lengths of time and examining the catalyst. The catalyst lifetime and activity can be determined. It may be found that the build up of char itself is acting as the catalyst and the slate is only a medium for supporting the char with a greater surface area than char on its own.

12.1.5 Catalyst Concentration

In the experiments presented in this thesis, only one concentration of catalyst was investigated for each type and configuration of catalyst. In future work ball bearings could be added to the secondary bed to alter the concentration and the thermal sites upon which to react *(Horne, 1996)*. The relationship between thermal and catalytic cracking and the importance of char deposition could be studied to further improve liquid fuel quality.

12.1.6 Slate Reaction Investigation

The method that is employed by the successful slate catalyst to produce a more stable pyrolysis liquid should be sought. This could be attempted by using model compounds

such as those mentioned in Section 2.3 to ascertain upon which components of the pyrolysis vapours the slate acts.

12.2 Process Modifications

12.2.1 Addition of Steam

The addition of steam to the pyrolysis process was found to have a beneficial effect on the product by promoting thermal cracking *(Williams, 1997; 1998; Vassilatos, 1990)*. It is recommended that that effect be tested when slate catalyst is used.

12.2.2 Modification of Condensation Temperature

The temperature of condensation should be modified to alter the product composition. The 'time-temperature envelope' of pyrolysis liquid production can alter the product by extending or reducing the secondary reactions. This can be done by using a chilled liquid rather than tap water through the sloping Liebig condenser. One consideration however would be that this would increase the cost of a plant should the process be scaled up.

It is suggested that reducing the temperature of liquid collection will allow more of the chemicals that, in the configuration presented in this thesis, are collected in the acetone condenser. They will therefore condense at the same time as the bulk of the liquid.

12.3 Further Testing of Current Process

12.3.1 Tarry Liquid Analysis

This thesis has assumed that the composition of the liquid that remains on the glassware is of the same composition as the pyrolysis liquid collected in the oil pot. By the fact that it has remained on the walls of the condenser suggests that this is not correct. It appears more tarry and it is suggested that it has a higher sugar content. A comparison of the composition of this liquid and the main bulk of the pyrolysis liquid collected should be carried out, particularly finding the sugar content.

12.4 Chemistry Recommendations

12.4.1 Lignin Ratio

It was discovered in Section 5.4.2, 'Lignin Results' in the 'Discussion of Liquid Product Chemical Analysis Results' Section, that at an average pyrolysis run temperature of 475°C an anomaly occurred when the percent lignin found was compared to the percent organic yield. It should be discovered if an interesting chemical phenomenon occurs at this temperature, but not lower or higher temperatures. This temperature corresponds to the organic yield peak. It would follow that if the lignin yield stayed the same, the ratio would decrease (Equation 48) or if it increased with the organic yield, the ratio would stay the same. The ratio actually increases. It would be interesting to find the chemical cause of this, to enable its promotion. This is particularly important due to the link between lignin and stability.

12.4.2 Acidity of Pyrolysis Liquid

Although this project has addressed the problem of instability in terms of viscosity change, it was discussed in Section 7.4 that there was no change of pH with catalyst type or mode of incorporation of the catalyst into the pyrolysis process. In fact, it was found through accelerated ageing experiments, that the acidity was still changing with the age of the pyrolysis liquid, if only slightly. This is another phenomenon that would better be addressed in the field of chemistry. The addition of chemicals to reduce the number of free protons and to stop their production should be investigated to help pyrolysis liquid become less acidic. This is a current hurdle for pyrolysis liquid becoming a commercial product and technology, as specialist storage and handling is currently required.

12.4.3 Homogeneity of Pyrolysis Liquid

In Section 8.4, the homogeneity of the pyrolysis liquid produced from the large fluid bed using a slate fluid bed, was examined. The testing was done using the physical property of viscosity and viscosity change. This could also be done chemically, using HPLC for example, to compare the composition of the liquid to the position in the container from which the sample was taken, over time. The localised pattern of

chemicals found may indicate the degradation path of the pyrolysis liquid and the cause of this. This may confirm the hypothesis in Section 8.4 that it is the presence of microfine char that settles towards the bottom of the liquid container, that influences the homogeneity of the pyrolysis liquid. The direct measurement of the microfine char is particularly difficult because of the viscosity of the pyrolysis liquid. Even with the addition of solvents, for example methanol, the pressure drop across a filter builds very quickly. Examining the chemical composition could be an alternative method for observing the microfine char composition as the catalytic effect of char has been proven.

13 Nomenclature

The following symbols and letters have been used to represent the following expressions:

Term	Units	Definition
AdjHPLC%	wt%	Weight percent chemical concentration in HPLC sample
A_i	m^2	Cross sectional area of cyclone gas inlet
A_T	m^2	Area of heat transfer
C	-	Viscometer specific calibration constant (applies when the flow time is not less than 200 seconds)
Cp_w	J/kg K	Specific heat capacity of cooling water (constant mass)
d	m	Diameter (or inner diameter)
D	m	Outer diameter
d_o	m	Diameter of cyclone outlet
e	-	Particle voidage
e_{mf}	-	Particle voidage at minimum fluidising conditions
F	N	Total force on particle
g	m/s^2	Acceleration due to gravity
G	kg/s	Mass flow-rate
Ga	-	Galileo number (Equation 6)
HPLC%	wt%	Weight percent of chemical found by HPLC
ID	mm	Internal diameter
k_G	W/m K	Thermal conductivity of glass
l	m	Characteristic length
M	kg	Mass
Mf	g	Mass of dry wood feed pyrolysed
Mpl	g	Mass of product liquid recovered from pyrolysis
Mt	g	Mass of pyrolysis liquid
Mw	g	Mass of water
P	Pa	Pressure
PL%	wt%	Weight percent concentration of chemical in pyrolysis liquid sample from reaction
Q	W	Heat transfer load
Re	-	Reynolds number (Equation 5)

Re_t	-	Reynolds number under terminal falling velocity conditions
s	m^2	Tube flow area
STDev	-	Standard deviation
T	K	Temperature
T_{cold}	K	Cold side temperature
T_{hot}	K	Hot side temperature
T_{Pout}	K	Inlet pyrolysis liquid temperature
T_{Pout}	K	Outlet pyrolysis liquid temperature
T_{Win}	K	Inlet water temperature
T_{Wout}	K	Outlet water temperature
U	W/m^2 K	Heat transfer coefficient
u	m/s	Velocity
u_{mf}	m/s	Minimum fluidising velocity
u_o	m/s	Superficial gas velocity
u_t	m/s	Particle terminal velocity
$u_{t, dmin}$	m/s	Terminal falling velocity of smallest particle retained by cyclone
V	m^3	Volume
Vs	µl	HPLC injection sample volume of standard
Vu	µl	HPLC injection sample volume of sample with unknown concentration
W_W	kg/s	Mass flow-rate of cooling water
x_G	m	Wall thickness of glass for heat transfer
XLT	g	Mass of lignin
Z	m	Length of cyclone
θ_{lm}	K	Logarithmic mean temperature difference (Equation 20)
μ_W	N s/m^2	Viscosity of water
π	-	Pi = 3.142
ρ	kg/m^3	Density
ρ_b	kg/m^3	Bulk density – mass of a group of particles per volume of particles including voids between particles
ρ_p	kg/m^3	Particle density – mass of a particle per particle volume were the particle non-porous
ρ_W	kg/m^3	Density of water

Σ_s (area of peak)	mVolt.s	Sum of selected chromatograph peak areas
Σ_t (peak)	-	Total number of chromatograph peaks

14 References

14.1 Contents of References

		Page
1	Aabloo to Adjaye	237
2	Adjaye to Bridgwater	238
3	Bridgwater to Churin	239
4	Conti to Diebold	240
5	Diebold to Donnot	241
6	Elamin to Gevert	242
7	Goldstein to Hanniff	243
8	Horne to Kaiser	244
9	Katikaneni to Leppämäki	245
10	Longley to Meier	246
11	Meier to Perry	247
12	Perry to Rogers	248
13	Robinson to Sharma	249
14	Sharma to Vassilatos	250
15	Vassilatos to Wunder	251

14.2 Alphabetical References

References are arranged alphabetically then chronologically for each primary author. Where a primary author has published more than once in a year, a hash mark differentiates between the publications.

A

Aabloo, A, French, A.D., Mikelsaar, R-H., 'Packing Energy Calculations on the Crystalline Structure of Cellulose I' in Cellulose and Cellulose Derivatives' Eds. Kennedy, J.F., Phillips, G.O., Williams, P.O. Pp 51-56. (Woodhead, 1995)

Adjaye, J.D., Sharma, R.K., Bakhshi, N.N., 'Catalytic Upgrading of Wood Derived Bio-Oil Over HZSM-5: Effect of Co-Feeding Steam' in Advances in Thermal Biomass

Conversion Elsevier Applied Science: New York (1994), Eds. Bridgwater, A.V., Kuester, J.L., Pp. 1032-1046

Adjaye, J.D., Bakhshi, N.N., 'Catalytic Conversion of a Biomass-Derived Oil to Fuels and Chemicals II: Chemical Kinetics, Parameter Estimation and Model Predictions' in 'Biomass and Bioenergy' Vol. 8 No. 4. Pp 265-277 (Elsevier Science, 1995)

Agblevor, F.A. and Besler, S., 'Inorganic Compounds in Biomass Feedstocks. 1. Effect on the Quality of Fast Pyrolysis Oils', in 'Energy and Fuels', Vol. 10, Pp. 293-298, 1996

Allen, T., 'Particle Size Measurement, Volume 2 – Surface Area and Pore Size Determination', Fifth Edition, Pp. 47 (Chapman and Hall, 1997)

B

Baker, E.G., Elliott, D.C., 'Catalytic Upgrading of Biomass Pyrolysis Oils' in Research in Thermochemical Biomass Conversion Eds. Bridgwater, A.V., Kuester, J.L., Elsevier Applied Science: London (1988), Pp. 883-895

Baldauf, W. Balfans, U., 'Upgrading of Fast Pyrolysis Liquids at Veba Oel AG', in 'Biomass Gasification and Pyrolysis – State of the Art and Future Prospects', Eds. Kaltschmitt, M. and Bridgwater, A.V. Pp. 392-398 (CPL Press, 1997)

Barrow, G.M., 'Physical Chemistry', Fifth edition, McGraw Hill, 1988, Pp 45

Bitowft, B., Andersson, L.A. and Bjerle, I., 'Fast pyrolysis of sawdust in an entrained flow reactor', in Fuel, vol. 68, pp. 561-566, 1989.

Bodman, S., McWhinnie, W.R., 'Enhancement of Hydrocracking Reactivities of Liquifaction Extracts With Novel Catalysts', British Coal Research Association Contract No. B32(a), Periodic Report No. 3, January 1997, Aston University.

Boocock, D.G.B., Konor, S.K., Leung, A. Liu, J., Ly, L.D., 'Liquid Hydrocarbons From the Extraction and Catalytic Pyrolysis of Sewage Sludge', in Advances in Thermal Biomass Conversion Ed. Bridgwater, A.V., Blackie (1994) Pp. 986-999

Bridgwater, A.V., Bridge, S.A., 'Review of Biomass Pyrolysis Technologies' in 'Biomass Pyrolysis Liquids Upgrading and Utilisation' Eds. Bridgwater, A.V. and Grassi, G. Pp 11-92 (Elsevier Science, 1991)

Bridgwater, A.V., 'Opportunities for Biomass Pyrolysis Liquids Production and Upgrading' in Energy and Fuels, 1992, No.6 (American Chemical Society, 1992)

Bridgwater, A.V., 'Catalysis in Thermal Biomass Conversion' in Applied Catalysis A General 116 Pp. 5-47, (Elsevier Science Publishers BV, Amsterdam, 1994)

Bridgwater, A.V., 'Production of High Grade Chemicals from Catalytic Pyrolysis of Biomass' in Catalyst Today 29 (1996) Elsevier Pp. 285-295

Bridgwater, A.V., 'Catalytic Upgrading Options For Biomass Fast Pyrolysis Liquids And Vapours' in 'Catalytic Pyrolysis Of Biomass For Improved Liquid Fuel Quality', Final Report, European Commission Contract JOR CT95-0081. Meier, D. *et al.* 1998

Burch, R., 'Pillared Clays' in Catalysis Today Vol. 2, Nos. 2-3 (Feb 1998) Pp. 185-368

Butterworth, D., 'Introduction to Heat Transfer', Engineering Design Guide 18, Oxford University Press, 1977. Pp 5.

C

Cartlidge, S., Haas, A. 'The 'G' Modification, Zeolite Acidity Optimised for Premium Gasoline Octane', in 'Science and Technology', Vol 44 (2), Pp. 63-66 (1991)

Chen, N.Y., Walsh, D.E., Koenig, L.R., 'Fluidised Bed Upgrading of Wood Pyrolysis Liquids and Related Compounds' in 'Pyrolysis Oils from Biomass – Producing, Analysing and Upgrading' Eds. Soltes, E.J., and Milne, T.A., American Chemical Society Symposium Series No. 376, Washington, DC (1988). Pp. 277-289

Churin, E., Maggi, R., Grange, P., Delnom, B. 'Characterisation and Upgrading of a Bio-Oil Pyrolysis of Biomass' in Research in Thermal Biomass Conversion' Elsevier Applied Science: New York (1988), Eds. Bridgwater, A.V., Kuester, J.L., Pp. 896-909

Churin, E., Grange, P., Delmon, B., 'Catalytic Upgrading of Pyrolysis Oils' in 'Biomass for Energy and Industry' Eds. Grassi, G. Gosse, G. and Santos. G., Pp. 2.621-2.626 (Elsvier applied Science, London, 1990)

Churin, E. 'Upgrading of Pyrolysis Oils By Hydrotreatment' in 'Biomass Pyrolysis Liquids Upgrading and Utilisation'. Eds. Bridgwater, A.V. and Grassi, G.,(Elsevier Applied Science 1991)

Conti, L., Scano, G., Boufala, J., Trebbi, G., Rennachi, A., Malloggi, S., 'Bench Scale Plant for Continuos hydrotreating of Oils from Biomass', in 'Advances in Thermochemical Biomass Conversion'. Ed. Bridgwater, A.V., 1460-1464 (Blackie, 1994)

Cooke, L.A., 'The Use of Catalysts for Upgrading Primary Pyrolysis Vapours from the Fast Pyrolysis of Biomass'. PhD Thesis, Aston University, Birmingham, UK. 1999

Coulson, J.M., Richardson, J.F., 'Chemical Engineering Volume 2' Fourth Edition. Pp. 226 (Pergamon, 1991)

Coulson, J.M., Richardson, J.F., 'Chemical Engineering Volume 2' Fourth Edition. Pp. 104 (Pergamon, 1991#2)

Coulson, J.M., Richardson, J.F., 'Chemical Engineering Volume 2' Fourth Edition. Pp. 344 (Pergamon, 1991#3)

D

Dao, L.H., Haniff, M., Houle, A., Lamothe, D., 'Reactions of Model Compounds of Biomass Pyrolysis Oils over ZSM-5 Catalysts' in 'Pyrolysis Oils from Biomass – Producing, Analysing and Upgrading' Eds. Soltes, E.J., and Milne, T.A., American Chemical Society Symposium Series No. 376, Washington, DC (1988). Pp. 328-344

Diddams, P., 'The Role and Operation of FCC Catalysts Made By Grace Davison', in Joule Contract 0081 Contractors Workshop 12-14 February 1997, Solihull, UK, Record of Meeting

Diebold, J.P., Evans, R.J., Levie, B.E., Milne, T.A. and Scahill, J.W., 'Low Pressure Upgrading of Primary Oils from Biomass', Solar Energy Research Institute Report, contract no. B-L5950-A-Q for U.S. Dept. of Energy, 1986

Diebold, J.P., Chum, H.L., Evans, R.J., Milne, T.A., Reed, T.B., Scahill, J.W., 'Low-Pressure Upgrading of Primary Pyrolysis Oils from Biomass and Organic Wastes' in 'Energy from Biomass and Wastes X', Ed. Klass, D. Pp 801-830 (IGT Chicago, 1987)

Diebold, J.P., Power, A., 'Engineering Aspects of the Vortex Pyrolysis Reactor to Produce Primary Pyrolysis Oil Vapours for use in Resins and Adhesives', in Research in Thermal Biomass Conversion' Elsevier Applied Science: New York (1988#1), Eds. Bridgwater, A.V., Kuester, J.L., Pp. 609-628

Diebold, J.P., Scahill, J.W., 'Biomass to Gasoline' in 'Pyrolysis Oils from Biomass – Producing, Analysing and Upgrading' Eds. Soltes, E.J., and Milne, T.A., American Chemical Society Symposium Series No. 376, Washington, DC (1988#2). Pp. 264-276

Diebold, J., Phillips, Tyndall, D., Scahill, J., Feik, C. and Czernik, S., 'Catalytic Upgrading of Biocrude Oil Vapours to Produce Hydrocarbons for Oil Refinery Applications'. In 'Proceedings of 208th National Meeting of American Chemical Society: Div. Fuel Chem'. Vol. 39, No.4, Pp. 1043-1047, 1994

Diebold, J., Phillips, Czernik, S., Scahill, J., Phillips, S., Feik, C. and 'Hot Gas Filtration to Remove Char from Pyrolysis Vapours Produced in a Vortex Reactor at NRE'. Presented at 'Specialist Workshop on Biomass Properties and Combustion', Estes Park, Colorado, September 26 - 28, 1994#2

Diebold, J.P., Milne, T.A., Czernik, S., Oasmaa, A., Bridgwater, A.V., Cuevas, A., Gust, S., Huffman, D., Piskorz, J., 'Proposed Specifications for Various Grades of Pyrolysis Liquid', in 'Developments in Thermochemical Biomass conversion', Eds. Bridgwater, A.V. and Boocock, D.G.B., Vol. 1, 1997#1, Chapman and Hall, Pp 433-447

Diebold, J.P., Bridgwater, A.V. 'Overview of Fast Pyrolysis of Biomass for the Production of Liquid Fuels' in 'Developments in Thermochemical Biomass Conversion' Eds. Bridgwater, A.V. and Boocock, D,G,B, Vol. 1. Pp 5-26 (Blackie, 1997#2)

Diebold, J.P., Czernik, S. 'Additives to Lower and Stabilise the Viscosity of Pyrolysis Oils During Storage' in 'Energy and Fuels' Vol. 11 No. 5 Pp 1081-1091 (American Chemical Society, 1997#3)

Donnot, A., Magne, P., Deglise, X. 'Kinetic Parameter of the Cracking Reaction of Tar from Wood Pyrolysis; Comparison of Dolomite with Industrial Catalysts' in 'Journal of Analytical and Applied Pyrolysis', 22 Pp. 47-59 (1991)

Donnot, A., Magne, P., Deglise, X. 'Method of Determining Catalyst Lifetime in the Cracking Reaction of Tar from Wood Pyrolysis' in 'Journal of Analytical and Applied Pyrolysis', 22 Pp. 39-46 (1991#2)

E

Elamin, A., Rezzoug, S., Capart, R., Gelus, M., 'Catalytic Hydrotreatment of Wood Solvolysis Oil', in Advances in Thermochemical Biomass Conversion' Ed. Bridgwater, A.V. Pp 1415-1423 (Blackie, 1994)

Elliott, D.C., Baker, E.G., 'Hydrotreating Biomass Liquids to Produce Hydrocarbon Fuels' in 'Energy from Biomass and Wastes X', Ed. Klass, D. Pp 765-784 (IGT Chicago, 1987)

Elliott, D.C., 'Upgrading Liquid Products: Notes from the Workshop at the International Conference 'Research in Thermal Biomass Conversion' in 'Research in Thermal Biomass Conversion' Elsevier Applied Science: New York (1988), Eds. Bridgwater, A.V., Kuester, J.L., Pp. 1170

Evans, R.J., Milne, T. 'Molecular- Beam, Mass-Spectrometric Studies of Wood Vapour and Model Compounds over an HZSM-5 Catalyst' in 'Pyrolysis Oils from Biomass – Producing, Analysing and Upgrading' Eds. Soltes, E.J., and Milne, T.A., American Chemical Society Symposium Series No. 376, Washington, DC (1988). Pp. 311-327

F

Faix, O., Meier, D., Grobe, I., 'Studies on Isolated Lignins and Lignins in Woody Materials by Pyrolysis Gas Chromatography Mass Spectrometry and Off-Line Pyrolysis Gas Chromatography with Flame Ionisation Detection' Journal of Analysis and Applied Pyrolysis, 11, (1987), Pp. 403-416

Fischer Catalogue, The. From 'Fischer Scientific UK Ltd', Bishop Meadow Road, Loughborough, Leics, LE11 5RG, (1997)

G

Gevert, B.S., Otterstedt, J-E., 'Upgrading of Liquified Biomass To Transportation Fuels by Extraction' in 'Energy from Biomass and Wastes X', Ed. Klass, D. Pp 845-854 (IGT Chicago, 1987)

Gevert, B.S., 'Hydroprocessing of Oil from Biomass Liquifaction', in Advances in Thermochemical Biomass Conversion' Ed. Bridgwater, A.V. Pp 1424-1431 (Blackie, 1994)

Goldstein, S.I., 'Organic Chemicals from Biomass', CRC Press Inc., Boca Raton, Florida, 1981)

Goss, I.G., Smith, P.J., Wilson, R.C.L. (Eds.) 'Understanding the Earth. A Reader in the Earth Sciences'. 2nd Edition. The Open University Press, 1972.

Grace, W.R. & Co., 'Grace Davison Guide to Fluid Catalytic Cracking' Part Two. 1996 Grace GMBH, In der Hollerhecke 1, D-67547, WORMS. DE.

Graham, R.G., Bergougnou, M.A. and Overend, R.P., 'Fast Pyrolysis of Biomass', in 'Journal of Analytical and Applied Pyrolysis', vol. 6, Pp. 95-135, (Elsevier, 1984) (primary and secondary reactions typically in fast pyrolysis, how reactions happen)

Grassi , G., Bridgwater, A.V., 'Biomass for Energy and Environment, Agriculture and Industry in Europe', (EC EUR 14683 1992)

Güell, A.J., Li, C-Z., Herod, A.A., Stokes, B.J., Hancock, P., Kandiyoti, R., 'Mild Hydropyrolysis of Biomass Materials: Effect of Pressure on Product Tar Structures', in 'Advances in Thermochemical Biomass Conversion'. Ed. Bridgwater, A.V., 1053-1067 (Blackie, 1994)

H

Hague, R.A., Bridgwater, A.V., 'Investigation into the Stability of Fast Pyrolysis Liquid - Effect of Time and Temperature' in Meier, D. *et al*, 'Catalytic Pyrolysis of Biomass For Improved Liquid Fuel Quality', European Commission Contract Number JOR CT95-0081, 1998

Hague, R.A. 'The Pre-Treatment and Pyrolysis of Biomass for the Production of Liquids for Fuels and Speciality Chemicals'. PhD Thesis, Aston University, Birmingham, UK. September 1998#2

Hague, R.A. and Bridgwater, A.V., 'Investigation into the Stability of Fast Pyrolysis Liquid - Effect of Time and Temperature' Unpublished Results, Aston University, 1998#3

Hanniff, M.I., Dao, L.H., 'Conversion of Biomass Carbohydrates into Hydrocarbon Products' in 'Energy from Biomass and Wastes X', Ed. Klass, D. Pp 831-844 (IGT Chicago, 1987)

Horne, P.A., Williams, P.T., 'Catalysis of Model Biomass Compounds Over Zeolite ZSM-5 Catalyst' in 'Proceedings of 7th European Conference on Biomass, 1992

Horne, P.A., Williams, P.T., 'Premium Quality Fuels and Chemicals from the Fluidised Bed Pyrolysis of Biomass with Zeolite Catalyst Upgrading' in 'Renewable Energy' Vol. 5, Part II. Pp 810-812. (Elsevier Science, 1994)

Horne, P.A., Williams, P.T., 'The Effect of Zeolite ZSM-5 Catalyst deactivation During the Upgrading of Biomass-Derived Pyrolytic Vapours' in 'Journal of Analytical and Applied Pyrolysis' (Elsevier Science, 1995)

Horne, P.A., Nugranad, N., Williams, P.T., 'Catalytic Co-Processing of Biomass-Derived Pyrolysis Vapours and Methanol' in 'Journal of Analytical and Applied Pyrolysis' (Elsevier Science, 1995#2)

Horne, P.A., Williams, P.T., 'Upgrading of Biomass-Derived Pyrolytic Vapours Over Zeolite ZSM-5 Catalyst: Effect of Catalytic Dilution on Product Yields' in 'Fuel' Vol. 75, No. 9. Pp 1043-1050 (Elsevier Science, 1996)

Horne, P.A., Williams, P.T., 'Reaction of Oxygenated Biomass Pyrolysis Model Compounds Over a ZSM-5 Catalyst' in 'Renewable Energy' Vol. 7, No.2, Pp 131-144. (Elsevier Science, 1996#2)

Howard, J.R., 'Fluidised Bed technology – Principles and Applications', (Adam Hilger, New York, 1989)

J

Jäger, M., Kohler, J., Deimling, S., 'Electronic Upgrading of Flash Pyrolysis Oil' in 'Biomass for Energy and Industry', Proceedings of the International Conference Würzburg, 1998

Johnson, D.K., Chum, H.L., 'Pyrolysis Oils from Biomass – Producing, Analysing and Upgrading' Eds. Soltes, E.J., and Milne, T.A., American Chemical Society Symposium Series, Washington, DC (1988).

K

Kaiser, M., 'Upgrading of Fast Pyrolysis Liquids' in 'Biomass Gasification and Pyrolysis – State of the Art and Future Prospects', Eds. Kaltschmitt, M. and Bridgwater, A.V. Pp. 399-406 (CPL Press, 1997)

Katikaneni, S.P.R., Idem, R.O., Bakhshi, N.N., 'Catalytic Conversion of a Biomass-derived Oil Using Various Catalysts' in 'Biomass Gasification and Pyrolysis – State of the Art and Future Prospects', Eds. Kaltschmitt, M. and Bridgwater, A.V. Pp. 411-421 (CPL Press, 1997)

Kunii, D., Levenspiel, O., 'Fluidisation Engineering'. Butterworth-Heinemann, Stoneham, (1991).

L

Lahousse, C., Maggi, R., Delmon, B., 'Characteristics of a HZSM-5 Catalyst used in Bio-Oil Upgrading' in 'Biomass for Energy and Industry', Proceedings of the International Conference Würzburg, Germany 8-11 June 1998. Pp 1654-1657

Laurent, E., Pierret, C., Grange, P., Delmon, B., 'Control of the Deoxygenation of Pyrolytic Oils by Hydrotreatment', in 'Biomass for Energy, Industry and Environment, 6th EC Conference'. Eds. Grassi, G., Collina, A. and Zibetta, H., Elsevier 1992, Pp 665 – 671

Laurent, E., Grange, P., Delmon, B., 'Hydrodeoxygenation of Model Oxygenated Compounds: Simulation of the Hydro-purification of Bio-oils', in 'Advances in Thermochemical Biomass Conversion'. Ed. Bridgwater, A.V., 1403-1414 (Blackie, 1994#1)

Laurent, E., Grange, P., Delmon, B., 'Study of the Hydrodeoxygenation of Carbonyl, Carboxylic and Guaiacyl Groups over Sulphided CoMo/γ-Al_2O_3 and NiMo/γ-Al_2O_3 Catalysts. I: Catalytic Reaction Schemes' in 'Applied Catalyst A' No. 109 Pp 77-96 (Elsevier Science, 1994#2)

Leech, J., 'Running a Duel Fuel Diesel Engine on Crude Pyrolysis Oil', in 'Biomass Gasification and Pyrolysis – State of the Art and Future Prospects', Eds. Kaltschmitt, M. and Bridgwater, A.V. Pp. 495-497 (CPL Press, 1997)

Leppämäki, E.A., Kuoppala, E.T., Krause, A.O.I., Nokkosmaki, 'New Rapid Method to Pre-screen Catalyst for Pyrolysis Oil's Vapour Phase Upgrading', in 'Biomass Gasification and Pyrolysis – State of the Art and Future Prospects', Eds. Kaltschmitt, M. and Bridgwater, A.V. Pp. 407-410 (CPL Press, 1997)

Longley, C.J., Fung, D.P.C., 'Potential Applications and Markets for Biomass-Derived Levoglucosan', in 'Advances in Thermochemical Biomass Conversion'. Ed. Bridgwater, A.V., Pp. 1484-1494 (Blackie, 1994)

M

Maggi, R.E. and Elliott, D.C., 'Upgrading Overview', in 'Developments in Thermochemical Biomass Conversion, Vol. 1', Eds. Bridgwater, A.V. and Boocock, D.G.B. Pp. 575-588 (Blackie, 1997)

Marquevich, M., Montane, D., Wang, D., Czernik, S., Chornet, E., 'Production of Hydrogen by Catalytic Steam Reforming of Residual Streams from Biomass Conversion Processes' in 'Biomass for Energy and Industry', Proceedings of the International Conference Würzburg, 1998

Marshall, A.J., 'Catalytic Conversion of Pyrolysis Oil in the Vapour Phase' , Masters of Applied Science Thesis, the University of Waterloo, Canada. (1984)

McMurry, J., 'Organic Chemistry' Third Edition Pp. 88 (Brooks/Cole Publishing Company, 1992)

McMurry, J., 'Organic Chemistry' Third Edition Pp. 50 - 59 (Brooks/Cole Publishing Company, 1992#2)

McWhinnie, W., 'Pillared Clays' in Joule Contract 0081 Contractors Workshop 12-14 February 1997, Solihull, UK, Record of Meeting

Meier, D. in Minutes of Meeting of JOR3-CT95-0081, Thesaloniki, November, 21-22, 1996

Meier, D. 'Analysis and Characteristics of Bio-Oil' in Joule Contract 0081 Contractors Workshop 12-14 February 1997, Solihull, UK, Record of Meeting

Meier, D., Oasmaa, A. and Peacocke, G.V.C., 'Properties of Fast Pyrolysis Liquids: Status of Test Methods', in 'Developments in Thermochemical Biomass Conversion', Eds: Bridgwater, A.V. and Boocock, D.G.V., Pp. 391-408, (Blackie, 1997#2)

Meier, D., Faix, O., 'Production and Analysis of Oils Obtained by Catalytic Hydroliquifaction of Wood', in 'Research in Thermal Biomass Conversion' Eds.

Bridgwater, A.V., Kuester, J.L. Pp 804-815 (Elsevier Applied Science: New York, 1988#1)

Meier, D. *et al*, 'Catalytic Pyrolysis of Biomass For Improved Liquid Fuel Quality', European Commission Contract Number JOR CT95-0081, 1998#2

Milne, T.A., Evans, R.J., Filley, J., 'Molecular Beam Spectrometric Study of HZSM-5 Activity During Wood Pyrolytic Products Conversion' in Research in Thermochemical Biomass Conversion, Eds. Bridgwater, A.V. and Kuester, J.L. Pp. 910-926 (Elsevier, 1988)

Milne, T.A., Agblevor, F., Davis, M., Deutch, S. and Johnson, D., 'A Review of the Chemical Composition of Fast Pyrolysis Oils from Biomass', in 'Developments in Thermochemical Biomass Conversion', Eds: Bridgwater, A.V. and Boocock, D.G.V., Pp. 409-424, (Blackie, 1997)

Morrison, D.E., 'The Use of Pillared Clays in the Catalysis of Biomass' MSc Thesis, University of Aston in Birmingham, UK. March 1995

O

Oasmaa, A., Sipila, K. 'Pyrolysis Oil Properties: Use of Pyrolysis Oil as Fuel in Medium-Speed Diesel Engines' in 'Bio-oil Production and Utilisation' Eds. Bridgewater, A.V. and Hogan, E.N. (CPL Press, 1996)

P

Peacocke, G.V.C., 'Ablative Pyrolysis of Biomass', PhD Thesis, University of Aston in Birmingham, UK. October 1994

Perry, R.J., Green, D. 'Perry's Chemical Engineering Handbook'. Pp. 9_8. McGraw International Press, 1984 #1

Perry, R.J., Green, D. 'Perry's Chemical Engineering Handbook'. Pp. 9_13. McGraw International Press, 1984 #2

Perry, R.J., Green, D. 'Perry's Chemical Engineering Handbook'. Pp. 3_78. McGraw International Press, 1984 #3

Perry, R.J., Green, D. 'Perry's Chemical Engineering Handbook'. Pp. 23_52. McGraw International Press, 1984 #4

Perry, R.J., Green, D. 'Perry's Chemical Engineering Handbook'. Pp. 3_247. McGraw International Press, 1984 #5

Pinnavaia, T.J., Tozou, M-S., Landau, S.D., Journal of the American Chemical Society, 1985, 107, Pp. 4783-4785

PSL Calibration Laboratory Certification, 1998 in accordance with ISO3104, ISO3105, BS188, IP Method 71 and ASTM Method D445

R

Radlein, D., Piskorz ,J., 'Production of Chemicals from Bio-Oil' in 'Biomass Gasification and Pyrolysis – State of the Art and Future Prospects'. Eds. Kaltschmitt, M. and Bridgwater, A.V. CPL Press (1997), Pp. 471-481.

Ratcliff, M.A., Johnson, D.K., Posey, F.L., Maholland, M.A., Cowley, S.W., Chum, H.L., 'Hydrode0oxygenation of a Lignin Model Compound', in 'Research in Thermal Biomass Conversion' Eds. Bridgwater, A.V., Kuester, J.L. Pp 941-955 (Elsevier Applied Science: New York, 1988)

Rejal, B., Evans, R.J., Milne, T.A., Diebold, J.P., Scahill, J., 'The Conversion of Biobased Feedstocks to Liquid Fuels Through Pyrolysis', in 'Energy from Biomass and Wastes XV' Ed. Klass, D.L. Pp 855-876 (IGT, 1992)

Renaud, M., Grandmaison, J.L., Roy, C. and Kaliaguine, S., 'Low Pressure Upgrading of Vacuum Pyrolysis Oils from Wood', in 'Pyrolysis Oils from Biomass: Producing, Analysing, and Upgrading', Eds. Soltes, E.J., Milne, T.A. (American Chemical Society Symposium Series, no. 376, pp. 290-310, 1988)

Richards, G.N., 'Chemistry of Polysaccharides and Lignocellulosics', in 'Advances in Thermochemical Biomass Conversion', Ed: Bridgwater, A.V., Pp. 727-745, (Blackie Academic and Professional, 1994)

Roberts, I., 'Error Analysis of Yield Calculations and Other Quality Assessments Following Experimental Non-Catalytic 100 g/h Fast Pyrolysis' Third Year MEng Project, Aston University, UK, 1999

Rogers, G.F.C., Mayhew, Y.R., 'Thermodynamic and Transport Properties of Fluids, SI Units'. Fourth Edition, Blackwell Publishers, 1988

Robinson, N., 'Physical Property Characteristics of Fast Pyrolysis Liquids', Internal Report, Energy Research Group, Aston University, 1996

Rupp, M., 'Utilisation of Pyrolysis Liquids in Refineries' in Bridgwater, A.V. and Grassi, G., 'Biomass Pyrolysis Liquids Upgrading and Utilisation' (Elsevier Applied Science 1991) Pp 219-226

S

Salt, L.E., Sinclair, R. (Eds) 'Oxford Encyclopaedia Volume VI, Farming and Fisheries' Oxford University Press, 1952

Samolada, M.C., Grigoriadou, E., Kiparissides, Z., Vasalos, I.A., 'Selective O-Alkylation of Phenol with Methanol over Sulphates Supported on γ–Al_2O_3' in 'Journal of Catalysis' No. 152. Pp 52-62, (Academic Press, 1995)

Scahill, J., Diebold, J., 'Engineering Aspects of Upgrading Pyrolysis Oil Using Zeolites' in Research in 'Thermochemical Biomass Conversion' Eds. Bridgwater, A.V., Kuester, J.L., Elsevier Applied Science: New York (1988), Pp. 927-940

Schoonheydt, R.A., Van Den Eynde, J., Tubbax, H., Leeman, H., Stuyckens, M., Lenotte, I., Stone, W.E.E., 'The Al Pillaring of Clays. Part 1. Pillaring With Dilute and Concentrated Al Solutions' in 'Clays and Clay Minerals' 1993, Vol. 41 No. 5. Pp. 598-607

Scott, D.S. and Piskorz, J., 'Flash Pyrolysis of Wood in a Fluidised Bed', in Proceedings of American Chemical Society Symposium 'Fuels from Biomass', Chapter 23, Ed: Klass, D., Pp. 421-434, (Ann Arbor Science Publishers, 1981)

Scott, D.S. and Piskorz, J., 'Continuous Flash Pyrolysis of Wood for Production of Liquid Fuels', in Canadian Journal of Chemical. Engineering, vol. 62, Pp. 404-412, 1984

Scott, D.S., Piskorz, J., Radlein, Majerski, P. 'Process for the Thermal Conversion of Biomass to Liquids', US Patent 5605551, 1987

Sharma, R.K., Bakhshi, N.N., 'Catalytic Upgrading of Biomass-Derived Oils to Transportation Fuels and Chemicals' in Canadian Journal of Chemical Engineering. Vol 69, October 1991 Pp. 1071-1081

Sharma, R.K. and Bakshi, N.N., 'Upgrading of Wood Derived Bio-Oil Over HZSM-5 Catalyst Using Various Diluents', Biosource Technol. 35, 57-66, (1991#2)

Sinnott, R.K., 'Coulson and Richardson's Chemical Engineering Volume 6 (Design)' 2nd Edition. Pergamon Press 1993. Pp.403

Solantausta, Y., Sipila, K., 'Pyrolysis in Finland', in 'Biomass Pyrolysis Liquids Upgrading and Utilisation', Eds. Bridgwater, A.V. and Grassi, G. Pp 327-340 (Elsevier Applied Science, 1991)

Solantausta, Y. and Oasmaa, A., 'Utilisation of Biomass Pyrolysis Oil in Power Production', in 'Energy from Biomass: Progress in Thermochemical Conversion', Proceedings of EC Contractor's Meeting, 7 Oct 92, Florence, Italy, Pp. 137-141, ECSC-EEC-EAEC, 1994

Stocker, M., 'Recently Developed Meso-Porous Catalysts' in Joule Contract 0081 Contractors Workshop 12-14 February 1997, Solihull, UK, Record of Meeting

Stradal, J.A., Underwood, G.L., 'Process for Producing Hydroxyacetaldehyde', United States Patent No. 5,393,542, 1996

Stroud, K.A., 'Engineering Mathematics', Third Edition, 1987, Macmillan Education, Pp. 835

T

Theander, O. 'Cellulose, Hemicellulose and Extractives', in 'Fundamentals of Thermochemical Biomass Conversion', Eds: Overend, R.P., Milne, T.A. and Mudge, L.K., Pp. 35-60, (Elsevier Applied Science, 1985)

Tiplady, I.R., Peacocke, G.V.C., Bridgwater, A.V., 'Physical Properties of Fast Pyrolysis Liquids from the Union Fenosa Pilot Plant', Aston University, 1996, unpublished

Toft, A.J. 'A Comparison of Integrated Biomass to Electricity Systems'. PhD Thesis, University of Aston in Birmingham, UK. October 1996

V

Vassilatos, V., 'Thermal and Catalytic Cracking of Tar in Biomass Pyrolysis Gas', Masters Thesis, Department of Chemical Technology, Royal Institute of Technology, Stockholm, 1990

Vassilatos, V., Taralas, G., Stöström, K., Björnbom, E., 'Catalytic Cracking of Tar in Biomass Pyrolysis Gas in the Presence of Calcined Dolomite' in 'Canadian Journal of Chemical Engineering', Vol. 70, 1008-1013, 1992

Venderbosch, R.H., Janse, A.M.C., Radovanovic, M., Prins, W., Van Swaaij, W.P.M., 'Pyrolysis of Pine Wood in a Small Integrated Pilot Plant Rotating Cone Reactor' in 'Biomass Gasification and Pyrolysis – State of the Art and Future Prospects'. Eds. Kaltschmitt, M. and Bridgwater, A.V. Pp. 345-353 (CPL Press, 1997)

W

Weekes, A.L., Salter, E.H., Bridgwater, A.V., 'The Addition of Chemical Modifiers to Improve the Stability of Pyrolysis Liquids' in Meier, D. *et al*, 'Catalytic Pyrolysis of Biomass For Improved Liquid Fuel Quality', European Commission Contract Number JOR CT95-0081, 1998

Williams, P.T., Nugrand, N., Horne, P.A., 'Influence of Steam on the Formation of Polycyclic Aromatic Hydrocarbons in Zeolite Catalytic Upgrading of Biomass Pyrolysis Oils' in 'Biomass Gasification and Pyrolysis – State of the Art and Future Prospects'. Eds. Kaltschmitt, M. and Bridgwater, A.V. Pp. 422-430 (CPL Press, 1997)

Williams, P.T., Nugrand, N., 'Aromatic Hydrocarbons in the Catalytic Upgrading of Biomass Pyrolysis Oils in the presence of Steam', in 'Biomass for Energy and Industry', Proceedings of the International Conference Würzburg, Germany 8-11 June 1998. Pp 1589-1592

Wulzinger, P., Meier, D., in Meier, D. *et al*, 'Catalytic Pyrolysis of Biomass For Improved Liquid Fuel Quality', European Commission Contract Number JOR CT95-0081, 1998

Wulzinger, P., 'Catalytic Upgrading of Pyrolysis Liquids', PhD Thesis, Institute for Wood Chemistry, Hamburg, Germany, May 1999. (In German)

Wunder, B., 'Fluidisation Characteristics and Particle Entrainment of Multi-Solid Bubbling Beds Related to a Fast Pyrolysis Reactor', Final Thesis in Energy and Process Engineering at the Technical University, Berlin, 1999

Appendix A – Publications

The following is a list of publications that were produced during the course of this work.

'Aston University Research Review 1997/8 Chemical Engineering & Applied Chemistry'
'Catalytic Pyrolysis for Bio-Oil Quality Improvement', EH Salter and AV Bridgwater in 'Biomass for Energy and Industry', Proceedings of the International Conference Würzburg, Germany, 8th – 11th June 1998.

'Catalytic Fast Pyrolysis of Biomass' E H Salter, N M Robinson, G C Peacocke, D Ristorcelli, H Sheena and A V Bridgwater in IChemE Research Event Proceedings, 1998.

'Catalytic Pyrolysis for Improved Liquid Fuel Quality', EH Salter and AV Bridgwater in the European Commission Public Report, contract JOR CT95-0081in the framework of the Non Nuclear Energy Programme, Joule III, January 1999.

'Catalytic Pyrolysis for Improved Liquid Fuel Quality', EH Salter in 'Proceedings of the 4th Biomass Conference of the Americas', Oakland, California, USA, 29th August – 2nd September 1999.

Appendix B – Results Proforma

Aston Small Fluidised Bed Pyrolysis Reactor 1of 2

Date: / /	Feedstock:	Type	Size	Ratio
Run name:	Wood			
Temp aim:	Catalyst			

Cooling Water

Volume		Temp
Time		

Apparatus mass /g:	Before	After
Feeder + feed + tube		
Reactor top (+ wire)		
Reactor body		
Crucible + sand		
Crucible		
Reactor body + sand		
Char pot		
Transfer tube		
All together (+ wire)		

	Before	After
Condenser		
Oil pot		
2ry Condenser		
Oil pot 2		
EP		
Cotton filter (no springs)		
Condenser arm		

Sample jars	Before	After
a		
b		
c		

Ethanol washing	Empty	Full
Filter paper		
RotaVap flask (no lid)		

Feeder calibration	Time /min	Mass /g	Flow /g/h
Run 1			
Run 2			
Run 3			
Run 4			
Run 5			

Flow-rate settings	
Entraining nitrogen	
Feeder top	
Fluidising nitrogen	
Stirrer speed	
Entrain tube size	

Feed water content	Beaker	+ wood	1	2	3	4
1						
2						
3						

Water content measurements Date: / /

Oil dilutions	Oil sample /g	MeOH /g
Oil pot 1		
Oil pot 2		

Karl Fischer testing	Syringe Mass				
	Before /g	After /g	Difference /g	Water content	Units
Dilution methanol #1					
Dilution methanol #2					
Dilution methanol #3					
Dilution methanol #4					
Oil pot 1 #1					
Oil pot 1 #2					
Oil pot 1 #3					
Oil pot 1 #4					
Oil pot 2 #1					
Oil pot 2 #2					
Oil pot 2 #3					
Oil pot 2 #4					
Ethanol washings #1					
Ethanol washings #2					
Ethanol washings #3					
Ethanol to wash #1					
Ethanol to wash #2					
Ethanol to wash #3					
Ethanol to wash #4					

Aston Small Fluidised Bed Pyrolysis Reactor 2 of 2

Date: / /
Run name:

2ry Set T

Time /min	Reactor T	Furnace T	Set Pt T	Delta Pf	Delta Pf b	Gas meter vol	Gas T	2ry In T	2ry Out T
0									
1									
2									
3									
4									
5									
6									
7									
8									
9									
10									
11									
12									
13									
14									
15									
16									
17									
18									
19									
20									
25									
30									
35									
40									
45									
50									
55									
60									
61									
62									
63									
64									

Time of day at end

Run Comments:

Time of day at end

EP mA	
EP kV	

Viscosity measurements

Date				
Storage time				
Storage temp				
Temp of test				
Vicom no.				
Code no.				
Constant				
Time of day #1				
Test time #1				
Time of day #2				
Test time #2				
Time of day #3				
Test time #3				

Water bath obs

Weight in	
Weight out	
Ph in	
Ph out	

Appendix C – Excel Spreadsheets

Table 65 Mass Balance Spreadsheet, Mass Balance Tab 1 of 2

Aston Small Fluidised Bed Pyrolysis Reactor				EHS39	Fill in red, grey boxes appear atomatically.			
				22.06.93				
Feed	beech	150-500 micron						
Catalyst amount	0.00	%	Catalyst type	Y-zeolite cc in 1ry reactor				
Feed entrain tube	1.70	mm		10.0g				
Pre-run feed calibration			Assume-	i) temperature held constant between readings				
weight (g)	time (mins)	flow rate (g/h)		ii) gas meter readings move in equal steps				
Length of run /min	46.50	111.6		iii) same proportion of char in all liquids as				
				liquid remnant in condensers.				
Settings	Rotameter read	Total l						
Feed entrain (l/min)	1.5	69.8						
Feed top (l/min)	1.2	55.8						
Fluidising gas (l/min)	10.0	465.0						
Stirrer speed	1.25	590.6	total l of N2 in					
Sand (g)	125.50							
Moisture Content of feed (cat & wood combined)				dry wood basis	wet wood basis			
Moisture content	empty beaker	& wood	& dry wood	%moisture	%moisture			
I	29.427	30.944	30.822	8.746	8.042			
II	28.264	31.828	31.545	8.625	7.941			
III	29.634	31.741	31.568	8.945	8.211			
			Average	8.772	8.064			
Assumption	none							
		Assume: %water in wood catalyst mix can be aportioned to the wood and catalyst alike						
			Wet wood basis		Dry wood basis			
			IN	OUT	IN	OUT		
	before run	after run	difference	difference				
Wood and catalyst fed								
feeder+feed+tube	1007.2	913.1	94.10					
Wood fed (on a wet basis)			94.10		86.51		1.86	g/min
Catalyst fed (on air dry basis)			0.00		0.00			
Moisture in feed (cat&wood)			7.59		7.59		water	
Reactor weights - char produced (incl. sand and maybe catalyst)								
Reactor top+wire+mesh	681.0	680.5		0.00				
Reactor body	1749.6	1749.6		0.00		Any sand carried over is		
Cruicable+sand +cat	183.4	185.3		1.90		accounted for in the char pot		
Cruicable	57.9	57.8		-0.10				
Reactor body+sand+cat	1874.6	1876.1	128.60	1.50				
Char pot	136.7	145.2	sand ^	8.50				
Transfer tube	87.1	87.6		0.50				
Sand+cat	125.50	127.5		2.00				
		Total		11.00			11.00	char found in reactor
All together + wire	2778.1	2790.2		12.10				and catalyst
Glassware weights - liquids produced (incl. some char and catalyst)								
Condenser	119.1	121.5		2.47				
Oil pot	55.4	98.1		42.74				
Condenser 2	571.5	571.7		0.20				
Oil pot 2	23.4	33.1		9.73				
EP	770.2	774.1		3.90				
Cotton filter + wool	202.3	205.6		3.30	Assume: Micro char in oil is negligable			
Condenser arm	17.5	17.8		0.37	and all char is in filter paper.			
		Total		62.71			62.17	total liquid (oil&water) recovered
Sample jars	empty	full					3.23	*char/cat found in liquids (samples ar*
a	6.68	29.61	22.93 g				11.54	total char + catalyst (reactor and l
b	6.35	25.87	19.52 g				11.54	char alone
c (EP)	0.00	0.00	0.00 g					
d (OP2)	6.34	16.07	9.73 g					
		Total	52.18				44.85	total organic liquid
% of char in liquids collected							17.32	total water found in products
	empty	full					9.73	water produced by pyrolysis
Filter paper	2.290	2.832	0.54					
RotaVap flask	312.05	559.60	247.75					
Char free pyr liqs in flask			9.99	E58-D67-D64(Liquid in glassware)-(liquid in sample jars)-(char collected)				
Ethanol added			237.76	D68-D69				
% char/cat in pre filtered liqs			5.15	D67/(E58-D64)*100				

Table 66 Mass Balance Spreadsheet, Mass Balance Tab 2 of 2

EXPERIMENTAL									
Grey boxes will update automatically									
Gas losses due to blockages =		19	dm3	Feeder problems:	11.5min to 16 min				
Readings taken throughout run									
Time (mins)	Reactor (°C)	Furnace (°C)	Furnace SP (°	a P Feeder (" H2O)	? Fluid Bed (" H2O)	Gas (dm3)	EP Inlet (°C)		
0	455	455	460	25	23	819			
1.0	451	461	460	40	38	-			
2.0	452	464	462	41	37	-			
3.0	451	464	462	40	36	858			
4.0	452	463	463	39	34	574			
5.0	452	462	463	39	34	888			
6.0	451	460	462	37	34	902			
7.0	451	462	462	33	31	-			
8.0	451	462	462	34	30	929			
9.0	451	463	462	33	30	943			
10.0	451	464	462	33	29	956			
11.0	452	463	461	33	29	-			
12.0									
13.0									
14.0									
15.0									
16.0	469	465	461	34	29	994			
17.0	466	464	461	35	30	1008			
18 0	463	463	461	34	30	1021			
19.0	459	461	461	36	31	-			
20 0	456	461	461	35	30	1048			
21.0	453	461	461	36	31	-			
22.0	451	461	461	36	31	1075			
23.0	450	464	461	35	31	1089			
24.0	449	460	461	37	33	1102			
25.0	449	464	461	36	32	1116			
26.0	**449**	**464**	**461**	**36**	**32**	**1129**			
27.0	**449**	**464**	**461**	**36**	**32**	**1142**			
28.0	**449**	**464**	**461**	**36**	**32**	**1155**			
29.0	**449**	**464**	**461**	**36**	**32**	**1168**			
30.0	445	461	464	41	39	1184			
31.0	**445**	**461**	**464**	**41**	**39**	**1197**			
32.0	**445**	**461**	**464**	**41**	**39**	**1210**			
33 0	**445**	**461**	**464**	**41**	**39**	**1223**			
34.0	**445**	**461**	**464**	**41**	**39**	**1236**			
35.0	448	469	470	43	40	1253			
36.0	**448**	**469**	**470**	**43**	**40**	**1266**			
37.0	**448**	**469**	**470**	**43**	**40**	**1279**			
38.0	**448**	**469**	**470**	**43**	**40**	**1292**			
39.0	**448**	**469**	**470**	**43**	**40**	**1305**			
40.0	450	469	468	46	44	1322			
41.0	**450**	**469**	**468**	**46**	**44**	**1335**			
42.0	**450**	**469**	**468**	**46**	**44**	**1348**			
43.0	**450**	**469**	**468**	**46**	**44**	**1361**			
44 0	**450**	**469**	**468**	**46**	**44**	**1374**			
45.0	450	473	469	50	45	1390			
46.0	**450**	**473**	**469**	**50**	**45**	**1403**			
47.0	**450**	**473**	**469**	**50**	**45**	**1416**			
48.0	**450**	**473**	**469**	**50**	**45**	**1429**			
49.0	**450**	**473**	**469**	**50**	**45**	**1442**			
50.0	455	469	467	50	47	1458			
51.0	**460**	**467**	**467**	**50**	**47**	**1472**			
52.0	**0**	**0**	**0**	**0**	**0**	**0**			
53.0	**0**	**0**	**0**	**0**	**0**	**0**			
54 0	**0**	**0**	**0**	**0**	**0**	**0**			
55.0	0	0	0	0	0	0			
56.0	**0**	**0**	**0**	**0**	**0**	**0**			
57.0	**0**	**0**	**0**	**0**	**0**	**0**			
58.0	**0**	**0**	**0**	**0**	**0**	**0**			
59.0	**0**	**0**	**0**	**0**	**0**	**0**	Assume MWt of gas is 30		
60.0	**0**	**0**	**0**	**0**	**0**	0			
Average temps	**451.40**	**464.13**	**463.42**	**38.60**	**35.07**	**634.00**	dm3 total gas volume out		
	reactor	furnace	set point						
						The following is only comparative			

Table 67 Mass Balance Spreadsheet, Water Tab

Water Content Measurements									
Add red cells, add information, then unitalic them. Any italic cells, information has not yet been inputted.									
O		Oil sample for dilution (g)						Results	
M		Methanol used in dilution (g)				**OP1**		17.075	%
T		Total weight of prepared sample for injection (g)				**OP2**		63.606	%
Ow		Water content of oil (%)				**EW**		0.000	%
Mw		Water content of dilution methanol (%)				**OP1**		7.964	g
Tw		Total water content of mixture (%)				**OP2**		6.189	g
Ew		Water content of ethanol used for washings (%)				**EW**		0.000	g
						Total		14.153	g
	O/T = Ow/Tw								
	Ow =	**((Tw * T) - (Mw * M)) / O**							
Methanol	%		**Methanol 2**	%		If 3 rather than 4 samples are taken,			
1	0.04797		1	*0.09386*		enter 0 for the at position 4.			
2	0.05874		2	*0.09386*		This will not effect average.			
3	0.04376		3	*0.09386*					
4	0.05264		4	*0.09386*					
Mw =	**0.05078**		**Mw =**	**0.09386**					
Oil Pot +EP				%					
O	0.1812	g	1	0.685					
M	4.8390	g	2	0.691					
T	5.0202	g	3	0.665		In cell G27,check which methanol			
			4	0.620		refered to, B20 or E20			
			Tw	0.66525	**Ow =**	17.075	%		
Oil Pot 2				%		7.964	g		
O	0.2652	g	1	2.370		mass of water collected from OP1			
M	7.0726	g	2	2.327					
T	7.3378	g	3	2.319		In cell G33,check which methanol			
			4	2.375		refered to, B20 or E20			
			Tw	2.34775	**Ow =**	63.606	%		
						6.189	g		
						mass of water collected from OP2			
Ethanol					Only for use with 3 product system				
1	0.060	%			If use, amend cell D69 to include G34 and G40				
2	0.061	%							
3	0.049	%							
4	0.052	%							
Ew =	**0.056**								
	RO + E =	**O**	RO	Raw oil					
	ROw + Ew =	**Ow**	E	Ethanol					
	ROw =	**Ow - Ew**	O	Oil sample used for Karl Fisher					
			(in the case of the ethanol washings, this is pyrolysis liquids diluted in ethanol)						
Ethanol washings									
1	1.325		RO	9.99					
2	1.335		E	237.76					
3	1.330		O	247.75					
4	0.000								
Ow =	1.330	%							
ROw =	31.667	%							
	3.163	g							
mass of water still remaining on glassware walls after recovery									
Total water found in products			17.316	g	F66 = B63+B28+G34				
Total water produced during run			9.727	g	D67 = D66-'Mass Balance'!F36				
					'Mass Balance'!F36 = moisture in feed				

Table 68 Mass Balance Spreadsheet, Gas Tab

Gas Analysis - Put standards into the appropriate red or black sections below then fill in sample data below this.								
Gas analysis average will appear automatically								
		Sample1	Sample2	Sample3				
Gas (% in sample)	Average	t=25	t=35	t=45	Gas Density	Total Gas out g		
Methane	0.084	0.086	0.079	0.088	0.717	0.38		
Carbon dioxide	0.562	0.586	0.546	0.555	1.980	7.06		
Ethene	0.011	0.015	0.009	0.009	1.260	0.09		
Ethane	0.007	0.007	0.006	0.007	1.350	0.06		
Hydrogen	0.041	0.051	0.034	0.038	0.090	0.02		
Propene	0.017	0.030	0.007	0.015	1.920	0.21		
Propane	0.387	0.000	1.160	0.000	2.000	4.90		
Carbon monoxide	0.908	1.622	0.008	1.095	1.250	7.20		
n-Butane	0.000	0.000	0.000	0.000	2.700	0.00		
n-Butene	0.000	0.000	0.000	0.000		0.00		
Oxygen	*0.000*	0.000	0.000	0.000	*1.430*	0.00		
TOTAL						19.923		

Table 69 Mass Balance Spreadsheet, Summary Tab

Summary Sheet									
						Internal volume of reactor		326	m^3
run no.	EHS39		Reactor only res. time (s) =		0.46	Density of sand		2.6695	g/m^3
ave. r. temp	451.40		Total hot space res. time (s) =		0.55	Hot space volume		377.86	m^3
ave. f. temp	464.13								
% catalyst	0.00				F3= (reactor vol-sand vol)/(1000*reactor temp)*pressure				
					F3= (hot space vol-sand vol)/(1000*reactor temp)*pressure				
Products	Mass (g)	Yields (%)	Normalised (%)						
gas	19.92	23.03	23.15						
organics	44.85	51.85	52.13						
char	11.54	13.34	13.41						
water	9.73	11.24	11.30						
wood in	86.51	99.46	100.00						

Appendix D – Catalyst Screening Graphs and Tables

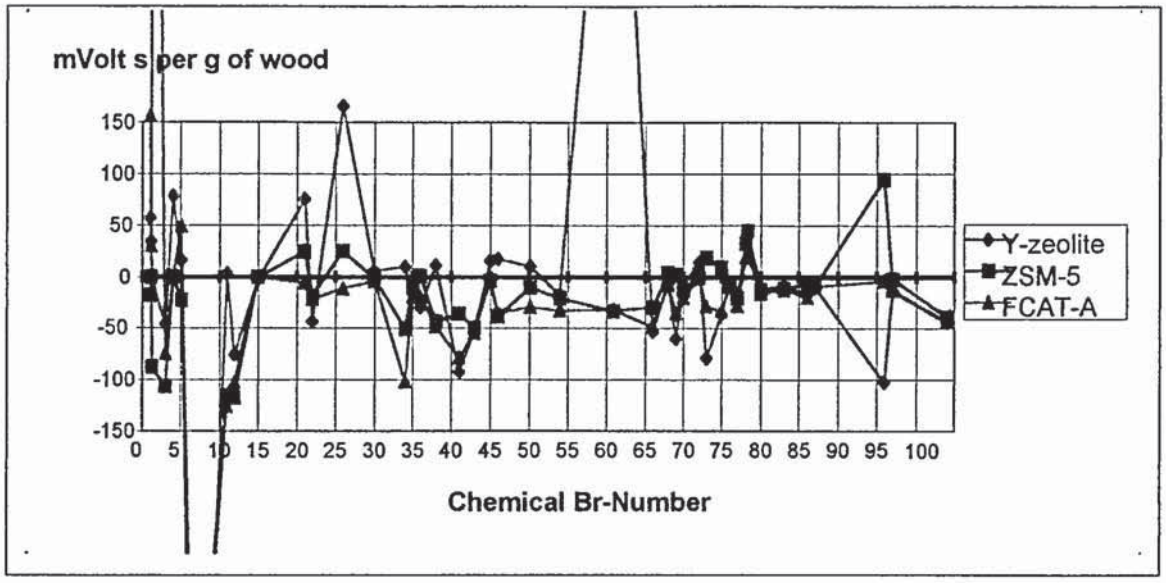

Figure 12 Chromatograph Peak Area Minus Blank, Zeolites 1 of 2

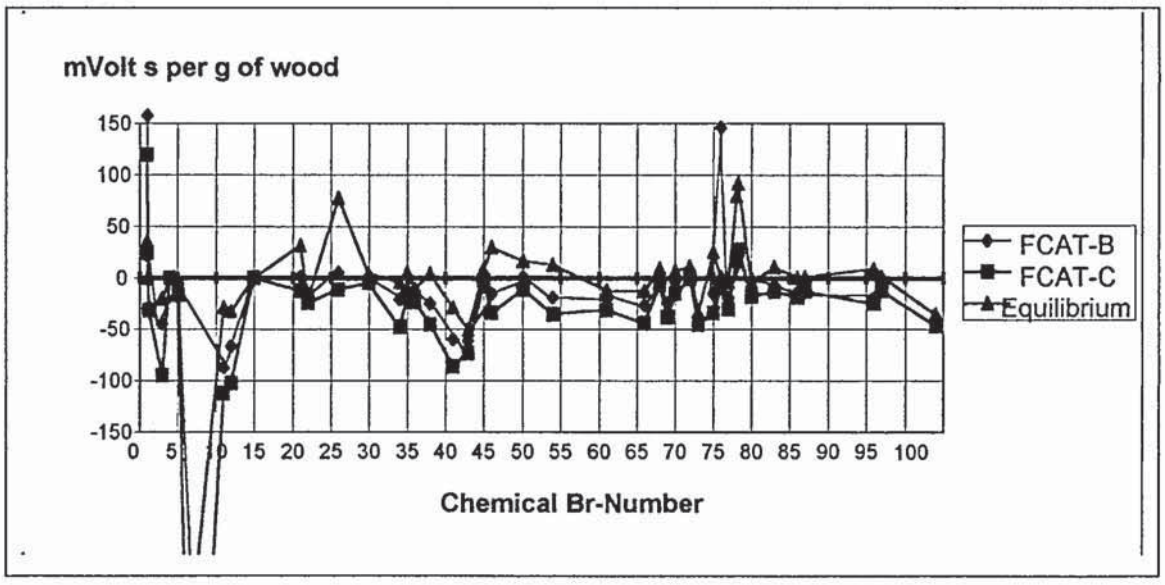

Figure 74 Chromatograph Peak Area Minus Blank, Zeolites 2 of 2

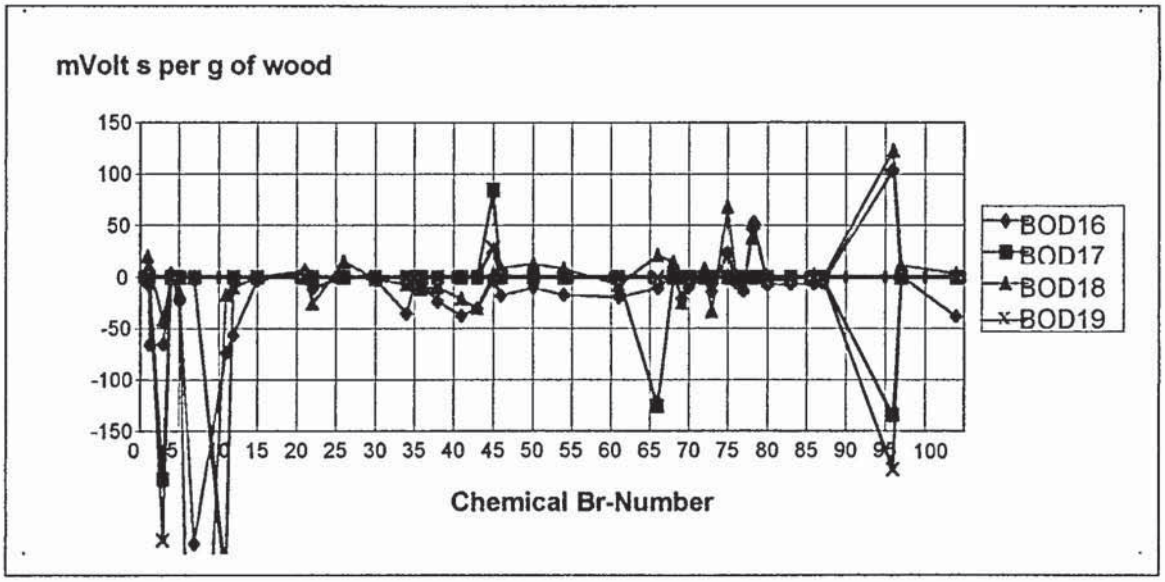

Figure 75 Chromatograph Peak Area Minus Blank, Clays 1 of 2

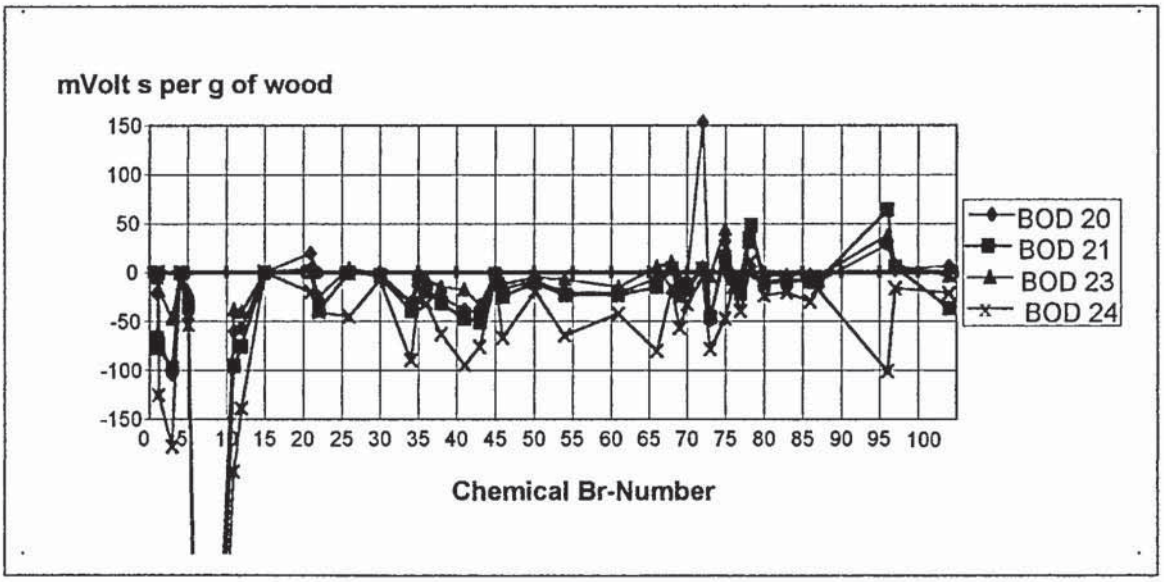

Figure 76 Chromatograph Peak Area Minus Blank, Clays 2 of 2

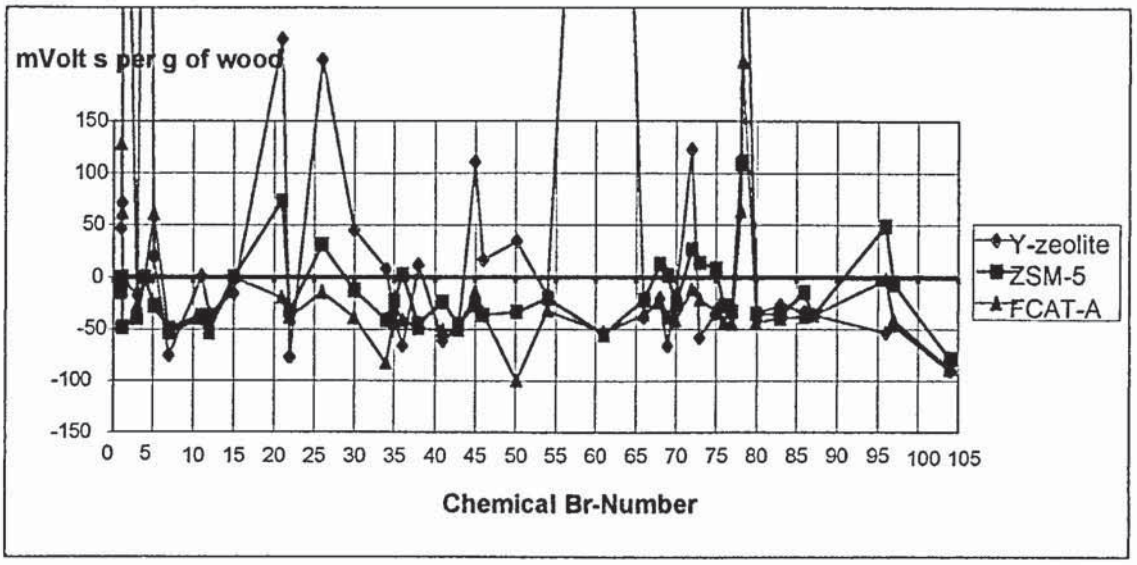

Figure 13 Chromatograph Peak Area Difference as % of Blank, Zeolites 1 of 2

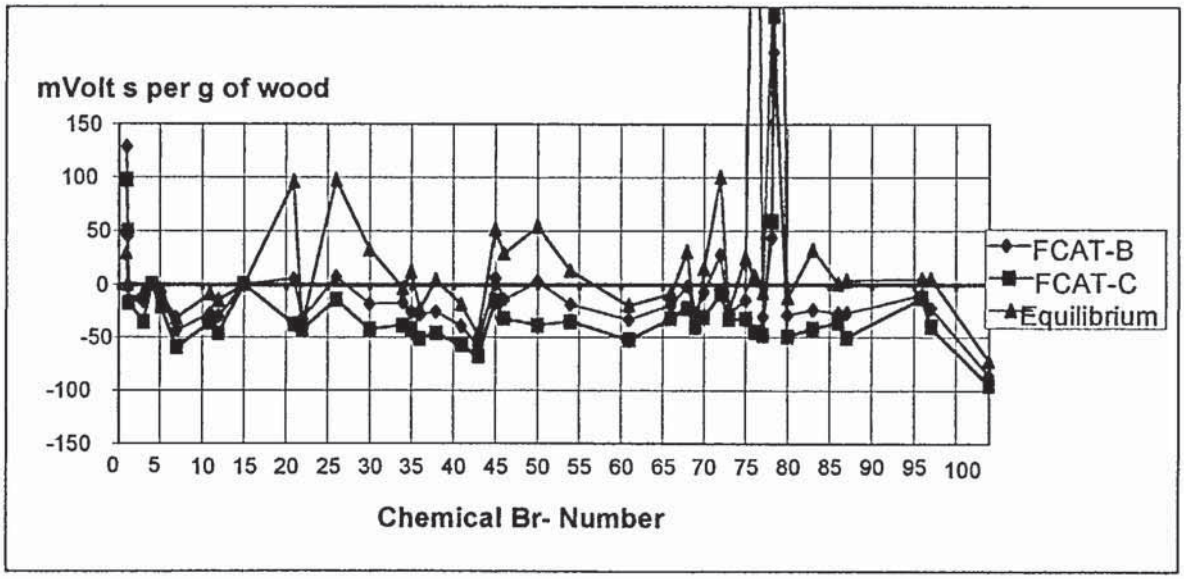

Figure 77 Chromatograph Peak Area Difference as % of Blank, Zeolites 2 of 2

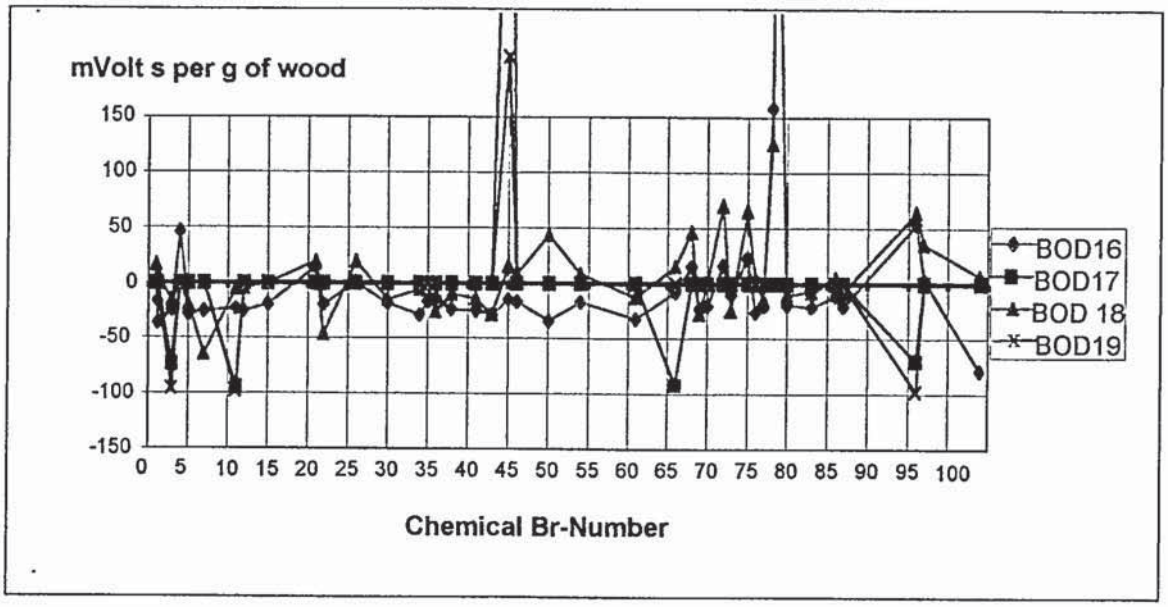

Figure 78 Chromatograph Peak Area Difference as % of Blank, Clays 1 of 2

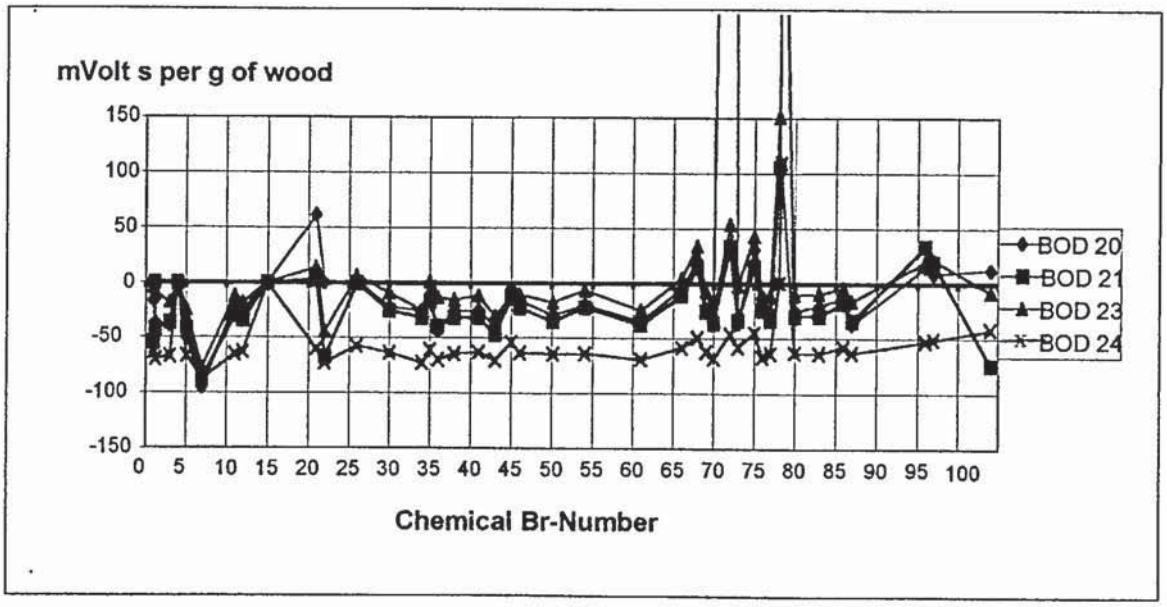

Figure 79 Chromatograph Peak Area Difference as % of Blank, Clays 2 of 2

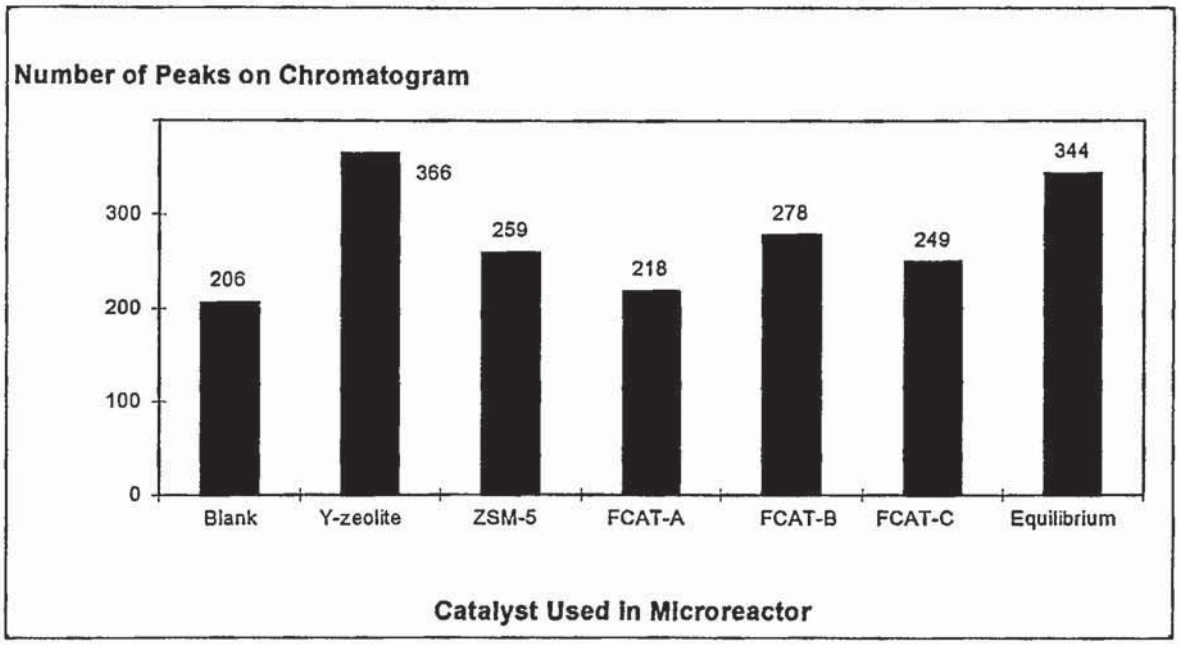

Figure 14 *Comparison of the Number of Peaks Resulting from Catalyst Addition to the Pyrolysis Micro-reactor, Zeolites*

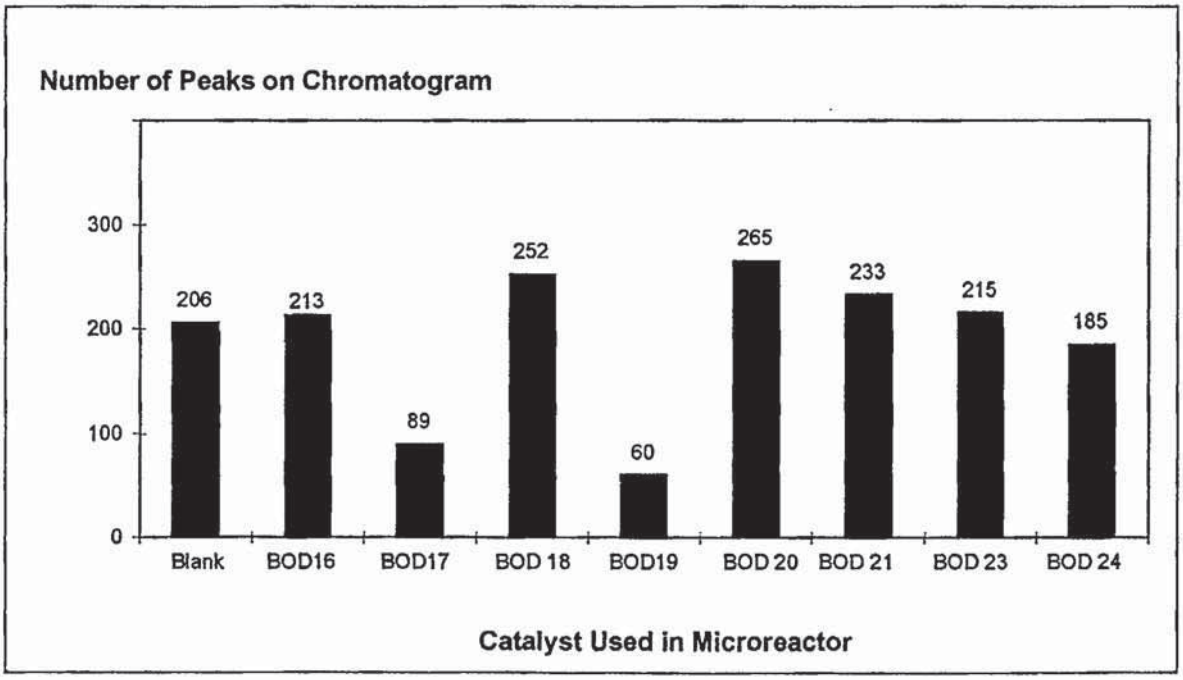

Figure 80 *Comparison of the Number of Peaks Resulting from Catalyst Addition to the Pyrolysis Micro-reactor, Clays*

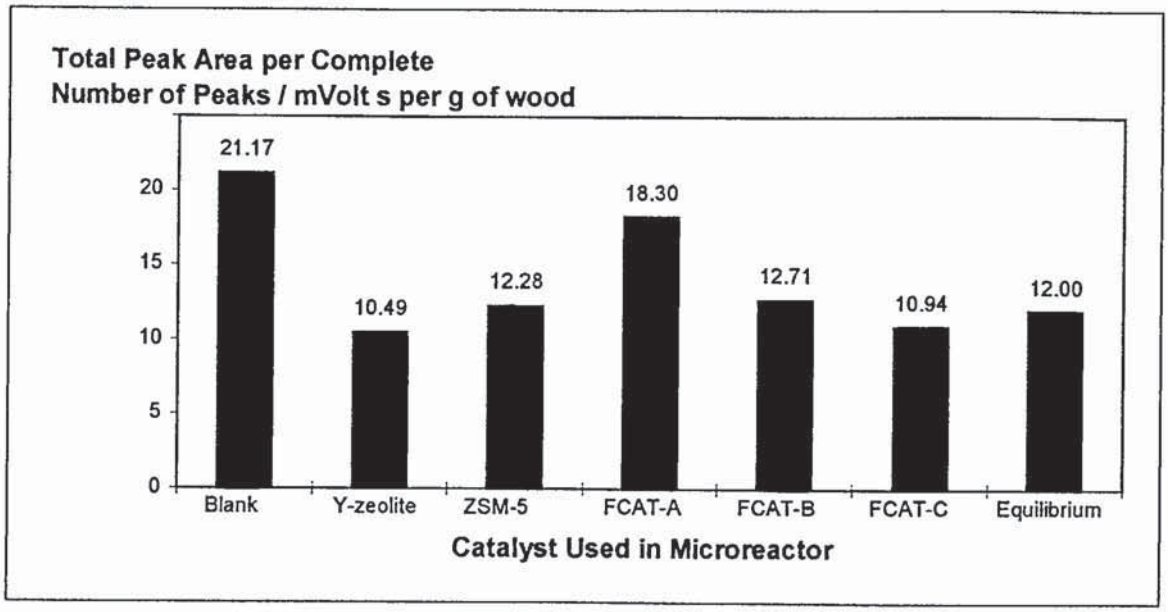

Figure 15 Average GC Peak Area, Zeolites

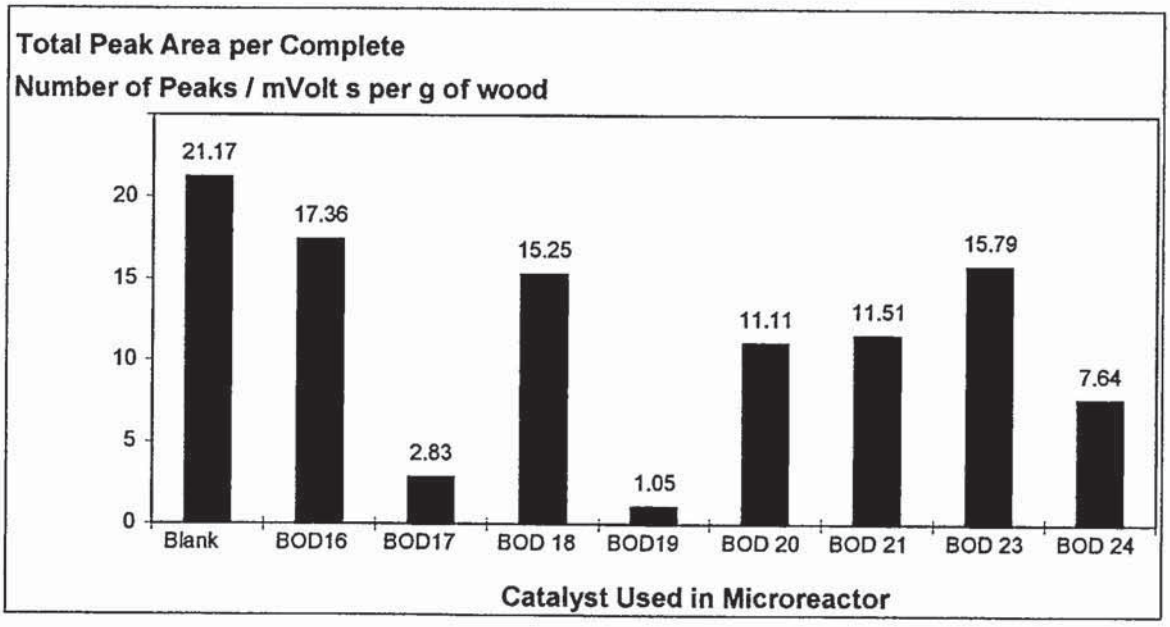

Figure 81 Average GC Peak Area, Clays

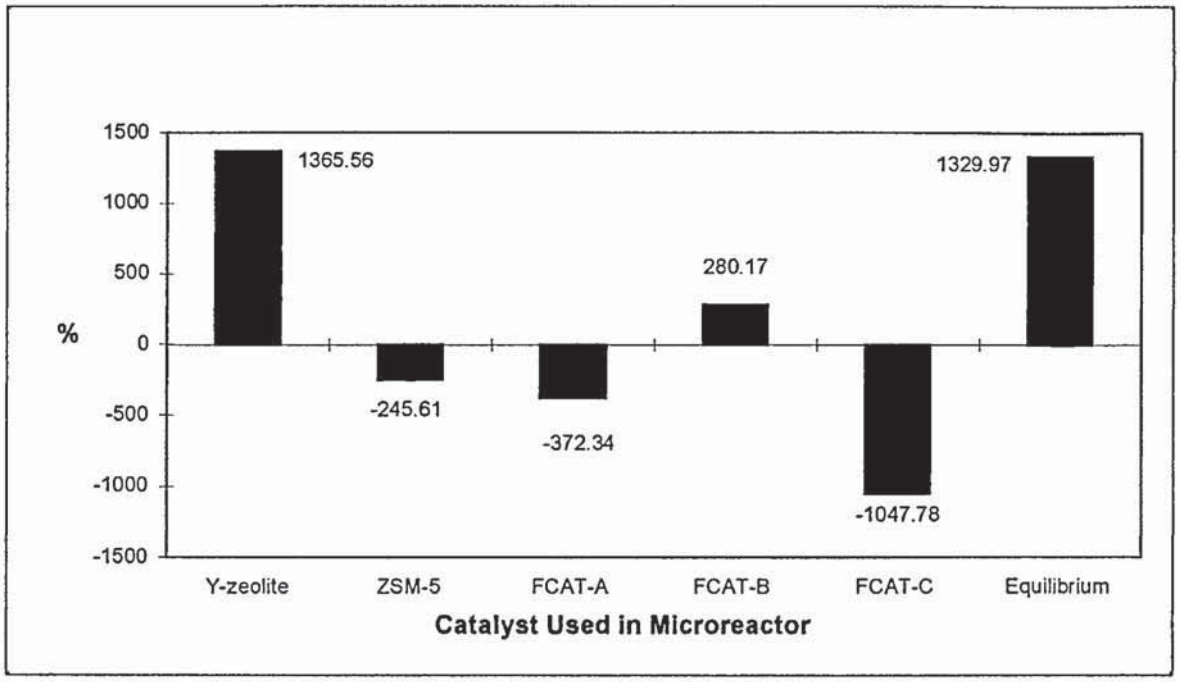

Figure 16 *Total Sum of Peak Area Difference as % of Blank area for Selected Chemicals, Zeolites*

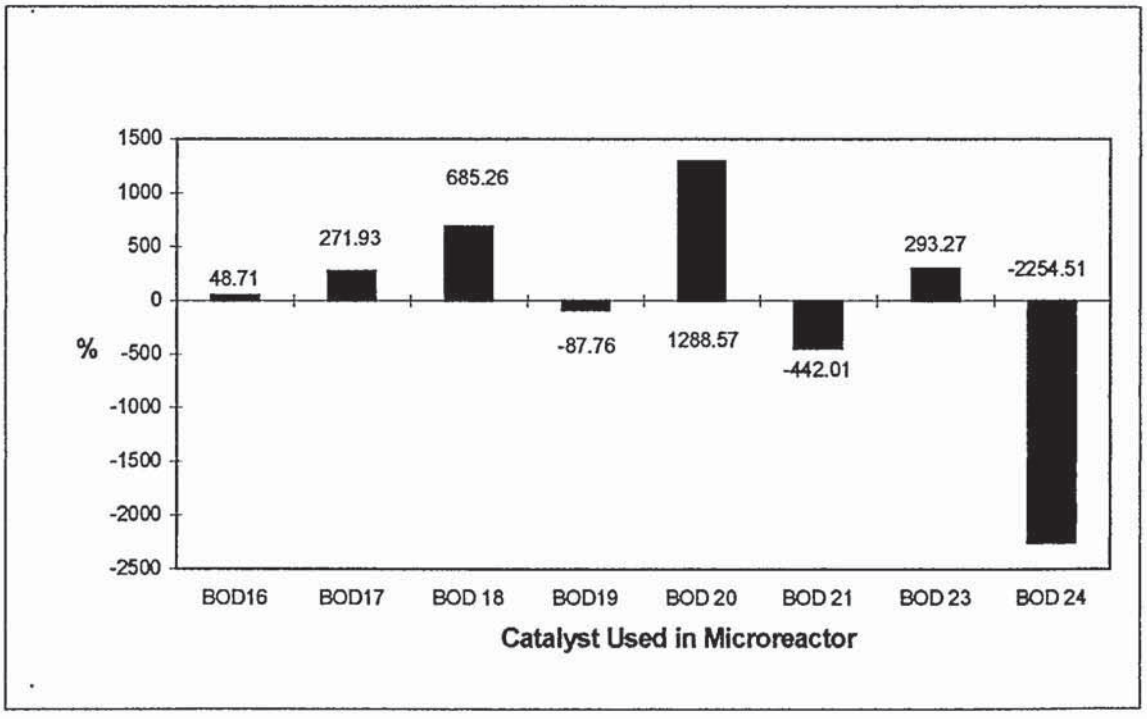

Figure 82 *Total Sum of Peak Area Difference as % of Blank area for Selected Chemicals, Clays*

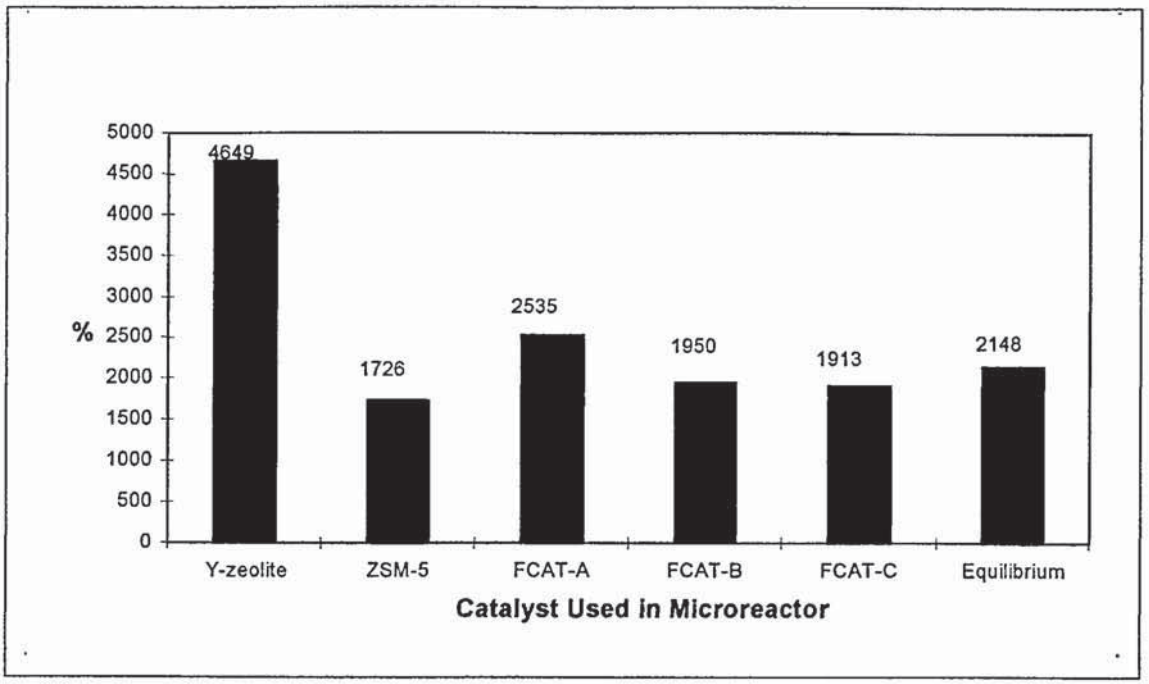

Figure 17 ***Sum of Peak Area Difference as % of Blank Peak Area for Selected Chemicals (Absolute Values), Zeolites***

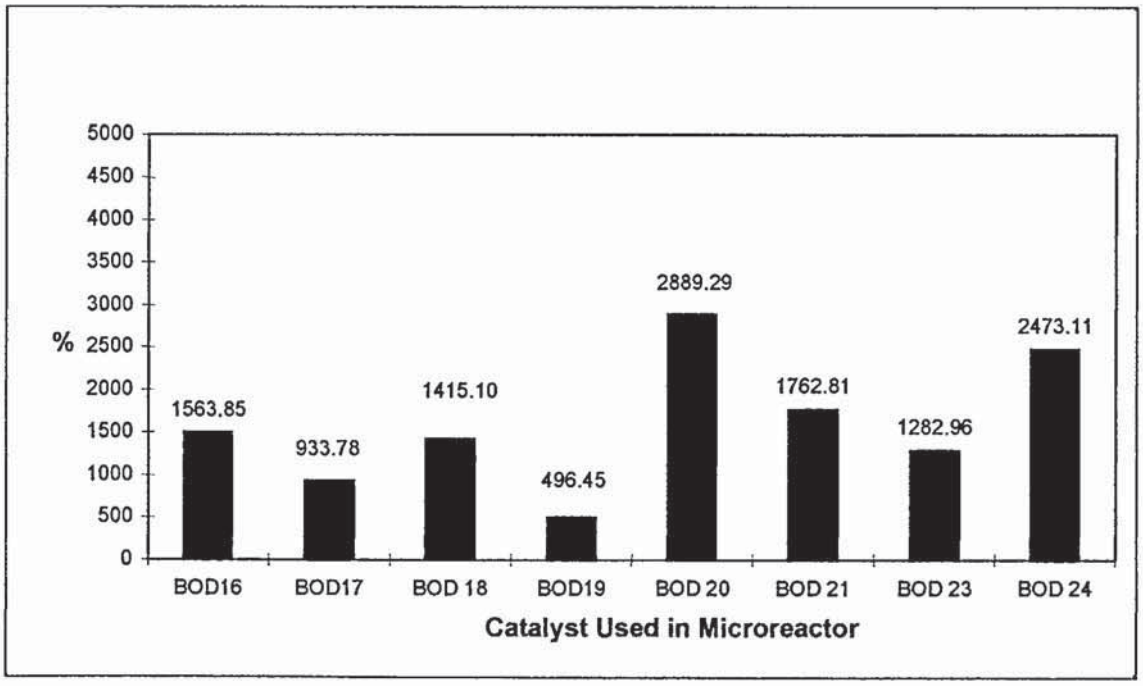

Figure 83 ***Sum of Peak Area Difference as % of Blank Peak Area for Selected Chemicals (Absolute Values), Clays***

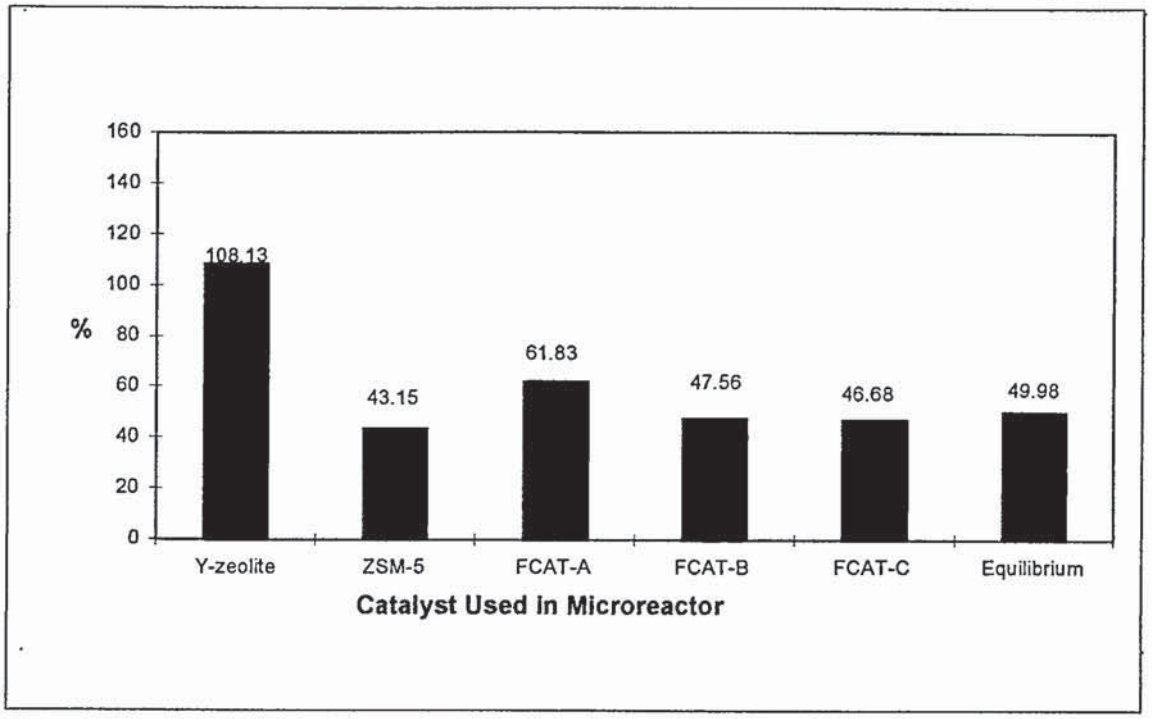

Figure 18 *Average Peak Area Difference as % of Blank Peak Area (Absolute Values), Zeolites*

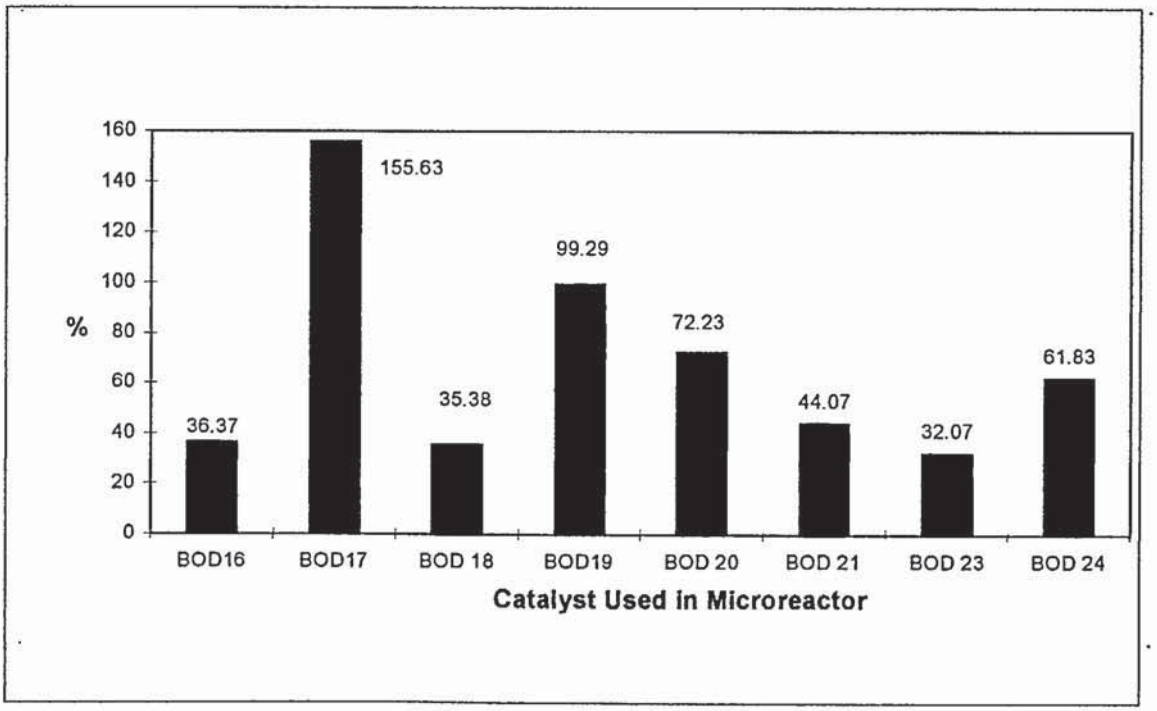

Figure 84 *Average Peak Area Difference as % of Blank Peak Area (Absolute Values), Clays*

Table 70 Identification of Detected Chemicals in Micro-reactor Screening

(Italics - Not used in analysis)

Br-Nr (see below)	Chemical Name c-Carbohydrates, h-hydroxy phenol, g-guaiacyl, s-syringyl		Br-Nr	Chemical Name c-Carbohydrates, h-hydroxy phenol, g-guaiacyl, s-syringyl	
1	CO2	c	50.1	Methyl-butyraldehyde derivative	c
1.1	Formaldehyde	c	*52*	*gamma lactone derivative*	c
1.2	Water (pyro)	c	54	4-Methyl guaiacol	c
3	Propanal-2-one	c	61	4-Hydroxy-3-methyl-(5H)-Furanone	c
4	2-Methylfuran	c	66	4-Vinyl guaiacol	g
5.1	2,3-Butandione	c	68	Eugenol	g
7	Hydroxyacetaldehyde	c	69	5-Hydroxymethyl-2-furaldehyde	c
11	Acetic acid	c	*69.1*	*gamma lactone derivative*	c
12	Acetol	c	70	Syringol	s
13	*1,2-Dihydroxyethene*	c	71	2-Hydroxy-butanedial	c
15	3-Methylfuran	c	72	Isoeugenol (cis)	g
16	*2-Propenoic acid methylester*	c	73	2-Hydroxymethyl-5-hydroxy-2,3-dihydro-(4H)-pyran-4-one	c
18	*3-Hydroxypropanal*	c	75	Isoeugenol (trans)	g
19	*3-Butenal-2-one*	c	76	4-Methyl syringol	s
20	*(3H)-Furan-2-one*	c	77	Vanillin	g
21	(2H)-Furan-3-one	c	78.1	G-C=C=C *	g
22	3-Furaldehyde	c	78.3	G-C=C=C *	g
24	*Butanedial*	c	80	Homovanillin	g
25	*2-Hydroxy-3-oxobutanal*	c	83	Acetoguaiacone	g
26	2-Furaldehyde	c	86	4-Vinyl syringol	s
28	*2-Furfuryl alcahol*	c	87	Guaiacyl acetone	g
29 / 29.1	*1-Acetyloxypropane-2-one / 2-Ethyl-butanal*	c	*92.1*	*Isomer of Conferyl alcohol*	g
30	Dihydro-methyl-furanone	c	96	Levoglucosan	c
34	Dihydro-methyl-furanone	c	97	4-propenyl syringol (trans)	s
35	Dihydro-methyl-furanone	c	*98*	*Dihydroconiferyl alcohol (G VII)*	g
36	4-Hydroxy-5,6-Dihydro-(2H)-	c	*99*	*Syringaldehyde*	s

	pyran-2-one				
38	(5H)-Furan-2-one	c	*101*	*Anhydrosugar:unknown*	c
41	4-Hydroxy-5,6-Dihydro-(2H)-pyran-2-one	c	*102*	*Acetosyringone*	s
43	Methyl-dihydro-(2H)-pyran-2-one	c	*103*	*Coniferyl alcohol(trans)*	g
45	Phenol	h	104	Coniferyaldehyde	g
46	Guaiacol	c			

Notes: * The exact structures of 78.1 and 78.3, G-C=C=C, are not known. The G represents Guaiacyl.

Br-Nr is the Bremer Number. Bremer of the IWC, Hamburg made a standard for analytical pyrolysis. Each of these spectra were given a number for simplifying the comparison of results.

Appendix E – Mass Balance Tabulated Results

Table 33 ***Runs on 150 g/h Apparatus, Beech Wood Feed***

Run no.	EHS	*18*	33	50	16	17	21	*19*	22	23	20	42
Catalyst type		-	-	-	-	-	-	-	-	-	-	-
Av. Run Temp (°C)		*452*	453	475	478	491	501	*502*	523	523	549	447
Run time (min)		*38*	45	45	51	42	46	*63*	42	46	29	38
Flow-rate (g/h)		*112*	133	133	101	123	112	*54*	118	104	146	113
Hot space residence time (s)		*0.51*	0.54	0.52	0.62	0.51	0.50	*0.56*	0.47	0.48	0.45	0.56
Product Yield (%)	**gas**	*12.0*	15.0	14.2	10.1	14.0	16.3	*16.8*	18.6	17.0	25.2	11.9
	organics	*75.3*	59.1	61.0	71.7	64.3	63.2	*56.9*	63.5	60.3	54.5	64.2
	char	*15.0*	11.8	12.1	11.6	10.7	9.5	*9.3*	10.4	8.7	7.6	11.5
	water	*7.4*	8.2	13.6	8.0	6.4	6.5	*2.0*	8.6	7.4	11.9	8.0
	liquids	*82.7*	67.3	74.6	79.7	70.7	69.7	*58.9*	72.1	67.7	66.4	72.2
Closure (%)	**wood in**	***109.8***	**94.0**	**100.9**	**101.4**	**95.4**	**95.5**	***85.0***	**101.1**	**93.4**	**99.1**	**95.5**
							Average	**97.4**	**STDev[a]**	**3.2**	**95%[b]**	**7.3**

Notes: (a) Standard deviation

(b) Standard deviation with a 95 % confidence limit based on 9 points *(Straud, 1987)*.

Table 71 ***Runs on 150 g/h Apparatus, Beech Wood Feed, Slate Fluid Bed***

Run no.	EHS	*26*	31	40	25	24	29	27	28	32
Catalyst type		***Slate fluid bed 96g***	**Slate fluid bed 100g**	**Slate fluid bed 100g**	**Slate fluid bed 97g**	**Slate fluid bed 91g**	**Slate fluid bed 95g**	**Slate fluid bed 94g**	**Slate fluid bed 96g**	**Slate fluid bed 97g**
Av. Run Temp (°C)		*447*	451	452	474	501	501	522	549	550
Run time (min)		*55*	57	48	51	50	57	51	50	47
Flow-rate (g/h)		*99*	91	121	106	108	95	114	96	111
Hot space residence time (s)		*0.82*	0.86	0.76	0.74	0.52	0.74	0.69	0.68	0.66
Product Yield (%)	**gas**	*12.6*	11.8	13.9	12.3	14.4	14.0	16.5	20.6	21.0
	organics	*81.9*	63.7	64.0	65.2	58.6	64.7	59.9	52.6	59.0
	char	*14.2*	17.8	13.7	11.3	8.8	10.3	10.1	9.0	9.3
	water	*9.2*	9.7	8.1	8.5	7.5	6.9	10.7	5.9	5.8
	liquids	*91.1*	73.4	72.1	73.7	66.0	71.6	70.6	58.4	64.7
Closure (%)	**wood in**	***117.8***	**103.0**	**99.7**	**97.4**	**89.3**	**95.9**	**97.2**	**88.0**	**95.1**
					Average	**95.7**	**STDev[(a)]**	**5.0**	**95%[(b)]**	**11.5**

Notes: (a) Standard deviation

(b) Standard deviation with a 95 % confidence limit based on 8 points *(Straud, 1987)*.

Table 72 ***Runs on 150 g/h Apparatus, Beech Wood Feed, Y-Zeolite Close-Coupled in Primary Reactor***

Run no.	EHS	39	34	35	36	37	38
Catalyst type		**Y-zeolite cc in 1ry reactor**	**Y-zeolite cc in 1ry reactor**	**Y-zeolite cc in 1ry reactor**	**Y-zeolite cc in 1ry reactor**	**Y-zeolite cc in 1ry reactor**	**Y-zeolite cc in 1ry reactor**
Av. Run Temp (°C)		451	453	478	502	525	550
Run time (min)		47	34	49	44	46	43
Flow-rate (g/h)		112	99	109	105	121	123
Hot space residence time (s)		0.55	0.52	0.51	0.50	0.48	0.47
Product Yield (%)	**gas**	23.0	16.9	16.7	16.6	21.4	25.4
	organics	51.8	62.2	57.2	55.7	54.4	49.8
	char	13.3	12.0	12.1	11.2	10.3	8.4
	water	11.2	7.7	9.7	10.8	11.2	11.7
	liquids	63.1	69.9	67.0	66.6	65.6	61.6
Closure (%)	**wood in**	**99.5**	**98.7**	**95.8**	**94.3**	**97.4**	**95.3**
		Average	**96.8**	**STDev[(a)]**	**2.0**	**95%[(b)]**	**5.0**

Notes: (a) Standard deviation

(b) Standard deviation with a 95 % confidence limit based on 6 points *(Straud, 1987)*.

Table 73 ***Runs on 150 g/h Apparatus, Beech Wood Feed, Char Co-Fed and Char in the Secondary Reactor***

Run no.	EHS	43	57	44	45	46	47	*48*
Catalyst type		**Char co-fed**	**Char co-fed**	**Char co-fed**	**Char 2ry reactor 9.85g**	**Char 2ry reactor 4.0g**	**Char 2ry reactor 4.3g**	***Char 2ry reactor 4.4g***
Catalyst %		9.09	9.09	9.090	0	0	0	*0*
Av. Run Temp (°C)		450	501	526	452	501	524	*556*
Run time (min)		56	44	34	40	17	37	*38*
Flow-rate (g/h)		112	101	149	111	79	132	*98*
Hot space residence time (s)		0.62	0.53	0.50	0.77	0.48	0.52	*0.49*
Product Yield (%)	**gas**	13.0	15.7	17.1	40.4	36.9	26.6	*21.8*
	organics	57.6	67.2	54.7	30.5	43.9	46.6	*44.4*
	char	19.9	12.6	19.0	14.3	5.3	8.5	*8.6*
	water	7.9	0.8	7.6	8.4	13.0	5.7	*5.8*
	liquids	65.4	68.0	62.3	38.9	56.9	52.3	*50.2*
Closure (%)	**wood in**	**98.4**	**96.3**	**98.3**	**93.6**	**99.1**	**87.3**	***80.6***
			Average	**97.7**		**Average**	**93.3**	
			STDev[a]	**1.2**		**STDev[a]**	**5.9**	
			95%[b]	**3.8**		**95%[b]**	**18.8**	

Notes: (a) Standard deviation (b) Standard deviation with a 95 % confidence limit based on 3 points *(Straud, 1987).*

Table 74 ***Runs on 150 g/h Apparatus, Beech Wood Feed, Char Fluid Bed, Slate Co-Fed and Slate in the Secondary Reactor***

Run no.		52	49	51	54	53	56	55
Catalyst type		**Char fluid bed**	**Char fluid bed**	**Char fluid bed**	**Slate co-fed**	**Slate co-fed**	**Slate co-fed**	**Slate 2ry reactor 30.4g**
Catalyst %		0.00	0.00	0.00	9.09	9.09	9.09	0.00
Av. Run Temp (°C)		475	499	525	478	501	526	504
Run time (min)		41	39	42	38	49	60	47
Flow-rate (g/h)		114	145	125	60	96	92	80
Hot space residence time (s)		0.60	0.58	0.54	1.01	0.53	0.48	0.49
Product Yield (%)	**gas**	19.0	10.9	15.9	13.2	33.0	39.4	33.3
	organics	61.8	59.4	54.7	59.9	62.1	59.9	42.7
	char	9.0	6.3	4.6	14.1	14.0	7.0	9.3
	water	5.7	9.9	6.8	7.0	5.3	7.6	6.0
	liquids	67.5	69.3	61.5	66.9	67.5	67.5	48.7
Closure (%)	**wood in**	**95.5**	**86.5**	**82.0**	**94.3**	**114.4**	**113.9**	**91.3**
			Average	**88.0**		**Average**	**107.5**	
			STDev[a]	**6.9**		**STDev[a]**	**11.5**	
			95%[b]	**21.9**		**95%[b]**	**36.5**	

Notes: (a) Standard deviation (b) Standard deviation with a 95 % confidence limit based on 3 points *(Straud, 1987)*.

Table 75 ***Runs on 150 g/h Apparatus, Pine Wood Feed (Commissioning Configuration)***

Run name	EHS	2	3	*5*	6	4	8	7	9
Catalyst type		-	-	-	-	**GD ZSM5**	**GD ZSM5**	**BDH-Y in 1ry bed 10g**	**BDH-Y in 1ry bed 10g**
Catalyst %		0	0	*0*	0	10	10	0	10
Av. Run Temp (°C)		510.93	474.89	*506.07*	508.41	473.34	505.28	502.14	509.74
Run time (min)		60.00	60.00	*60.00*	60.00	60.00	60.00	51.00	60.00
Flow-rate (g/h)		40.44	41.00	*35.10*	56.18	40.11	33.43	67.41	53.37
Hot space residence time (s)		15.36	16.53	*16.56*	16.18	17.07	20.64	12.31	21.62
Product Yield (%)	**gas**	12.13	13.07	*13.44*	12.17	8.26	21.81	6.32	5.03
	organics	57.51	64.47	*49.73*	63.12	55.12	66.50	53.69	56.43
	char	19.25	7.87	*7.53*	9.40	12.76	1.85	9.57	10.13
	water	14.18	10.84	*9.11*	14.15	13.27	13.86	16.15	14.99
	liquids	71.70	75.31	*58.84*	77.27	68.39	80.36	69.84	71.41
Closure (%)	**wood in**	**103.07**	**96.25**	***79.81***	**98.85**	**89.40**	**104.02**	**85.73**	**86.57**

Appendix F – Mass Balance Graphical Results

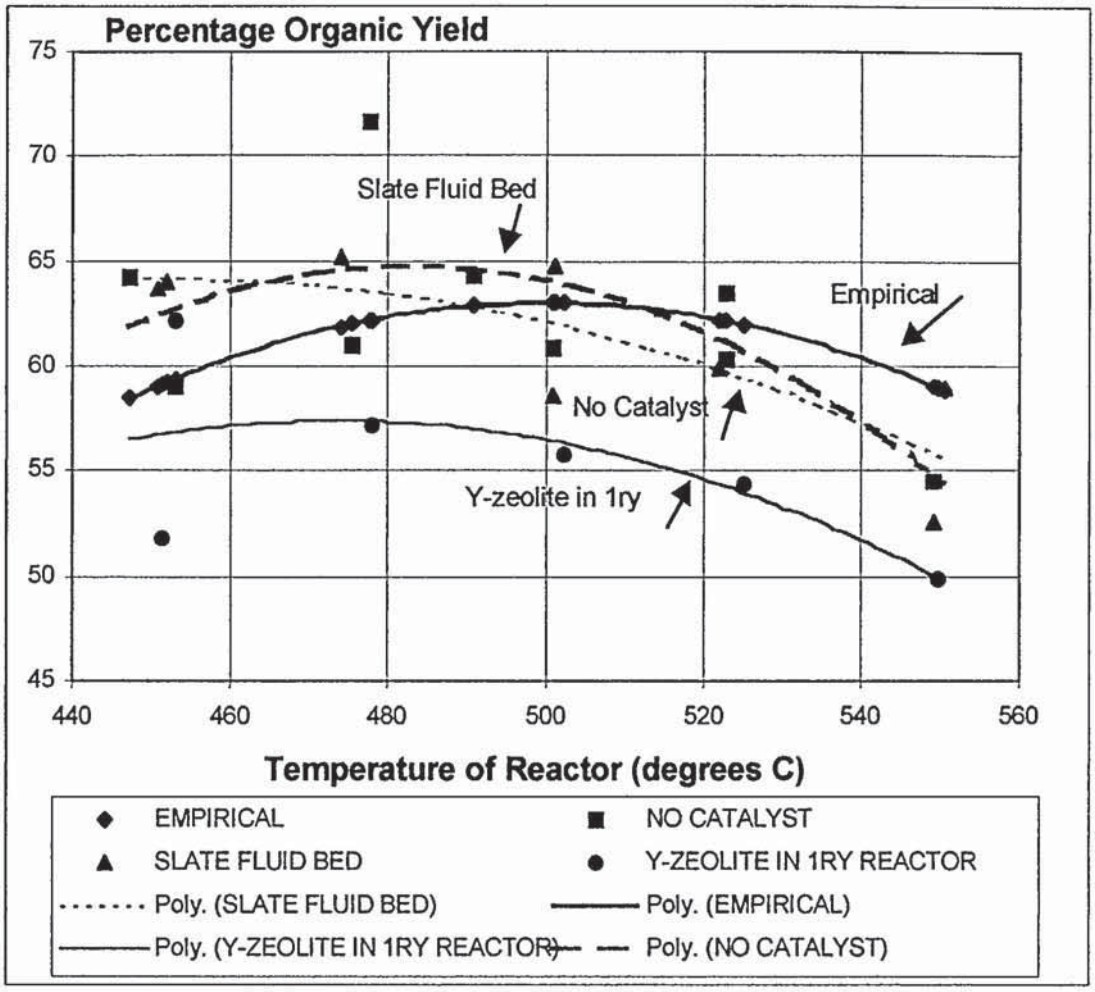

Figure 85 Organic Yield Results from 150 g/h Apparatus (Scale 45 – 75 %)

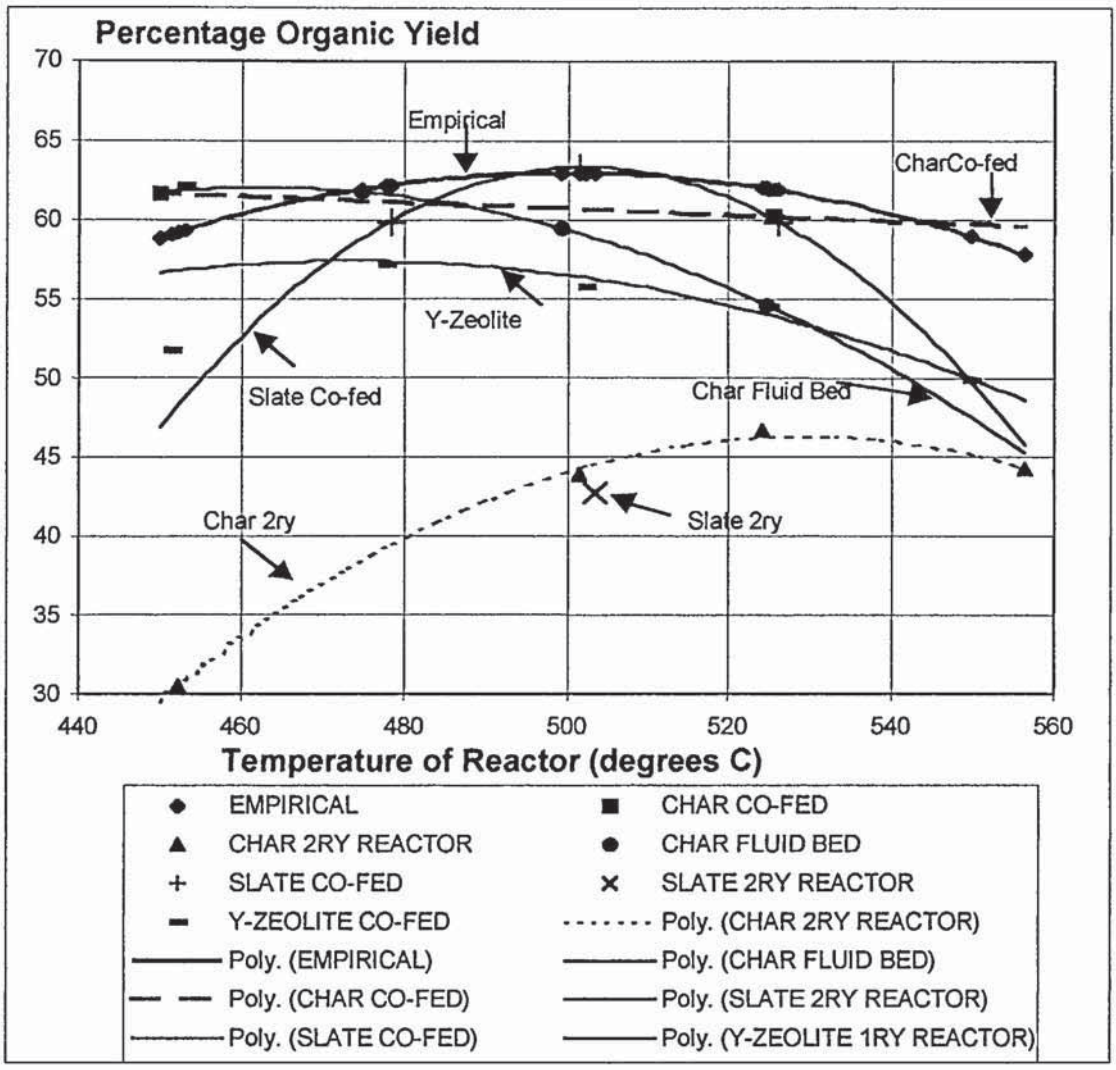

Figure 86 Organic Yield Results from 150 g/h Apparatus (Scale 30 – 65 %)

Appendix G – Water Content Graphs and Tables

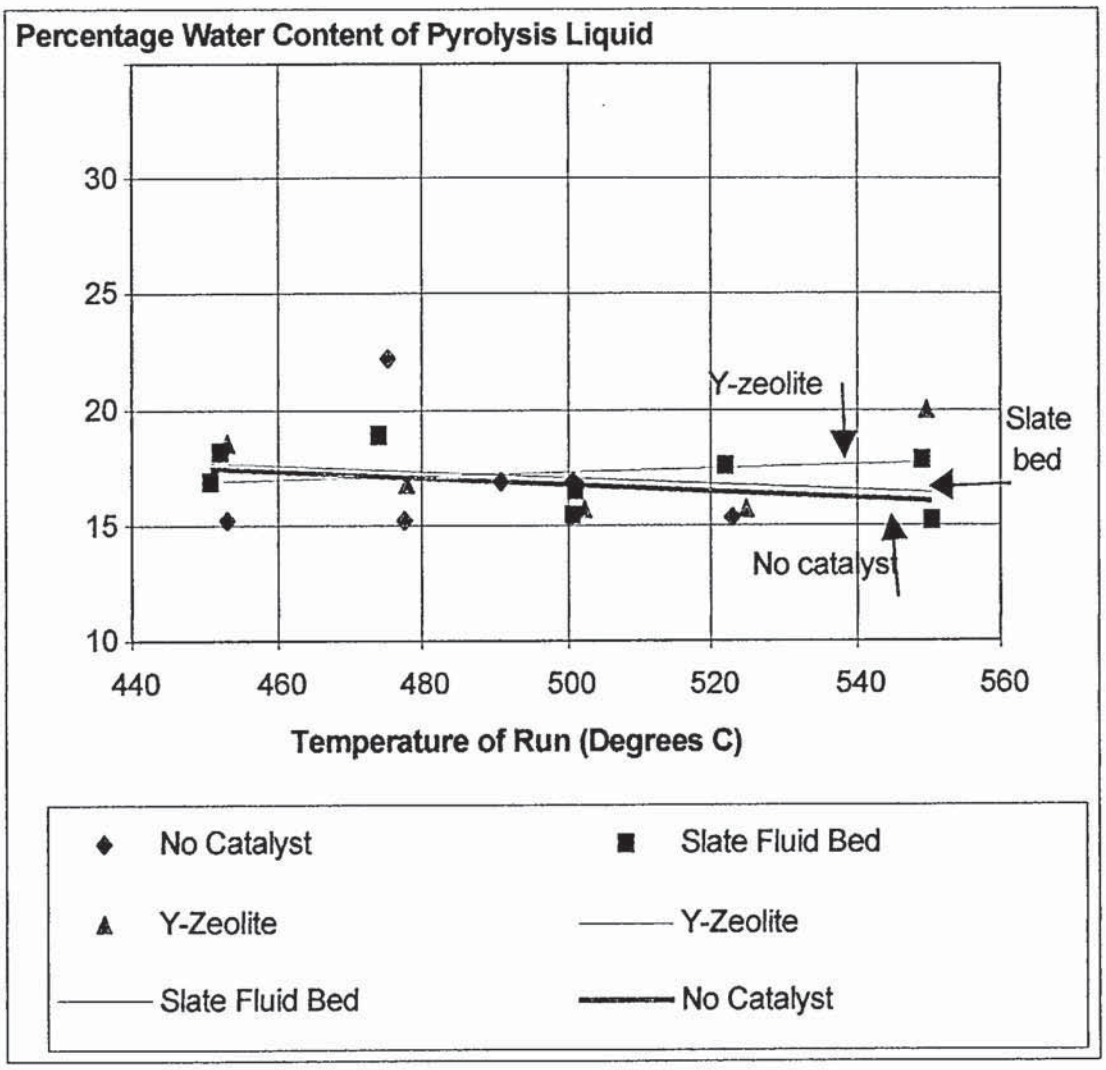

Figure 87 Percentage Water Content of Pyrolysis Liquids 1 of 2

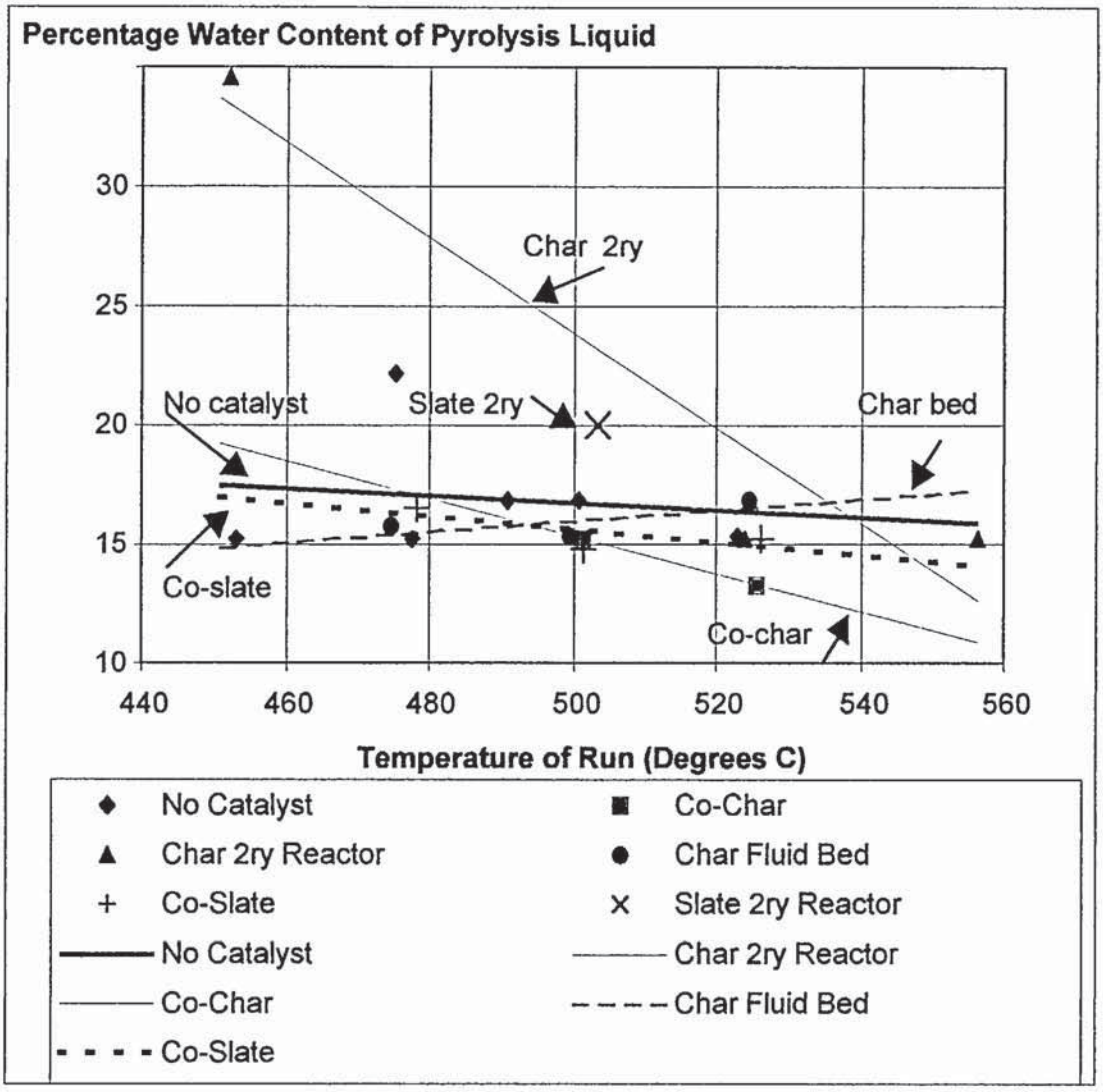

Figure 88 Percentage Water Content of Pyrolysis Liquids 2 of 2

Table 76 Line Fit for Graphs, Figure 87 and Figure 88

Experiment Set	R^2 Value
No Catalyst	0.018
Y-Zeolite	0.023
Slate Fluid Bed	0.140
No Catalyst	0.018
Char 2^{ry} Reactor	0.907
Co-Fed Char	1.000
Char Fluid Bed	0.507
Co-Fed Slate	0.492

The equation used as the 'model' in the following Table 77 to Table 81 is the equation of the straight line of the non-catalytic runs, Equation 44.

Table 77 Calculation of Percentage Difference from 'Model' (No catalyst) Water Content for No Catalyst Runs

	No Catalyst				
Run No. (EHS..)	33	50	17	21	23
Temperature of Run (°C)	453.13	475.36	490.79	500.77	522.96
Actual Water Content (%)	15.20	22.15	16.82	16.90	15.37
Model Water Content (%)	18.10	17.60	17.26	17.03	16.54
Percentage Difference between Measured and Model Water Content	16.00	-25.84	2.51	0.78	7.04
			Average	STDev[(a)]	95%[(b)]
			0.10	15.65	40.23

Notes: (a) Standard deviation

(b) Standard deviation with a 95 % confidence limit based on 5 points *(Straud, 1987)*.

Table 78 ***Calculation of Percentage Difference from 'Model' (No catalyst) Water Content for Slate Fluid Bed Runs***

	Slate Fluid Bed					
Run No. (EHS..)	31	40	29	27	28	32
Temperature of Run (°C)	450.96	452.10	501.08	522.02	549.24	550.48
Actual Water Content (%)	16.83	18.16	16.54	17.64	17.81	15.22
Model Water Content (%)	18.14	18.12	17.03	16.56	15.95	15.92
Percentage Difference between Measured and Model Water Content	7.23	-0.23	2.85	-6.52	-11.63	4.41
				Average	STDev[(a)]	95%[(b)]
				-0.65	7.14	17.47

Notes: (a) Standard deviation

(b) Standard deviation with a 95 % confidence limit based on 6 points *(Straud, 1987)*.

Table 79 ***Calculation of Percentage Difference from 'Model' (No catalyst) Water Content for Y-Zeolite In-bed and Co-fed Char Runs***

	Y-Zeolite In-Bed				Co-fed Char		
Run No. (EHS..)	34	35	36	37	57	44	
Temperature of Run (°C)	453.11	477.91	502.35	525.00	501.33	525.54	
Actual Water Content (%)	18.48	16.74	15.64	15.68	15.22	13.29	
Model Water Content (%)	18.10	17.54	17.00	16.49	17.02	16.48	
Percentage Difference between Measured and Model Water Content	-2.15	4.57	7.97	4.93	10.57	19.34	
		Average	STDev[(a)]	95%[(b)]	Average	STDev[(a)]	95%[(b)]
		3.83	4.27	11.85	14.95	6.20	26.68

Notes: (a) Standard deviation

(b) Standard deviation with a 95 % confidence limit based on 4 or 2 points *(Straud, 1987)*.

Table 80 ***Calculation of Percentage Difference from 'Model' (No catalyst) Water Content for Char in Secondary Reactor and Char Fluid Bed Runs***

	Char Secondary Reactor			Char Fluid Bed		
Run No. (EHS..)	45	47	48	52	49	51
Temperature of Run (°C)	452.12	523.95	556.28	474.83	499.43	524.64
Actual Water Content (%)	34.62	15.20	15.22	15.77	15.36	16.89
Model Water Content (%)	18.12	16.52	15.79	17.61	17.06	16.50
Percentage Difference between Measured and Model Water Content	-91.06	7.97	3.63	10.45	9.97	-2.34
	Average	STDev[a]	95%[b]	Average	STDev[a]	95%[b]
	-26.49	55.96	178.06	6.02	7.25	23.07
Excluding run 45[c]:	5.80	3.07	13.21			

Notes:
(a) Standard deviation
(b) Standard deviation with a 95 % confidence limit based on 3 points *(Straud, 1987)*.
(c) Because of the unacceptable standard deviation of EHS45, the spurious point has been removed from the calculations.

Table 81 ***Calculation of Percentage Difference from 'Model' (No catalyst) Water Content for Co-fed Slate and Slate Secondary Bed Runs***

	Co-fed Slate			Slate Secondary Bed
Run No. (EHS..)	54	53	56	55
Temperature of Run (°C)	478.29	501.49	526.15	503.53
Actual Water Content (%)	16.57	14.75	15.22	20.04
Model Water Content (%)	17.53	17.02	16.47	16.97
Percentage Difference between Measured and Model Water Content	5.51	13.32	7.56	-18.08
	Average	STDev[(a)]	95%[(b)]	Average
	8.80	4.05	12.89	-18.08

Notes: (a) Standard deviation

(b) Standard deviation with a 95 % confidence limit based on 3 points *(Straud, 1987)*.

Appendix H – HPLC Analysis Technique and Tabulated Results

Analysis of Resulting HPLC Chromatographs

Identification of individual peaks is based on retention times. A chromatogram obtained from an unknown sample of aqueous phase liquid is compared to that of the standard. The standard contains many of the expected chemicals from wood pyrolysis. These are shown in Table 82. HPLC software identifies and measures peaks automatically against that of the standard. Problems arise when the software does not analyse the chromatogram correctly. This happens especially when peaks are not fully resolved (they do not reach the base line or have a shoulder attached to them). In this case the chromatograph must be examined carefully and analysed manually.

The area of each peak is calculated by the software and compared to the corresponding peak in the standard. Equation 56 is used to calculate the concentration of the chemical constituent by the computer.

$$\text{Wt\% concentration of unknown peak} = \frac{\text{Area of peak with unknown concentration}}{\text{Area of corresponding standard peak}} \times \text{Standard peak wt\% concentration}$$

Equation 56

The following calculations are then done using a 'Microsoft Excel Spreadsheet' (Equation 57 to Equation 62). They find the weight percent concentration of each chemical detected in the sample with unknown chemical concentrations, on a dry wood-fed basis. This 'unknown' sample is the aqueous fraction of the pyrolysis liquid. Table 83 describes the terms used in Equation 57 to Equation 62 and how they have been obtained. 'Sample' is referred to as the pyrolysis liquid and water that is added to the vial before lignin extraction. The meanings of the abbreviations can be found in Table 83.

$$\text{Mass fraction passing to HPLC column} = \frac{(Mt + Mw) - (Mt \times XLT)}{(Mt + Mw)}$$

Equation 57

$$\text{AdjHPLC\%} = \text{HPLC\%} \times \text{Mass fraction passing to HPLC column} \times \frac{Vs}{Vu}$$

Equation 58

$$PL\% = \frac{\text{AdjHPLC\%} \times (Mw + Mt)}{Mt}$$

Equation 59

$$\text{Mass of chemical in pyrolysis liquid} = \frac{PL\% \times Mpl}{100}$$

Equation 60

Table 82 HPLC 'Standard' Components in Order of Retention Times

Chemical (Alternative Name)	Code Name	Class	Typical Retention Times (minutes) [a]	Typical Concentration in Standard (wt%)
Cellobiose	CB	Sugar	9.37	0.026
Glucose	G	Sugar	11.37	0.034
Fructose	F	Sugar	12.57	0.076
Glyoxal (Ethane-1,2-dial)	GX	Aldehyde	12.87	0.022
Pyruvic Acid	PYA	Acid	12.90	0.157
Xylitol	X	Alcohol	14.68	0.027
Hydroxyacetaldehyde (Glycolaldehyde)	HA	Aldehyde	15.18	0.422
Levoglucosan	LG	Sugar	16.40	0.365
Lactic Acid	LA	Acid	16.41	0.183
Formaldehyde (Methanal)	FD	Aldehyde	17.08	0.255
Formic Acid (Methanoic Acid)	FC	Acid	17.67	0.314
Acetic Acid (Ethanoic Acid)	HOAc	Acid	19.18	0.379
Acetol (1-Hydroxy-2-Propanaone)	A	Alcohol	22.3	0.306
Methanol	MeOH	Alcohol	23.13	2.641
γ-Butyrolactone (Dihydro-2(3H)-furanone	BL	Ketone	27.65	0.433
2-Furoic Acid (Furan-2-cardoxylic Acid)	FUA	Acid	32.917	0.045
Cyclopentanedione	MCPD	Ketone	37.70	0.073
2-Buten-1-ol	BEL	Alcohol	40.70	0.084
2(5H)-Furanone	FUE	Ketone	42.22	0.145
Crotonaldehyde (2-Butenal)	CRA	Aldehyde	53.72	0.066

Notes: (a) Retention time when mobile phase is 0.005 Molar H_2SO_4 at 0.50 cc/min, 35°C

$$\text{Wt\% chemical on dry wood fed basis} = \frac{\text{Mass of chemical in pyrolysis liquid} \times 100}{\text{Mf}}$$

Equation 61

The weight percent of lignin in the pyrolysis liquid product can be found using Equation 62, then applying Equation 61 as for the weight percent of the chemicals found by HPLC.

$$\text{Mass of lignin in pyrolysis liquid} = \text{XLT} \times \text{Mpl}$$

Equation 62

Table 83 Terms Used in Equation 57 to Equation 62 (in order of appearance)

Term	Abbreviation	Calculated By
Mass of pyrolysis liquids initially in analysis preparation	Mt	Liquid weighed into vial
Mass of water added to Mt	Mw	Water weighed into vial
Lignin in raw liquid	XLT	Weight of vial after aqueous extraction and drying minus original weight of vial
Weight percent concentration in HPLC sample	AdjHPLC%	Adjusted using Equation 8
HPLC result	HPLC%	Weight percent of chemical as detected and computed by HPLC
Standard injection sample volume	Vs	Typically 5 µl
Unknown injection sample volume	Vu	Typically 5 µl
Weight percent concentration in pyrolysis liquid from reaction	PL%	Equation
Mass of product liquid recovered from pyrolysis	Mpl	From pyrolysis reaction mass balance
Mass of dry wood feed pyrolysed	Mf	From pyrolysis reaction mass balance

In the following Table 37, Table 84 to Table 87, Table 38 and Table 88 to Table 91, 'r' indicates that a sample has been re-analysed.

Table 37 ***HPLC Analysis - Main Fraction of Liquid, Wt% on Dry Wood Basis of Chemicals Found and Pyrolytic Lignin, No Catalyst***

Run No	EHS - No Catalyst	42	33	50	16	17	21	22	23	20
	Av. Run Temp (°C)	**447.32**	**453.13**	**475.36**	**477.62**	**490.79**	**500.77**	**522.91**	**522.96**	**549.18**
CB	Cellobiose	0.00	0.00	0.09	0.00	0.00	0.00	0.00	0.00	0.00
G	Glucose	0.01	0.27	0.45	0.30	0.26	0.00	0.00	0.00	0.16
F	Fructose	0.00	1.03	0.00	0.00	0.00	0.00	0.00	0.00	0.00
GX	Glyoxal	3.59	0.02	6.36	0.15	0.17	0.02	0.01	0.02	0.02
HA	**Hydroxyacetaldehyde**	**23.72**	**20.17**	**22.39**	**18.49**	**20.62**	**15.77**	**17.73**	**18.80**	**14.99**
LG	**Levoglucosan**	**4.62**	**3.01**	**4.21**	**5.06**	**4.56**	**1.74**	**1.85**	**1.96**	**2.50**
FD	Formaldehyde	4.93	2.29	4.57	2.89	3.15	1.06	1.44	1.72	2.20
FC	Formic Acid	0.00	4.01	0.00	4.60	4.50	2.00	2.11	3.02	2.72
HOAc	Acetic Acid	5.35	4.55	5.34	3.86	4.01	3.27	3.41	4.12	4.40
A	Acetol	2.66	2.85	3.46	1.09	1.15	1.00	0.99	0.96	1.25
BL	Butyrolactone	5.37	0.00	0.00	0.00	0.00	0.00	0.00	0.00	0.00
FUA	Furoic Acid	0.00	0.18	0.00	0.00	0.00	0.00	0.00	0.00	0.00
BEL	2-Buten-1-ol	0.23	0.00	0.36	0.00	0.00	0.00	0.00	0.00	0.00
FUE	2(5H)-Furanone	0.00	0.00	0.00	0.60	0.46	0.49	0.00	0.39	0.33
	Pyrolytic Lignin	2.16	3.22	5.28	3.53	3.39	2.63	3.44	1.88	1.67

Table 84 ***HPLC Analysis - Main Fraction of Liquid, Wt% on Dry Wood Basis of Chemicals Found and Pyrolytic Lignin, Slate Fluid Bed***

Run No	EHS – Slate Fluid Bed	31	40	25	25r	24	29	27	28	32
	Av. Run Temp (°C)	**450.96**	**452.10**	**473.96**	**473.96**	**500.75**	**501.08**	**522.02**	**549.24**	**550.48**
CB	Cellobiose	0.00	0.00	0.00	0.00	0.00	0.00	0.00	0.00	0.00
G	Glucose	0.00	0.33	0.00	0.51	0.00	0.19	0.00	0.00	0.00
F	Fructose	0.76	0.00	0.41	0.00	0.42	0.68	0.39	0.47	0.28
GX	Glyoxal	0.02	3.73	0.02	0.02	0.02	0.02	0.02	0.02	0.12
PYA	Pyruvic Acid	0.00	0.00	0.73	0.00	0.60	0.00	0.00	0.00	0.00
HA	**Hydroxyacetaldehyde**	**11.39**	**19.81**	**19.77**	**19.75**	**17.52**	**18.45**	**16.23**	**20.32**	**10.33**
LG	**Levoglucosan**	**1.52**	**3.77**	**2.16**	**4.17**	**1.85**	**2.30**	**1.55**	**2.21**	**1.54**
FD	Formaldehyde	1.49	3.19	1.38	1.86	1.06	2.35	0.47	1.83	1.30
FC	Formic Acid	1.53	5.41	2.37	5.88	1.87	1.79	0.00	2.72	1.08
HOAc	Acetic Acid	2.38	5.51	4.03	5.55	3.17	3.71	3.78	4.00	2.44
A	Acetol	0.96	2.54	1.23	2.82	0.92	1.18	1.02	0.93	0.90
FUA	Furoic Acid	0.00	0.12	0.00	0.00	0.00	0.00	0.00	0.00	0.15
BEL	2-Buten-1-ol	0.00	0.23	0.00	0.00	0.35	0.00	0.00	0.00	0.00
FUE	2(5H)-Furanone	0.00	0.00	0.45	0.09	0.37	0.28	0.34	0.22	0.00
	Pyrolytic Lignin	2.32	1.94	6.05	4.77	2.26	3.57	2.41	1.92	4.66

Table 85 ***HPLC Analysis - Main Fraction of Liquid, Wt% on Dry Wood Basis of Chemicals Found and Pyrolytic Lignin, Y-Zeolite Close Coupled in Primary Reactor***

Run No	EHS – Y-zeolite cc in 1ry reactor	39	34	35	36	37	38
	Av. Run Temp (°C)	**451.40**	**453.11**	**477.91**	**502.35**	**525.00**	**549.73**
CB	Cellobiose	0.00	0.03	0.05	0.07	0.06	0.00
G	Glucose	0.28	0.38	0.48	0.27	0.23	0.17
F	Fructose	0.00	0.88	1.12	0.90	0.43	0.00
GX	Glyoxal	2.72	1.43	1.83	1.97	1.05	1.33
X	Xylitol	2.69	0.84	1.04	0.96	0.36	0.67
HA	**Hydroxyacetaldehyde**	**13.38**	**10.44**	**13.97**	**12.13**	**9.36**	**10.45**
LG	**Levoglucosan**	**2.78**	**2.05**	**2.37**	**2.14**	**2.00**	**2.04**
FD	Formaldehyde	2.13	1.53	1.83	1.58	1.25	2.42
FC	Formic Acid	3.70	2.52	2.91	2.50	1.78	0.00
HOAc	Acetic Acid	3.82	3.16	3.61	2.92	2.30	2.45
A	Acetol	2.37	1.85	2.19	1.72	1.32	1.64
FUA	Furoic Acid	0.13	0.03	0.29	0.08	0.07	0.00
MCPD	Cyclopentanedione	0.11	0.00	0.00	0.00	0.07	0.00
BEL	2-Buten-1-ol	0.23	0.00	0.00	0.00	0.14	0.13
CRA	Crotonaldehyde	0.02	0.00	0.00	0.00	0.01	0.00
	Pyrolytic Lignin	1.99	3.88	4.90	3.67	2.77	2.29

Table 86 ***HPLC Analysis - Main Fraction of Liquid, Wt% on Dry Wood Basis of Chemicals Found and Pyrolytic Lignin, Char Co-Fed and Char in Secondary Reactor***

Run No	EHS – Char Co-fed	43	57	44	EHS – Char in 2ry Reactor	45	46	47	48
	Av. Run Temp (°C)	**449.95**	**501.33**	**525.54**	**Av. Run Temp (°C)**	**452.12**	**501.42**	**523.95**	**556.28**
G	Glucose	0.00	0.25	0.32	Glucose	0.05	0.04	0.09	0.01
GX	Glyoxal	3.35	6.67	3.41	Glyoxal	1.11	0.77	2.07	0.90
X	Xylitol	0.00	0.00	0.00	Xylitol	0.96	0.48	1.15	0.58
HA	**Hydroxyacetaldehyde**	**22.83**	**16.31**	**20.63**	**Hydroxyacetaldehyde**	**2.81**	**3.83**	**8.67**	**4.83**
LG	**Levoglucosan**	**4.56**	**3.44**	**3.90**	**Levoglucosan**	**2.07**	**0.88**	**2.32**	**1.65**
FD	Formaldehyde	4.98	3.65	6.01	Formaldehyde	1.63	0.96	2.40	0.35
HOAc	Acetic Acid	5.19	3.54	4.71	Acetic Acid	2.66	1.18	3.09	1.83
A	Acetol	2.64	2.69	1.33	Acetol	1.45	0.82	2.02	1.05
BL	Butyrolactone	1.75	0.00	1.46	Butyrolactone	0.00	0.00	0.00	0.00
MCPD	Cyclopentanedione	0.00	0.00	0.00	Cyclopentanedione	0.35	0.06	0.28	0.09
BEL	2-Buten-1-ol	0.25	0.27	0.00	Butanol	0.08	0.07	0.13	0.08
FUE	2(5H)-Furanone	0.00	0.75	0.00	Furanone	0.00	0.00	0.00	0.00
	Pyrolytic Lignin	2.70	6.00	4.36	Pyrolytic Lignin	2.24	0.07	2.10	2.61

Table 87 ***HPLC Analysis - Main Fraction of Liquid, Wt% on Dry Wood Basis of Chemicals Found and Pyrolytic Lignin, Char Fluid Bed, Slate Co-Fed and Slate in Secondary Reactor***

Run No	EHS – Char Fluid Bed	52	49	51	EHS – Slate Co-fed	54	53	56	Slate in 2ry Reactor	55
	Av. Run Temp (°C)	**474.83**	**499.43**	**524.64**	**Av. Run Temp (°C)**	**478.29**	**501.49**	**526.15**	**Av. Run Temp (°C)**	**503.53**
CB	Cellobiose	0.02	0.07	0.09	Cellobiose	0.00	0.00	0.09	Cellobiose	0.00
G	Glucose	0.03	0.30	0.45	Glucose	0.00	0.37	0.29	Glucose	0.00
GX/PYA	Glyoxal	1.45	1.06	6.36	Glyoxal	4.56	5.48	3.49	Glyoxal	0.00
X	Xylitol	0.00	1.26	0.00	Xylitol	0.00	0.00	0.00	Xylitol	0.00
HA	**Hydroxyacetaldehyde**	**7.14**	**11.76**	**22.39**	**Hydroxyacetaldehyde**	**12.89**	**15.43**	**13.63**	**Hydroxyacetaldehyde**	**9.89**
LG	**Levoglucosan**	**2.00**	**3.35**	**4.21**	**Levoglucosan**	**2.53**	**3.80**	**3.41**	**Levoglucosan**	**1.57**
FD	Formaldehyde	1.67	1.93	4.57	Formaldehyde	3.04	3.75	8.74	Formaldehyde	2.09
FC	Formic Acid	0.00	3.50	0.00	Formic Acid	0.00	0.00	0.00	Formic Acid	0.00
HOAc	Acetic Acid	2.14	3.88	5.34	Acetic Acid	3.31	4.06	2.75	Acetic Acid	2.69
A	Acetol	1.38	2.38	3.46	Acetol	1.98	2.22	2.16	Acetol	1.72
BL	Butyrolactone	0.15	0.00	0.00	Butyrolactone	0.51	0.87	0.00	Butyrolactone	0.30
BEL	2-Buten-1-ol	0.00	0.00	0.36	Butanol	0.00	0.00	0.21	Butanol	0.00
FUE	2(5H)-Furanone	0.00	0.00	0.00	Furanone	0.00	0.00	0.54	Furanone	0.00
	Pyrolytic Lignin	6.55	5.71	5.28	Pyrolytic Lignin	4.34	6.96	5.81	Pyrolytic Lignin	2.47

Table 38 ***HPLC Analysis - Secondary Fraction of Liquid, Wt% on Dry Wood Basis of Chemicals Found and Pyrolytic Lignin, No Catalyst***

Run No	**EHS - No Catalyst**	**42**	**33**	**50**	**16**	**17**	**17r**	**21**	**22**	**23**	**20**
	Av. Run Temp (°C)	**447.32**	**453.13**	**475.36**	**477.62**	**490.79**	**490.79**	**500.77**	**522.91**	**522.96**	**549.18**
F	Fructose	0.78	0.00	0.82	0.00	0.00	0.00	0.00	0.00	0.00	0.00
GX	Glyoxal	0.00	0.08	0.00	0.00	0.00	0.00	0.00	0.00	0.00	0.00
X	Xylitol	3.23	0.27	4.21	0.00	0.00	0.00	0.00	0.00	0.00	0.00
HA	**Hydroxyacetaldehyde**	**4.32**	**0.56**	**6.86**	**0.95**	**0.13**	**0.84**	**3.16**	**0.78**	**0.98**	**0.51**
LG	Levoglucosan	0.30	0.04	0.51	0.10	0.00	0.00	0.00	0.00	0.00	0.00
LA	Lactic Acid	0.00	0.00	0.00	0.00	0.00	0.11	0.00	0.00	0.00	0.00
FD	Formaldehyde	4.53	0.65	7.54	1.40	0.19	0.82	3.43	1.00	1.08	0.77
FC	Formic Acid	0.00	0.25	0.00	0.50	0.09	0.34	0.00	0.00	0.00	0.00
HOAc	Acetic Acid	3.34	0.46	4.65	0.61	0.16	0.69	2.23	0.62	0.65	0.58
A	Acetol	1.03	0.16	1.40	0.17	0.03	0.21	0.60	0.21	0.19	0.12
MeOH	Methanol	2.11	0.28	3.22	0.31	0.00	0.31	1.23	0.34	0.35	0.35
MCPD	Cyclopentanedione	0.00	0.00	0.12	0.00	0.00	0.00	0.00	0.00	0.00	0.00
BEL	2-Buten-1-ol	0.00	0.00	0.02	0.00	0.00	0.00	0.00	0.00	0.00	0.00
FUE	2(5H)-Furanone	0.00	0.00	0.00	0.00	0.00	0.00	0.00	0.02	0.02	0.00
	Pyrolytic lignin	0.26	0.02	0.02	0.02	0.02	0.01	0.03	0.02	0.01	0.01

Table 88 ***HPLC Analysis - Secondary Fraction of Liquid, Wt% on Dry Wood Basis of Chemicals Found and Pyrolytic Lignin, Slate Fluid Bed***

Run No	EHS – Slate Fluid Bed	31	40	25	24	29	27	28	28r	32
	Av. Run Temp (°C)	**450.96**	**452.10**	**473.96**	**500.75**	**501.08**	**522.02**	**549.24**	**549.24**	**550.48**
G	Glucose	0.00	0.00	0.00	0.00	0.31	0.00	0.00	0.08	0.08
F	Fructose	0.60	0.00	0.00	0.00	0.31	0.00	0.00	0.00	0.59
GX	Glyoxal	0.02	0.33	0.00	0.00	0.02	0.00	0.00	0.48	0.00
X	Xylitol	3.86	3.38	0.00	0.00	0.00	0.00	0.00	2.35	3.13
HA	**Hydroxyacetaldehyde**	**4.05**	**2.38**	**0.00**	**1.01**	**19.12**	**0.30**	**4.46**	**2.42**	**3.50**
LG	Levoglucosan	0.00	0.04	0.00	0.00	5.23	0.00	0.00	0.00	0.00
FD	Formaldehyde	5.80	4.72	0.60	0.98	2.99	0.65	7.27	5.16	0.00
FC	Formic Acid	2.58	1.50	0.00	0.00	4.75	0.00	0.00	0.00	0.00
HOAc	Acetic Acid	4.85	22.74	0.32	0.62	3.99	0.36	5.07	3.61	4.53
A	Acetol	1.15	1.26	0.07	0.16	1.13	0.11	1.55	0.85	1.05
MeOH	Methanol	3.06	3.11	0.18	0.27	0.00	0.14	2.40	3.74	3.95
FUE	2(5H)-Furanone	0.00	0.00	0.00	0.00	0.62	0.01	0.00	0.00	0.00
	Pyrolytic Lignin	0.19	0.05	0.01	0.03	0.07	0.01	0.06	0.08	0.16

Table 89 ***HPLC Analysis - Secondary Fraction of Liquid, Wt% on Dry Wood Basis of Chemicals Found and Pyrolytic Lignin, Y-Zeolite Close Coupled in the Primary Reactor***

Run No	**EHS – Y-zeolite cc in 1ry reactor**	**39**	**34r**	**34**	**35**	**36**	**37**	**38**
	Av. Run Temp (°C)	**451.40**	**453.11**	**453.11**	**477.91**	**502.35**	**525.00**	**549.73**
G	Glucose	0.00	0.00	0.00	0.00	0.00	0.00	0.03
F	Fructose	0.00	0.00	0.39	0.00	0.00	0.00	0.00
GX	Glyoxal	0.37	0.24	0.00	0.08	0.12	0.00	0.19
X	Xylitol	0.00	0.93	1.78	0.25	0.29	0.00	0.53
HA	**Hydroxyacetaldehyde**	**2.77**	**1.97**	**2.24**	**0.58**	**0.65**	**2.35**	**2.10**
LG	Levoglucosan	0.27	0.15	0.00	0.05	0.06	0.21	0.21
FD	Formaldehyde	3.73	3.41	3.94	0.71	0.86	3.10	2.94
FC	Formic Acid	1.35	0.89	0.00	0.33	0.27	0.00	0.00
HOAc	Acetic Acid	3.34	2.28	2.67	0.57	0.63	2.11	2.23
A	Acetol	0.88	0.75	0.75	0.16	0.18	0.53	1.16
MeOH	Methanol	2.49	1.06	1.23	0.39	0.46	1.33	1.68
BEL	2-Buten-1-ol	0.00	0.01	0.00	0.00	0.00	0.02	0.02
	Pyrolytic Lignin	0.91	0.09	0.11	0.02	0.02	0.04	0.08

Table 90 ***HPLC Analysis - Secondary Fraction of Liquid, Wt% on Dry Wood Basis of Chemicals Found and Pyrolytic Lignin, Char Co-Fed and Char in the Secondary Reactor***

Run No	EHS – Char Co-fed	43	57	44	EHS – Char in 2ry Reactor	45	46	47	48
	Av. Run Temp (°C)	**449.95**	**501.33**	**525.54**	**Av. Run Temp (°C)**	**452.12**	**501.42**	**523.95**	**556.28**
F	Fructose	0.00	0.00	0.47	Fructose	0.00	0.00	0.00	0.00
GX	Glyoxal	0.31	0.00	0.00	Glyoxal	0.02	0.12	0.20	0.06
X	Xylitol	2.33	2.86	2.22	Xylitol	0.29	0.68	1.03	0.38
HA	**Hydroxyacetaldehyde**	**3.26**	**5.31**	**3.24**	**Hydroxyacetaldehyde**	**0.24**	**1.01**	**1.71**	**0.49**
LG	Levoglucosan	3.26	0.44	0.23	Levoglucosan	0.03	0.09	0.15	0.04
FD	Formaldehyde	3.67	5.98	4.21	Formaldehyde	0.71	1.23	2.57	0.85
HOAc	Acetic Acid	2.91	3.60	2.81	Acetic Acid	1.10	1.68	2.53	0.96
A	Acetol	0.98	0.92	0.84	Acetol	0.33	0.55	0.80	0.19
MeOH	Methanol	1.91	2.33	2.40	Methanol	0.71	1.20	2.76	0.12
BL	Butyrolactone	0.00	0.00	0.00	Butyrolactone	0.00	0.00	4.74	1.46
FUA	Furoic Acid	0.00	0.00	0.00	Furoic Acid	0.00	0.00	0.13	0.00
MCPD	Cyclopentanedione	0.00	0.10	0.00	Cyclopentanedione	0.00	0.00	0.21	0.29
BEL	2-Buten-1-ol	0.00	0.04	0.00	Butanol	0.00	0.00	0.03	0.00
FUE	2(5H)-Furanone	0.00	0.12	0.00	Furanone	0.00	0.00	0.00	0.00
	Pyrolytic Lignin	0.18	0.03	0.19	Pyrolytic Lignin	0.07	0.07	0.09	0.05

Table 91 ***HPLC Analysis - Secondary Fraction of Liquid, Wt% on Dry Wood Basis of Chemicals Found and Pyrolytic Lignin, Char Fluid Bed, Slate Co-Fed and Slate in the Secondary Reactor***

Run No	EHS – Char Fluid Bed	52	49	51	EHS – Slate Co-fed	54	53	56	Slate in 2ry Reactor	55
	Av. Run Temp (°C)	**474.83**	**499.43**	**524.64**	**Av. Run Temp (°C)**	**478.29**	**501.49**	**526.15**	**Av. Run Temp (°C)**	**503.53**
G	Glucose	0.00	0.07	0.00	Glucose	0.00	0.00	0.00	Glucose	0.00
F	Fructose	0.00	0.00	0.82	Fructose	0.00	0.00	0.00	Fructose	0.00
GX	Glyoxal	0.00	0.26	0.00	Glyoxal	0.00	0.00	0.00	Glyoxal	0.00
X	Xylitol	2.39	1.70	4.21	Xylitol	2.14	3.15	1.98	Xylitol	0.47
HA	**Hydroxyacetaldehyde**	**3.96**	**2.16**	**6.86**	**Hydroxyacetaldehyde**	**3.63**	**5.11**	**4.40**	**Hydroxyacetaldehyde**	**2.04**
LG	Levoglucosan	0.35	0.21	0.51	Levoglucosan	0.00	0.00	0.34	Levoglucosan	0.00
FD	Formaldehyde	4.58	3.28	7.54	Formaldehyde	3.54	5.32	4.66	Formaldehyde	3.52
HOAc	Acetic Acid	3.47	2.35	4.65	Acetic Acid	3.25	3.63	3.05	Acetic Acid	2.07
A	Acetol	1.37	0.76	1.40	Acetol	1.02	1.03	0.93	Acetol	0.67
MeOH	Methanol	2.03	2.24	3.22	Methanol	1.72	1.81	1.85	Methanol	0.91
BL	Butyrolactone	0.00	0.00	0.00	Butyrolactone	0.12	0.06	0.00	Butyrolactone	0.18
MCPD	Cyclopentanedione	0.15	0.17	0.12	Cyclopentanedione	0.00	0.11	0.00	Cyclopentanedione	0.00
BEL	2-Buten-1-ol	0.05	0.03	0.02	Butanol	0.00	0.00	0.02	Butanol	0.00
FUE	2(5H)-Furanone	0.00	0.00	0.00	Furanone	0.00	0.00	0.08	Furanone	0.00
	Pyrolytic lignin	0.07	0.14	0.02	Pyrolytic lignin	0.07	0.15	0.03	Pyrolytic lignin	0.03

Table 92 Numbering of Catalyst Systems for Table 93 and Table 94

Catalyst System	Identifying Number
No catalyst	1
Slate fluid bed	2
Slate co-fed	3
Slate in secondary reactor	4
Y-zeolite close coupled in primary reactor	5
Char fluid bed	6
Char co-fed	7
Char in secondary reactor	8

Table 93 looks at the main fraction of pyrolysis liquid and Table 94 the secondary liquid. Points have been emboldened and repeated to highlight unusual or notable results.

Table 93 Initial Assessment of HPLC Results, Main Fraction of Liquid

(See Table 92 for Identifying Number code)

Chem Code	Catalyst System Identifying Number Code							
	1	2	3	4	5	6	7	8
CB	×	×	×	×	✓✓	✓✓	×	×
G	✓	××	✓	××	✓	✓	✓	✓
F	×	✓✓	×	×	✓✓	×	×	×
GX	✓	✓	✓	××	✓	✓	✓	✓
PYA	×	×	×	×	×	×	×	×
X	×	×	×	×	✓✓	×	×	✓✓
HA	✓	✓	✓	✓	✓	✓	✓	✓
LG	✓	✓	✓	✓	✓	✓	✓	✓
LA	×	×	×	×	×	×	×	×
FD	✓	✓	✓	✓	✓	✓	✓	✓
FC	✓	✓	×	×	✓	×	×	×
HOAc	✓	✓	✓	✓	✓	✓	✓	✓
A	✓	✓	✓	✓	✓	✓	✓	✓
MeOH	×	×	×	×	×	×	×	×
BL	×	×	✓✓	✓✓	×	×	✓✓	×
FUA	×	×	×	×	✓✓	×	×	×
MCPD	×	×	×	×	×	×	×	✓✓
BEL	×	×	×	×	×	×	✓✓	✓✓
FUE	✓✓	✓✓	×	×	×	×	×	×
CRA	×	×	×	×	×	×	×	×

Table 94 ***Initial Assessment of HPLC Results, Secondary Fraction of Liquid***

(See Table 92 for Identifying Number code)

Chem Code	Catalyst System Identifying Number Code							
	1	2	3	4	5	6	7	8
CB	×	×	×	×	×	×	×	×
G	×	×	×	×	×	×	×	×
F	×	×	×	×	×	×	×	×
GX	×	×	×	×	✓✓	×	×	✓✓
PYA	×	×	×	×	×	×	×	×
X	××	××	✓	✓	✓	✓	✓	✓
HA	✓	✓	✓	✓	✓	✓	✓	✓
LG	×	×	×	×	✓✓	✓✓	×	✓✓
LA	×	×	×	×	×	×	✓✓	×
FD	✓	✓	✓	✓	✓	✓	××	✓
FC	✓	✓	×	×	✓	×	✓	×
HOAc	✓	✓	✓	✓	✓	✓	✓	✓
A	✓	✓	✓	✓	✓	✓	××	✓
MeOH	✓	✓	✓	✓	✓	✓	××	✓
BL	×	×	✓✓	✓✓	×	×	×	✓✓
FUA	×	×	×	×	×	×	×	×
MCPD	×	×	×	×	×	✓✓	×	✓✓
BEL	×	×	×	×	×	×	×	×
FUE	×	×	×	×	×	×	×	×
CRA	×	×	×	×	×	×	×	×

Table 95 ***Calculation of Percentage Difference from 'Model' (No catalyst) Hydroxyacetaldehyde, Levoglucosan and Acetic Acid Content for Non-Catalytic Runs***

	No Catalyst										
Run No. (EHS..)	33	50	16	16r	17	17r	21	22	23	20	42
Temperature of Run (°C)	453.13	475.36	477.62	477.62	490.79	490.79	500.77	522.91	522.96	549.18	447.32
Actual Hydroxyacetaldehyde Content (%)	20.17	22.39	18.49	18.49	20.62	20.62	15.77	17.73	18.80	14.99	23.72
Model Hydroxyacetaldehyde Content (%)	21.62	20.09	19.94	19.94	19.07	19.07	18.42	17.03	17.03	15.45	22.02
Percentage Difference[a]	6.70	-11.43	7.27	7.27	-8.12	-8.12	14.37	-4.10	-10.40	2.99	-7.71
									Average	STDev[b]	95%[c]
									-1.03	8.95	19.7
Actual Levoglucosan Content (%)	3.01	4.21	5.06	5.06	4.56	4.56	1.74	1.85	1.96	2.50	4.62
Model Levoglucosan Content (%)	7.21	7.19	7.18	7.18	7.06	7.06	6.92	6.48	6.48	5.70	7.19
Percentage Difference[a]	58.22	41.50	29.55	29.55	35.44	35.44	74.93	71.40	69.81	56.21	35.71
									Average	STDev[b]	95%[c]
									48.89	17.61	38.8
Actual Acetic Acid Content (%)	4.55	5.34	3.86	3.86	4.01	4.01	3.27	3.41	4.12	4.40	5.35
Model Acetic Acid Content (%)	10.87	10.70	10.70	10.70	10.81	10.81	10.99	11.66	11.66	12.96	10.98
Percentage Difference[a]	58.19	50.12	63.96	63.96	62.90	62.90	70.21	70.75	64.69	66.09	51.32
									Average	STDev[b]	95%[c]
									62.28	6.68	

Notes: (a) Percentage Difference between Measured and Model Hydroxyacetaldehyde Content (b) Standard deviation

(c) Standard deviation with a 95 % confidence limit based on 11 points *(Straud, 1987)*.

Table 96 ***Calculation of Percentage Difference from 'Model' (No catalyst) Hydroxyacetaldehyde, Levoglucosan and Acetic Acid Content for Slate Fluid Bed Runs***

	Slate Fluid Bed									
Run No. (EHS..)	31	40	25	25 r	24	29	27	28	28	32
Temperature of Run (°C)	450.96	452.10	473.96	473.96	500.75	501.08	522.02	549.24	549.24	550.48
Actual Hydroxyacetaldehyde Content (%)	11.39	19.81	19.77	19.75	17.52	18.45	16.23	20.32	20.32	10.33
Model Hydroxyacetaldehyde Content (%)	21.77	21.69	20.19	20.19	18.42	18.40	17.08	15.45	15.45	15.38
Percentage Difference[(a)]	47.66	8.67	2.05	2.15	4.90	-0.25	5.01	-31.48	-31.48	32.80
								Average	STDev[(b)]	95%[(c)]
								4.00	24.27	54.1
Actual Levoglucosan Content (%)	1.52	3.77	2.16	4.17	1.85	2.30	1.55	2.21	2.21	1.54
Model Levoglucosan Content (%)	7.21	7.21	7.20	7.20	6.92	6.92	6.50	5.70	5.70	5.65
Percentage Difference[(a)]	78.92	47.78	70.00	42.10	73.35	66.74	76.24	61.29	61.29	72.82
								Average	STDev[(b)]	95%[(c)]
								65.05	12.15	27.1
Actual Acetic Acid Content (%)	2.38	5.51	4.03	5.55	3.17	3.71	3.78	4.00	4.00	2.44
Model Acetic Acid Content (%)	10.91	10.89	10.70	10.70	10.99	10.99	11.62	12.96	12.96	13.04
Percentage Difference[(a)]	78.18	49.45	62.37	48.14	71.11	66.25	67.50	69.18	69.18	81.31
								Average	STDev[(b)]	95%[(c)]
								66.27	10.73	

Notes: as Table 95

Table 97 ***Calculation of Percentage Difference from 'Model' (No catalyst) Hydroxyacetaldehyde, Levoglucosan and Acetic Acid Content for Y-Zeolite in Primary Reactor and Char Co-fed Runs***

	Y-Zeolite in Primary Reactor							Char Co-fed		
Run No. (EHS..)	39	34	34	35	36	37	38	43	57	44
Temperature of Run (°C)	451.40	453.11	453.11	477.91	502.35	525.00	549.73	449.95	501.33	525.54
Actual Hydroxyacetaldehyde Content (%)	13.38	10.44	10.44	13.97	12.13	9.36	10.45	22.83	16.31	20.63
Model Hydroxyacetaldehyde Content (%)	21.74	21.62	21.62	19.92	18.32	16.90	15.42	21.84	18.39	16.87
Percentage Difference[a]	38.44	51.70	51.70	29.86	33.79	44.60	32.23	-4.55	11.27	-22.32
					Average	STDev[b]	95%[c]	Average	STDev[b]	95%[c]
					40.33	9.11	21.5	-5.20	16.80	53.4
Actual Levoglucosan Content (%)	2.78	2.05	2.05	2.37	2.14	2.00	2.04	4.56	3.44	3.90
Model Levoglucosan Content (%)	7.21	7.21	7.21	7.18	6.90	6.43	5.68	7.20	6.92	6.41
Percentage Difference[a]	61.42	71.61	71.61	67.01	68.95	68.83	64.13	36.70	50.19	39.22
					Average	STDev[b]	95%[c]	Average	STDev[b]	95%[c]
					67.65	3.79	9.0	42.04	7.17	22.8
Actual Acetic Acid Content (%)	3.82	3.16	3.16	3.61	2.92	2.30	2.45	5.19	3.54	4.71
Model Acetic Acid Content (%)	10.90	10.87	10.87	10.71	11.02	11.74	12.99	10.93	11.00	11.76
Percentage Difference[a]	64.95	70.92	70.92	66.31	73.50	80.43	81.18	52.52	67.84	59.94
					Average	STDev[b]	95%[c]	Average	STDev[b]	95%[c]
					72.60	6.32		60.10	7.66	

Notes: as Table 95

Table 98 ***Calculation of Percentage Difference from 'Model' (No catalyst) Hydroxyacetaldehyde, Levoglucosan and Acetic Acid Content for Char in Secondary Reactor, Char Fluid Bed, Slate CO-fed and Slate in Secondary Reactor Runs***

	Char in Secondary Reactor				**Char Fluid Bed**			**Slate Co-fed**			**Slate 2ry Reactor**
Run No. (EHS..)	45	46	47	48	52	49	51	54	53	56	55
Temperature of Run (°C)	452.12	501.42	523.95	556.28	474.83	499.43	524.64	478.29	501.49	526.15	503.53
Actual Hydroxyacetaldehyde Content (%)	2.81	3.83	8.67	4.83	7.14	11.76	22.39	12.89	15.43	13.63	9.89
Model Hydroxyacetaldehyde Content (%)	21.69	18.38	16.97	15.04	20.13	18.51	16.92	19.90	18.38	16.83	18.25
Percentage Difference[a]	87.05	79.19	48.88	67.86	64.51	36.46	-32.29	35.20	16.02	19.02	45.78
		Average	STDev[b]	95%[c]	Average	STDev[b]	95%[c]	Average	STDev[b]	95%[c]	Average
		70.74	16.57	46.0	22.89	49.81	158.5	23.41	10.32	32.8	45.78
Actual Levoglucosan Content (%)	2.07	0.88	2.32	1.65	2.00	3.35	4.21	2.53	3.80	3.41	1.57
Model Levoglucosan Content (%)	7.21	6.91	6.45	5.44	7.19	6.94	6.44	7.17	6.91	6.40	6.88
Percentage Difference[a]	71.24	87.23	64.05	69.72	72.17	51.73	34.64	64.78	45.10	46.66	77.20
		Average	STDev[b]	95%[c]	Average	STDev[b]	95%[c]	Average	STDev[b]	95%[c]	Average
		73.06	9.94	27.6	52.85	18.79	59.8	52.18	10.94	34.8	77.20
Actual Acetic Acid Content (%)	2.66	1.18	3.09	1.83	2.14	3.88	5.34	3.31	4.06	2.75	2.69
Model Acetic Acid Content (%)	10.89	11.00	11.70	13.41	10.70	10.96	11.73	10.71	11.00	11.79	11.05
Percentage Difference[a]	75.55	89.27	73.54	86.35	79.97	64.58	54.48	69.13	63.10	76.67	75.68
		Average	STDev[b]	95%[c]	Average	STDev[b]	95%[c]	Average	STDev[b]	95%[c]	Average
		81.18	7.79		66.35	12.84		69.63	6.80		75.68

Notes: as Table 95

Table 99 ***Calculation of Percentage Difference from 'Model' (No catalyst) Pyrolytic Lignin Content for Non-Catalytic Runs***

	No Catalyst										
Run No. (EHS..)	33	50	16	16r	17	17r	21	22	23	20	42
Av. Run Temp (°C)	453.13	475.36	477.62	477.62	490.79	490.79	500.77	522.91	522.96	549.18	447.32
Lignin Ratio (Lignin:Organic Yield)	5.45	8.65	4.93	4.93	5.28	5.28	4.33	5.42	3.11	3.06	3.36
Actual Pyrolytic Lignin Content (%)	3.22	5.28	3.53	3.53	3.39	3.39	2.63	3.44	1.88	1.67	2.16
Model Pyrolytic Lignin Content (%)	9.81	10.97	11.06	11.06	11.48	11.48	11.68	11.78	11.78	11.26	9.43
Percentage Difference between Measured and Model Lignin Content	67.17	51.88	68.06	68.06	70.43	70.43	77.45	70.78	84.08	85.20	77.10
									Average	STDev[(a)]	95%[(b)]
									71.88	9.17	20.1

Notes: (a) Standard deviation

(b) Standard deviation with a 95 % confidence limit based on 11 points *(Straud, 1987)*.

Table 100 Calculation of Percentage Difference from 'Model' (No catalyst) Pyrolytic Lignin Content for Slate Fluid Bed Runs

	Slate Fluid Bed									
Run No. (EHS..)	31	40	25	25r	24	29	27	28	28	32
Av. Run Temp (°C)	450.96	452.10	473.96	473.96	500.75	501.08	522.02	549.24	549.24	550.48
Lignin Ratio (Lignin:Organic Yield)	3.64	3.03	9.28	7.31	3.86	5.51	4.02	3.66	3.66	7.91
Actual Pyrolytic Lignin Content (%)	2.32	1.94	6.05	4.77	2.26	3.57	2.41	1.92	1.92	4.66
Model Pyrolytic Lignin Content (%)	9.67	9.75	10.91	10.91	11.68	11.69	11.78	11.26	11.26	11.21
Percentage Difference between Measured and Model Lignin Content	76.03	80.09	44.51	56.32	80.66	69.49	79.53	82.92	82.92	58.41
								Average	STDev[(a)]	95%[(b)]
								71.09	13.48	30.0

Notes: (a) Standard deviation

(b) Standard deviation with a 95 % confidence limit based on 10 points *(Straud, 1987)*.

Table 101 ***Calculation of Percentage Difference from 'Model' (No catalyst) Pyrolytic Lignin Content for Y-Zeolite in Primary Reactor and Char Co-fed Runs***

	Y-Zeolite in Primary Reactor							Char Co-fed		
Run No. (EHS..)	39	34	34	35	36	37	38	43	57	44
Av. Run Temp (°C)	451.40	453.11	453.11	477.91	502.35	525.00	549.73	449.95	501.33	525.54
Lignin Ratio (Lignin:Organic Yield)	3.84	6.25	6.25	8.56	6.59	5.09	4.59	4.38	8.94	7.24
Actual Pyrolytic Lignin Content (%)	1.99	3.88	3.88	4.90	3.67	2.77	2.29	2.70	6.00	4.36
Model Pyrolytic Lignin Content (%)	9.70	9.81	9.81	11.07	11.71	11.76	11.24	9.61	11.69	11.76
Percentage Difference between Measured and Model Lignin Content	79.48	60.43	60.43	55.72	68.63	76.45	79.64	71.86	48.65	62.93
					Average	STDev[(a)]	95%[(b)]	Average	STDev[(a)]	95%[(b)]
					68.68	10.01	23.7	61.15	11.70	37.2

Notes: (a) Standard deviation

(b) Standard deviation with a 95 % confidence limit based on 7 or 3 points *(Straud, 1987)*.

Table 102 ***Calculation of Percentage Difference from 'Model' (No catalyst) Pyrolytic Lignin Content for Char in Secondary Reactor, Char Fluid Bed, Slate Co-fed and Slate in Secondary Reactor Runs***

	Char in Secondary Reactor				Char Fluid Bed			Slate Co-fed			Slate 2ry Reactor
Run No. (EHS..)	45	46	47	48	52	49	51	54	53	56	55
Av. Run Temp (°C)	452.12	501.42	523.95	556.28	474.83	499.43	524.64	478.29	501.49	526.15	503.53
Lignin Ratio (Lignin:Organic Yield)	7.36	0.16	4.50	5.90	10.61	9.60	9.66	7.24	10.99	9.70	5.79
Actual Pyrolytic Lignin Content (%)	2.24	0.07	2.10	2.61	6.55	5.71	5.28	4.34	6.96	5.81	2.47
Model Pyrolytic Lignin Content (%)	9.75	11.69	11.77	11.00	10.95	11.66	11.77	11.08	11.69	11.75	11.72
Percentage Difference between Measured and Model Lignin Content	77.01	99.41	82.19	76.25	40.14	51.06	55.15	60.87	40.48	50.58	78.90
		Average	STDev[(a)]	95%[(b)]	Average	STDev[(a)]	95%[(b)]	Average	STDev[(a)]	95%[(b)]	Average
		83.72	10.79	30.0	48.78	7.76	24.7	50.64	10.19	32.4	78.90

Notes: (a) Standard deviation

(b) Standard deviation with a 95 % confidence limit based on 4 or 3 points *(Straud, 1987)*.

Appendix J – HPLC Graphical Results

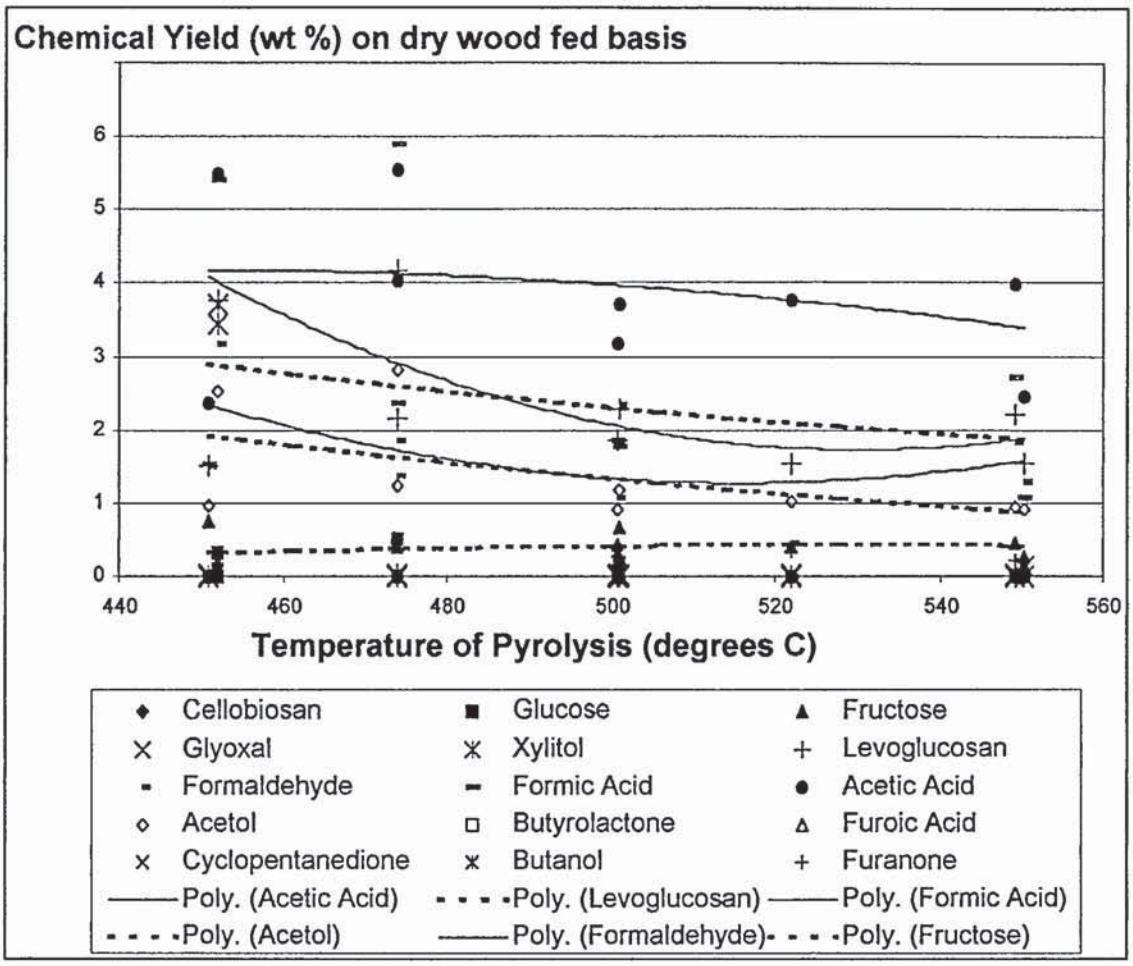

Figure 89 ***Example Chemicals Occurring in Pyrolysis Liquid from a Slate Fluid Bed at Different Temperatures***

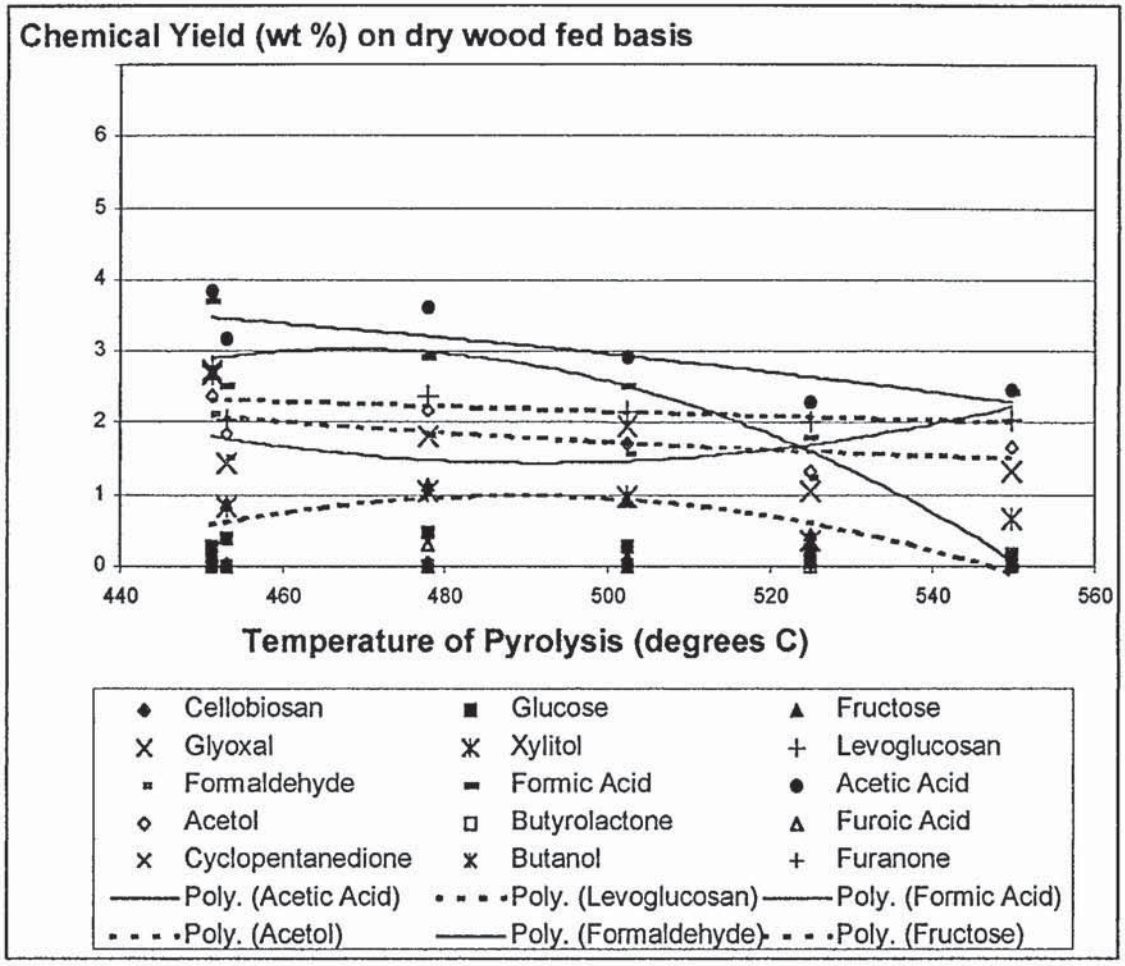

Figure 90 ***Example Chemicals Occurring in Pyrolysis Liquid Y-Zeolite Close-Coupled in the Primary Reactor at Different Temperatures***

Appendix K – Viscosity Tabulated Results

Table 103 Viscosity Calculations for EHS17, Stored at 25 ℃ in Viscometer. Temperature of Run 490.79 ℃. Water Content 6.37 %.

Time from run (hrs)	23.92	48.00	72.00	95.92	120.17	167.12	267.67	341.00	675.95
Viscometer No.	4	4	4	4	4	4	4	4	4
Viscometer Code	9334	9334	9334	9334	9334	9334	9334	9334	9334
Constant, C ((mm^2/s)/s)	0.09621	0.09621	0.09621	0.09621	0.09621	0.09621	0.09621	0.09621	0.09621
Test time #1 seconds	608.77	635.46	736.19	764.00	779.02	798.44	878.34	938.16	1127.13
Test time #2 seconds	64.81	632.59	735.86	762.56	779.02	795.95	872.71	0.00	1108.08
Test time #3 seconds	0.00	0.00	0.00	763.09	0.00	0.00	0.00	0.00	0.00
Average Test Time, t, (s)	606.79	634.03	736.03	763.22	779.02	797.20	875.53	938.16	1117.61
μ_1=Ct (mm^2/s)	58.38	61.00	70.81	73.43	74.95	76.70	84.23	90.26	107.52

Table 104 Calculation of Percentage Difference from 'Model' (No catalyst) Initial Viscosity for Non-Catalytic Runs

	No Catalyst				
Run No. (EHS.)	33	50	17	21	23
Temperature of Run (°C)	453.13	475.36	490.79	500.77	522.96
Actual Initial Viscosity (mm^2/s)	62.99	38.66	58.38	69.89	59.70
Model Initial Viscosity (mm^2/s)	52.59	55.31	57.19	58.41	61.12
Percentage Difference between Measured and Model Initial Viscosity	-19.77	30.10	-2.07	-19.65	2.33
			Average	STDev[(a)]	95%[(b)]
			-1.81	20.47	52.6

Notes: (a) Standard deviation

(b) Standard deviation with a 95 % confidence limit based on 5 points *(Straud, 1987)*.

Table 105 Calculation of Percentage Difference from 'Model' (No catalyst) Initial Viscosity for Slate Fluid Bed Runs

	Slate Fluid Bed					
Run No. (EHS.)	31	40	29	27	28	32
Temperature of Run (°C)	450.96	452.10	501.08	522.02	549.24	550.48
Actual Initial Viscosity (mm^2/s)	48.66	44.87	54.31	50.90	52.82	59.24
Model Initial Viscosity (mm^2/s)	52.33	52.46	58.45	61.01	64.33	64.49
Percentage Difference between Measured and Model Initial Viscosity	7.01	14.47	7.08	16.57	17.89	8.14
				Average	STDev[(a)]	95%[(b)]
				11.86	5.01	12.3

Notes: (a) Standard deviation

(b) Standard deviation with a 95 % confidence limit based on 6 points *(Straud, 1987)*.

Table 106 ***Calculation of Percentage Difference from 'Model' (No catalyst) Initial Viscosity for Y-Zeolite in Primary Reactor and Char Co-fed Runs***

	Y-Zeolite in Primary Reactor				Char Co-fed		
Run No. (EHS.)	34	35	36	37	57	44	
Temperature of Run (°C)	453.11	477.91	502.35	525.00	501.33	525.54	
Actual Initial Viscosity (mm^2/s)	46.35	53.52	62.22	64.67	70.71	81.86	
Model Initial Viscosity (mm^2/s)	52.59	55.62	58.61	61.37	58.48	61.44	
Percentage Difference between Measured and Model Initial Viscosity	11.87	3.78	-6.17	-5.37	-20.92	-33.24	
	Average	STDev[(a)]	95%[(b)]		Average	STDev[(a)]	95%[(b)]
	1.03	8.52	23.7		-27.08	8.72	37.5

Notes: (a) Standard deviation

(b) Standard deviation with a 95 % confidence limit based on 4 or 2 points *(Straud, 1987)*.

Table 107 ***Calculation of Percentage Difference from 'Model' (No catalyst) Initial Viscosity for Char in Secondary Reactor and Char Fluid Bed Runs***

	Char in Secondary Reactor			Char Fluid Bed		
Run No. (EHS.)	45	47	48	52	49	51
Temperature of Run (°C)	452.12	523.95	556.28	474.83	499.43	524.64
Actual Initial Viscosity (mm^2/s)	20.04	90.59	78.89	53.62	59.46	55.02
Model Initial Viscosity (mm^2/s)	52.47	61.24	65.20	55.24	58.25	61.33
Percentage Difference between Measured and Model Initial Viscosity	61.81	-47.91	-21.01	2.93	-2.07	10.29
	Average	STDev[(a)]	95%[(b)]	Average	STDev[(a)]	95%[(b)]
	-2.37	57.19	182.0	3.71	6.22	19.8

Notes: (a) Standard deviation

(b) Standard deviation with a 95 % confidence limit based on 3 points *(Straud, 1987)*.

Table 108 ***Calculation of Percentage Difference from 'Model' (No catalyst) Initial Viscosity for Slate Co-fed and Slate in Secondary Reactor Runs***

	Slate Co-fed			Slate 2ry Reactor
Run No. (EHS..)	54	53	56	55
Temperature of Run (°C)	478.29	501.49	526.15	503.53
Actual Initial Viscosity (mm^2/s)	50.51	58.81	79.08	24.41
Model Initial Viscosity (mm^2/s)	55.66	58.50	61.51	58.75
Percentage Difference between Measured and Model Initial Viscosity	9.25	-0.53	-28.56	58.45
	Average	STDev[(a)]	95%[(b)]	Average
	-6.61	19.63	62.5	58.45

Notes: (a) Standard deviation

(b) Standard deviation with a 95 % confidence limit based on 3 points *(Straud, 1987)*.

Table 109 ***Line Fit for Initial Viscosity Graphs, Figure 91 and Figure 92***

Experiment Set	No. Points	Line Type	R^2 Value
No Catalyst	5	Linear	0.073
Y-Zeolite	4	Linear	0.194
Slate Fluid Bed	6	Linear	0.467
Char 2^{ry} Reactor	3	Linear	0.800
Co-Fed Char	2	Linear	1.000
Char Fluid Bed	3	Linear	0.049
Co-Fed Slate	3	Linear	0.952

Appendix L – Viscosity Graphical Results

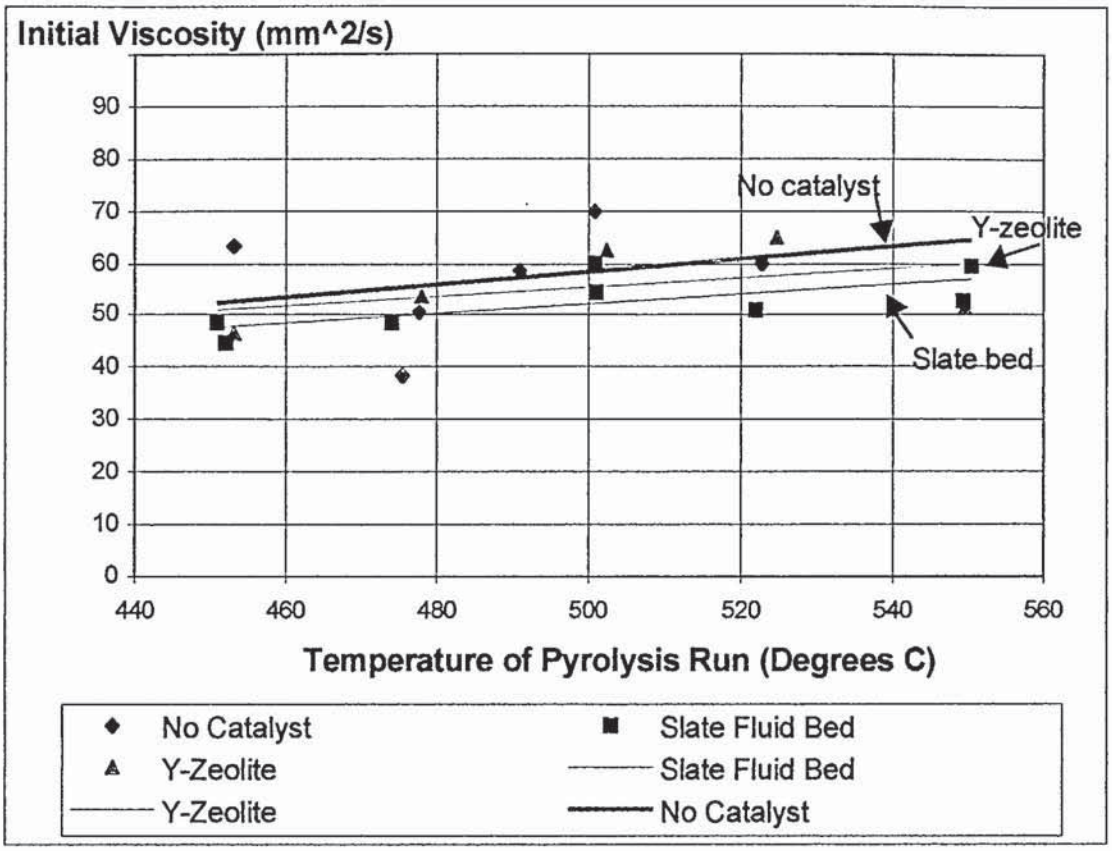

Figure 91 Initial Viscosity of Main Pyrolysis Liquid 1 of 2

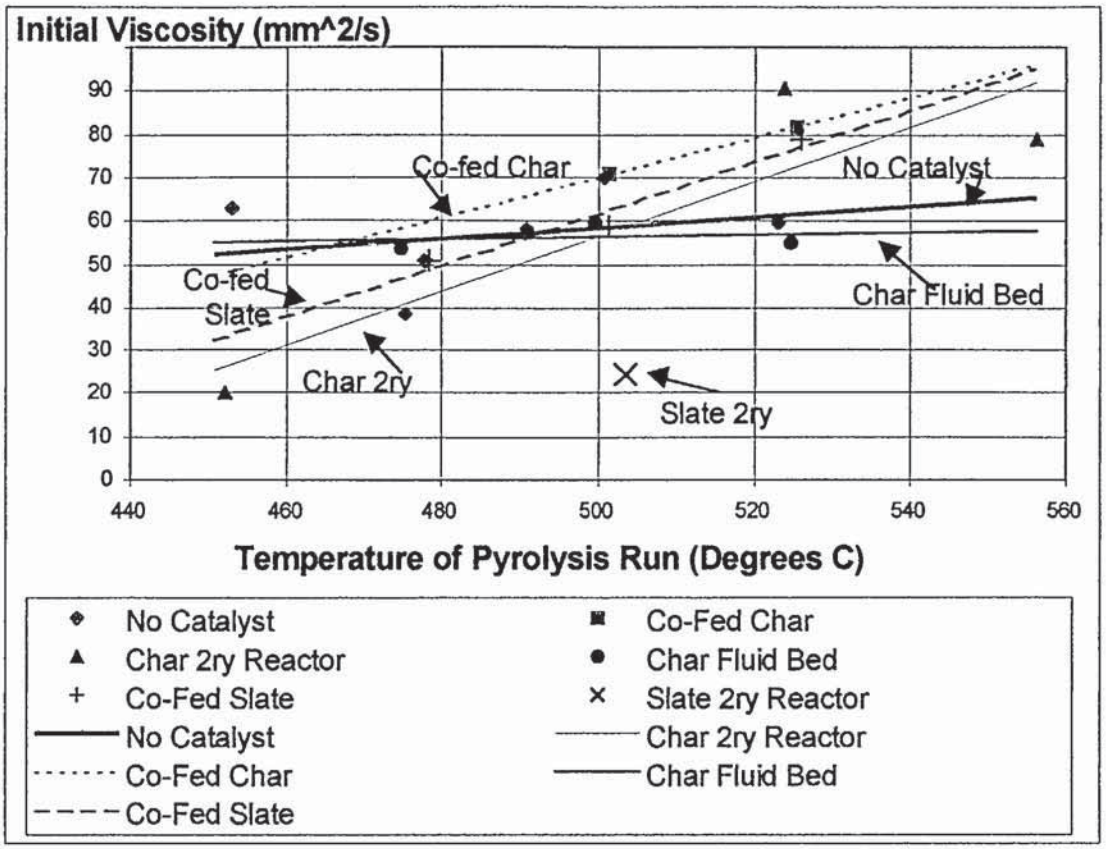

Figure 92 Initial Viscosity of Main Pyrolysis Liquid 2 of 2

Appendix M – Stability Tabulated Results

Table 110 *Calculation of Percentage Difference from 'Model' (No catalyst) AVI and Adjusted AVI for Non-Catalytic Runs*

	No Catalyst				
Run No. (EHS..)	33	50	17	21	23
Temperature of Run (°C)	453.13	475.36	490.79	500.77	522.96
Actual AVI (mm^2/s)	1.53	2.34	1.38	2.27	2.48
Model AVI (mm^2/s)	1.46	1.74	1.94	2.07	2.36
Percentage Difference between Measured and Model AVI	-4.62	-33.93	29.13	-9.44	-5.14
			Average	STDev[(a)]	95%[(b)]
			-4.80	22.48	71.5
Actual Adjusted AVI (mm^2/s)	0.79	2.84	0.94	1.57	1.33
Model Adjusted AVI (mm^2/s)	1.27	1.34	1.39	1.42	1.48
Percentage Difference between Measured and Model Adjusted AVI	37.69	-111.86	32.20	-10.53	10.11
			Average	STDev[(a)]	95%[(b)]
			-8.48	60.88	193.7

Notes: (a) Standard deviation

(b) Standard deviation with a 95 % confidence limit based on 5 points *(Straud, 1987)*.

Table 111 ***Calculation of Percentage Difference from 'Model' (No catalyst) AVI and Adjusted AVI for Slate Fluid Bed Runs***

	Slate Fluid Bed					
Run No. (EHS.)	31	40	29	27	28	32
Temperature of Run (°C)	450.96	452.10	501.08	522.02	549.24	550.48
Actual AVI (mm^2/s)	1.96	1.51	1.42	1.20	1.51	2.08
Model AVI (mm^2/s)	1.43	1.44	2.08	2.35	2.70	2.71
Percentage Difference between Measured and Model AVI	-37.03	-4.49	31.46	49.07	43.91	23.46
				Average	STDev[(a)]	95%[(b)]
				17.73	32.81	80.3
Actual Adjusted AVI (mm^2/s)	1.34	1.23	0.93	0.91	1.18	1.08
Model Adjusted AVI (mm^2/s)	1.27	1.27	1.42	1.48	1.56	1.57
Percentage Difference between Measured and Model Adjusted AVI	-5.69	3.01	34.31	38.30	24.35	30.70
				Average	STDev[(a)]	95%[(b)]
				20.83	17.99	44.0

Notes: (a) Standard deviation

(b) Standard deviation with a 95 % confidence limit based on 6 points *(Straud, 1987)*.

Table 112 ***Calculation of Percentage Difference from 'Model' (No catalyst) AVI and Adjusted AVI for Y-Zeolite in Primary Reactor and Char Co-fed Runs***

	Y-Zeolite in Primary Reactor				Char Co-fed		
Run No. (EHS.)	34	35	36	37	57	44	
Temperature of Run (°C)	453.11	477.91	502.35	525.00	501.33	525.54	
Actual AVI (mm^2/s)	1.38	1.06	1.70	1.84	1.41	1.46	
Model AVI (mm^2/s)	1.46	1.78	2.09	2.39	2.08	2.39	
Percentage Difference between Measured and Model AVI	5.56	40.46	19.01	22.97	32.39	38.96	
	Average	STDev[(a)]	95%[(b)]		Average	STDev[(a)]	95%[(b)]
	22.00	14.39	40.0		35.67	4.64	20.0
Actual Adjusted AVI (mm^2/s)	1.17	0.71	0.96	1.04	0.73	0.48	
Model Adjusted AVI (mm^2/s)	1.27	1.35	1.42	1.49	1.42	1.49	
Percentage Difference between Measured and Model Adjusted AVI	8.26	47.06	32.68	29.92	48.21	67.73	
	Average	STDev[(a)]	95%[(b)]		Average	STDev[(a)]	95%[(b)]
	29.48	16.02	44.5		57.97	13.80	59.4

Notes: (a) Standard deviation

(b) Standard deviation with a 95 % confidence limit based on 4 or 2 points *(Straud, 1987)*.

Table 113 ***Calculation of Percentage Difference from 'Model' (No catalyst) AVI and Adjusted AVI for Char in Secondary Reactor and Char Fluid Bed Runs***

	Char in Secondary Reactor			Char Fluid Bed		
Run No. (EHS.)	45	47	48	52	49	51
Temperature of Run (°C)	452.12	523.95	556.28	474.83	499.43	524.64
Actual AVI (mm^2/s)	0.58	4.04	2.65	1.04	1.39	1.26
Model AVI (mm^2/s)	1.44	2.37	2.79	1.74	2.06	2.38
Percentage Difference between Measured and Model AVI	59.96	-70.15	4.93	40.43	32.34	47.26
	Average	STDev[(a)]	95%[(b)]	Average	STDev[(a)]	95%[(b)]
	-1.76	65.31	207.8	40.01	7.47	23.8
Actual Adjusted AVI (mm^2/s)	1.42	2.10	1.38	0.60	0.75	0.86
Model Adjusted AVI (mm^2/s)	1.27	1.49	1.58	1.34	1.41	1.49
Percentage Difference between Measured and Model Adjusted AVI	-12.13	-41.22	12.52	55.36	47.20	41.88
	Average	STDev[(a)]	95%[(b)]	Average	STDev[(a)]	95%[(b)]
	-13.61	26.90	85.6	48.15	6.79	21.6

Notes: (a) Standard deviation

(b) Standard deviation with a 95 % confidence limit based on 3 points *(Straud, 1987)*.

Table 114 ***Calculation of Percentage Difference from 'Model' (No catalyst) AVI and Adjusted AVI for Slate Co-fed and Slate in Secondary Reactor Runs***

	Slate Co-fed			Slate 2ry Reactor
Run No. (EHS..)	54	53	56	55
Temperature of Run (°C)	478.29	501.49	526.15	503.53
Actual AVI (mm^2/s)	1.84	2.15	2.58	2.14
Model AVI (mm^2/s)	1.78	2.08	2.40	2.11
Percentage Difference between Measured and Model AVI	-3.20	-3.08	-7.43	-1.43
	Average	STDev[(a)]	95%[(b)]	Average
	-4.57	2.48	7.9	-1.43
Actual Adjusted AVI (mm^2/s)	1.21	1.02	1.35	2.15
Model Adjusted AVI (mm^2/s)	1.35	1.42	1.49	1.42
Percentage Difference between Measured and Model Adjusted AVI	10.41	28.12	9.77	-50.71
	Average	STDev[(a)]	95%[(b)]	Average
	16.10	10.41	33.1	-50.71

Notes: (a) Standard deviation

(b) Standard deviation with a 95 % confidence limit based on 3 points *(Straud, 1987)*.

Table 115 ***Line Fit for Aston Viscosity Index Graphs, Figure 93 and Figure 94***

Experiment Set	No. Points	Line Type	R^2 Value
No Catalyst	5	Linear	0.338
Y-Zeolite	4	Linear	0.546
Slate Fluid Bed	6	Linear	0.012
Char 2^{ry} Reactor	3	Linear	0.568
Co-Fed Char	2	Linear	1.000
Char Fluid Bed	3	Linear	0.370
Co-Fed Slate	3	Linear	0.994

Table 116 Line Fit for Adjusted Aston Viscosity Index Graphs, Figure 95 and Figure 96

Experiment Set	No. Points	Line Type	R^2 Value
No Catalyst	5	Linear	0.008
Y-Zeolite	4	Linear	0.365
Slate Fluid Bed	6	Linear	0.118
Char 2^{ry} Reactor	3	Linear	0.027
Co-Fed Char	2	Linear	1.000
Char Fluid Bed	3	Linear	0.995

Appendix N – Stability Graphical Results

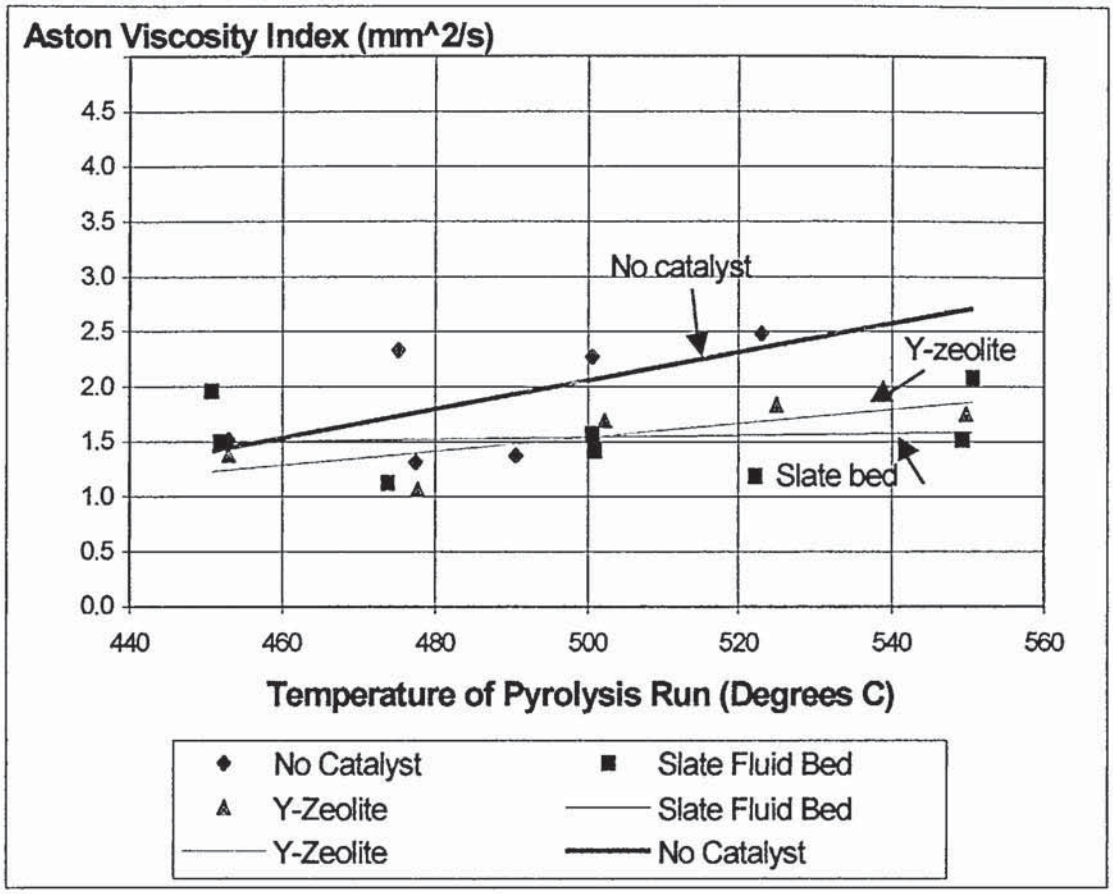

Figure 93 Aston Viscosity Index of Pyrolysis Liquid, 1 of 2

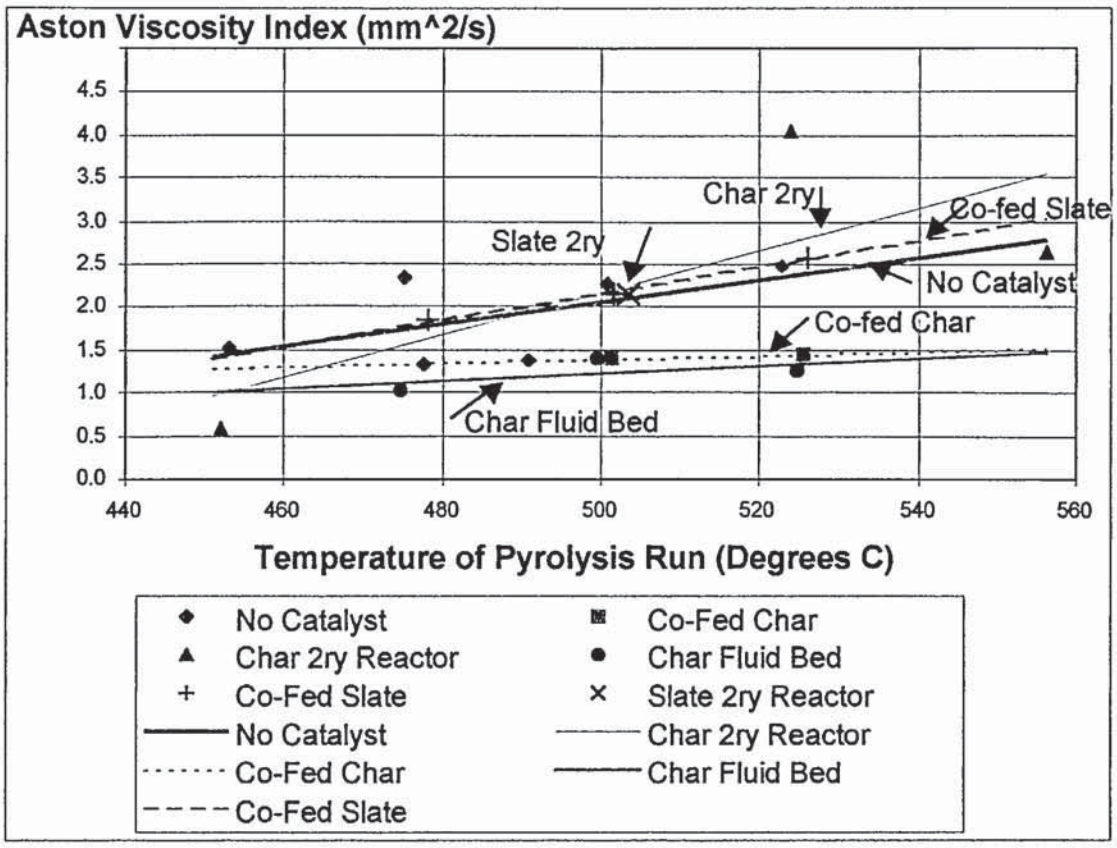

Figure 94 Aston Viscosity Index of Pyrolysis Liquid, 2 of 2

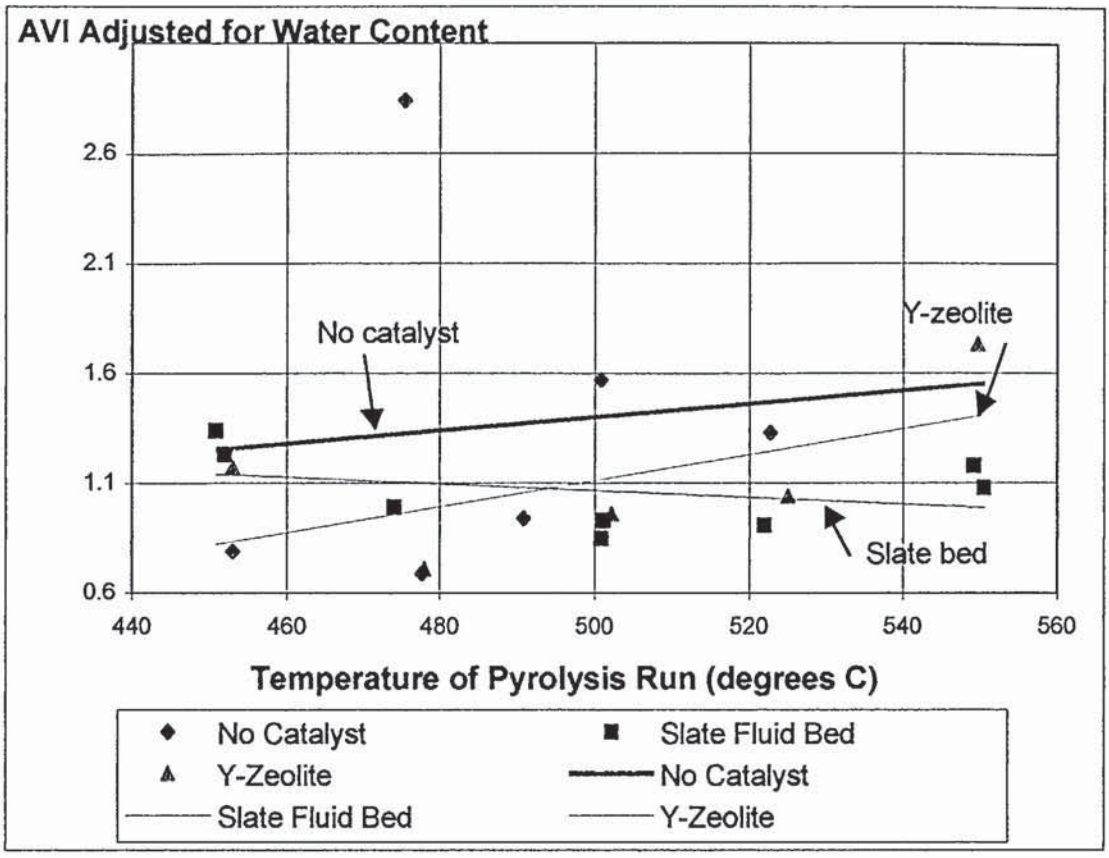

Figure 95 AVI Adjusted for Water Content of Pyrolysis Liquid, 1 of 2

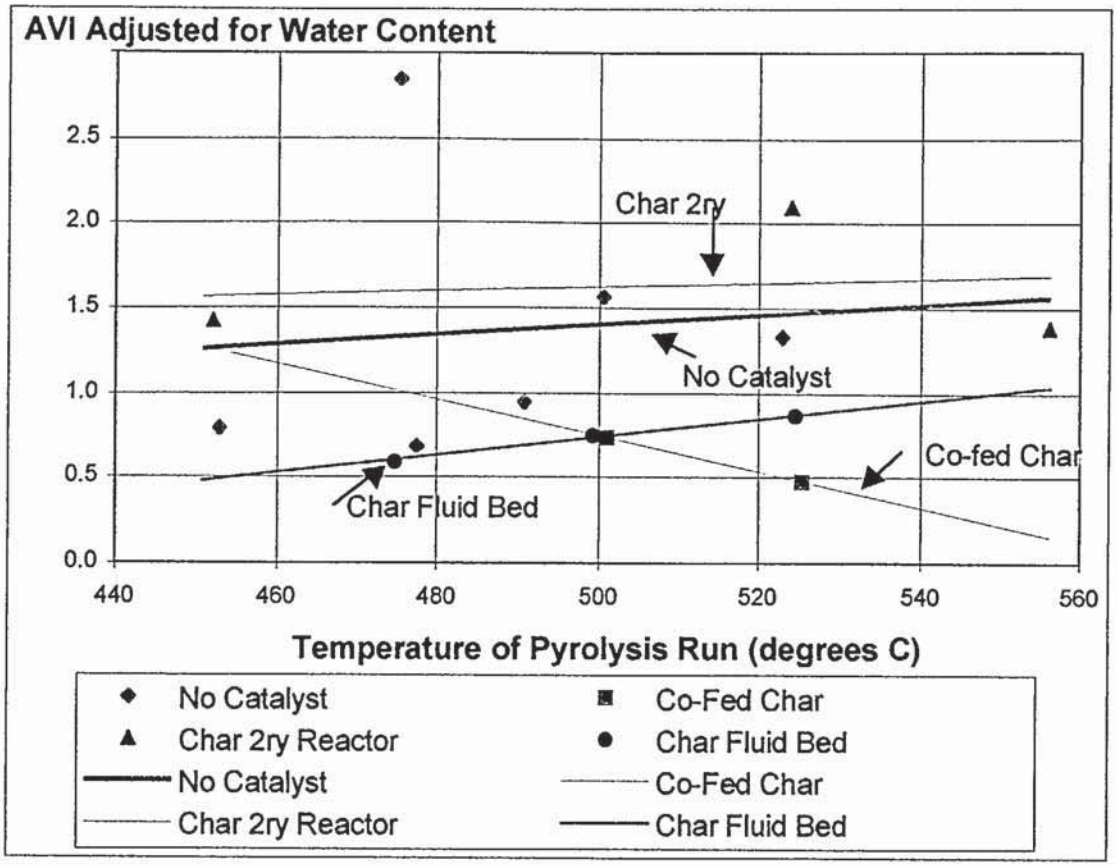

Figure 96 AVI Adjusted for Water Content of Pyrolysis Liquid, 2 of 2

Appendix P – Large Fluid Bed Viscosity and Homogeneity Testing Results

Table 117 Viscosity and Homogeneity Results for Pyrolysis Liquid from Run LFB46

Sample Position	Time from End of Run (h)	Initial Viscosity (mm^2/s)	Secondary Viscosity (mm^2/s)	Water Content (%)	Aston Viscosity Index	Adjusted Aston Viscosity Index
Shake a	161.0	34.6	64.4	20.6	0.86	0.91
Shake a	258.0	37.2	72.2	30.2	0.94	1.90
Shake a	258.5	37.6	70.2	21.9	0.87	1.03
Shake a	261.0	44.1	74.6	17.8	0.69	0.54
Top	1145.5	52.9	75.0	23.2	0.42	0.55
Mid	1145.5	54.1	82.1	20.6	0.52	0.55
Bottom	1145.5	56.7	75.9	20.1	0.34	0.34
Shake a	1145.5	54.1	71.5	20.8	0.32	0.35
Shake b	1145.5	52.5	85.8	19.8	0.63	0.62
Top	1507.5	45.3	-	-	-	-
Mid	1507.5	45.5	-	-	-	-
Bottom	1507.5	46.6	-	-	-	-
Shake a	1507.5	46.1	-	-	-	-
Shake b	1507.5	45.7	-	-	-	-
Top	2080.5	57.6	77.9	14.9	0.35	0.17
Mid	2080.5	56.6	73.2	8.4	0.29	-0.05
Bottom	2080.5	57.3	92.7	14.9	0.62	0.31
Shake a	2080.5	56.7	74.2	8.9	0.31	-0.04
Shake b	2080.5	58.5	-	13.9	-	-

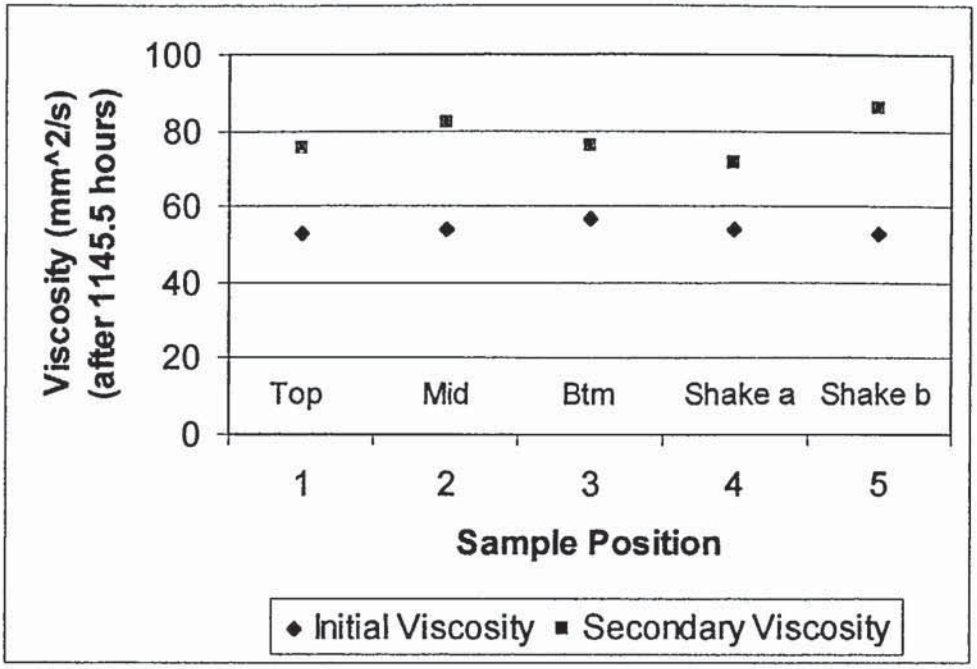

Figure 97 *Initial and Secondary Viscosities of LFB46 Pyrolysis Liquid after 48 Days*

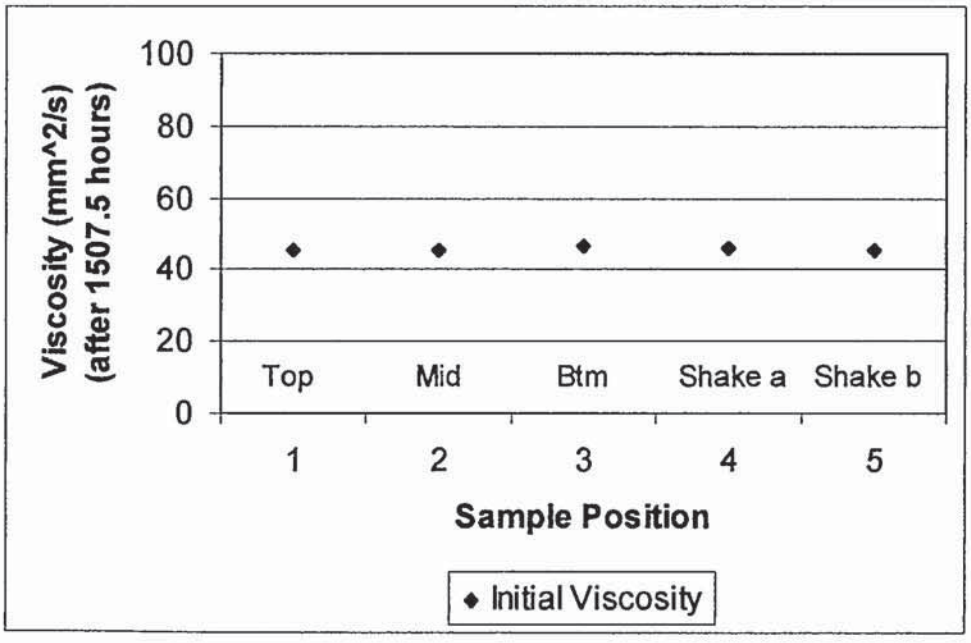

Figure 98 *Initial Viscosity of LFB46 Pyrolysis Liquid after 63 Days*

(No secondary results due to Karl Fischer apparatus problems)

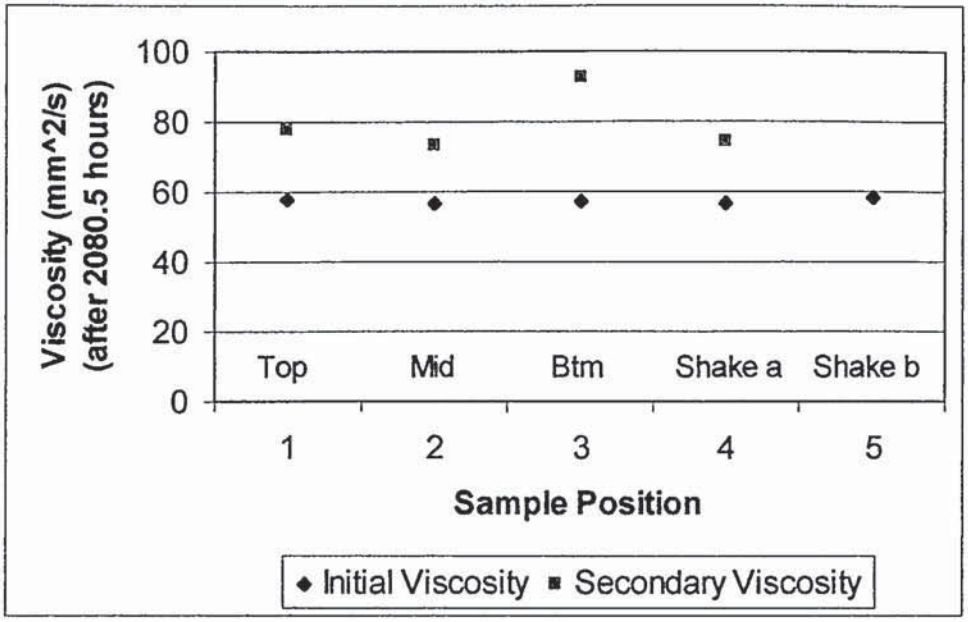

Figure 99 *Initial and Secondary Viscosities of LFB46 Pyrolysis Liquid after 87 Days*

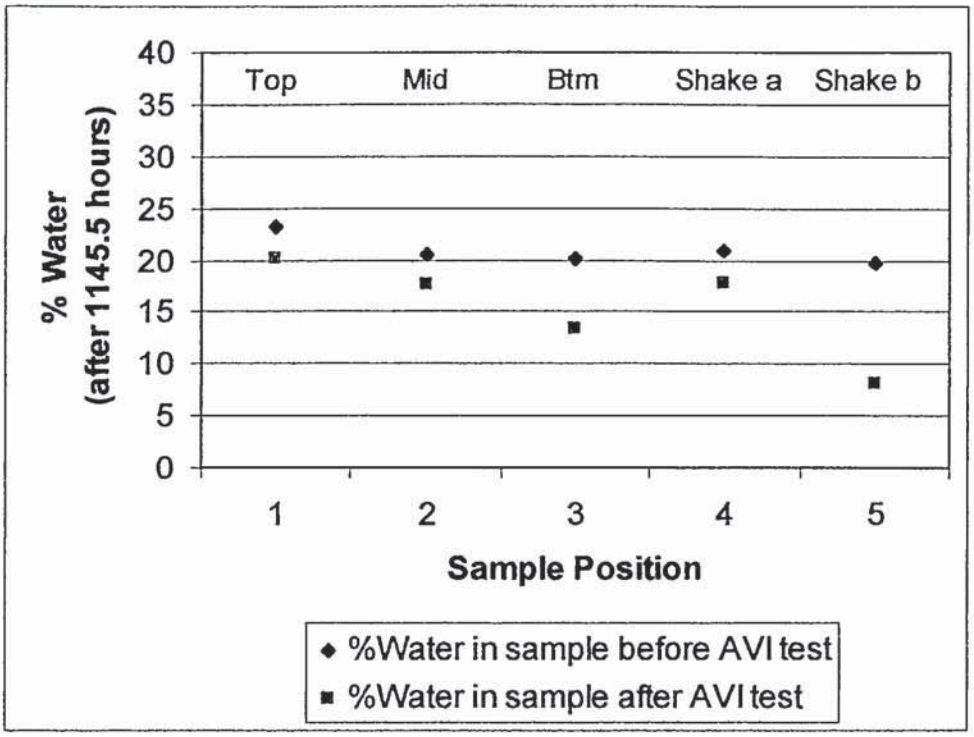

Figure 100 Percentage Water Content of LFB46 Pyrolysis Liquid after 48 Days, before and after Stability Testing

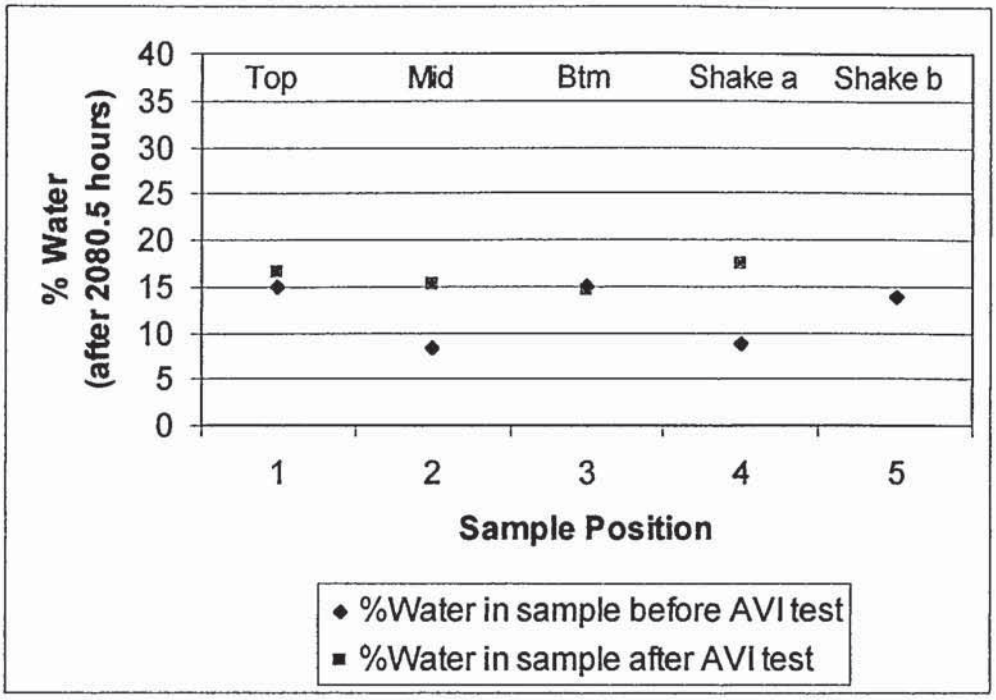

Figure 101 *Percentage Water Content of LFB46 Pyrolysis Liquid after 87 Days, before and after Stability Testing*

Procedure for Homogeneity Testing

1) Record the time that the pyrolysis run ends.
2) Store pyrolysis liquid in screw-lidded storage container made of opaque polypropylene. Dimensions shown in Figure 102. Store in dark cupboard.
3) Oven-dry four 15 ml sample jars and lids, then cool in desiccater.
4) Using a pipette, take 15 ml of pyrolysis liquid from the following locations; put them in the dried sample jars, seal and label them and record the time of sampling:
   a) top: 2 cm from top liquid surface
   b) mid: centre of vessel
   c) bottom: 2 cm from bottom of vessel
5) Shake the inverted, closed vessel and pipette a sample from the centre of it (sample name: 'shake a').
6) Re-shake the inverted, closed vessel and pipette another sample from the centre of it (sample name: 'shake b').
7) Return the storage vessel to the dark cupboard with the lid sealed.
8) Test each sample for water content, initial viscosity and secondary viscosity as described in Chapters 5, 6 and 7.
9) Repeat steps 3) to 8) at suitable time intervals, long enough for the pyrolysis liquid to fully settle following being shaken.

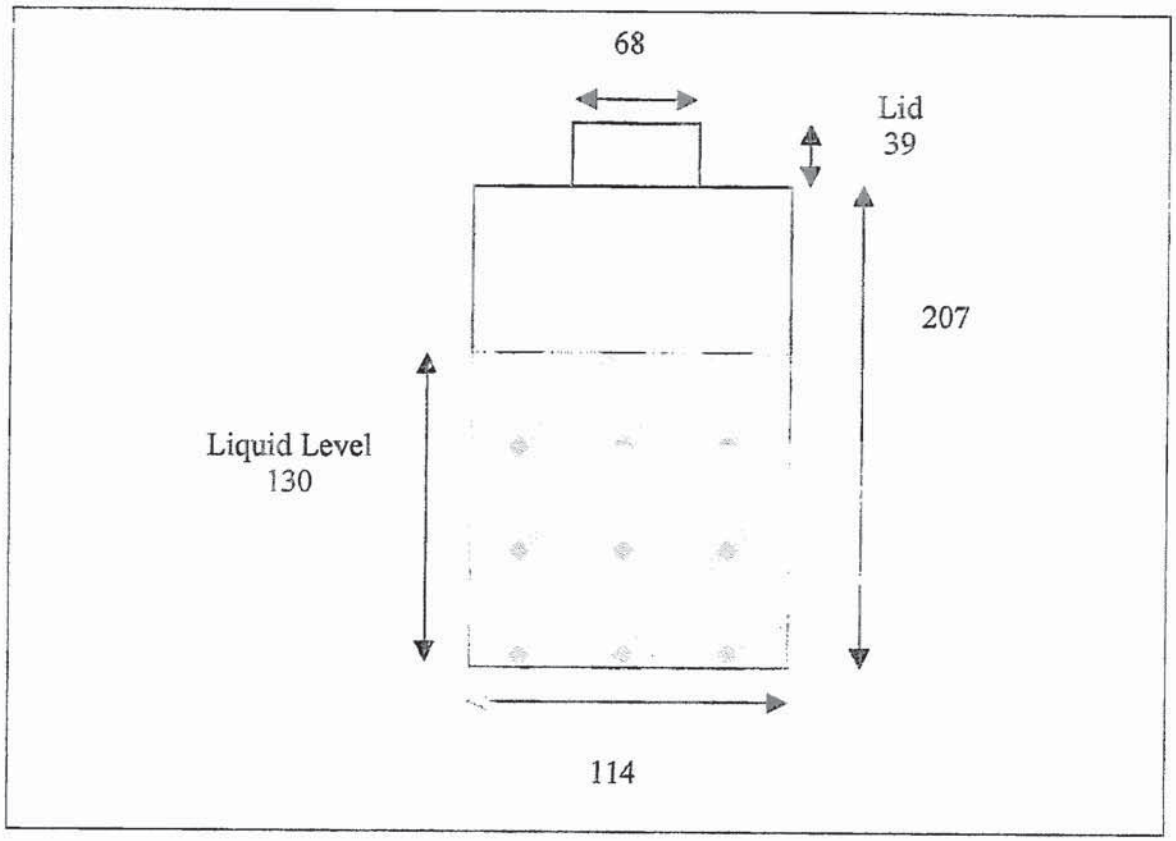

Figure 102 ***Dimensions of Pyrolysis Liquid Storage Vessel for Large Fluid Bed Liquid to be used for Homogeneity Testing (in mm, not to scale)***

Appendix Q – Scanning Electron Microscopy Pictures

The length of the white line in each picture represents the length shown to the right of each picture, in µm.

Figure 103 BDH-Y Zeolite: Fresh

Figure 104 BDH-Y Zeolite: 1 Use and Regeneration

Figure 105 BDH-Y Zeolite: Coked

Figure 106 BDH-Y Zeolite: 1 Hour Regeneration

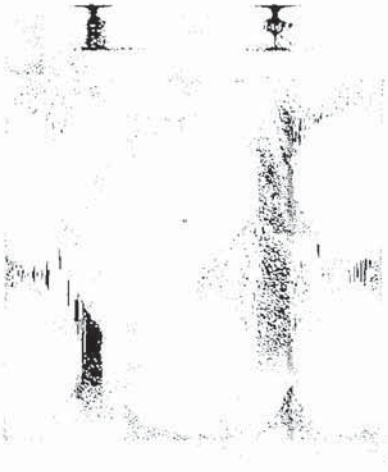

ure 107 ...H-Y Z...: 24 Hour Regeneration

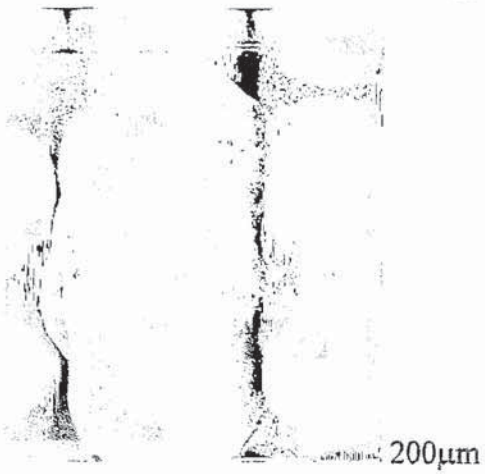

Figure 108 Fluid Bed Sand: Coked

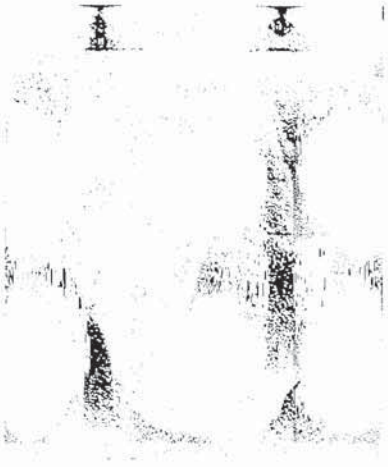

...re 109 ...id Bed ...: 1 Hour Regeneration

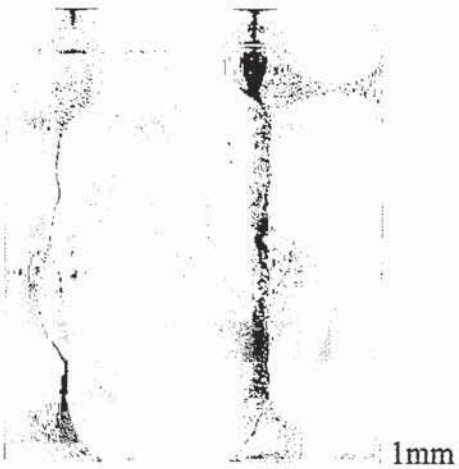

Figure 110 Fluid Bed Sand: 24 Hour Regeneration

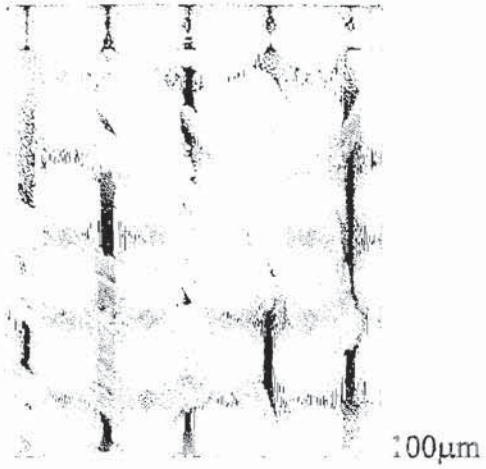

Figure 111 Char from Charpot

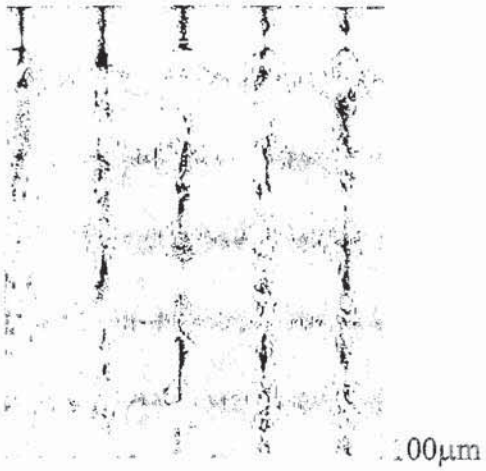

Figure 112 Expanded Slate: Coked

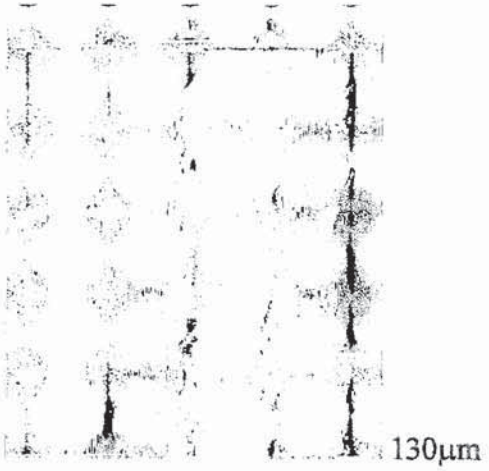

Figure 113 Expanded Slate: 1 Hour Regeneration

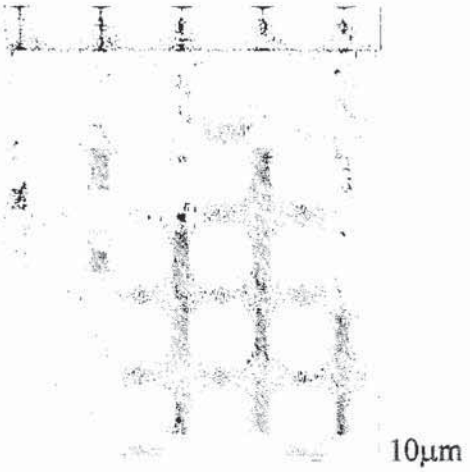

Figure 114 Expanded Slate: 24 Hour Regeneration

Figure 115 [illegible]

Figure 116 Field Bed Sand: Coated

Figure 117 Field Bed Sand: 1st Wash
[illegible]

Figure 118 Field Bed Sand: 2nd Wash
[illegible]

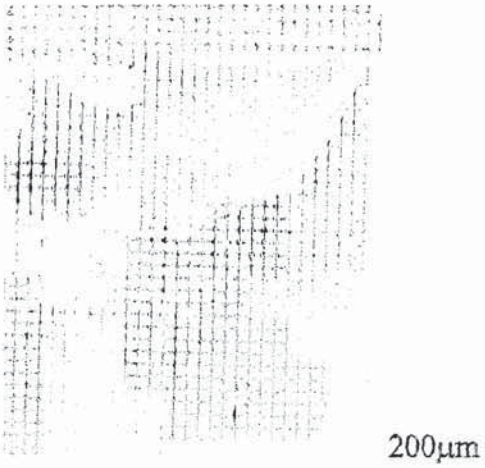

Figure 119 Char from Charpot

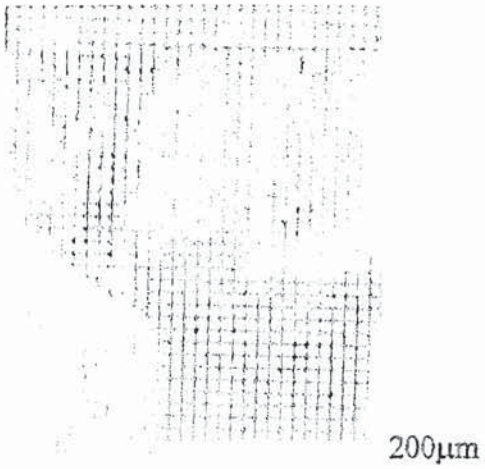

Figure 120 Char from Filter Paper

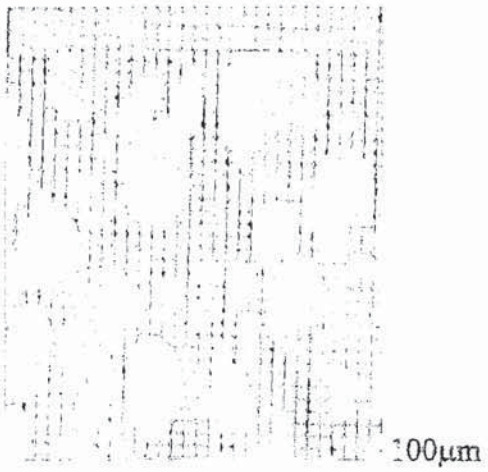

Figure 121 Grace ZSM-5 Zeolite

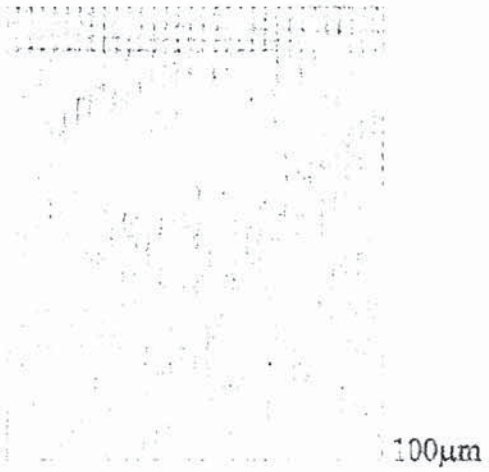

Figure 122 Char from Charpot

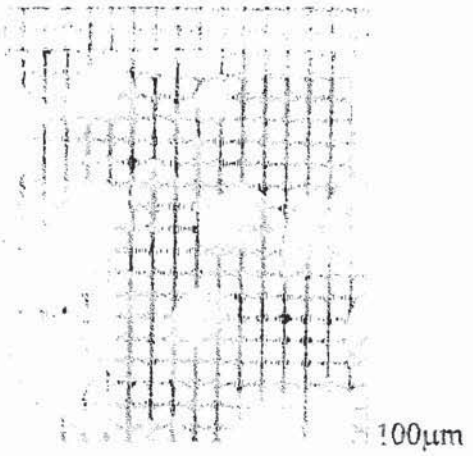

Figure 123 Char from Filter Paper

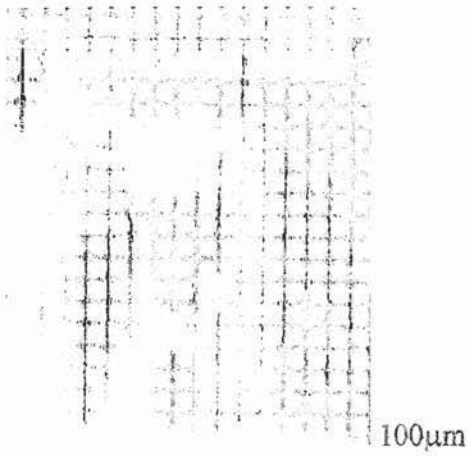

Figure 124 Char from [illegible]

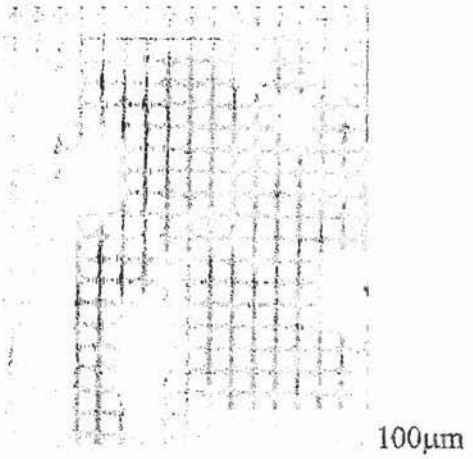

Figure 125 Char from Filter Paper

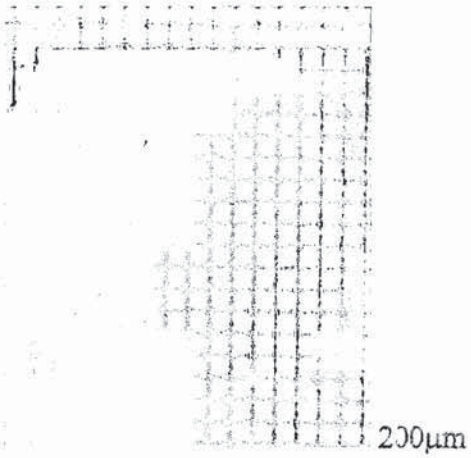

Figure 126 Fluid Bed Sand and BDH-Y Zeolite

Appendix R – Catalyst Screening Chromatographs and Acetate Overlay

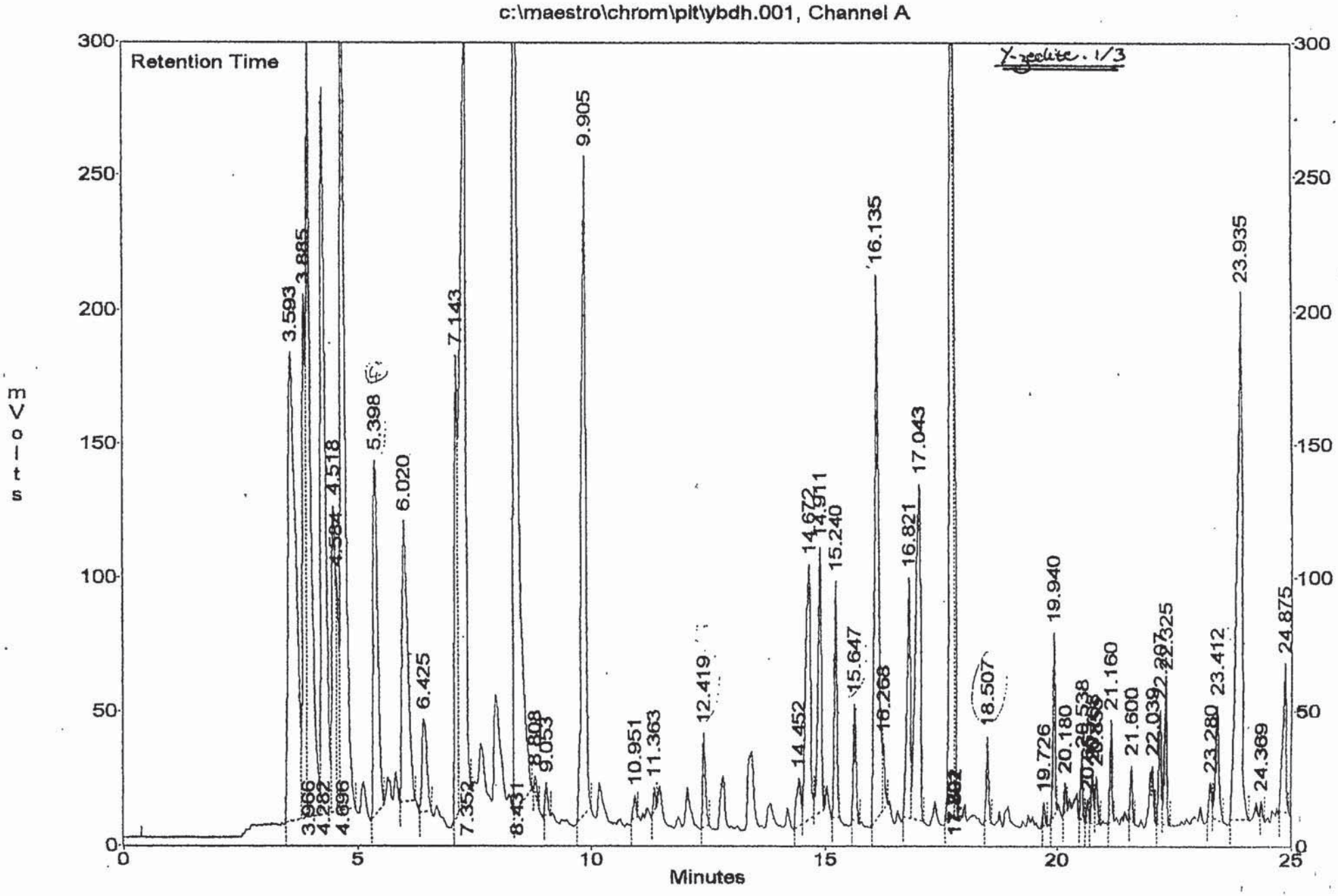
c:\maestro\chrom\plt\ybdh.001, Channel A
Retention Time
Y-zeolite. 1/3
mV
Minutes
3.593
3.885
3.966
4.282
4.518
4.696
5.398
6.020
6.425
7.143
7.352
8.451
9.053
9.905
10.951
11.363
12.419
14.452
14.672
14.911
15.240
15.647
16.135
16.268
16.821
17.043
18.507
19.726
19.940
20.180
21.160
21.600
22.039
22.325
23.280
23.412
23.935
24.369
24.875

OHNE KAT

c:\maestro\chrom\pit\pine.001, Channel A

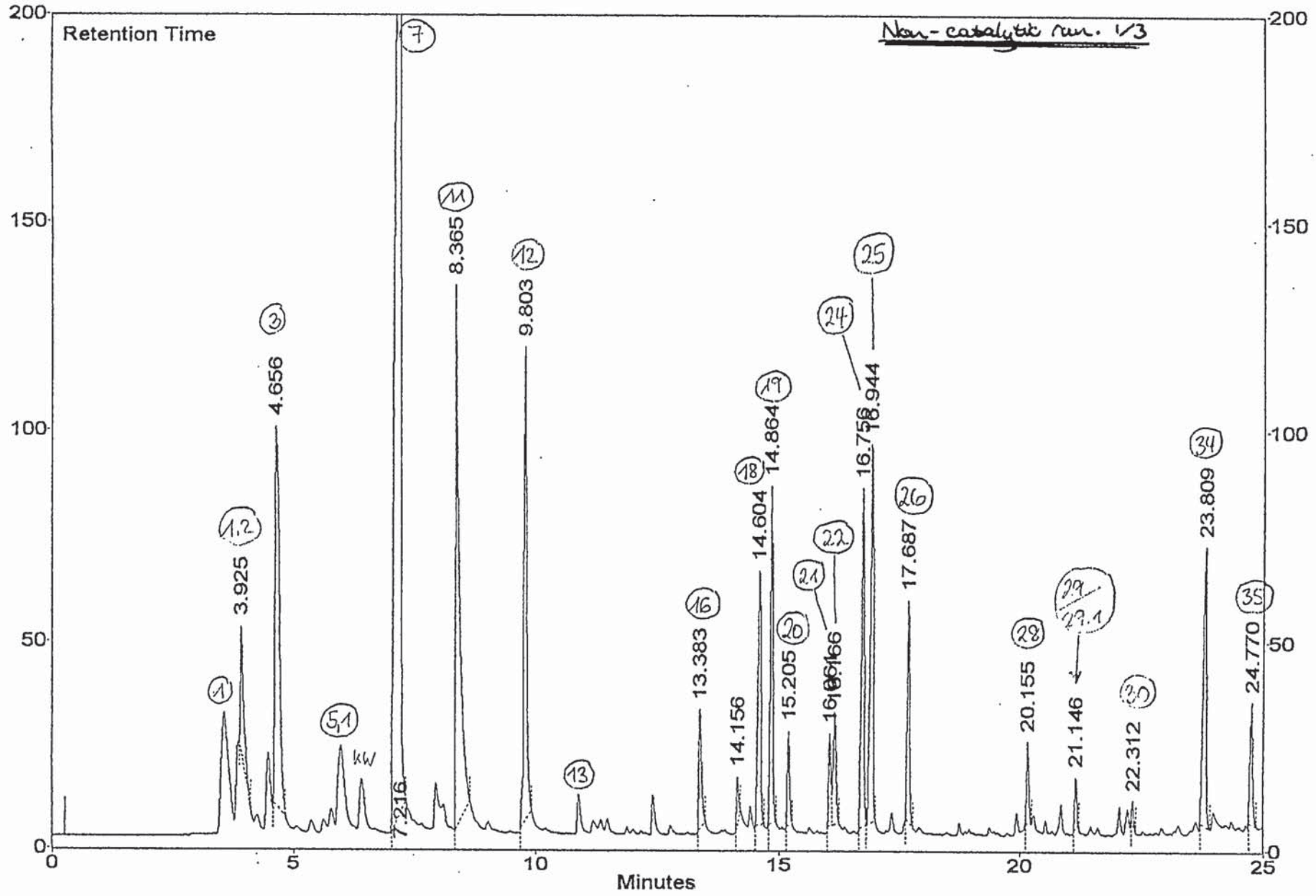

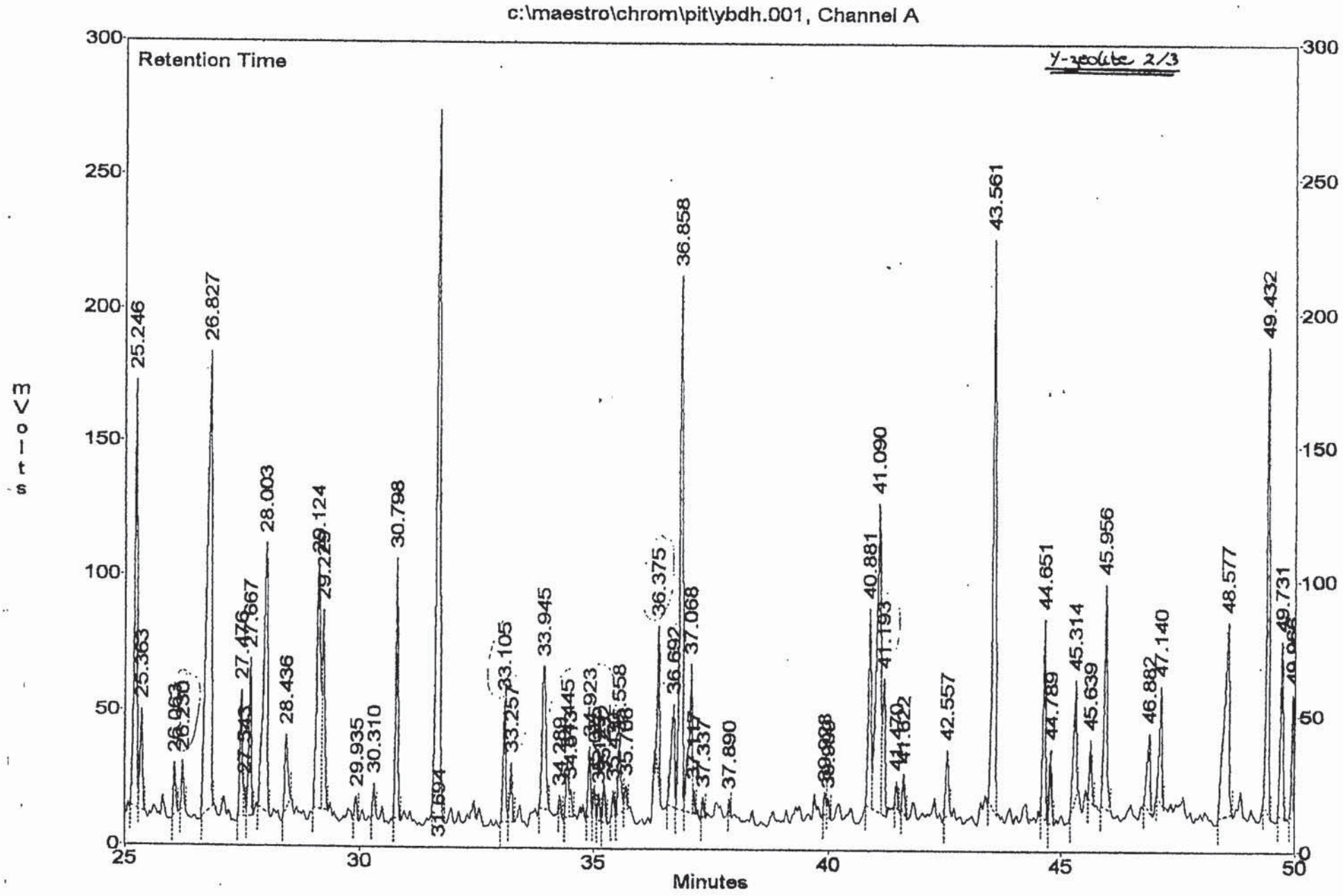
c:\maestro\chrom\pit\ybdh.001, Channel A
Retention Time
Y-zeolite 2/3
Minutes
25.246
25.363
26.827
28.003
28.436
29.124
29.935
30.310
30.798
31.694
33.105
33.257
33.945
36.375
36.692
36.858
37.068
37.317
37.890
40.881
41.090
41.193
42.557
43.561
44.651
44.789
45.314
45.639
45.956
46.882
47.140
48.577
49.432
49.731

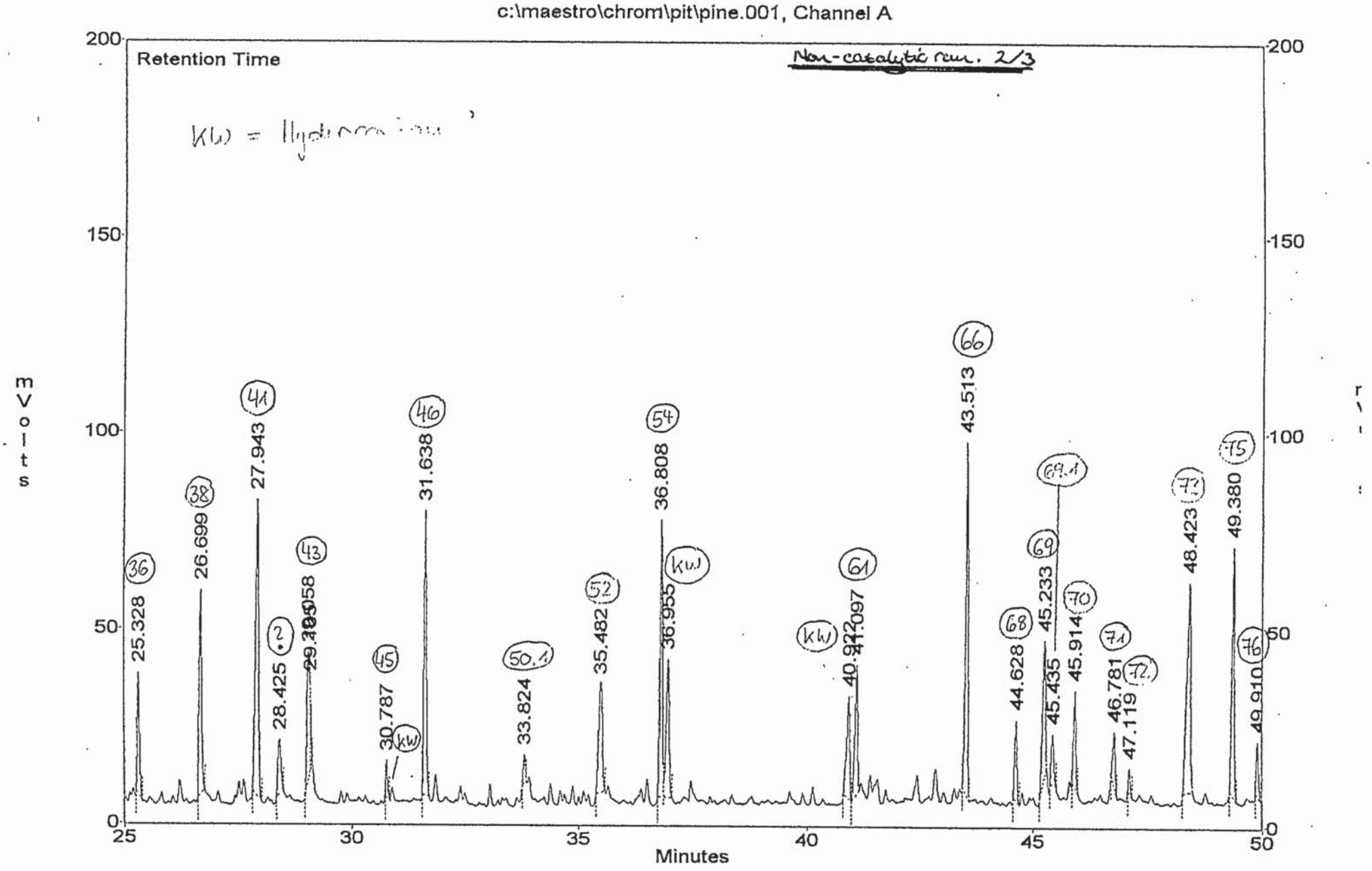
c:\maestro\chrom\pit\pine.001, Channel A
Retention Time
Non-catalytic run. 2/3
KW = Hydrocarbons
Minutes
25.328
26.699
27.943
28.425
30.787
31.638
33.824
35.482
36.808
36.955
40.922
41.097
43.513
44.628
45.233
45.435
45.914
46.781
47.119
48.423
49.380
49.910

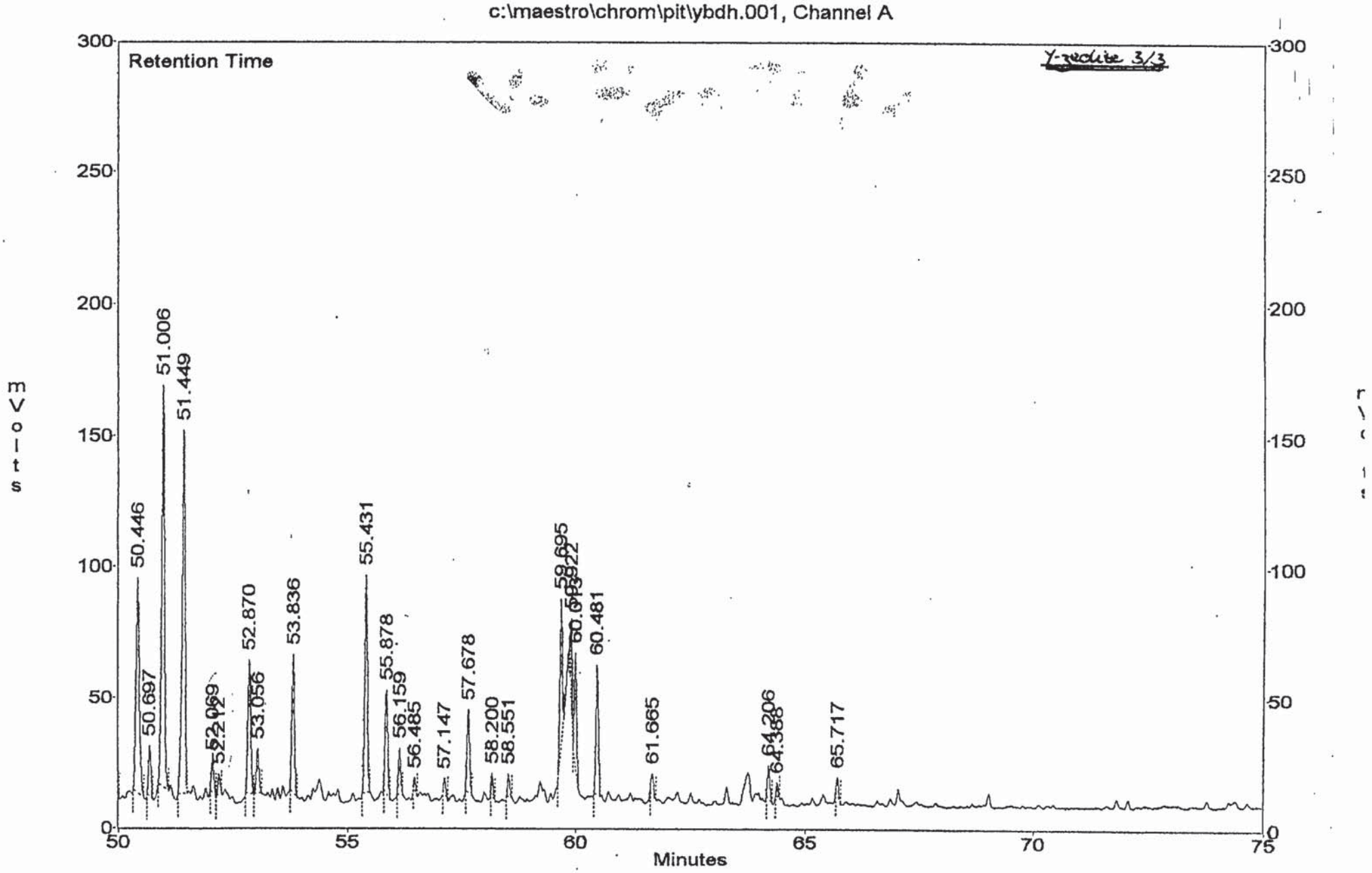
c:\maestro\chrom\pit\ybdh.001, Channel A
Retention Time
Y-zeolite 3/3
mAU
Minutes
50.446
50.697
51.006
51.449
52.069
52.202
52.870
53.056
53.836
55.431
55.878
56.159
56.485
57.147
57.678
58.200
58.551
59.695
60.481
61.665
64.206
64.388
65.717

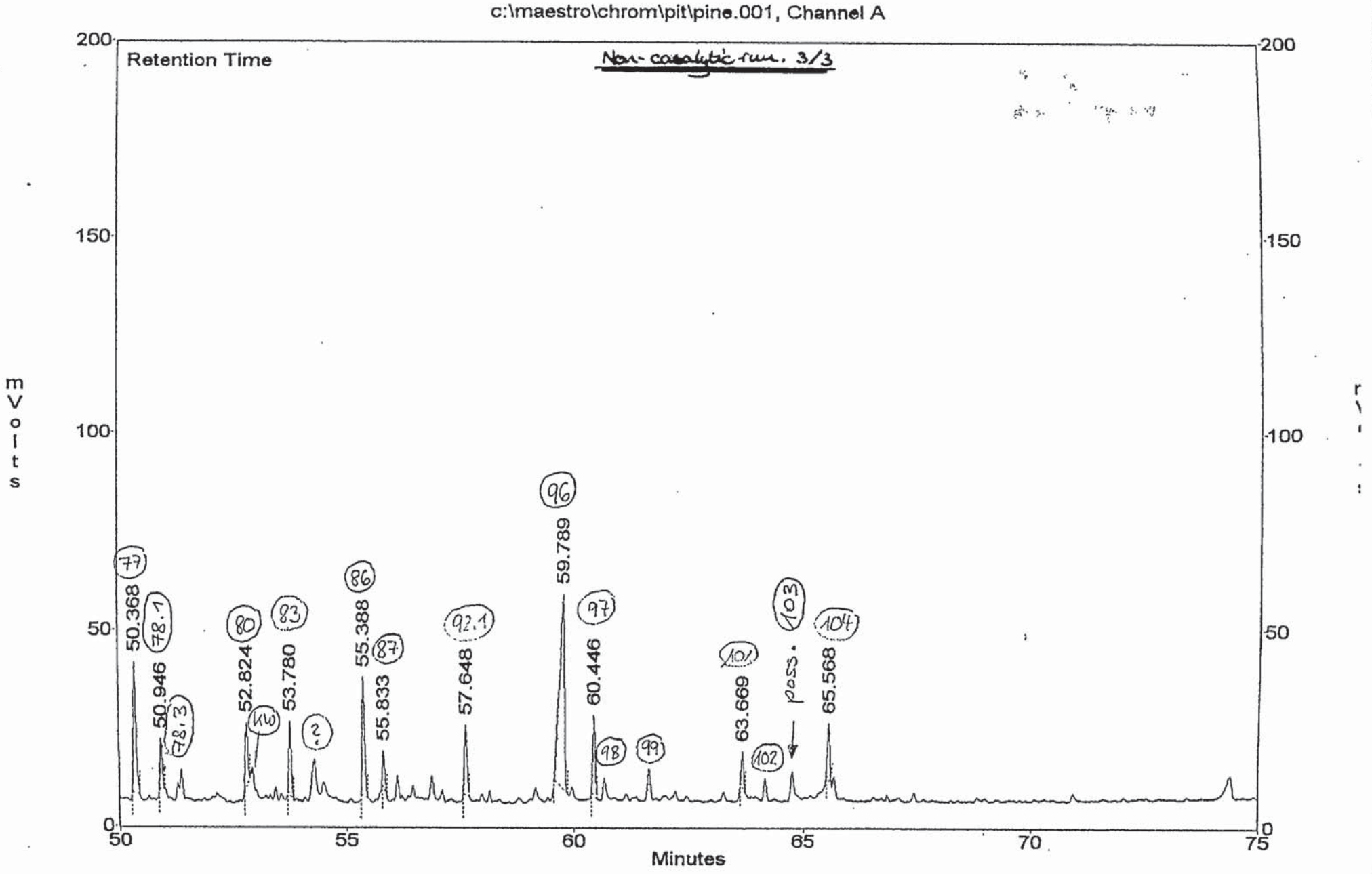
c:\maestro\chrom\pit\pine.001, Channel A
Retention Time
Non-catalytic run. 3/3
mVolts
Minutes
200
150
100
50
0
50
55
60
65
70
75
50.368
50.946
52.824
53.780
55.388
55.833
57.648
59.789
60.446
63.669
65.568
poss.
77
78.1
78.3
80
83
86
87
92.1
96
97
98
99
101
102
103
104